

## **General Disclaimer**

### **One or more of the Following Statements may affect this Document**

- This document has been reproduced from the best copy furnished by the organizational source. It is being released in the interest of making available as much information as possible.
- This document may contain data, which exceeds the sheet parameters. It was furnished in this condition by the organizational source and is the best copy available.
- This document may contain tone-on-tone or color graphs, charts and/or pictures, which have been reproduced in black and white.
- This document is paginated as submitted by the original source.
- Portions of this document are not fully legible due to the historical nature of some of the material. However, it is the best reproduction available from the original submission.

# **NOISE CHARACTERISTICS OF THE SKYLAB S-193 ALTIMETER ALTITUDE MEASUREMENTS**

(NASA-CR-141403) NOISE CHARACTERISTICS OF  
THE SKYLAB S-193 ALTIMETER ALTITUDE  
MEASUREMENTS Final Report, Nov. 1974 - Aug.  
1975 (Business and Technological Systems,  
Inc.) 212 p HC \$7.75 CSCL 14B

N76-11539

Unclassified  
01589

William E. Hatch

## FINAL REPORT

**Report No. BTS-TR-75-23**

Prepared Under Contract No. NAS6-2631 by  
Business and Technological Systems, Inc.  
Aerospace Building  
Seabrook, Maryland 20801



November 1975



## National Aeronautics and Space Administration

**Wallops Flight Center**  
Wallops Island, Virginia 23337  
AC 804 824-3411

1. Report No. NASA CR-141403	2. Government Accession No.	3. Recipient's Catalog No.
4. Title and Subtitle NOISE CHARACTERISTICS OF THE SKYLAB S-193 ALTIMETER ALTITUDE MEASUREMENTS		5. Report Date October 1975
		6. Performing Organization Code
7. Author(s) William E. Hatch (Business and Technological Systems, Inc. Seabrook, Maryland 20801)		8. Performing Organization Report No. BTS-TR-75-23
9. Performing Organization Name and Address Business and Technological Systems, Inc. Aerospace Building, Suite 605 10210 Greenbelt Road Seabrook, Maryland 20801		10. Work Unit No.
12. Sponsoring Agency Name and Address National Aeronautics and Space Administration Wallop Flight Center Directorate of Applied Science Wallop Island, Virginia 23337		11. Contract or Grant No. NAS6-2631
15. Supplementary Notes This is a final report.		13. Type of Report and Period Covered Contractor Report November 1974 - August 1975
16. Abstract This report presents the statistical characteristics of the SKYLAB S-193 altimeter altitude noise. These results are reported in a concise format for use and analysis by the scientific community. In most instances the results have been grouped according to satellite pointing so that the effects of pointing on the statistical characteristics can be readily seen. The altimeter measurements and the processing techniques are described. The mathematical descriptions of the computer programs used for these results are included.		14. Sponsoring Agency Code
17. Key Words (Suggested by Author(s)) SKYLAB Altimeter, Altitude Noise Characteristics, Spectral Analysis, Pointing Effects		18. Distribution Statement Unclassified - Unlimited STAR Category 43
19. Security Classif. (of this report) Unclassified	20. Security Classif. (of this page) Unclassified	21. No. of Pages 211
22. Price*		

ACKNOWLEDGMENTS

The results included in this report could not have been achieved without contributions from several individuals. Mr. Joseph McGoogan and Mr. Clifford Leitao of NASA/Wallops provided valuable technical assistance in relating statistics derived from the data analysis to S-193 hardware performance characteristics. Mr. Thomas Taylor and Mr. Robert Kelly of Scientific Applications, Inc. coordinated the computer processing of over 250 data arcs. Ms. Carol Hammond and Mr. Dan Chin of Business and Technological Systems, Inc. provided support for updating the SAMPFL and RAP programs so that a large amount of data could be processed and quickly interpreted.

## TABLE OF CONTENTS

	<u>Page</u>
1.0 INTRODUCTION.....	1-1
2.0 ALTIMETER DATA PROCESSING.....	2-1
2.1 Measurement Description.....	2-1
2.2 Evaluation of Residual Statistics.....	2-4
2.2.1 Summary of Residual Statistics.....	2-4
2.2.2 Detail Noise Statistics.....	2-6
2.3 References.....	2-11
3.0 STATISTICAL SUMMARY.....	3-1
3.1 Distribution of Residual Sigmas.....	3-22
3.2 Distribution of Significant Frequency Bands.....	3-28
3.3 References.....	3-37
4.0 NOISE STATISTICS FOR SELECTED DATA ARCS.....	4-1
4.1 Mode 1 Results.....	4-4
4.2 Mode 3 Results.....	4-48
4.3 Mode 5 Results.....	4-86
4.4 Comparison of Power Spectrum with Autoregressive Model Transfer Function.....	4-128
APPENDIX A - RAP Program Mathematical Description.....	A-1
APPENDIX B - SAMPL Program Mathematical Description.....	B-1

## 1.0 INTRODUCTION

The purpose of this document is to present statistical characteristics of the SKYLAB S-193 altimeter altitude noise measurement process in a concise format for use and analysis by the Scientific Community. The data contained in this report is obtained from all three SKYLAB missions (SL-2, SL-3, SL-4). Section 2 describes the statistical processing techniques, Section 3 presents summary residual statistics for 184 data arcs and Section 4 contains detailed noise statistics for 27 selected data arcs. Appendices A and B contain mathematical descriptions of the computer programs used for this data processing.

## 2.0 ALTIMETER DATA PROCESSING

### 2.1 Measurement Description

The altimeter range residuals are defined as the differences between the eight per second altimeter measurements to the sea surface and the calculated altitude from the spacecraft to a reference ellipsoid. This calculated altitude is derived from a short arc orbit determination using S-Band and C-Band tracking data as described in reference [2]. The calculated altitude includes corrections for pulsewidth, bandwidth and other operating parameters. A 2.79 meter correction for refraction was also applied. Errors in the calculated altitude are constant over the altimeter data arc thus contributing a constant bias error. The noise on the altimeter measurements is a function of received signal to noise ratio, the statistical independence of the returns and tracking servo bandwidth. For a near beamwidth limited system such as the S-193 (in the 100 ns pulsewidth mode) the received peak power is a very sensitive function of pointing angle with respect to nadir. An increase in pointing angle will (1) introduce a bias error (2) reduce signal power and (3) change the return signal waveshape. The reduction in signal power will increase the measurement noise variance and reduce the tracking servo bandwidth thus altering both the noise magnitude and power spectrum. However, the change in the received waveshape will have the largest effect on the servo bandwidth for it changes the characteristics of the error detection.

Altimeter range measurements were analyzed for three major operating modes, (Table 2.1) modes 1, 3 and 5. Each operating mode has three data acquisition submodes (DAS-1, DAS-2 and DAS-3) which vary in length from 16 seconds to 103 seconds. In this report a data arc is defined as the residuals recorded during one altimeter mode/submode. Each such arc is uniquely identified by a map number as assigned in reference [2] and the submode designation. Hardware problems which influenced the analysis and statistical summaries presented in this report included the following:

- The pulse compression (Mode-5 DAS-2) was inoperative for all data arcs prior to Map 73. As a result for these data arcs the altimeter processor operating characteristics were nearly identical to Mode-1 DAS-2
- The antenna gain was reduced to 28 db during SKYLAB IV. This affected every data arc after Map 76.

A more detailed description of the altimeter experiment and hardware is given in reference [2].

TABLE 2.1 ALTIMETER DATA ACQUISITION MODES/SUBMODES

MODE 1 PULSE SHAPE EXPERIMENT																
TRANSMITTER					ANT.	RECEIVER		SIGNAL PROC.	SQUARE LAW SAMPLING							TYPICAL RUNNING TIME SEC.
SUB-MODE	PULSE MODE	FREQ. GHZ	PULSE WIDTH NSEC.	POINTING ANGLE DEGREES	IF FILTER BANDWIDTH MHZ	CAL. PATH ATTN. DB	ALTITUDE TRACK OR COUNTER	# OF SAMPLE POSITIONS	# OF SCH GATES PER POSITION	SCH GATE SPACING NSEC.	RETURNS SAMPLED PER FRAME	# OF FRAMES OF DATA	# OF SAMPLES OBTAINED			
DAS-1	SINGLE-250 FPS	13.9	100	SUB-SATELLITE	10	N/A	ALT. TRACK	3	8	25	104	50	41,600	52.00		
DAS-2	"	"	"	"	100	"	"	"	"	"	"	61	50,752	63.44		
DAS-3	"	"	"	0.431° PITCH	"	"	"	"	"	"	"	61	50,752	63.44		

MODE 2 TIME CORRELATION EXPERIMENT																
TRANSMITTER					ANT.	RECEIVER		SIGNAL PROC.	SQUARE LAW SAMPLING							TYPICAL RUNNING TIME SEC.
SUB-MODE	PULSE MODE	FREQ. GHZ	PULSE WIDTH NSEC.	POINTING ANGLE DEGREES	IF FILTER BANDWIDTH MHZ	CAL. PATH ATTN. DB	ALTITUDE TRACK OR COUNTER	# OF SAMPLE POSITIONS	# OF SCH GATES PER POSITION	SCH GATE SPACING NSEC.	RETURNS SAMPLED PER FRAME	# OF FRAMES OF DATA	# OF SAMPLES OBTAINED			
DAS-1	"	13.9	100	SUB-SATELLITE	10	N/A	ALT. TRACK	3	8	25	104	16	13,312	16.64		
DAS-2	DUAL-250 PULSE PAIRS/SEC	"	"	"	100	"	"	8	4	"	208	25	20,800	26.0		
DAS-3	"	"	20	"	"	"	"	16	"	10	"	98	61,536	101.07		

MODE 3 PULSE COMPRESSION - 20 NANOSECOND EXPERIMENT																
TRANSMITTER					ANT.	RECEIVER		SIGNAL PROC.	SQUARE LAW SAMPLING							TYPICAL RUNNING TIME SEC.
SUB-MODE	PULSE MODE	FREQ. GHZ	PULSE WIDTH NSEC.	POINTING ANGLE DEGREES	IF FILTER BANDWIDTH MHZ	CAL. PATH ATTN. DB	ALTITUDE TRACK OR COUNTER	# OF SAMPLE POSITIONS	# OF SCH GATES PER POSITION	SCH GATE SPACING NSEC.	RETURNS SAMPLED PER FRAME	# OF FRAMES OF DATA	# OF SAMPLES OBTAINED			
DAS-1	SINGLE-250 FPS	13.9	100	SUB-SATELLITE	10	N/A	ALT. TRACK	3	8	25	104	16	13,312	16.64		
DAS-2	"	"	130 (PC)	"	100	"	"	4	"	10	104	99	82,368	102.96		
DAS-3	"	"	20	"	"	"	"	"	"	"	104	51	47,432	53.04		

In Mode 1 DAS-3 the antenna pointing angle is offset  $.431^\circ$  in pitch from its nadir pointing position to evaluate the effect of known pointing angle variation. Pointing angle can be estimated (1) from an analysis of the tracker response and automatic gain control (AGC) and (2) from an analysis of the return waveform. The pointing angles as tabulated in this report, have been estimated by the first method which is accurate to within a few tenths of a degree for pointing angles from  $.75^\circ$  through  $1.7^\circ$ .

## 2.2 Evaluation of Residual Statistics

In addition to broadband (Bandwidth 2 Hz) measurement noise the altimeter residual data contains low frequency effects due to geoid variations. Thus evaluation of the noise statistics consisted of (1) selection of a reasonable number of data arcs (approximately 184), which visually contain a minimal amount of geoid variations, (2) computation of summary residual statistics for all of these data arcs, and (3) high pass filtering and computation of detailed noise characteristics for twenty-seven typical data arcs spanning all nine altimeter operating modes/submodes and three pointing angle ranges (low, moderate, and high).

### 2.2.1 Summary Residual Statistics

The summary residual statistics as compiled from the RAP program output include:

- Mean
- Standard deviation
- F Statistic for assessment of variance homogeneity
- Chi square statistic to assess distribution normality
- Listing of significant power spectral components
- Listing of significant autocorrelation coefficients

A detailed description of the computation as performed in RAP is contained in Appendix A. The F statistic is computed by partitioning the data arc into four segments, computing a mean and sum of squares about the mean for each segment and then comparing the pooled sums of squares about the segment means with the sum of the squared deviations of the segment means from the overall means. The chi square statistic measures the goodness of fit of the residual histogram to the normal distribution.

In RAP the power spectrum is computed and scaled such that if the residuals are a white noise process then each spectral component is an independently distributed chi square variate with two degrees of freedom. The raw power spectrum (i.e. before application of any window functions) is then divided into fifty cells containing an equal number of spectral coefficients. The coefficients are summed within each cell. Under the white noise assumption these sums are also independently distributed chi square variates with degrees of freedom equal to the sum of the

degrees of freedom of the coefficients within that cell. Thus if  $p$  coefficients are summed within a cell the resultant sum would have  $2p$  degrees of freedom. Significant frequency bands are then defined as those cells where this sum exceeds the 99th percentile of the appropriate chi square distribution. Thus, if the observed residual time series is not a white noise process, this approach identifies those frequency bands where the signal power is concentrated so as to cause significant deviations from the white noise assumption.

Similarly, for a white noise process the autocorrelation coefficients are asymptotically normal with mean zero and standard deviation  $1/\sqrt{N}$  where  $N$  is the sample size. Significant autocorrelation coefficients are defined as those coefficients whose absolute value exceeds  $2/\sqrt{N}$  (i.e. two sigma). As with the spectrum, this approach simply identifies the coefficients which are significantly different from their expected value (zero) under the white noise assumption.

These summary statistics are presented and discussed in Section 3.

### **2.2.2 Detail Noise Statistics**

To evaluate S-193 measurement noise characteristics in addition to computation of the above statistics, the longer data arcs (i.e. longer than 24 seconds) subject to detail analysis were high pass filtered by the program SAMPFL (Appendix B) to remove any low frequency geoid effects. This high pass filtering is accomplished by SAMPFL by (1) low pass filtering the data with a 99 point quadratic midpoint filter and (2) computing the high pass output as the difference between the input data and the low pass output. The low pass power transfer function plot (Figure 2.1) shows that cut off frequency for this filter is .0845 Hz. In reference [2] a low pass filter with the half power frequency of .164 Hz is recommended for recovery of geoid features from the SKYLAB S-193 data. Since the purpose of this study was to evaluate the S-193 measurement noise statistics, the data arcs processed had no prominent geoid features, therefore the .0845 Hz cutoff was adequate for rejection of any small geoid features or trends and yet retained most of the measurement noise power.

In reference [2] the S-193 tracking loop frequency domain transfer function is given as

$$H_T(jw) = \frac{70jw+280}{8(jw)^2+81jw+280} \frac{\sin wT/2}{wT/2} e^{-jwT/2} \quad (2.1)$$

where  $w$  is the radian frequency ( $2\pi f$ ) and  $T$  is the sampling period of .128 seconds. From the plot of  $|H_T(jw)|^2$  (Figure 2.2) it is obvious that the 99 point highpass filter removes only a small fraction of the broadband noise power.

After high pass filtering (where applicable) the following were computed and displayed.

- Summary statistics as defined in Section 2.2.1
- Time series plot
- Power spectrum plot
- Autocorrelation function plot
- Autoregressive model power transfer function plot

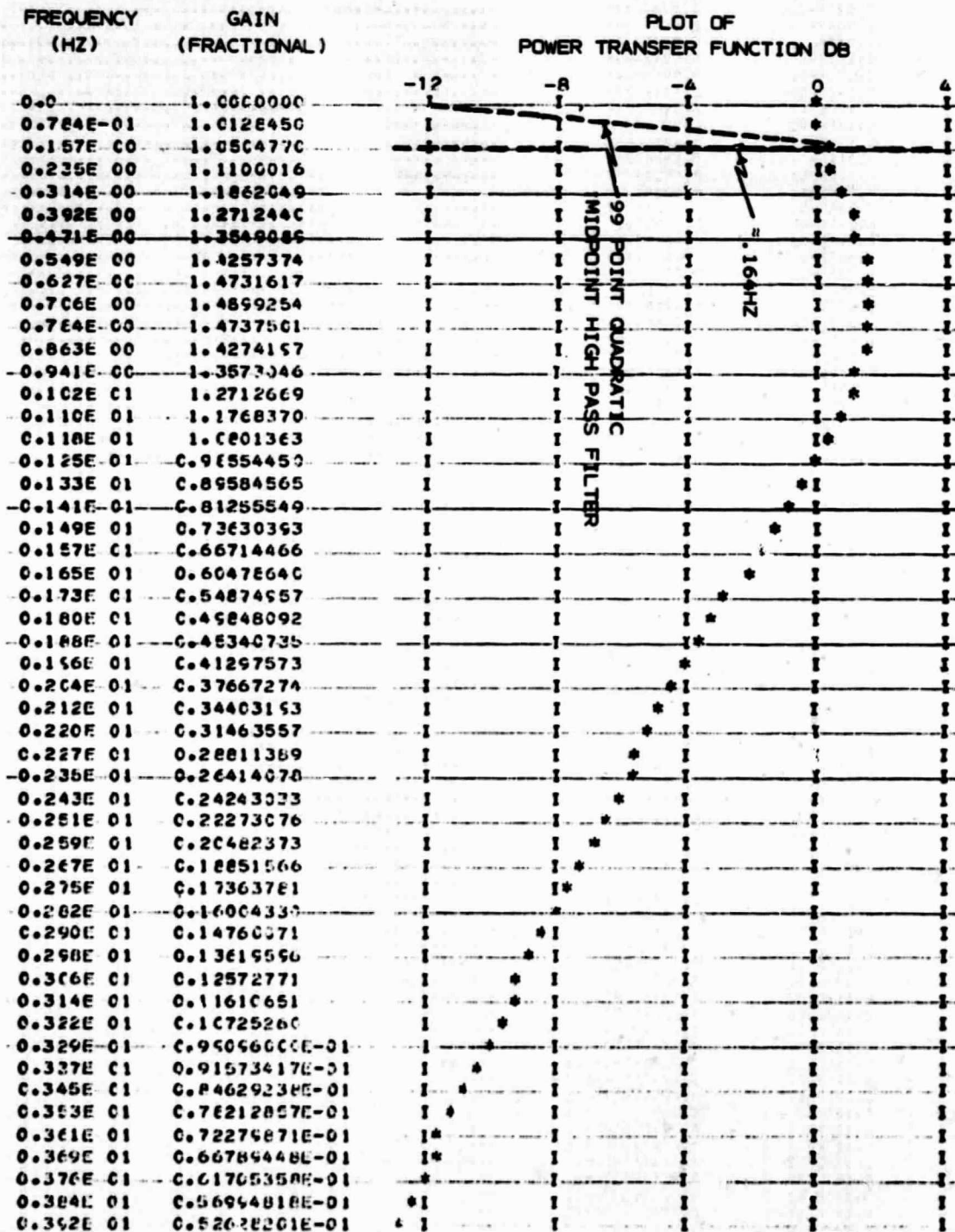
The summary statistics included mean, standard deviation, F statistic, chi square statistic, significant power spectral coefficients and significant auto-

POWER TRANSFER FUNCTION OF 99 POINT QUADRATIC MIDPOINT FILTER

FIGURE 2.1

FREQUENCY (HZ)	POWER TRANSFER (FRACTIONAL)
0.	0.9999999
0.17E-02	0.9999999
0.35E-02	0.9999973
0.52E-02	0.9999944
0.70E-02	0.9999917
0.88E-02	0.9999884
0.10E-01	0.9999849
0.125E-01	0.9999624
0.141E-01	0.9999327
0.157E-01	0.9999119
0.176E-01	0.9999010
0.194E-01	0.9997612
0.211E-01	0.9996275
0.225E-01	0.9953771
0.241E-01	0.9938145
0.254E-01	0.9918745
0.275E-01	0.9765721
0.295E-01	0.9647442
0.317E-01	0.9535247
0.334E-01	0.9797234
0.352E-01	0.9752219
0.370E-01	0.9702147
0.387E-01	0.9644425
0.405E-01	0.9579493
0.422E-01	0.9506562
0.440E-01	0.9455457
0.458E-01	0.9435545
0.475E-01	0.9276438
0.492E-01	0.9128377
0.514E-01	0.9010449
0.526E-01	0.8927164
0.546E-01	0.8744828
0.563E-01	0.8594934
0.581E-01	0.8435725
0.591E-01	0.8270474
0.611E-01	0.6919362
0.631E-01	0.7913512
0.651E-01	0.7705332
0.664E-01	0.7497725
0.686E-01	0.72e1054
0.704E-01	0.7053769
0.722E-01	0.6822382
0.739E-01	0.6561494
0.757E-01	0.6333766
0.774E-01	0.6079923
0.792E-01	0.5820756
0.811E-01	0.5557110
0.827E-01	0.5285943
0.845E-01	0.5020017
0.862E-01	0.4746464
0.880E-01	0.4476326
0.897E-01	0.4204547
0.915E-01	0.3934236
0.933E-01	0.3666356
0.951E-01	0.3402256
0.968E-01	0.3142337
0.985E-01	0.2882271
0.100E 00	0.2642614
0.102E 00	0.2470722
0.104E 00	0.2349147
0.106E 00	0.1946565
0.107E 00	0.1734445
0.109E 00	0.1533151
0.111E 00	0.1345114
0.113E 00	0.1164657
0.114E 00	0.9991917e-01
0.115E 00	0.1441447e-01
0.116E 00	0.7e14321e-01
0.120E 00	0.5762211e-01
0.121E 00	0.4656547e-01
0.123E 00	0.3551270e-01
0.125E 00	0.2772331e-01
0.127E 00	0.2132426e-01
0.128E 00	0.1411437e-01
0.131E 00	0.9114371e-02
0.132E 00	0.52471177e-02
0.134E 00	0.25211177e-02
0.135E 00	0.13011143e-02
0.137E 00	0.5317371e-04
0.139E 00	0.2721577e-03
0.141E 00	0.1317112e-02
0.143E 00	0.27157471e-02
0.144E 00	0.13157471e-02

FIGURE 2.2  
POWER TRANSFER FUNCTION  
S-193 PROCESSOR



correlation coefficients as defined above in Section 2.2.1. CALCOMP plots of the high pass filtered (where applicable) time series, power spectrum and auto-correlation function were generated using the plot tape output option of the RAP program. For plotting purposes, to present a smoother graph, the raw power spectrum was modified by two applications of the Hanning window to the Fourier coefficients as described in Appendix A, Section 2.6.

To provide an analytical estimate of the noise power spectra, an autoregressive model was fitted to the residual time series.

The power spectral density requires  $1 + N/2$  coefficients (where  $N$  is the sample size) to describe the detailed frequency characteristics of the data and the autocorrelation function requires  $N-1$  coefficients to describe the time domain correlation structure. These are descriptive statistics which make no assumption about the underlying process which generates the time series. The autoregressive model [1] assumes that a stationary time series  $\{X_t\}$  can be represented as finite sum of the form

$$X_t = \epsilon_t - \phi_1 X_{t-1} - \phi_2 X_{t-2} - \cdots - \phi_p X_{t-p} \quad (2.2)$$

where  $X_t$  is the observed value at time  $t$ ,  $\epsilon_t$  is a zero mean white noise process with variance  $\sigma^2$  and the  $\{\phi_i; i=1,2 \dots p\}$  are called the autoregressive coefficients. This is equivalent to assuming that  $\{X_t\}$  is generated by passing a discrete white noise process  $\{\epsilon_t\}$  through a digital filter with the transfer function  $H(Z)$  given by

$$H(Z) = \frac{1}{1 - \phi_1 Z^{-1} - \phi_2 Z^{-2} - \cdots - \phi_p Z^{-p}} \quad (2.3)$$

where  $Z = e^{j2\pi fT}$ ,  $f$  is the frequency in Hz,  $T$  is the sample time in seconds, and  $j = \sqrt{-1}$ .

A linear least squares procedure is implemented in RAP (Appendix A) to estimate the autoregression coefficients from the computed autocorrelation coefficients. For purposes of this study it was arbitrarily decided to estimate the first twenty autoregression coefficients. From these estimated coefficients the power transfer function  $|H(Z)|^2$  was computed and plotted over the frequency range (0-3.9 Hz). This plotted power transfer function is related to the power spectrum of the digital filter output,  $N(f)$ , by the scale factor  $\sigma^2$  as

$$N(f) = |H(e^{j2\pi fT})|^2 \sigma^2 \quad (2.4)$$

These detailed noise statistics are presented in Section 4.0.

2.3 References

1. Box and Jenkins, Time Series Analysis, Forecasting and Control, Holden-Day, 1970.
2. McGoogan, Leitao and Wells, "Summary of SKYLAB S-193 Altimeter Results", NASA TM-X-69355, NASA Wallops Flight Center, February 1975.

### 3.0 STATISTICAL SUMMARY

This section presents statistical summaries of altimeter range residual data from 184 data arcs. Table 3.1 gives the number of analyzed arcs for each mode/submode. Within a given mode/submode the antenna off nadir pointing angle is the principal factor which determines the altimeter hardware signal processing parameters. Therefore, in this section the residual statistics are tabulated as a function of pointing angle with the pointing angle ranges defined as follows:

Low - pointing angle  $\leq$  .6 degrees

Moderate - .6 degrees  $<$  pointing angle  $\leq$  .9 degrees

High - .9 degrees  $<$  pointing angle

In all cases the tracker determined pointing angle is used.

Tables 3.2 through 3.10 give the date (year, month, day), start time (hours, minutes, seconds), stop time, pointing angle and summary statistics as extracted from the RAP program output. The F statistic, which assesses the variance homogeneity over the data arc, has  $(3, N-3)$  degrees of freedom where N is the sample size. Large values of this F statistic would indicate a lack of such homogeneity. For the sample sizes given in tables 3.2 through 3.10 the 99th percentile of the F distribution is approximately 3.78. F values greater than this are marked with an asterisk (\*). Residual normality is assessed by computing a chi square statistic which measures the difference between the residual histogram and the normal distribution. The table entry (Normality Test) is the value of the chi square cumulative distribution function associated with the computed statistic. As discussed in Section 2.2.1, the significant frequency bands are those frequency bands where the grouped power spectral coefficient exceeds the 99th percentile of the chi square distribution with appropriate degrees of freedom. Significant autocorrelation coefficients are defined as those which exceed the plus or minus two sigma value for a white-noise process. If an autocorrelation function has all large positive coefficients the process is obviously non-stationary. The table entry contains either the lag indices of the significant coefficients or the abbreviation NON-STA. indicating that the process is non-stationary. Usually this non-stationarity occurs when the data contains geoid features which are large in comparison to the measurement noise level.

Section 3.1 presents the distribution of residual sigmas within each pointing angle range (low, moderate and high), and Section 3.2 describes the distribution of significant frequency bands.

TABLE 3.1  
NUMBER OF DATA ARCS FOR  
EACH MODE/SUBMODE

MODE	POINTING ANGLE RANGE	SUBMODE		
		DAS-1	DAS-2	DAS-3
MODE 1	LOW	6	6	6
	MODERATE	12	10	10
	HIGH	5	5	2
MODE 3	LOW	2	2	1
	MODERATE	2	2	2
	HIGH	5	6	3
MODE 5	LOW	10	9	6
	MODERATE	15	12	2
	HIGH	8	11	6

TABLE 3.2  
MODE 1 LOW POINTING ANGLE

MAP	PASS	MODE	DATE	START	STOP	POINT (DEGS)	SAMP.	MEAN	SIGMA	F STATISTIC	NORM. TEST	SIG. FREQ.	SIGNIFICANT AUTOCORRELATION COEFFICIENTS
							SIZE	(MTRS)	(MTRS)			FREQ. BANDS (HZ)	
3	4	1 DAS-1	730604	171111	171155	<.6°	280	46.7	1.89	2.33	.979	0-.0837	NON STA.
		1 DAS-3		171302	171401		400	57.0	1.73	.731	.361	0-.059 .391-.449	NON STA.
38	22	1 DAS-1	730902	142954	143034	<.6°	208	9.17	1.37	1.16	.641	0-.0376	10.11
		1 DAS-2		143040	143139		352	7.19	1.21	2.96	.666	NONE	8.19
		1 DAS-3		143157	143243		304	8.78	1.41	.277	.680	0-.128 .771-.822	NON STA.
39	22	1 DAS-1	730902	143342	143416	<.6°	208	17.9	1.95	1.22	.795	0-.112	NON STA.
		1 DAS-2		143430	143530		408	22.5	1.20	2.53	.827	0-.134	NON STA.
		1 DAS-3		143533	143633		408	23.3	1.30	.344	.746	0-.0574	NON STA.
40	22	DAS-3		143913	144013	<.5°	408	12.4	1.36	1.82	.727	0-.057	NON STA.
41	22	1 DAS-2	730902	144149	144251	<.5°	416	3.48	2.02	1.95	.938	0-.131	NON STA.
		DAS-3		144253	144353		408	-5.1	3.03	.214	.991	0-.134	NON STA.
85	55	1 DAS-1	731201	173026	173121	<.5°	364	31.0	1.77	.603	.692	0-.0429	NON STA.
		DAS-2		173127	173210		280	30.5	1.72	2.07	.526	0-.0279 .837-.865 1.172-1.200 1.339-1.367	1.8,9,12, 17,20
86	55	1(2)DAS-1	731201	173358	173442	<.5°	288	12.7	2.98	.992	.991	0-.136	NON STA.
		1(2)DAS-2		173445	173546		416	-3.16	2.13	5.11*	.956	0-.056 .300-.357 .826-.883 1.05-1.11	NON STA.

ORIGINAL PAGE IS  
OF POOR QUALITY

TABLE 3.2 (CONT.)

MAP	PASS	MODE	DATE	START	STOP	POINT (DEGS)	SAMP. SIZE	MEAN (MTRS)	SIGMA (MTRS)	F STATISTIC	NORM. TEST	SIG. FREQ. BANDS (HZ)	SIGNIFICANT AUTOCORRELATION COEFFICIENTS
86	55	1(2)DAS-3		173549	173649		408	-.03	1.95	.549	.945	0-.057 .536-.594 .689-.747 .919-.977	1,2,8-18
91	57	1 DAS-1	731202	182231	182256		192	38.9	1.84	.226	.989	.163-.203 .448	1-5
		1 DAS-2		182259	182323	<.5°	184	37.9	1.66	1.21	.718	.425 .934	1,7,8,12

TABLE 3.3  
MODE 1 MODERATE POINTING ANGLE

MAP	PASS	MODE	DATE	START	STOP	POINT (DEGS)	SAMP. SIZE	MEAN (MTRS)	SIGMA (MTRS)	F STATISTIC	NORM. TEST	SIG. FREQ. BANDS (HZ)	SIGNIFICANT AUTOCORRELATION COEFFICIENTS
201	97	1(2)DAS-1	740131	145526	145610	.75°	240	3.68	2.12	2.02	.997	0-.033 .846-.879	
		1(2)DAS-2		145614	145714		364	-1.5	2.39	1.36	.575	0-.1073	NON STA.
		1(2)DAS-3		145718	145816		342	-12.2	2.59	3.11	.303	0-.114	NON STA.
202	97	1(3)DAS-1	740131	150027	150110	.75°	280	-25.7	1.78	.774	.927	0-.0279	1-4.6-8. 12-13.15- 17.19
		1(3)DAS-2		150115	150215		360	-27.8	1.86	2.54	.539	0-.043	NON STA.
		1(3)DAS-3		150218	150318		364	-30	1.88	1.27	.625	0-.043 .193-.236 .645-.687	1,2,8,9,11. 12
203	97	1(4)DAS-1	730131	150921	150505	.75°	240	-31.6	1.88	.243	.997	0-.0325 1.107-1.139	1,8,14
		1(4)DAS-2		150509	150609		408	-35.5	2.34	1.83	.766	0-.057	NON STA.
		1(4)DAS-3		150611	150711		364	-39.3	1.82	.961	.981	.258-.300 .451-.494 .708-.816 1.03-1.07	1,2

TABLE 3.3 (CONT.)

MAP	PASS	MODE	DATE	START	STOP	POINT (DEGS)	SAMP. SIZE	MEAN (MTRS)	SIGMA (MTRS)	F STATISTIC	NORM. TEST	SIG. FREQ. BANDS (HZ)	SIGNIFICANT AUTOCORRELATION COEFFICIENTS
204	97	1(5)DAS-1	730131	150808	150851	.75°	240	-40.8	1.68	.135	.208	2.41-2.44	1.15
		1(5)DAS-2		150856	150955		400	-41.5	2.38	2.32	.929	0-.137 .859-.918	NON STA.
		1(5)DAS-3		150959	151058		352	-48.3	1.81	2.86	.888	0-.111 .400-.443 .533-.644 1.20-1.24	1.2.12-14
205	97	1(6)DAS-1	740131	151157	151249	.75°	280	-48.0	1.42	1.26	.987	NONE	NONE
		1(6)DAS-2		151252	151345		308	-46.1	1.73	.322	.331	0-.051 .304-.355 .457-.583 1.37-1.42	1.2.17
		1(6)DAS-3		151347	151448		368	-45.4	1.92	4.00*	.918	0-.106 .382-.488	NON STA.
206	97	1(7)DAS-2		151630	151725	.75°	312	-35.3	2.27	1.70	.581	0-.050 .977-1.03	NON STA.
		1(7)DAS-3		151734	151834		360	-26.4	2.79	5.01*	.981	0-.043 .586-.629	NON STA.

TABLE 3.3 (CONT.)

MAP	PASS	MODE	DATE	START	STOP	POINT (DEGS)	SAMP. SIZE	MEAN (MTRS)	SIGMA (MTRS)	F STATISTIC	NORM. TEST	SIG. FREQ. BANDS (HZ)	SIGNIFICANT AUTOCORRELATION COEFFICIENTS
207	97	1(3)DAS-1	740131	152208	152252	.75°	240	21.72	2.40	.577	.370	0-.098	NON STA.
208	97	1(9)DAS-1	740131	152553	152637	.75°	240	45.98	1.67	1.19	.995	NCNE	1.10
		1(9)DAS-2		152640	152741		416	43.1	2.42	2.26	.992	0-.056	NON STA.
		1(9)DAS-3		152744	152843		400	31.6	3.48	1.08	.875	0-.137	NON STA.
212	97	1(13)DAS-1	7430131	154059	154144	.75°	294	-60.1	1.78	1.70	.401	0-.0266 .797-.824	NON STA.
213	97	1(14)DAS-1	740131	154443	154527	.75°	240	-33.8	2.57	1.04	.651	0-.162	NON STA.
		1(14)DAS-2		154530	154630		360	-23.1	2.48	.173	.195	0-.174	NON STA.
		1(14)DAS-3		154634	154733		352	-18.2	2.35	1.70	.622	0-.111 .932-.977	NON STA.
214	97	1(15)DAS-1	740131	154832	154916	.85°	240	2.03	2.27	.774	.931	.326-.350 .911-.944	1,14,18,19
		1(15)DAS-2		154919	155018		294	1.30	3.56	2.62	.824	0-.132 .213-.292 .425-.452 .531-.558 .691-.717	NON STA.

TABLE 3.3 (CONT.)

VAP	PASS	MODE	DATE	START	STOP	POINT (DEGS)	SAMP. SIZE	MEAN (MTRS)	SIGMA (MTRS)	F STATISTIC	NORM. TEST	SIG. FREQ. BANDS (HZ)	SIGNIFICANT AUTOCORRELATION COEFFICIENTS
214	97	1(15)DAS-3		155022	155122		408	5.72	3.17	4.68 *		0-.057 .153-.287 .383-.440 .536-.670 .766-.623	1-3,5-7, 11-16
218	97	1(16)DAS-1	740131	155230	155323	.75°	224	2.65	2.53	3.64	.974	.698-.732 1.12-1.50	1,13,14
		1(16)DAS-2		155327	155427		360	.148	2.2	.916	.930	0-.0434 .391-.434 .521-.629 .781-.825	NON STA.
		1(16)DAS-3		155431	155529		342	-5.50	2.18	1.02	.999	0-.114 .342-.386 .490-.731 .822-.868	1,2,3,11-15

TABLE 3.4

## MODE-1 HIGH POINTING ANGLES

MAP	PASS	MODE	DATE	START	STOP	POINT (DEGS)	SAMP. SIZE	MEAN (MTRS)	SIGMA (MTRS)	F STATISTIC	NORM. TEST	SIG. FREQ. BANDS (HZ)	SIGNIFICANT AUTOCORRELATION COEFFICIENTS
6	7	1 DAS-1	730610	142819	142857	1.2°	192	89.0	5.30	1.16	.796	0-.081 .407-.529 .651-.692 .895	1-3,6-8, 10-13
		1 DAS-2		142901	143002		368	94.5	6.23	1.62	.101	0-.488	NON STA.
		1 DAS-3		143006	143106		352	146.3	8.55	10.13*	.995	0-.377	ALL
28	17	1 DAS-2	740669	134806	134847	1.3°	312	4.75	5.80	7.79*	.999	0-.500	1-7 12-17,19
		1 DAS-3		134856	134948		400	57.3	4.52	5.94*	.207	.0781-.371 .469-.605	1-5,
33	19	1 DAS-1	730812	023502	023547	1.07°	242	-69.8	3.03	.807	.974	.322-.355 .646-.678 .839-.872	1,15
		1 DAS-2		023703	023804		468	-30.9	5.91	5.26*	.761	0-.451 .534-.548	1-6,11-19
100	62	1 DAS-1	731207	144810	144853	1.3°	244	45.0	7.69	3.95*	.981	.209-.453 .628-.663	1-4, 6-12

ENTRANT PAGE **B**  
OF YOUR QUALITY

TABLE 3.4 (CONTINUED)

MAP	PASS	MODE	DATE	START	STOP	POINT (DEGS)	SAMP. SIZE	MEAN (MTRS)	SIGMA (MTRS)	F STATISTIC	NORM. TEST	SIG. FREQ. BANDS (HZ)	SIGNIFICANT AUTOCORRELATION COEFFICIENTS
108	68	1 DAS-1	731218	113318	113403	1.0°	242	60.05	2.57	.990	.967	.968-1.00	1,4,5
		1 DAS-2		113406	113506		360	61.1	2.40	2.64 <sup>*</sup>	.96 <sup>†</sup>	.326-.434 .586-.629 .716-.760 .977-1.02	1,2,5,6
148	93	1(2)DAS-1	730114	165602	165646	1.0°	240	56.6	4.29	2.75	.924	.130-.293 .391-.423 .521-.618 .716-.749 1.11-1.14	1,2
		1(3)DAS-2		165649	165719		132	57.9	4.44	1.41	.999	.237-.414 .592	1-4,7-20

TABLE 3.5

## MODE 3 LOW POINTING ANGLE

3-12

MAP	PASS	MODE	DATE	START	STOP	POINT (DEGS)	SAMP. SIZE	MEAN (MTRS)	SIGMA (MTRS)	F STATISTIC	NORM. TEST	SIG. FREQ. BANDS (HZ)	SIGNIFICANT AUTOCORRELATION COEFFICIENTS
45	24	3(3)DAS-1	730903	154440	154454	<.6°	104	-81.6	1.45	.952	.990	NONE	18
		3(3)DAS-2		154455	154517		114	-70.4	1.57	1.51	.181	.0685	1,2,4-8 10,11,14,17
		3(3)DAS-3		154600	154703		435	-85.7	1.79	4.17*	.991	0-.054	NON STA.
89	57	3 DAS-1	731202	161710	181724	<.5°	90	34.9	1.71	1.64	.586	.347	14
		3 DAS-2		181726	181748		114	48.6	1.94	2.91	.939	NONE	1

TABLE 3.6  
MODE-3 MODERATE POINTING ANGLE

3-13

MAP	PASS	MODE	DATE	START	STOP	POINT (DEGS)	SAMP. SIZE	MEAN (MTRS)	SIGMA (MTRS)	F STATISTIC	NORM. TEST	SIG. FREQ. BANDS (HZ)	SIGNIFICANT AUTOCORRELATION COEFFICIENTS
10	8	3 DAS-1	730611	152510.5	152525	.75°	112	-29.8	1.44	.581	.704	.349	None
		3 DAS-2		152526.5	152549		170	-30.2	1.42	.621	.838	1.65	1,14
		3 DAS-3		152552.5	152631		198	-31.7	1.55	.331	.610	0-.395	6,8,10,11 18,19
43	24	3(1)DAS-3	730903	153623	153801	.8°	104	-15.8	4.45	1.37	1.	0-.067	NON STA.
44	24	3(2)DAS-2	730903	154022	154043	.8°	110	-39.5	1.64	1.46	.506	.071	NON STA.

TABLE 3.7  
MODE-3 HIGH POINTING ANGLE

MAP	PASS	MODE	DATE	START	STOP	POINT (DEGS)	SAMP. SIZE	MEAN (MTRS)	SIGMA (MTRS)	F STATISTIC	NORM. TEST	SIG. FREQ. BANDS (HZ)	SIGNIFICANT AUTOCORRELATION COEFFICIENTS
8	7	3 DAS-1	730610	143629	143639	1.45°	76	130.8	7.39	4.7*	.997	.206 .411	1,2,3,4,5, 11,12,13,14,15
		3 DAS-2		143640	143704.5		184	131	9.2	3.69	.999	.0849 .170-.382	ALL
12	9	3(1)DAS-1	730612	131001	131015	1.1°	108	50.4	2.79	.428	.916	.940	1
		3(1)DAS-2		131016	131039		176	50.9	2.25	.100	.451	.133,.488	1
		3(1)DAS-3		131042	131203		526	52.0	2.69	1.30	.972	0-.061 .458-.519 .687-.742	1,11,12
13	9	3(2)DAS-1	730612	131536.5	131550	1.1°	104	40.5	4.27	.541	.845	.751,.977	1,2,5
		3(2)DAS-2		131551	131614		176	40.7	3.99	1.57	.300	.133,.266, .400,.444, .666	1,2,3
		3(2)DAS-3		131621	131755		612	43.1	6.45	10.39*	1.0	0-.600	1-6,14-20
29	17	3 DAS-1	730809	131512	135125	1.0°	100	42.0	3.00	3.70	.990	.469	1,17,18
		3 DAS-2		131527	135150		176	55.1	2.91	.402	.986	.355,.710	1,6,7
75	40	3 DAS-1	730914	170517	170531	1.0°	104	47.7	5.40	5.46*	.984	.0751,.376	1-5
		3 DAS-2		170532	170555		176	59.5	6.83	3.12	.786	.044-.088 .355-.533	1-4,6-10, 14-20
		3 DAS-3		170557	170655		256	63.9	6.06	3.95*	.960	.183-.458	ALL
135	81	3 DAS-2	740111	172926	172947	1.0°	160	52.3	2.35	.331	.893	.0977 .732 .977	1,7,10

TABLE 3.7  
MODE-3 HIGH POINTING ANGLE

MAP	PASS	MODE	DATE	START	STOP	POINT (DEGS)	SAMP. SIZE	MEAN (MTRS)	SIGMA (MTRS)	F STATISTIC	NORM. TEST	SIG. FREQ. BANDS (HZ)	SIGNIFICANT AUTOCORRELATION COEFFICIENTS
8	7	3 DAS-1	730610	143629	143639	1.45°	76	130.8	7.39	4.7*	.997	.206 .411	1,2,3,4,5, 11,12,13,14,15
		3 DAS-2		143640	143704.5		184	131	9.2	3.69	.999	.0849 .170-.382	ALL
12	9	3(1)DAS-1	730612	131001	131015	1.1°	108	50.4	2.79	.428	.916	.940	1
		3(1)DAS-2		131016	131039		176	50.9	2.25	.100	.451	.133,.488	1
		3(1)DAS-3		131042	131203		526	52.0	2.69	1.30	.972	0-.061 .458-.519 .687-.742	1,11,12
13	9	3(2)DAS-1	730612	131536.5	131550	1.1°	104	40.5	4.27	.541	.845	.751,.977	1,2,5
		3(2)DAS-2		131551	131614		176	40.7	3.99	1.57	.300	.133,.266, .400,.444, .666	1,2,3
		3(2)DAS-3		131621	131755		612	43.1	6.45	10.39*	1.0	0-.600	1-6,14-20
29	17	3 DAS-1	730809	131512	135125	1.0°	100	42.0	3.00	3.70	.990	.469	1,17,18
		3 DAS-2		131527	135150		176	55.1	2.91	.402	.986	.355,.710	1,6,7
75	40	3 DAS-1	730914	170517	170531	1.0°	104	47.7	5.40	5.46*	.984	.0751,.376	1-5
		3 DAS-2		170532	170555		176	59.5	6.83	3.12	.786	.044-.088 .355-.533	1-4,6-10, 14-20
		3 DAS-3		170557	170655		256	63.9	6.06	3.95*	.960	.183-.458	ALL
135	81	3 DAS-2	740111	172926	172947	1.0°	160	52.3	2.35	.331	.893	.0977 .732 .977	1,7,10

TABLE 3.8

## MODE 5 LOW POINTING ANGLE

MAP	PASS	MODE	DATE	START	STOP	POINT (DEGS)	SAMP. SIZE	MEAN (MTRS)	SIGMA (MTRS)	F STATISTIC	NORM. TEST	SIG. FREQ. BANDS (HZ)	SIGNIFICANT AUTOCORRELATION COEFFICIENTS
11	9	5 DAS-2	730612	130226.32	130319	.6°	352	40.1	1.30	.226	.993	0-.111	NON. STA.
		5 DAS-3		130336	130426		280	41.0	.945	14.6*	.908	.111-.140 .335-.363 .614-.698	
30	17	5 DAS-1	730809	135828	135843	<.5°	114	17.3	2.37	.995	.497	.548	1.13
		5 DAS-2		135845	140025		672	6.07	2.99	5.72*	.999	0-.128	
32	18	5 DAS-3	730811	153901.04	153941	<.5°	184	-37.5	.810	5.56*		.425 .977 1.10	1.4,11, 16,17
35	21	5(1)DAS-1	730901	152247	152302	<.6°	104	16.7	1.22	1.27	.371	NONE	NONE
46	25	5(1)DAS-1	730904	145138	145152	<.6°	108	-7.86	1.11	1.16	.430	.0723-.145	1,2,5,6,7
		5(1)DAS-3		155337	155428		342	-29.1	1.65	2.60	1.0	0-.114	
47	25	5(2)DAS-1	730904	145511	145523	<.5°	92	-32.3	1.10	.768	.931	NONE	16
		5(2)DAS-2		145526	145706		704	-39.6	3.04	6.98*	1.0	0-.144	NON STA.
		5(2)DAS-3		145709	145759		324	-49.4	1.85	1.17	1.0	0-.121	NON STA.
48	27	5 DAS-1	730906	211947	212000	<.6°	100	-4.71	1.45	.318	.946	.211	16.19
		5 DAS-2		212003	212134		650	-7.58	.931	6.57*	.808	0-.060	NON STA.
		5 DAS-3		212142	212236		352	-10.8	1.24	3.21	1.0	0-.111	NON. STA.

TABLE 3.8 (CONT.)

MAP	PASS	MODE	DATE	START	STOP	POINT (DEGS)	SAMP. SIZE	MEAN (MTRS)	SIGMA (MTRS)	F STATISTIC	NORM. TEST	SIG. FREQ. BANDS (HZ)	SIGNIFICANT AUTOCORRELATION COEFFICIENTS
50	28	5 DAS-2	730907	203582	203712	<.6°	720	-2.61	.828	.306	.731	0-.065	NON STA.
		5 DAS-3		203715	203805		324	-3.99	.878	.181	.535	0-.121	NON STA.
		5 DAS-1		203516	203529		100	-.758	1.22	.145	.669	.547	13,14,16
92	57	5(1)DAS-2	731202	182432	182604	<.5°	650	38.0	3.47	4.79*	1.0	0-.600	NON STA.
93	57	5(2)DAS-1	731202	182705	182715	<.5°	76	19.1	1.78	.186	.693	NONE	NONE
115	71	5(4)DAS-1	740101	133237	133251	.5°	108	17.54	1.72	.720	.518	.072,.174	1,2,5,11,13
		5(4)DAS-2		133254	133433		704	20.6	3.89	4.65*	1.0	0-.067	NON STA.
132	79	5(2)DAS-1	740109	154949	154959	.5°	76	57.7	1.38	.175	.950	.822	3,4,9,10 13,14,20
		5(2)DAS-2		155002	155141		704	67.1	3.52	8.86*	1.0	0-.067	NON STA.
233	86	5 DAS-1	740120	191815	191828	.6°	100	68.3	1.83	1.24	.540	.859	1,9-12,20
		5 DAS-2		191830	192010		720	82.8	1.58	1.08		0-.217 .304-.369 .456-.521 .760-.825	1-6,8-9

TABLE 3.9

## MODE 5 MODERATE POINTING ANGLE

ORIGINAL PAGE  
OF POOR QUALITY

3-17

MAP	PASS	MODE	DATE	START	STOP	POINT (DEGS)	SAMP. SIZE	MEAN (MTRS)	SIGMA (MTRS)	F STATISTIC	NORM. TEST	SIG. FREQ. BANDS (HZ)	SIGNIFICANT AUTOCORRELATION COEFFICIENTS
5	6	5 DAS-1	730609	151401	151546.5	.8°	114	91.3	1.50	.70	.656	NONE	NONE
18	11	5(2)DAS-1	730614	145400.5	145415	.7°	112	60.8	2.25	2.54	.975	.126..153 .767	1,2,3,15,16 19
		5(2)DAS-2		145417	145516		352	62.8	1.72	3.09	.999	0-.178	NON STA.
37	21	5(3)DAS-1	730901	153022	153036	.75°	108	-38.7	1.47	1.24	.383	NONE	1,4,6,7
73	39	5(1)DAS-1	730913	194549	194602	.85°	100	-54.6	2.31	.760	.762	.234	1-4,9,13
		5(1)DAS-3		194747	194838		342	-64.1	2.4	13.9*	1.0	0-.114	NON STA.
74	39	5(2)DAS-1	730913	194927	194940	.85°	100	-93.2	1.85	.648	.606	.148	8,20
		5(2)DAS-2		194946	195122		686	-89.8	2.47	3.11	1.	0-.057	NON STA.
		5(2)DAS-3		195125	195216		342	-100.3	1.83	24.5*	.999	0-.114	NON STA.
105	65	5 DAS-1	731215	000100	000113	.75°	100	-66.7	2.10	1.12	.576	NONE	1,4
106	67	5 DAS-1	731218	020019	020030	.75°	84	36.1	1.94	.414	.733	1.02	1,3,4,12

TABLE 3.9 (CONT.)

MAP	PASS	MODE	DATE	START	STOP	POINT (DEGS)	SAMP. SIZE	MEAN (MTRS)	SIGMA (MTRS)	F STATISTIC	NORM. TEST	SIG. FREQ. BANDS (HZ)	SIGNIFICANT AUTOCORRELATION COEFFICIENTS
106		S DAS-2		020033	020143		486	42.5	2.65	2.10	1.0	0-.113 .257-.354 .579-.627	NON STA.
109	68	S(1)DAS-2	731218	114511	114648	.75°	686	22.5	3.45	1.01	.978	0-.057	NON STA.
110	68	S(2)DAS-1	731218	114813	114827	.75°	104	-.144	2.09	1.17	.544	1.20	2
		S(2)DAS-2		114830	115010		650	7.21	2.17	9.82*	.998	0-.060 .216-.349 .433-.563 .649-.781 .865-.925	NON STA.
113	71	S(2)DAS-1	740101	132517	132532	.75°	114	35.41	1.71	1.51	.782	.411	1,18,20
		S(2)DAS-2		132534	132714		720	45.4	1.63	5.03*	1.0	0-.217 .380-.445 .608-.748 .836-.901	1-4,8-12, 16-20
114	71	S(3)DAS-1	740101	132859	132913	.75°	104	33.5	1.93	.731	.966	.451	1,8,16
		S(3)DAS-2		132916	133054		702	43.2	1.58	2.03	.591	0-.067	NON STA.
120	70	S(1)DAS-1	740108	163405	163416	.65°	84	56.2	1.91	2.34	.776	NONE	1
		S(1)DAS-2		163420	163550		704	59.7	3.38	2.06	1.0	0-.144	NON STA.

TABLE 3.9 (CONT.)

MAP	PASS	MODE	DATE	START	STOP	POINT (DEGS)	SAMP. SIZE	MEAN (MTRS)	SIGMA (MTRS)	F STATISTIC	NORM. TEST	SIG. FREQ. BANDS (HZ)	SIGNIFICANT AUTOCORRELATION COEFFICIENTS
129	78	S(2)DAS-2	740108	164444	164623	.75°	704	-33.3	3.43	2.01	.998	0-.0655	NON STA.
145	83	S(1)DAS-1	740114	153438	153452	.75°	104	2.03	2.21	.748	.557	.826;1.20	1,4,19,20
146	83	S(2)DAS-2	740114	153841	154021	.75°	704	-20.7	2.72	9.78*	.965	0-.067 .388-.610	NON STA.
151	85	S DAS-1	740118	204835	204848	.75°	100	78.4	2.02	1.45	.734	.391	1.15
216	97	S(1)DAS-1	740131	155628	155641	.75°	92	-5.14	2.40	.986	.944	.313	1,9,10,16
		S(1)DAS-2		155643	155823		650	8.37	2.55	3.19	1.0	0-.421	NON STA.
217	97	S(2)DAS-1	730131	155993	155956	.75°	100	12.6	1.89	.387	.620	1.56	1,15,18
		S(2)DAS-2		155959	160137		650	33.3	3.75	-1.12	.989	0-.132	NON STA.

TABLE 3.10

## MODE 5 HIGH POINTING ANGLE

MAP	PASS	MODE	DATE	START	STOP	POINT (DEGS)	SAMP. SIZE	MEAN (MTRS)	SIGMA (MTRS)	F STATISTIC	NORM. TEST	SIG. FREQ. BANDS (HZ)	SIGNIFICANT AUTOCORRELATION COEFFICIENTS
34	19	5 DAS-2	730812	024657	024829	1.1°	600	-23.5	3.56	9.31*	.530	0-.534	1-6,8-16 19.20
54	32	5(1)DAS-1	730901	130616	130628	1.6°	92	23.9	8.16	14.3*	.544	.170-.425	1-5,8-17
		5(1)DAS-2		130630	130810		768	19.3	5.15	20.9*	1.	0-.345	1-12,15-20
		5(1)DAS-3		130815	130902		360	12.8	9.33	27.3*	.997	0-.174	1-14,18-20
55	32	5(2)DAS-1	730911	130946	130957	1.2°	84	4.35	12.65	42.9*	1.0	.279-.372	1-5,9-19
		5(2)DAS-2		131001	131114		756	-7.05	6.64	49.9*	1.0	0-.279	1-12 16-20
		5(2)DAS-3		131143	131232		368	-6.13	5.25	4.43*	.998	0-.297	1-11 16-20
56	35	5(1)DAS-2	730912	125544	122727	1.4°	759	-5.04	6.42	22.1*	1.0	0-.335	1-12,16-20
		5(1)DAS-3		122730	122820		384	-5.5	4.87	3.14	1.0	0-.346	1-10,16-20
61	36	5(1)DAS-1	730912	165215	165228	1.25°	92	50.0	7.99	3.19	.999	.255-.340 .510	1-4,7-17
		5(1)DAS-2		165231	165411		650	52.3	3.40	4.94*	.981	0-.176 .361-.565	ALL
		5(1)DAS-3		165413	165503		280	58.5	3.98	1.53	.623	0-.0837 .167-.251 .335-.530 .614-.642	1-4,8-10, 15-18
62	36	5(2)DAS-1	730912	165553	165559	1.3°	46	62.1	6.99	3.50	.998	.340-.679	1-3,6-8, 15-20

TABLE 3.10 (CONT.)

MAP	PASS	MODE	DATE	START	STOP	POINT (DEGS)	SAMP. SIZE	MEAN (MTRS)	SIGMA (MTRS)	F STATISTIC	NORM. TEST	SIG. FREQ. BANDS (HZ)	SIGNIFICANT AUTOCORRELATION COEFFICIENTS
62	36	5(2)DAS-2	730912	165609	165737	1.3°	578	63.2	3.36	2.95	.997	0-.392 .541-.595	1-7,9-16
		5(2)DAS-3		165751	165835		240	65.5	3.04	2.57	.996	0.0651-.293 .391-.423	1-7,12-20
63	25/36	5(3)DAS-1	730912	165919	165930	1.4°	84	62.4	6.89	5.79*	.939	0.093-.186 .372-.465	1-4,9-15
		5(3)DAS-2		165932	170112		650	53.4	5.60	6.20*	1.0	0-.276	1-12,15-20
65	25/36	5(4)DAS-2	730912	171244	171423	1.3°	650	48.6	8.82	16.4*	1.0	0-.348	NON STA.
66	37	5 DAS-1	730912	201034	201049	1.4°	110	70.4	11.94	2.54	.969	0-.213 .855	ALL
		5 DAS-2		201056	201232		640	76.8	5.81	23.2*	1.0	0-.354	1-14,18-20
		5 DAS-3		201234	201325		294	84.6	4.46	10.6*	1.0	0-.239	ALL
71	38	5(2)DAS-1	730913	180952	181003	1.55°	84	41.6	9.27	10.53*	.995	0.093,.279	
99	61	5 DAS-1	731205	162108	162120	1.1°	92	-683	6.17	7.86*	.995	0.340,.510	1-3,6-12
		5 DAS-2		162120	162222		468	2.71	6.91	13.25*	1.0	0-.05 .133-.384 .534-.584	
134	79	5(4)DAS-1	740109	160044	160057	1.0	100	-68.1	1.93	1.86	.891	NONE	1,16
		5(4)DAS-2		160100	160239		650	-54.3	2.34	2.89	.916	0-.060 .144-.204 .288-.349 .505-.565 .793-.925	NON STA.

### 3.1 Distribution of Residual Sigmas

Within the program RAP the residual standard deviation, for a given data arc is computed as

$$\sigma = \left[ \frac{\sum_{i=1}^N x_i^2 - N\bar{x}^2}{N-1} \right]^{1/2} \quad (3.1)$$

where  $\{x_i\}$  are the altimeter range residuals,  $\bar{x}$  is the residual mean and  $N$  is the sample size. Thus  $\sigma$  is a measure of the dispersion of the data about the mean. Table 3.11 displays the overall residual sigmas for each mode/pointing angle range. Because of the small sample sizes data for Mode-3 low and moderate pointing angles has been grouped together. Figures 3.1, 3.2 and 3.3 show the distribution of residual sigmas in modes 1, 3 and 5 for each pointing angle range. In each case the overall sigma for each mode/pointing angle is defined as

$$\delta = \frac{\sum_j \sigma_j^2 N_j}{\sum_j N_j} \quad (3.2)$$

where  $\{\sigma_j\}$  are the arc sigmas and  $\{N_j\}$  are the arc sample sizes. In computing  $\delta$  for each data set obviously outlying  $\sigma_j$  were suppressed.

Figure 3.4 is a scatter diagram of residual sigma as defined in equation (3.1) versus tracker determined pointing angle. For pointing angles above .9 degrees each individual data point is shown. Due to the large number of data points below .9 degrees only the range of residual sigmas, with obvious outliers deleted, is shown. A least squares regression line was fitted to the 52 data points with pointing angles greater than .9 degrees yielding the statistical relationship:

$$\text{Residual Sigma} = 3.38 \text{ meters} + 7.34 * (\text{Pointing angle in degrees})$$

The corresponding correlation coefficient is .5306.

TABLE 3.11  
OVERALL RESIDUAL SIGMAS  
(METERS)

POINTING ANGLE RANGE	MODE-1	MODE- 3	MODE-5
LOW	1.56		1.27
MODERATE	2.43	1.64*	2.18
HIGH	5.51	5.28	5.68

\* INCLUDES BOTH LOW AND MODERATE  
POINTING ANGLE DATA.

FIGURE 3.1  
DISTRIBUTION OF MODE 1  
RESIDUAL STANDARD DEVIATION  
IN METERS

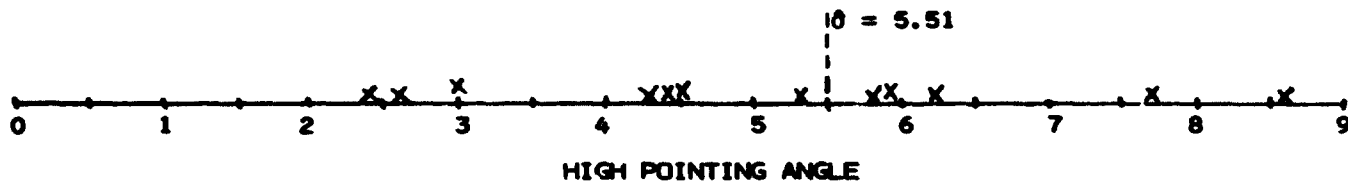
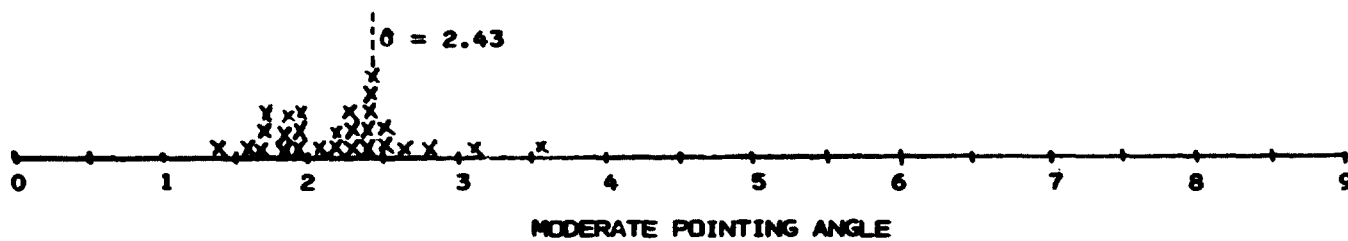
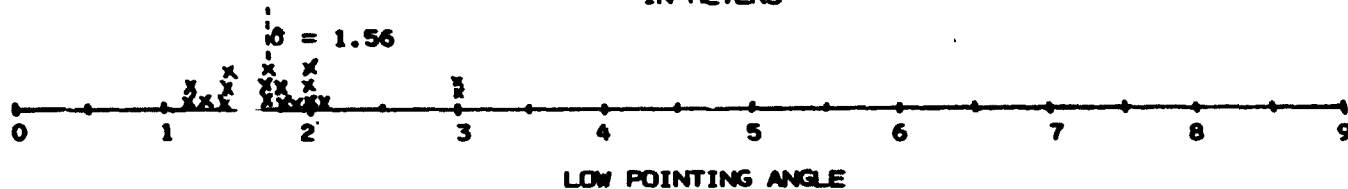


FIGURE 3.2  
DISTRIBUTION OF MODE 3  
RESIDUAL STANDARD DEVIATION  
IN METERS

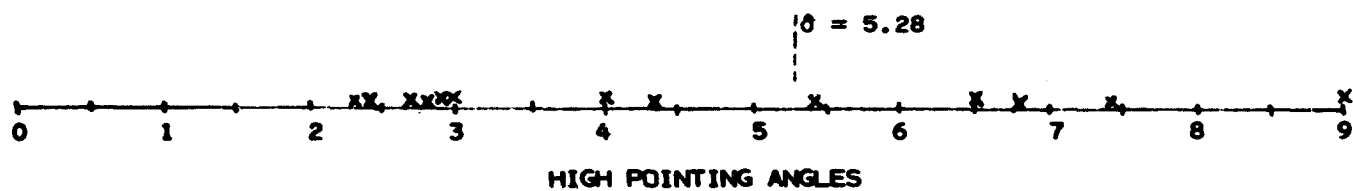
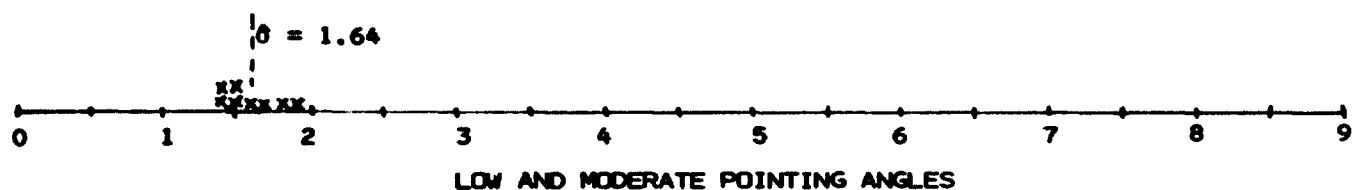


FIGURE 3.3  
DISTRIBUTION OF MODE 5  
RESIDUAL STANDARD DEVIATION  
IN METERS

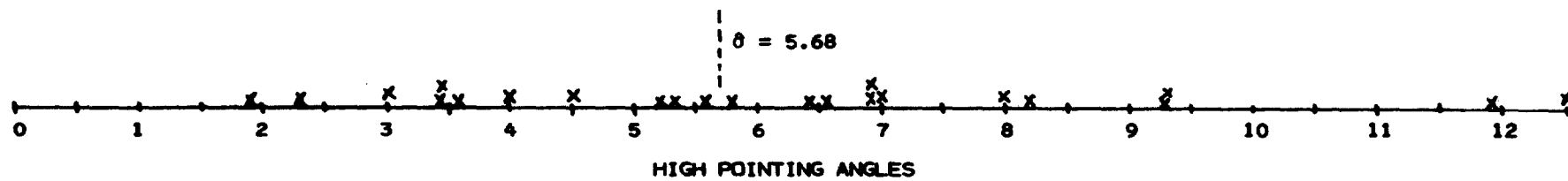
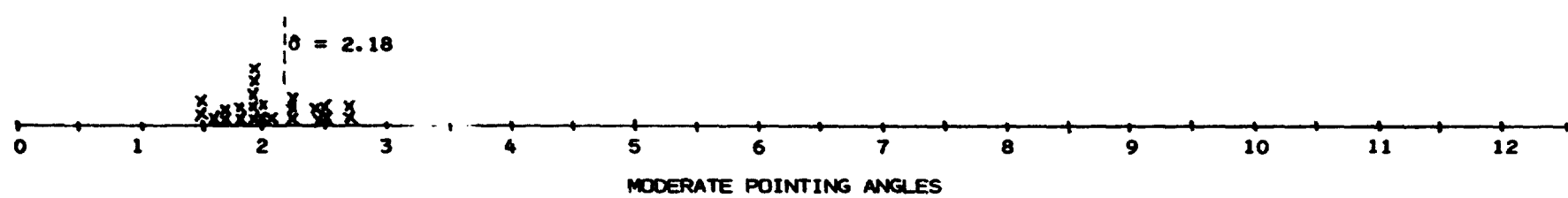
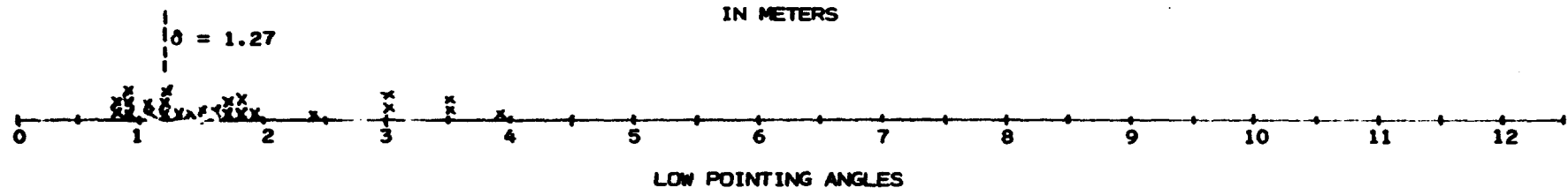
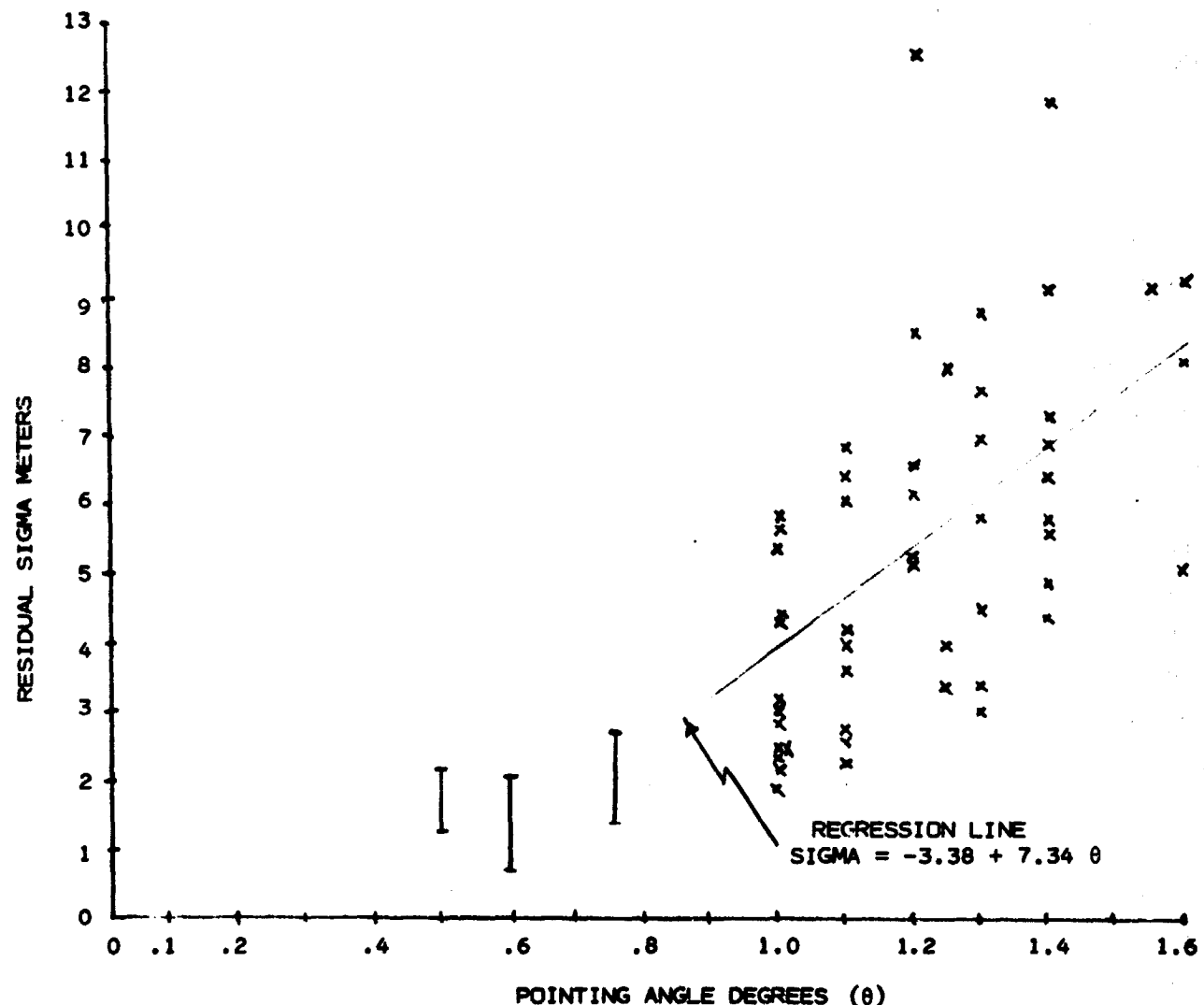


FIGURE 3.4  
RESIDUAL SIGMA  
VS.  
TRACKER DETERMINED POINTING ANGLE



### 3.2 Distribution of Significant Frequency Bands

Figure 3.5 is a typical plot of the grouped power spectral coefficients as described in Section 2.2.1. The frequency tabulated is the group center frequency. For example the frequency band associated with the first grouped coefficient (.0333 Hz center frequency) is zero Hz to .666 Hz. In this example the grouped coefficients had 8 degrees of freedom. The 99th percentile of the chi square distribution with 8 degrees of freedom is 20.1. The first two grouped coefficients exceed this value, therefore the significant frequency band is 0 Hz to .133 Hz. In this example there is a well defined low frequency signal and the measurement noise power is close to being uniformly distributed over the frequencies above .300 Hz.

Figures 3.6 through 3.13 are bar charts showing the location of significant frequency bands for each mode/pointing angle range. As discussed in reference [1], recoverable geoid features are contained in that part of the frequency spectrum below .164 Hz. In spite of having selected data arcs without prominent geoid features displayed on the residual time series plots, figures 3.6 through 3.13 indicate that most of the data arcs processed did contain significant power spectral components below .164 Hz. For the majority of arcs having low or moderate pointing angles these bands are well separated from significant higher frequency bands. This indicates that signal (i.e. geoid) and noise components of the range residual data can be separated with appropriate filtering techniques.

For high pointing angle arcs (figures 3.8, 3.10 and 3.13) this separability is not present. The measurement noise power is concentrated at lower frequencies which tend to overlap the 0-.164 Hz band containing recoverable geoid features. From reference [1] a reasonable explanation for this behavior is that at higher pointing angles the received waveform changes shape causing the altimeter tracking loop which acts as a low pass filter to become more "sluggish".

FIGURE 3.5

TYPICAL PLOT OF  
GROUPED POWER SPECTRAL COEFFICIENTS

## DB PLOT OF COEFFICIENTS

CENTER FREQUENCY (HZ)	COEFFICIENT	1 DIVISION = 6.0000000 DB
0.333E-01	* 94.376907	*****
0.999E-01	* 33.729055	*****
0.166E 00	11.777470	*****
0.233E 00	8.9357233	*****
0.300E 00	10.565467	*****
0.366E 00	6.7322653	*****
0.433E 00	5.7570267	*****
0.499E 00	4.9442987	*****
0.566E 00	12.214146	*****
0.633E 00	2.7122107	*****
0.699E 00	6.1173782	*****
0.766E 00	7.4255068	*****
0.832E 00	4.1044750	*****
0.899E 00	4.4849863	*****
0.965E 00	4.3598089	*****
0.103E 01	5.7130280	*****
0.110E 01	7.9702864	*****
0.117E 01	7.3848772	*****
0.123E 01	6.9888597	*****
0.130E 01	9.7422695	*****
0.136E 01	6.2496109	*****
0.143E 01	2.5783844	*****
0.150E 01	5.0625181	*****
0.156E 01	9.2757387	*****
0.163E 01	4.9122648	*****
0.170E 01	1.8779192	*****
0.176E 01	6.7043734	*****
0.183E 01	5.7798376	*****
0.190E 01	5.0946255	*****
0.196E 01	0.90594321	*****
0.203E 01	1.3609255	*****
0.210E 01	2.1177893	*****
0.216E 01	3.3948860	*****
0.223E 01	2.8880472	*****
0.230E 01	3.1496048	*****
0.236E 01	0.3881653	*****
0.243E 01	2.2418480	*****
0.250E 01	5.0065899	*****
0.256E 01	4.7177165	*****
0.263E 01	2.2005329	*****
0.270E 01	4.6028862	*****
0.276E 01	2.3550205	*****
0.283E 01	1.6099463	*****
0.290E 01	3.2948151	*****

CHI SQUARE  
99TH PERCENTILE

ORIGINAL PAGE IS  
OF POOR QUALITY

FIGURE 3.6  
DISTRIBUTION OF SIGNIFICANT  
FREQUENCY BANDS  
MODE 1 LOW POINTING ANGLES

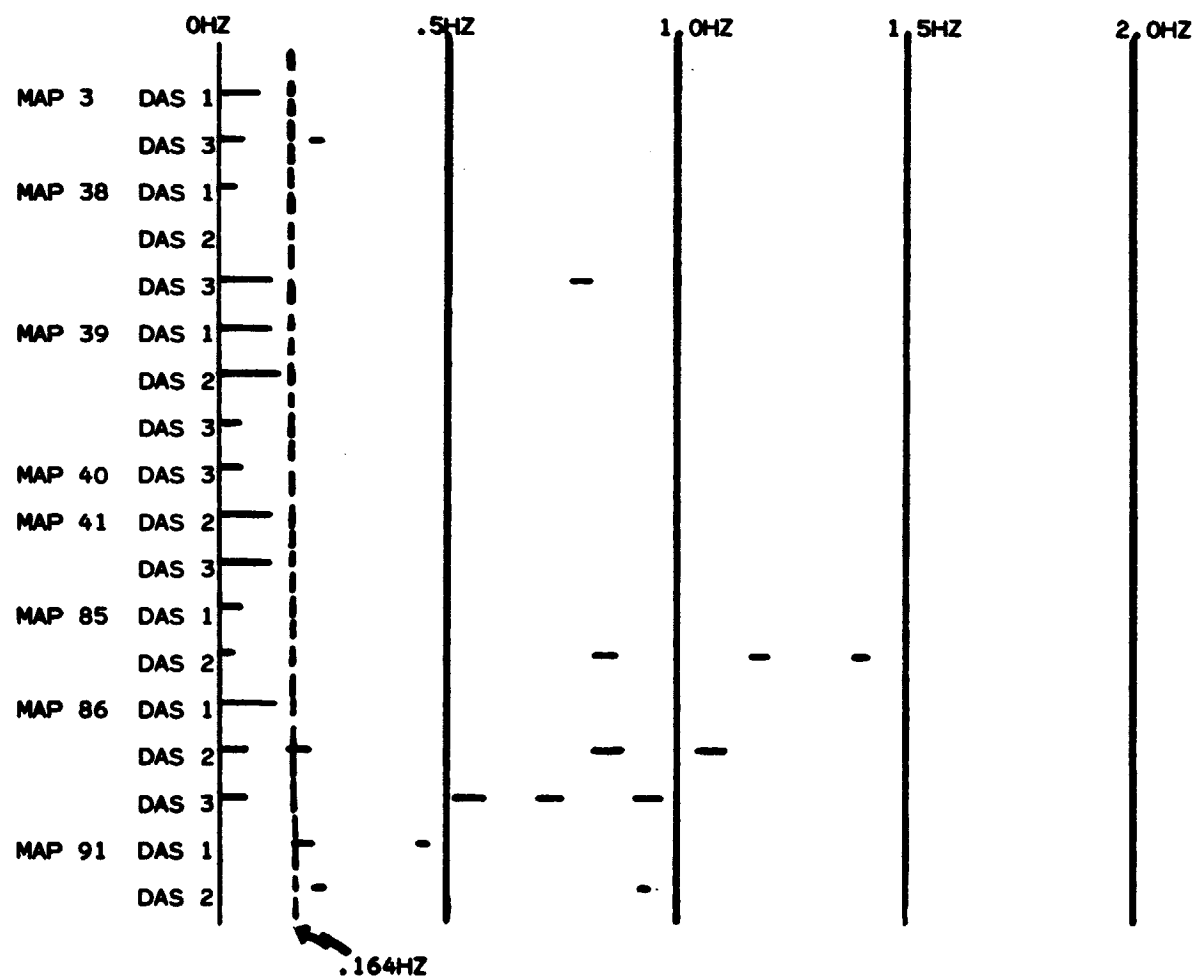
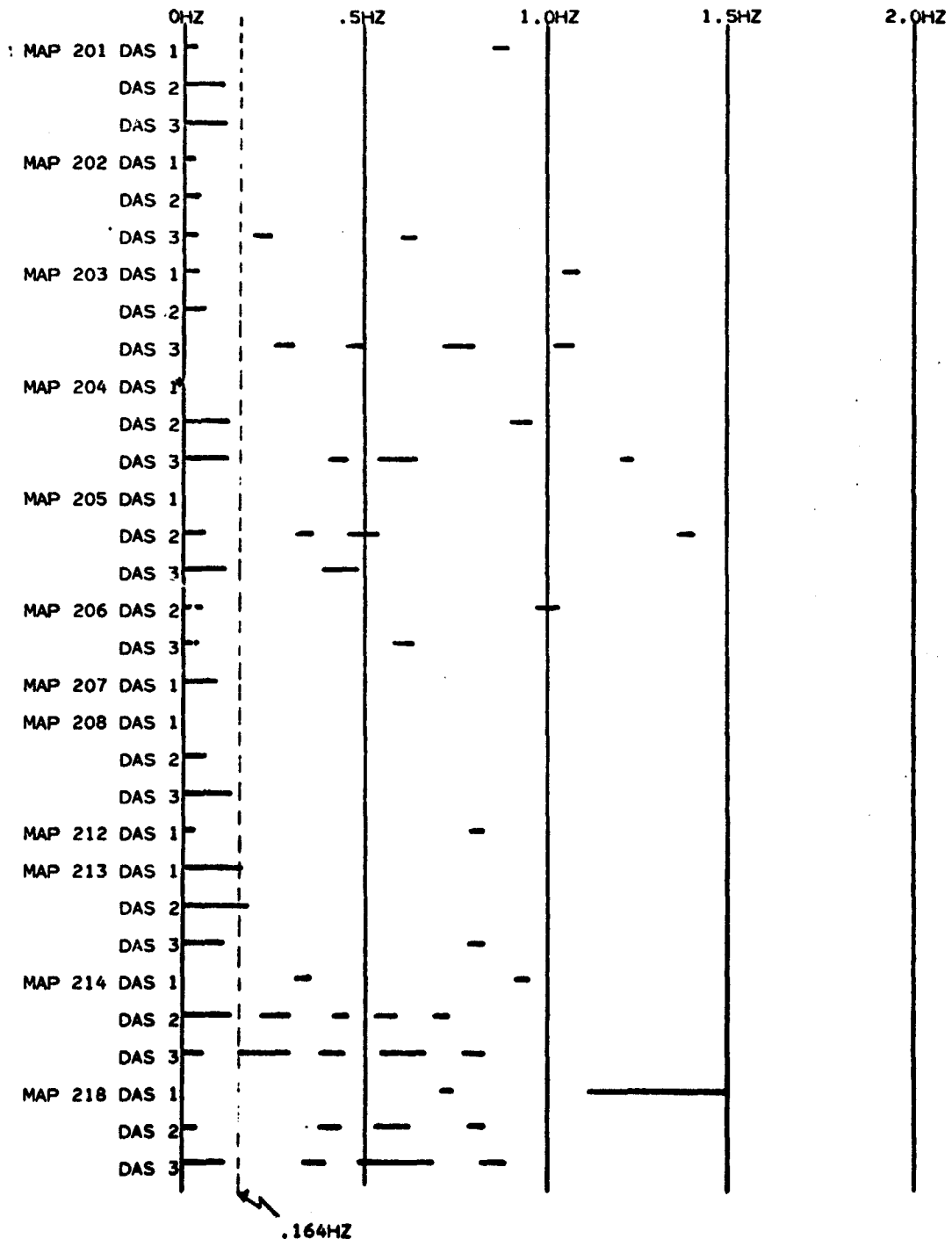


FIGURE 3.7  
DISTRIBUTION OF SIGNIFICANT  
FREQUENCY BANDS  
MODE 1 MODERATE POINTING ANGLES



\*MAP 204 DAS 1 SIGNIFICANT COEFFICIENTS AT 2.41-2.44HZ.

FIGURE 3.8  
DISTRIBUTION OF SIGNIFICANT  
FREQUENCY BANDS  
MODE 1 HIGH POINTING ANGLES

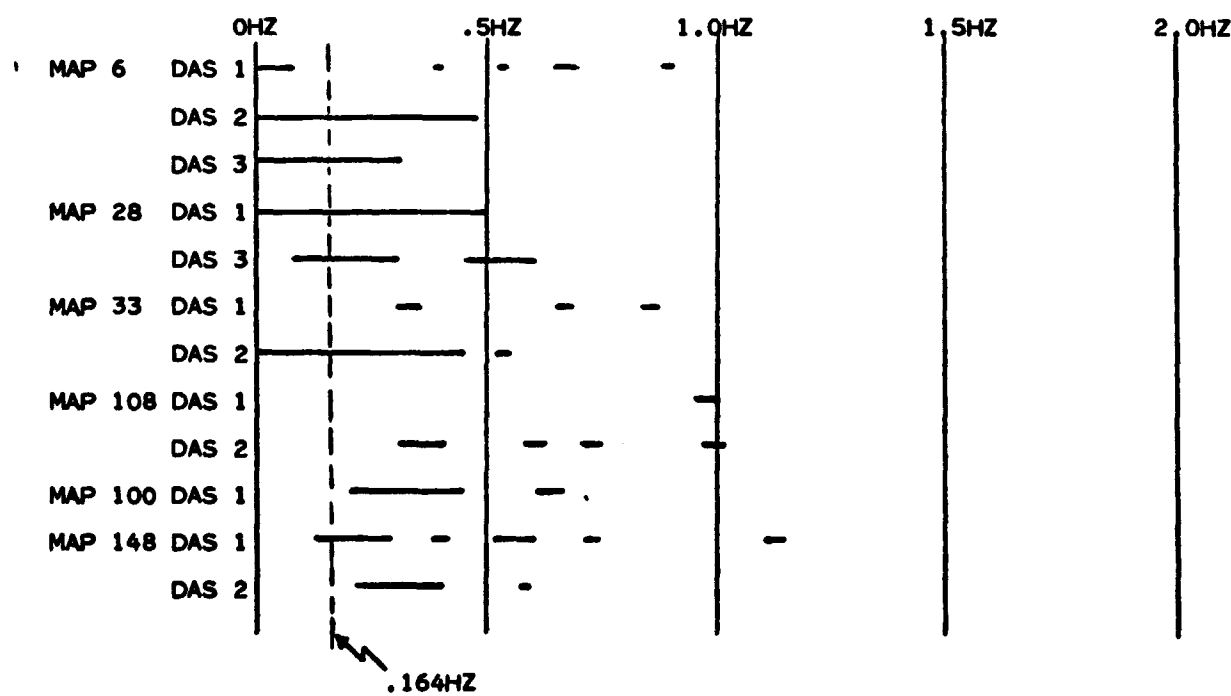


FIGURE 3.9  
DISTRIBUTION OF SIGNIFICANT  
FREQUENCY BANDS

MODE 3 LOW AND MODERATE POINTING ANGLES

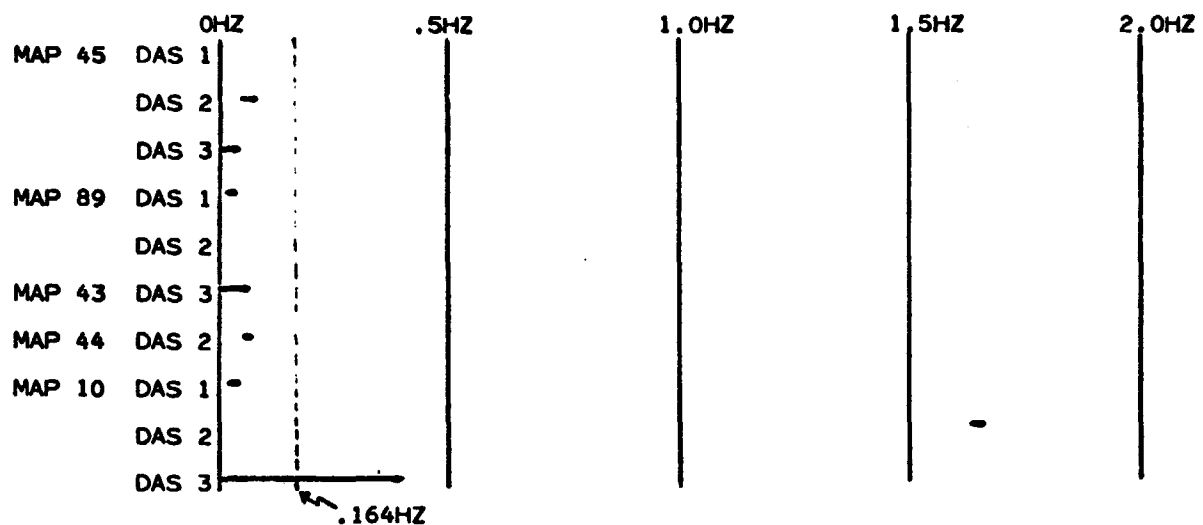


FIGURE 3.10  
DISTRIBUTION OF SIGNIFICANT  
FREQUENCY BANDS

MODE 3 HIGH POINTING ANGLES

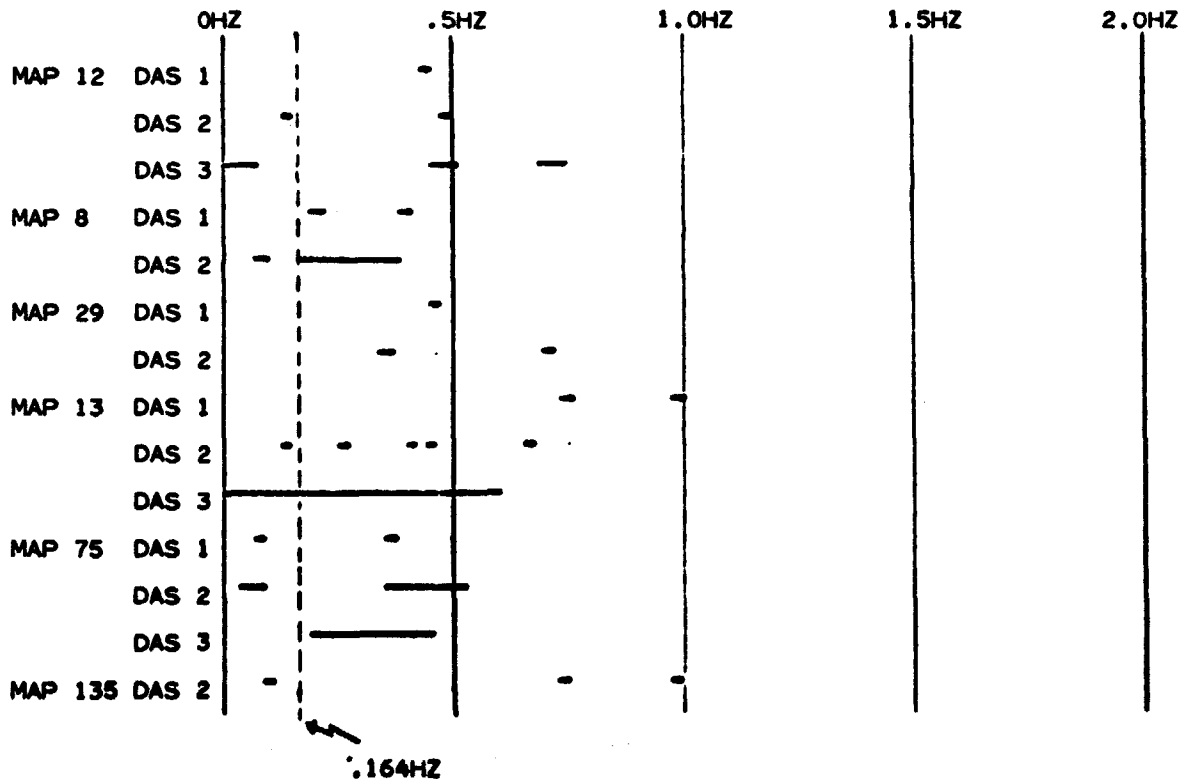


FIGURE 3.11  
DISTRIBUTION OF SIGNIFICANT  
FREQUENCY BANDS  
MODE 5 LOW POINTING ANGLES

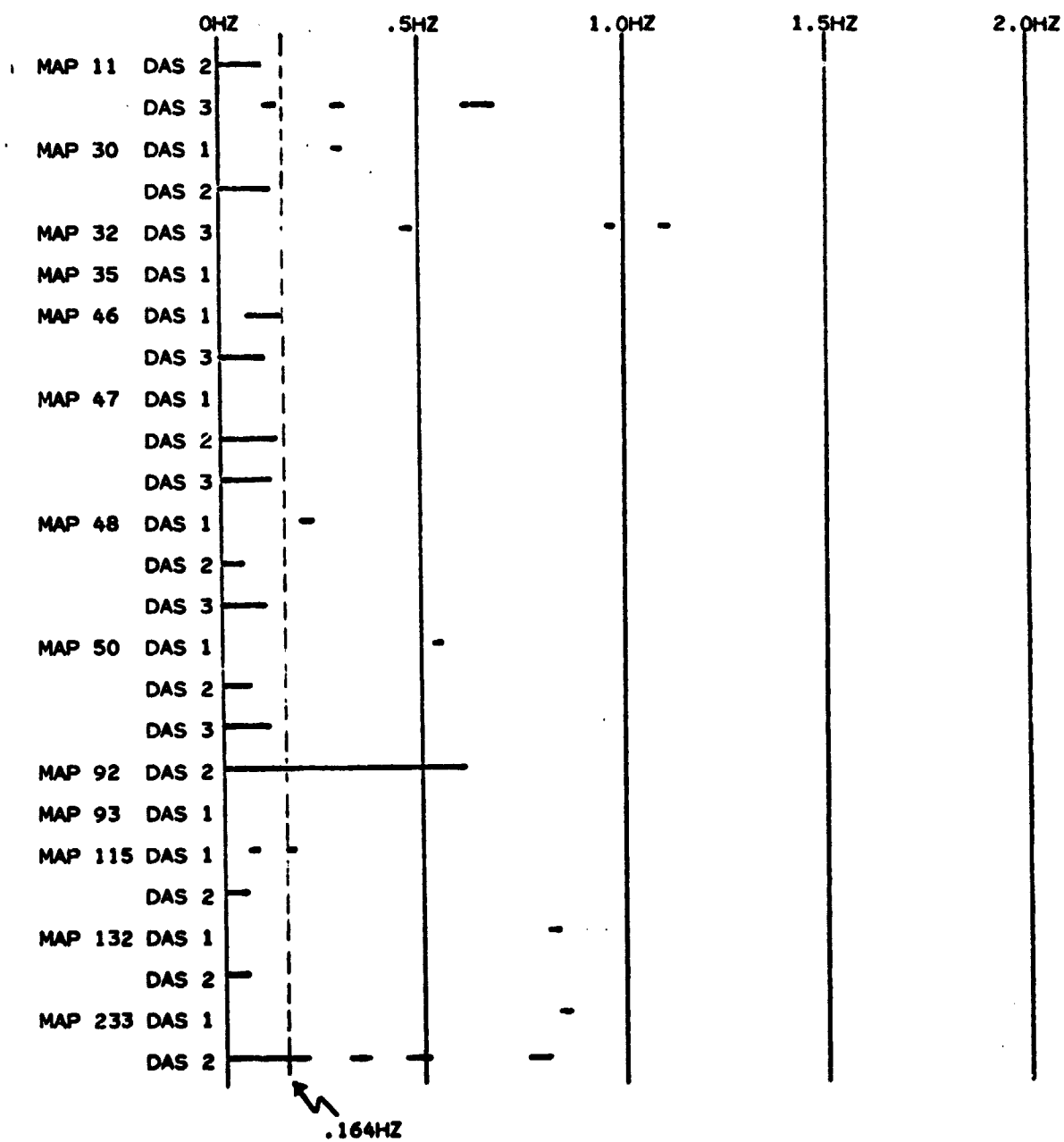


FIGURE 3.12  
DISTRIBUTION OF SIGNIFICANT  
FREQUENCY BANDS

MODE 5 MODERATE POINTING ANGLES

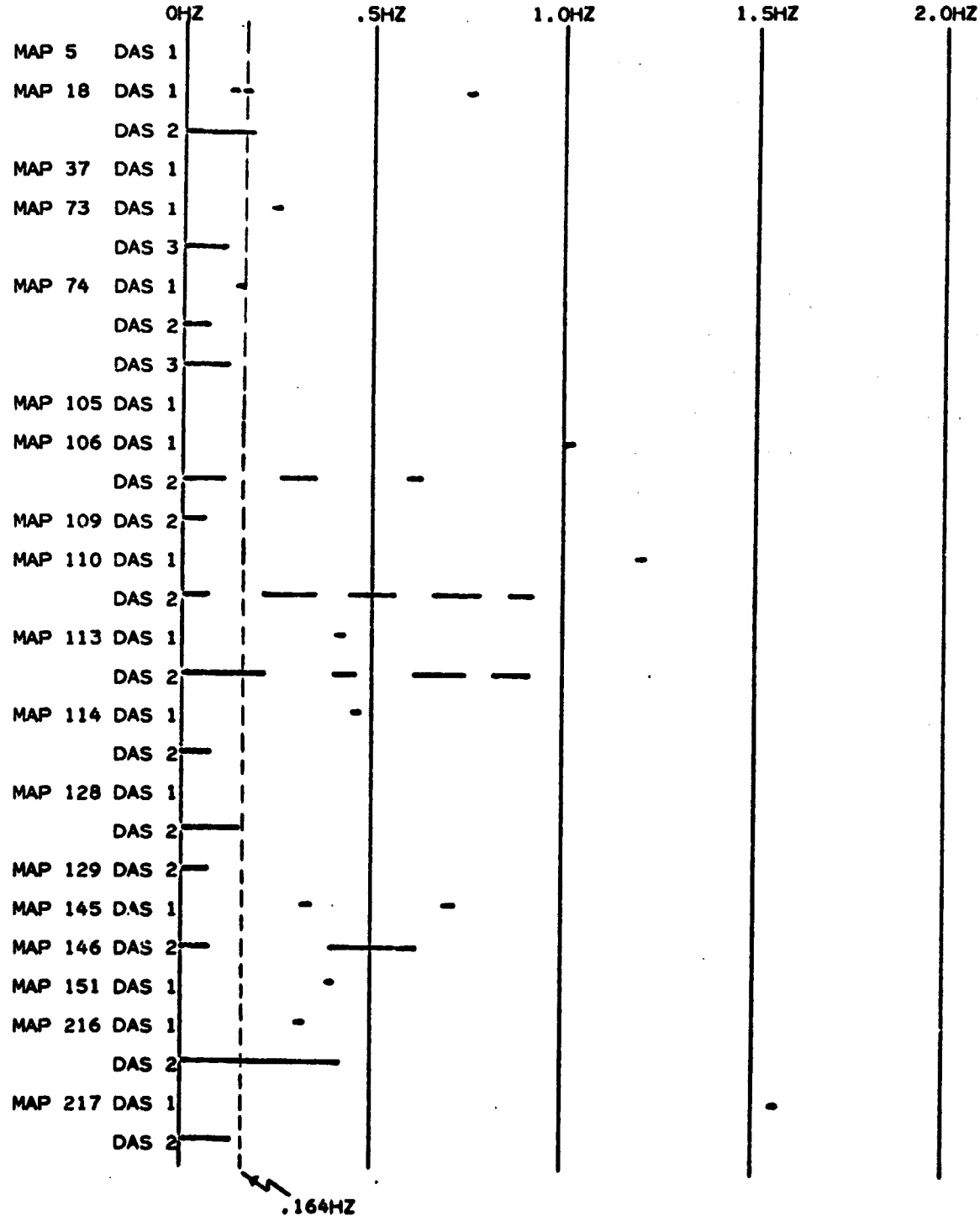
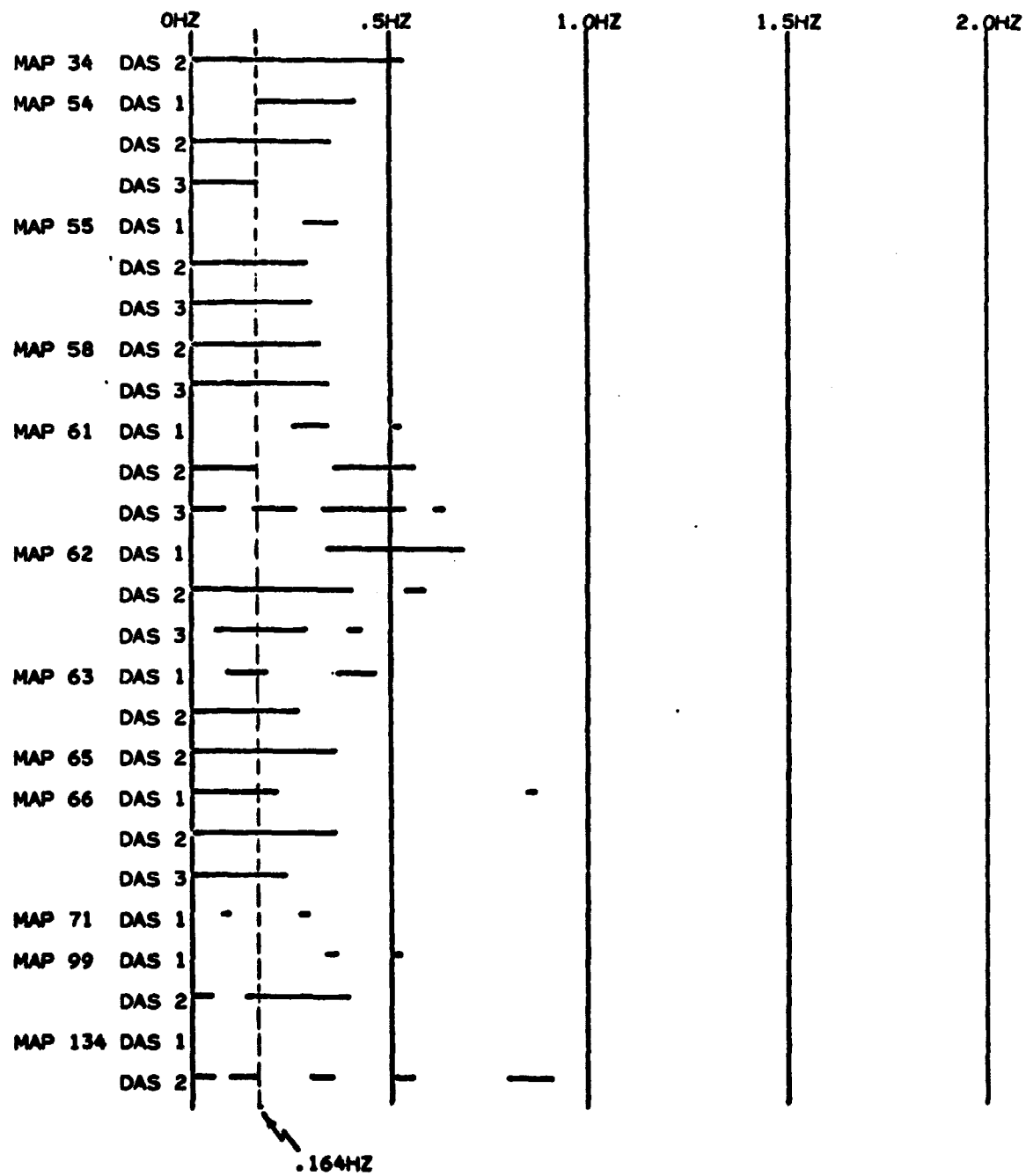


FIGURE 3.13  
 DISTRIBUTION OF SIGNIFICANT  
 FREQUENCY BANDS  
 MODE 5 HIGH POINTING ANGLES



3.3 References

1. McGoegan, Leitao and Wells, Summary of SKYLAB S-193 Altimeter Altitude Results, NASA TM X-69355, NASA Wallops Flight Center, February 1975.

#### 4.0 NOISE STATISTICS FOR SELECTED DATA ARCS

In the previous section (3.0), summary statistics have been presented for approximately 184 arcs of S-193 altimeter residuals. For a typical data arc these residuals can be modeled as

$$r(t) = s(t) + n(t)$$

Where  $s(t)$  is a low frequency, non-stationary signal due primarily to geoid variations and  $n(t)$  is stationary, broadband measurement noise. This section describes detailed evaluations of the statistical properties of the noise process,  $n(t)$ , for twenty-seven data arcs (Table 4.1) which were selected to span all data acquisition altimeter modes/submodes and the range of pointing angles (low, moderate, high). This evaluation was done by 1) selecting data arcs where  $s(t)$  was obviously small and/or at low frequencies, 2) in some cases high pass filtering the data to further attenuate  $s(t)$  and 3) computing descriptive statistics within the RAP program. The high pass filter, used to remove the signal  $s(t)$ , was obtained by low pass filtering the data with a 99 point quadratic midpoint filter and taking the high pass output as the difference between the filter midpoint value and the corresponding input data point. CALCOMP plots of the resultant time series, power spectrum and autocorrelation function were obtained using the optional RAP plot tape output. Also a 20th order autoregressive model of the noise process was formulated and the corresponding analytical power transfer function plotted.

In Section 3.2 it was shown that, for high pointing angles off nadir (i.e. greater than  $.9^\circ$ ) the frequency bands occupied by the signal  $s(t)$  and the noise  $n(t)$  show considerable overlap. Examination of the unfiltered data time series plots for all of the high pointing angle data arcs in Table 4.1 (Maps 6, 12 and 66) showed that  $s(t)$  for Map 6 DAS-2 includes the largest trend which is approximately .22 meters per second (Figure 4.1.29A). With the trend removed by a 99 point high pass filter the data standard deviation is decreased from 6.23 meters (unfiltered) to 5.30 meters (filtered) (Figure 4.1.29B). The power spectrum of the unfiltered data (Figure 4.1.30A) shows that the spectral components due to this trend (0 to .10 Hz) are smaller by approximately 4db than the dominating components due to the noise oscillations induced within the tracking loop (.20 to .26 Hz). Comparison with the filtered data power spectrum

TABLE 4.1  
RESIDUAL DATA ARCS SELECTED  
FOR DETAIL ANALYSIS

MAP	PASS	MODE	SUBMODE	TRACKER DETERMINED POINTING
39	22	1	DAS-1 DAS-2 DAS-3	<.6° (LOW)
205	97	1	DAS-1 DAS-2 DAS-3	.75° (MODERATE)
6	7	1	DAS-1 DAS-2 DAS-3	1.2° (HIGH)
45	24	3	DAS-1 DAS-2 DAS-3	<.6° (LOW)
10	8	3	DAS-1 DAS-2 DAS-3	.75° (MODERATE)
12	9	3	DAS-1 DAS-2 DAS-3	1.1° (HIGH)
47	25	5	DAS-1 DAS-2 DAS-3	<.5° (LOW)
74	39	5	DAS-1 DAS-2 DAS-3	.85° (MODERATE)
66	37	5	DAS-1 DAS-2 DAS-3	1.4° (HIGH)

(Figure 4.1.30B) showed that at frequencies above .25 Hz the shape of the filtered and unfiltered power spectra are identical. Thus the presence of this trend had only a 15% effect on the data standard deviation and did not dominate the power spectral plot. For these reasons it was decided to present time series plots, power spectral, autocorrelation functions and autoregressive transfer functions derived from unfiltered data for the nine arcs with large pointing angles off nadir. (Maps 6, 12 and 66). In addition, the 99 point filter was not applied for data arcs shorter than 30 seconds. This included Mode 3 DAS-1, Mode 3 DAS-2 and Mode 5 DAS-1.

#### 4.1 Mode 1 Results

From Table 2.1 the three mode 1 data acquisition submodes (DAS-1, DAS-2, and DAS-3) are 52 seconds, 63.44 seconds, and 63.44 seconds long respectively. During DAS-3 the antenna pointing is offset  $.431^\circ$  in pitch to evaluate the effect of a known change in pointing angle. Table 4.2 displays summary statistics for the 9 selected mode 1 data arcs. The corresponding time series plots, power spectra, autocorrelation functions and autoregressive model power transfer functions are displayed in Figures 4.1.1 through 4.1.36.

As would be expected with increasing pointing angle the noise standard deviations (Table 4.1 - Filtered Data) increase and the power spectra show a well defined attenuation at the higher frequencies.

At low pointing angles (Map 39) the measurement noise,  $n(t)$ , resembles a white noise process for all 3 submodes (DAS-1, DAS-2 and DAS-3). The power spectra (Figures 4.1.2, 4.1.6 and 4.1.12) are relatively flat and the corresponding autocorrelation functions (Figures 4.1.3, 4.1.7 and 4.1.11) have few coefficients which are significantly different from zero. The statistical characteristics of the data show no apparent change due to the  $.431^\circ$  pitch offset during DAS-3.

At moderate pointing angles (Map 205) during submode DAS-1 the power spectrum (Figure 4.1.14) and the autocorrelation function (Figure 4.1.15) indicate little or no departure from a white noise process. Submodes DAS-2 and DAS-3 show significant departures from a white noise process. The power spectra (Figures 4.1.18 and 4.1.22) show considerable attenuation at the higher frequencies with the DAS-2 spectrum starting to taper off between 1.5 and 1.6 Hz and the DAS-3 spectrum starting to taper off between 1.25 and 1.35 Hz. This difference in break frequencies could possibly be attributed to the  $.431^\circ$  pitch offset of the altimeter antenna during DAS-3. Comparison of the autocorrelation functions for DAS-2 and DAS-3 (Figures 4.1.19 and 4.1.23) shows that the DAS-3 data has more autocorrelation coefficients significantly greater than zero.

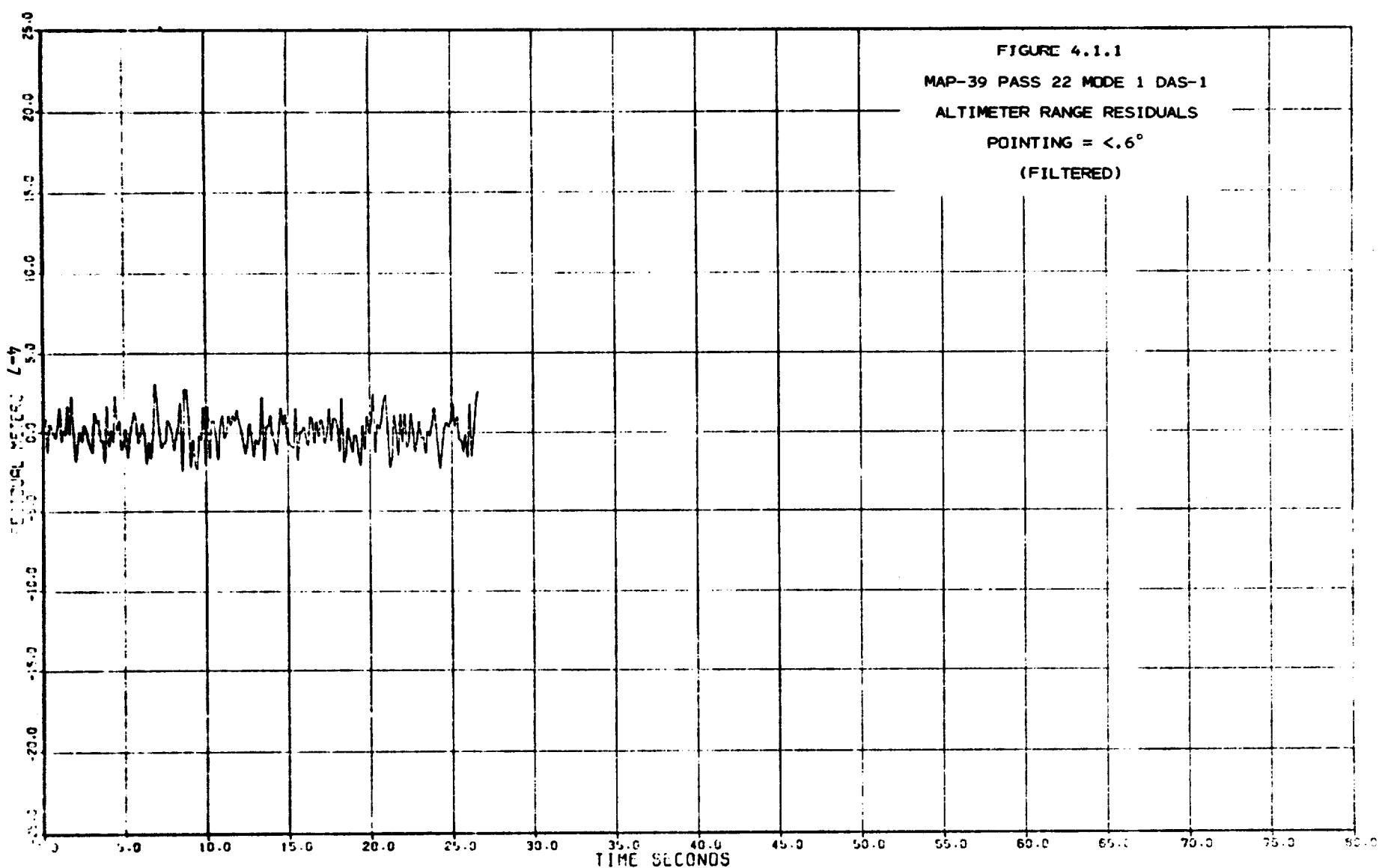
At high pointing angles (Map 6) the time series plots for all 3 submodes (Figures 4.1.25, 4.1.29 and 4.1.33) indicate that the noise process is dominated by low frequency oscillations which are approximately 23 meters peak to peak during DAS-1 and DAS-2 and as high as 35 meters peak to peak during DAS-3. The

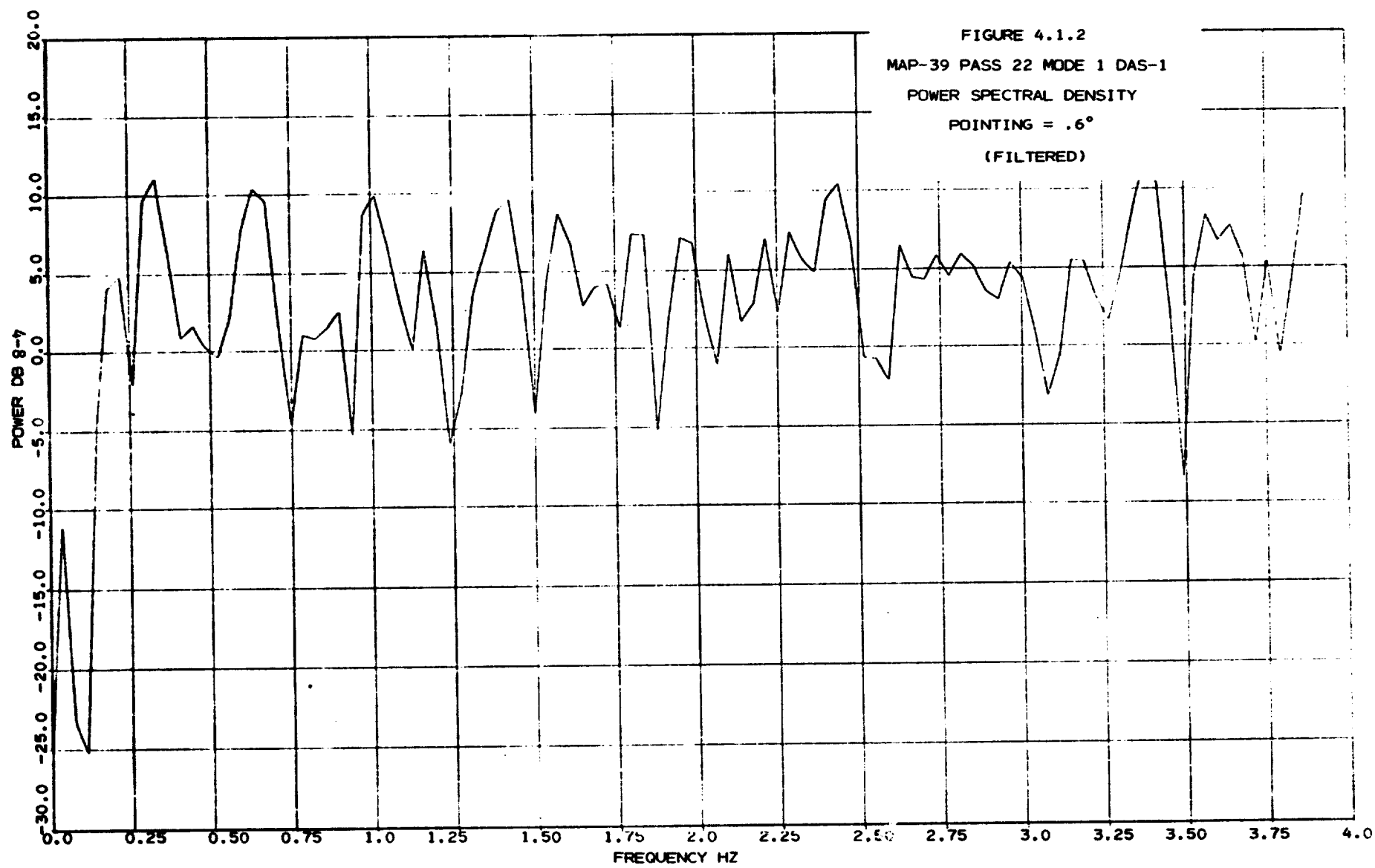
power spectral plots (Figures 4.1.26, 4.1.30A and 4.1.34) show that the principal oscillation frequency for DAS-1 is at .4 Hz, for DAS-2 between .19 Hz and .25 Hz and for DAS-3 between .22 and .35 Hz. The  $.431^\circ$  pitch offset during DAS-3 causes the noise sigma to increase from the DAS-2 value of 5.3 meters (Table 4.1) to 8.04 meters. Comparison of the DAS-2 and DAS-3 power spectral plots (Figures 4.1.30A and 4.1.34) show a much higher concentration of energy at the lower frequencies for DAS-3. At 1.0 Hz the DAS-2 power spectrum (Figure 4.1.30A) has decreased about 5 db from its peak value while the DAS-3 power spectrum (Figure 4.1.34) has decreased about 18 db.

TABLE 4.2  
MODE 1 DETAIL ANALYSIS

MAP	PASS	MODE	POINT (DEGS)	SAMP. SIZE	MEAN (MTRS)	SIGMA (MTRS)	F STATISTIC	NORM. TEST	SIG. FREQ. BANDS (HZ)	SIGNIFICANT AUTOCORRELATION COEFFICIENTS
39	22	*1 DAS-1	<.6°	208	17.9	1.16	1.28	.446	.676-.714	3,5
		*1 DAS-2		408	22.5	1.03	1.36	.929	2.37-2.43	8,12,16
		*1 DAS-3		408	23.3	1.12	.362	.995	1.53-1.59	8
205	97	*1(6)DAS-1	.75°	280	-48.0	1.89	1.35	.960	NONE	NONE
		*1(6)DAS-2		308	-46.1	1.69	.583	.846	.228-.355 .457-.583 .913-.964 1.37-1.42	1,9,10,14
		*1(6)DAS-3		368	-45.4	1.66	4.78	.082	.191-.223 .382-.488 .764-.807 .891-.934	1,2,11-14,19
6	7	1 DAS-1	1.2°	192	89.0	5.30	1.16	.796	0-.081 .407,.529 .651-.692 .895	1,2,15,16
		1 DAS-2		368	94.5	6.23	1.52	.101	0-.488	ALL
		1 DAS-3		352	146.3	8.55	10.13	.995	0-.510	ALL

\*INDICATES DATA FILTERED BY 99 POINT QUADRATIC MIDPOINT HIGH PASS FILTER





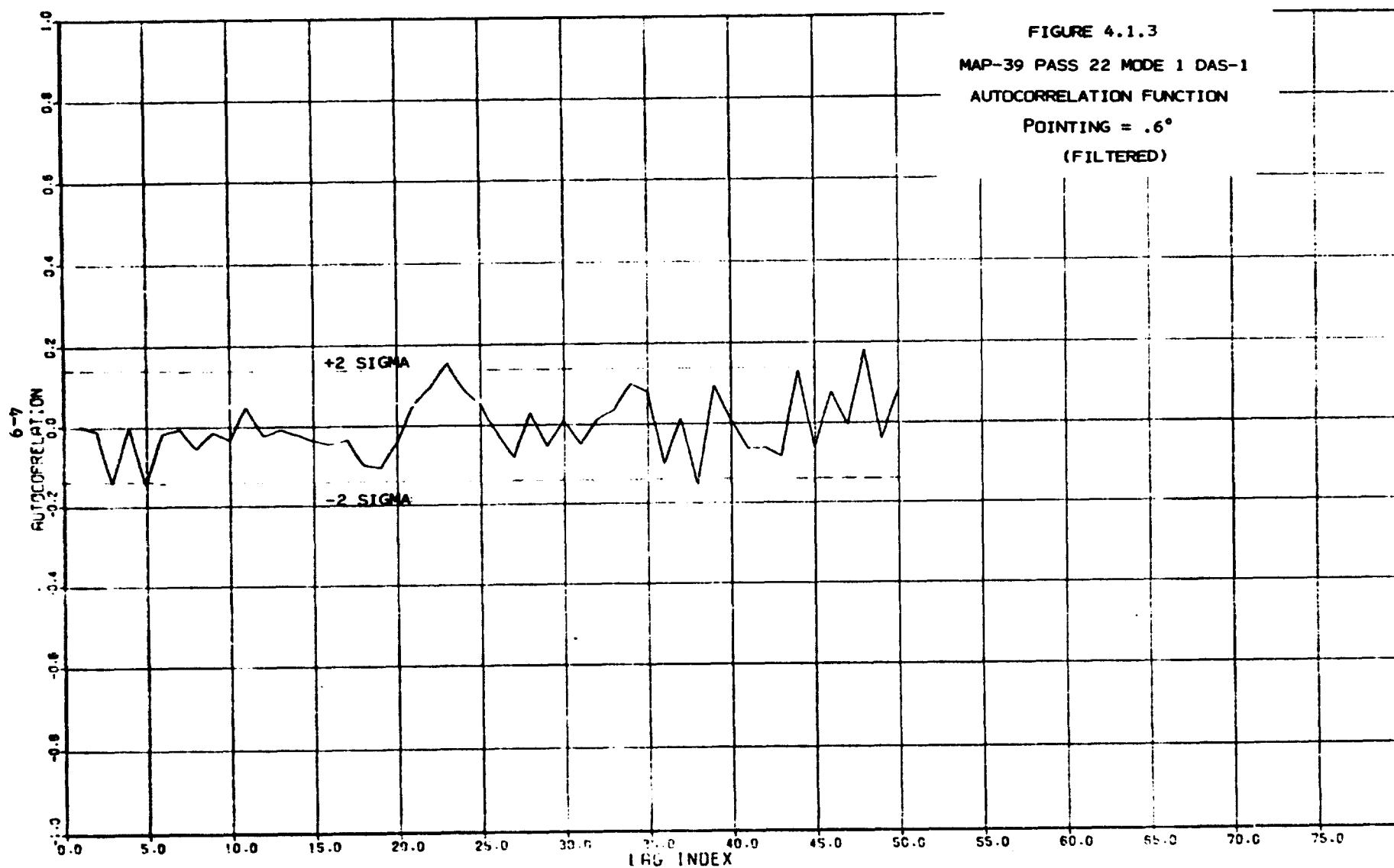
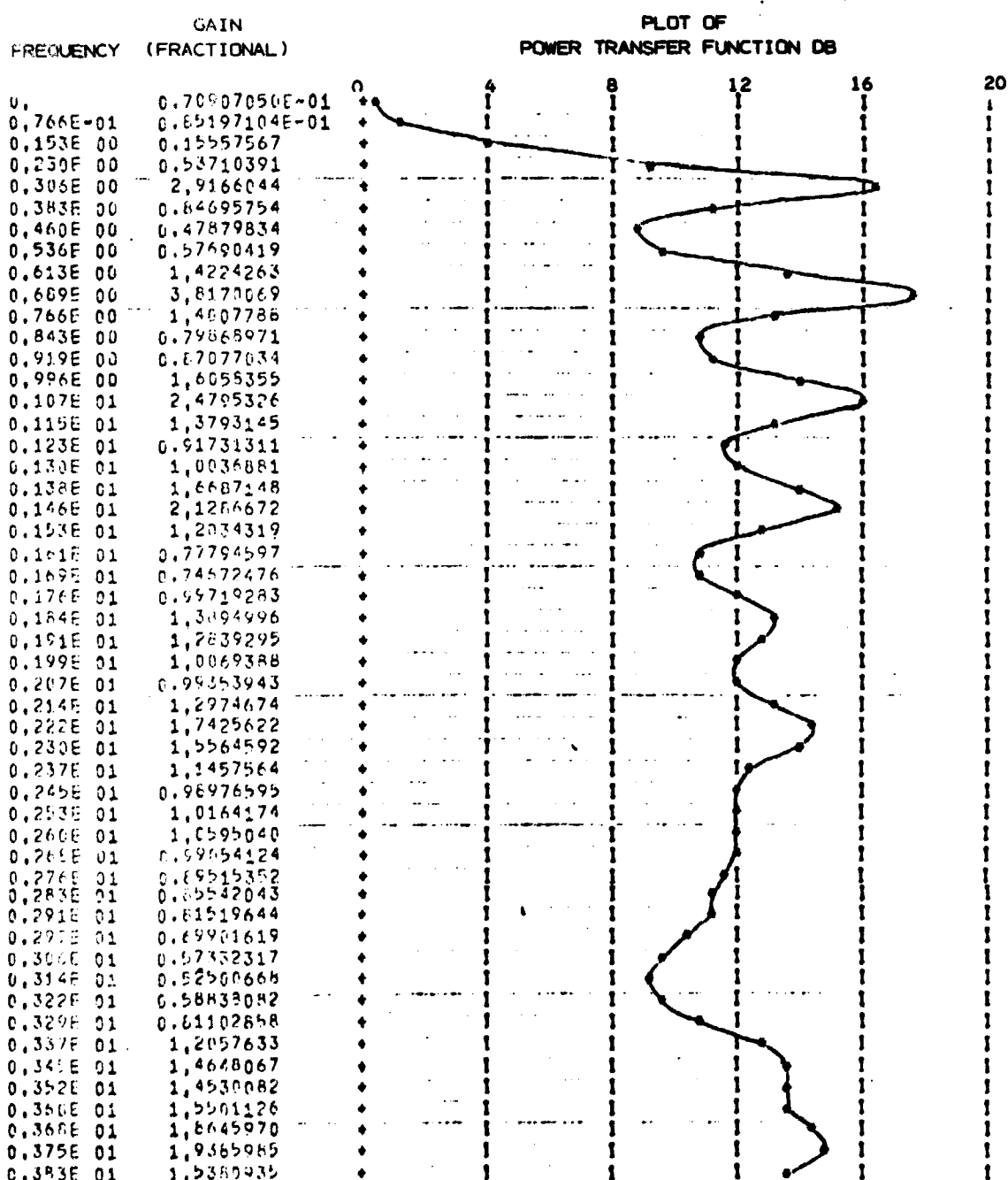
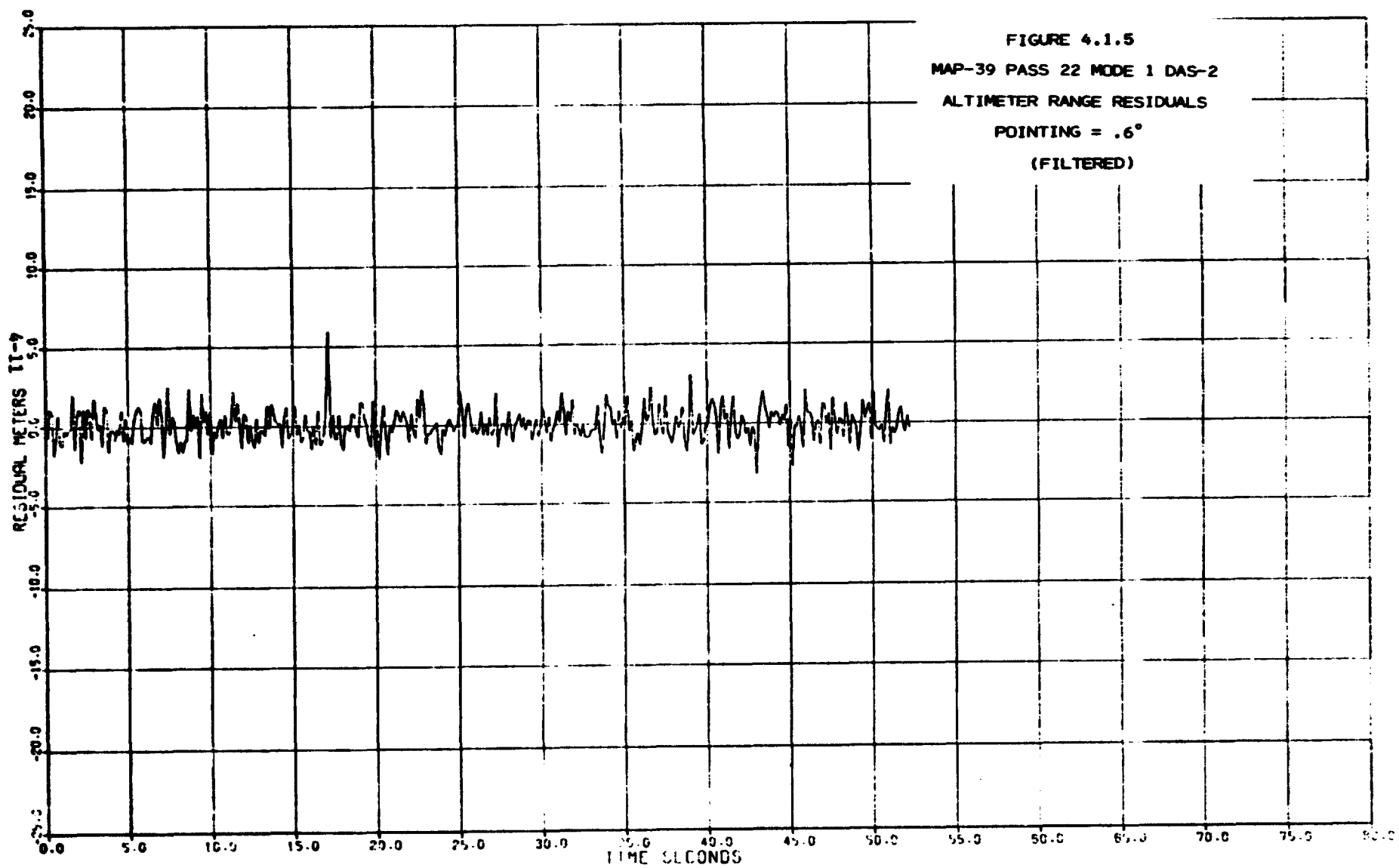
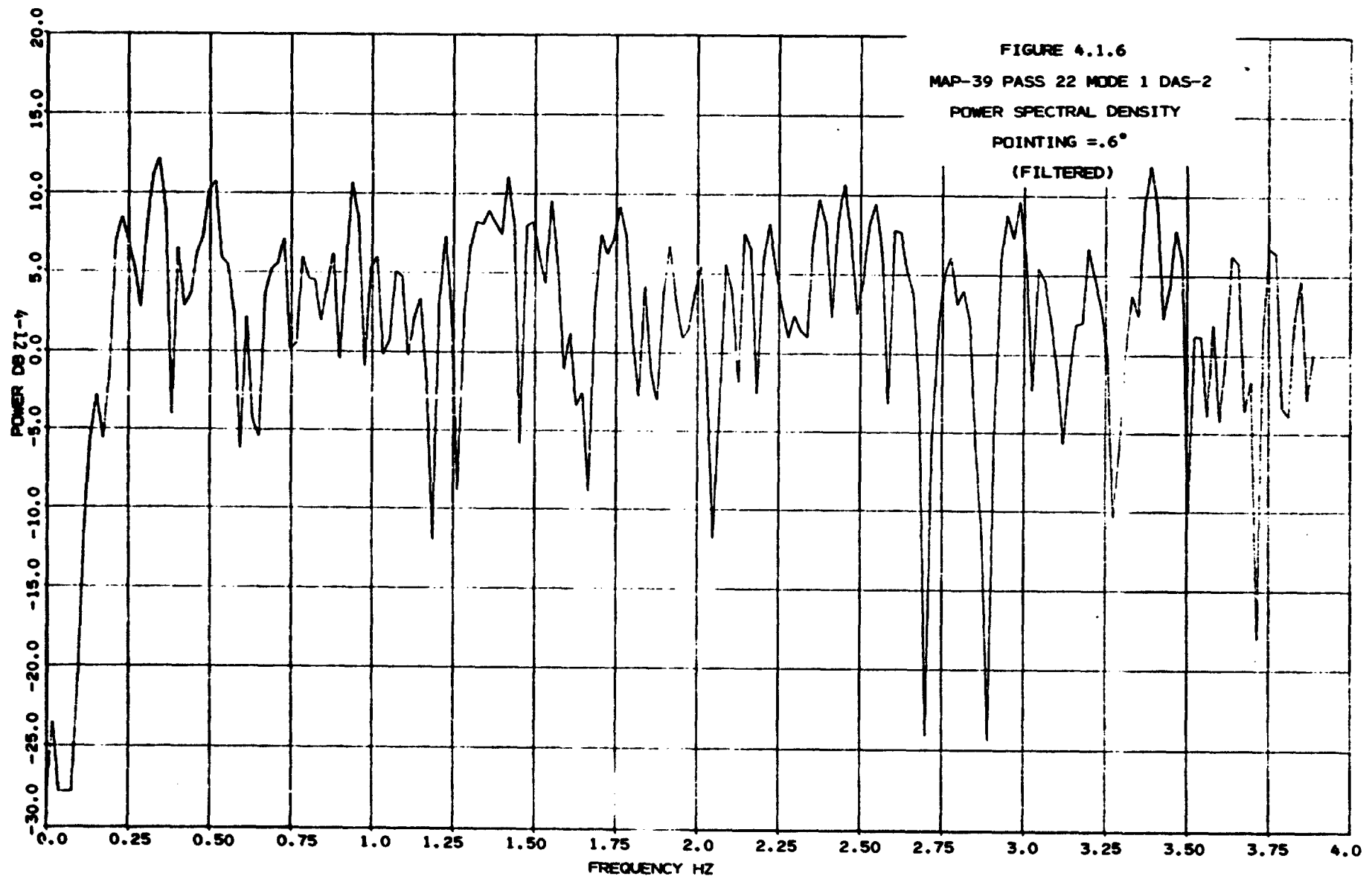


FIGURE 4.1.4

## AUTOREGRESSIVE MODEL

MAP-39 PASS-22 MODE-1 DAS-1  
(FILTERED)





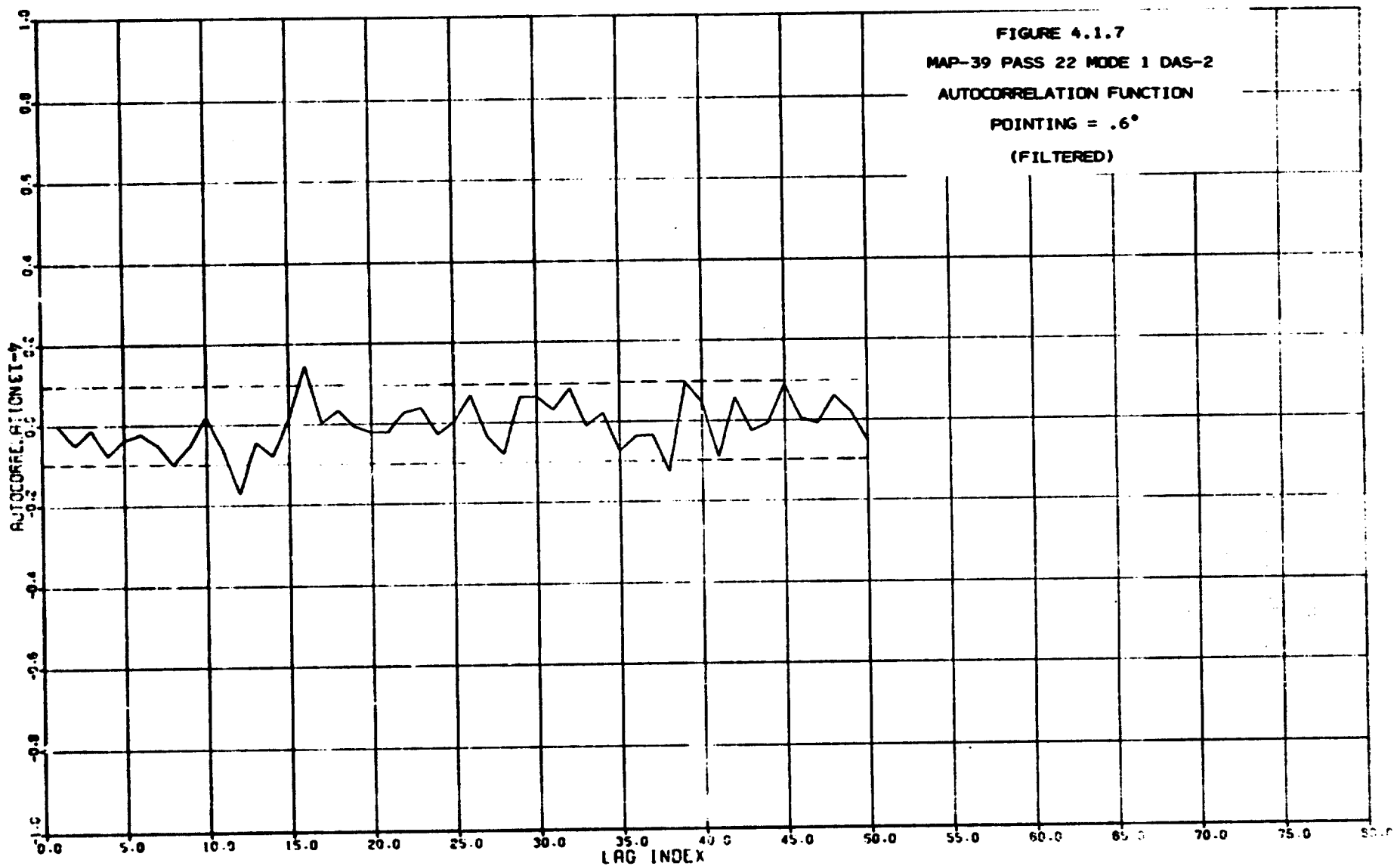
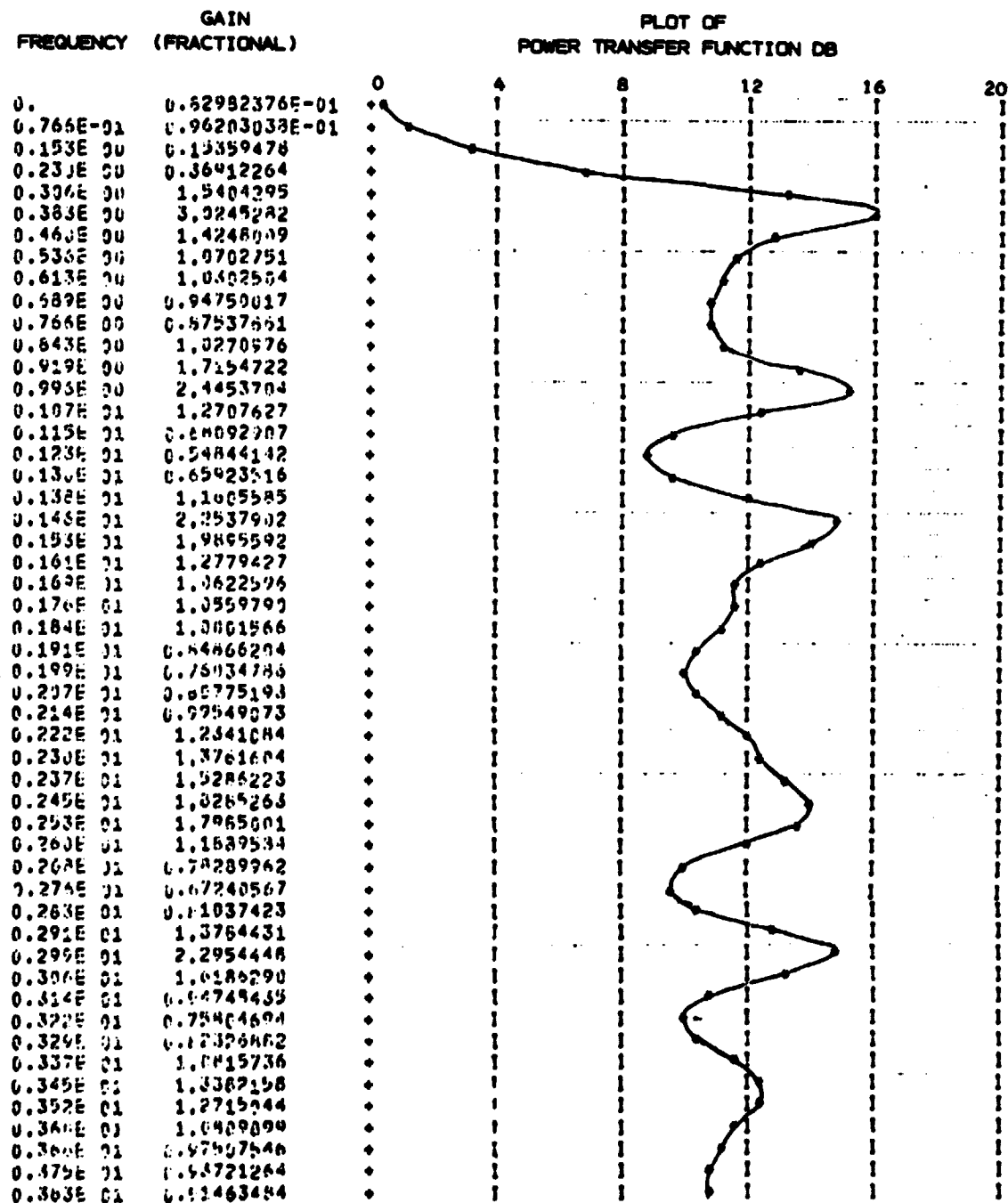
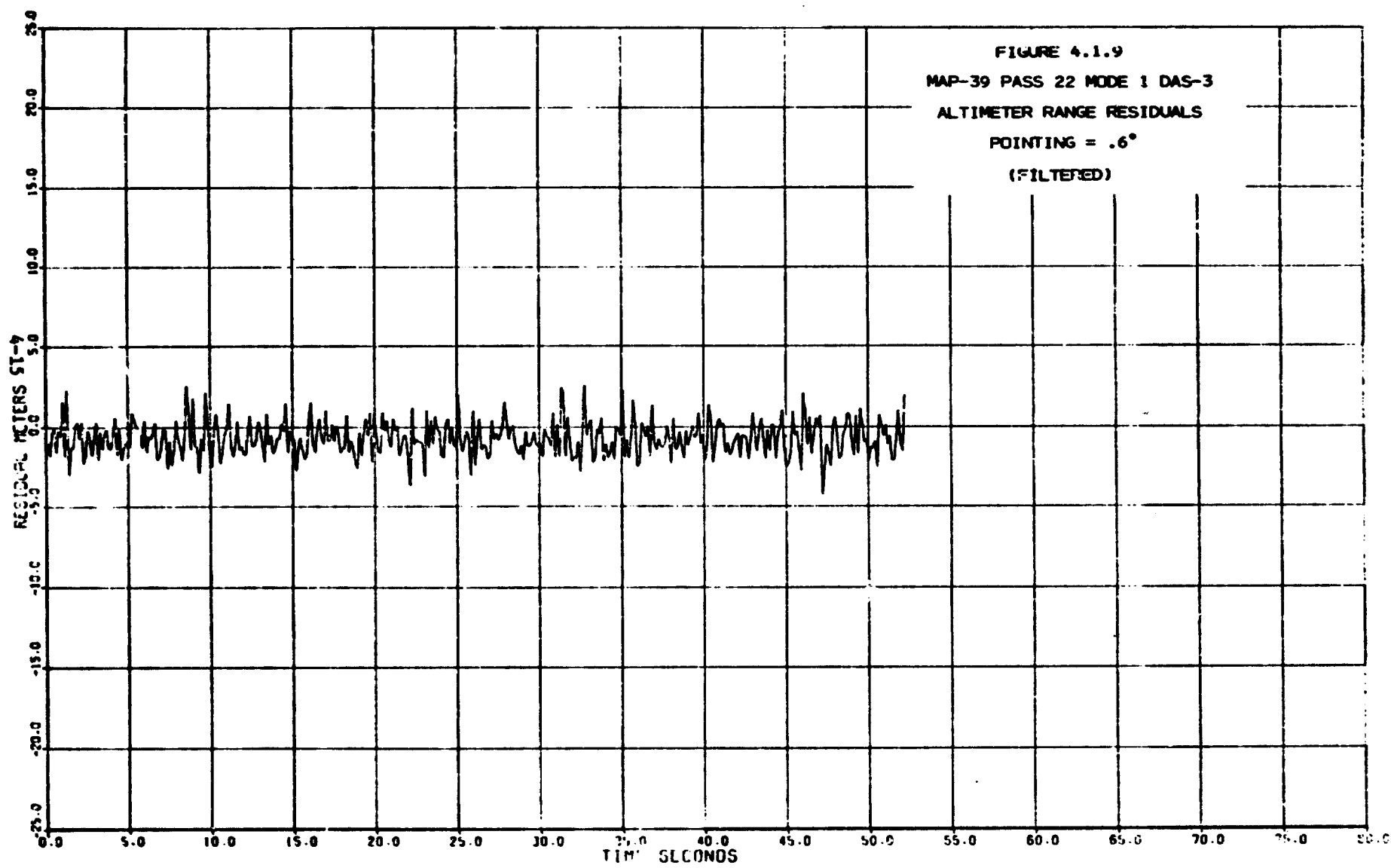
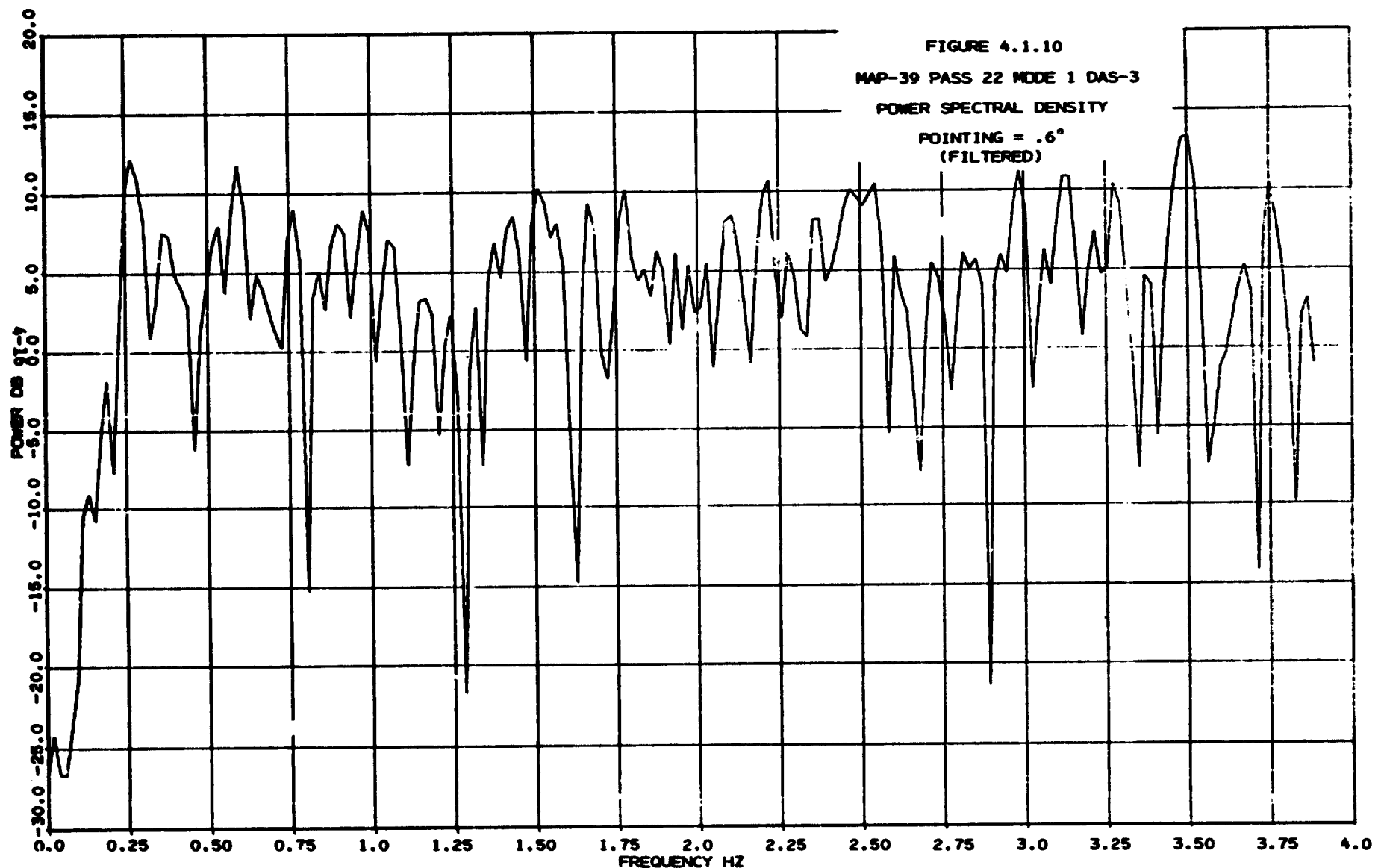


FIGURE 4.1.8  
 AUTOREGRESSIVE MODEL  
 MAP-39 PASS-22 MODEL-1 DAS-2  
 (FILTERED)







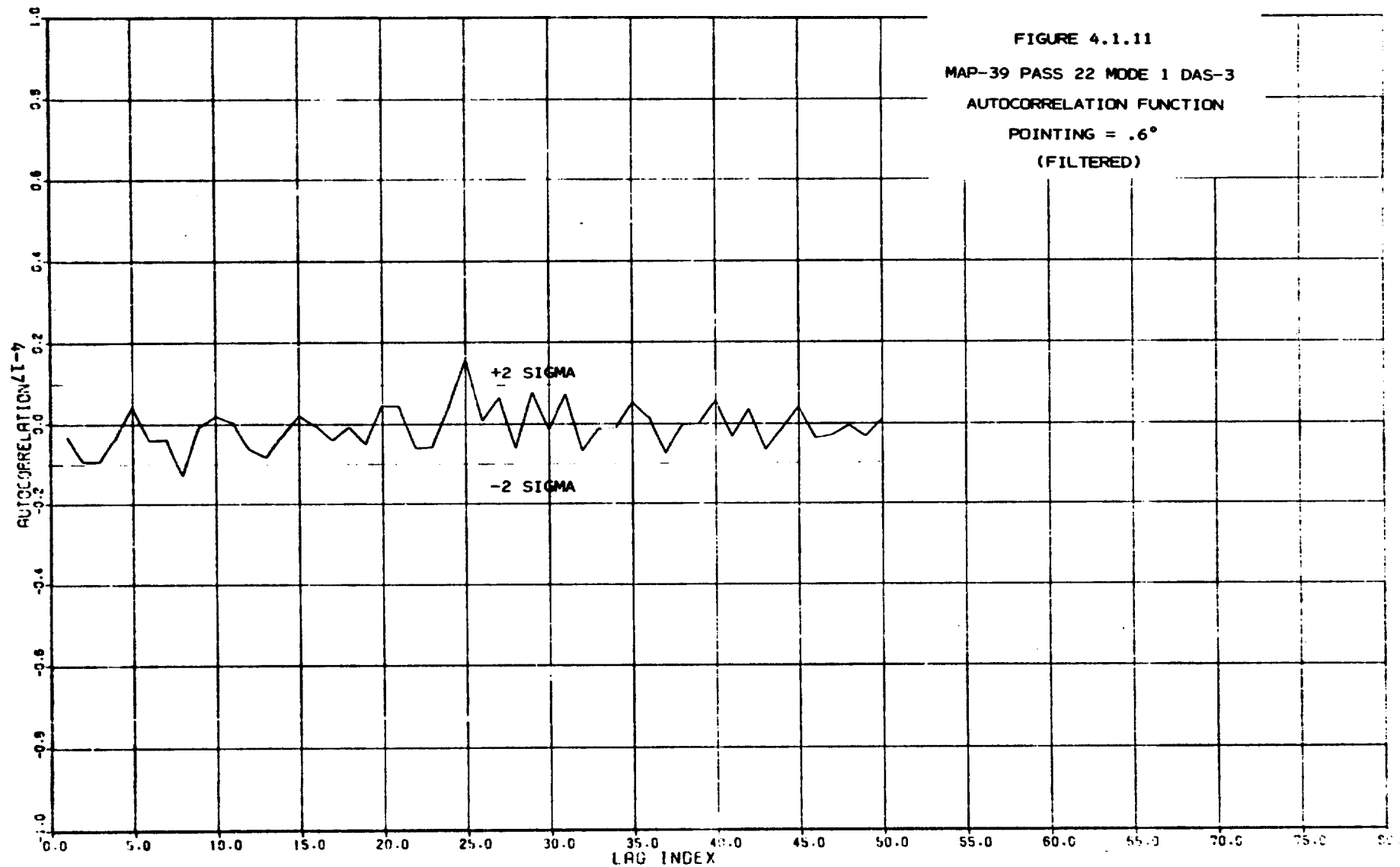


FIGURE 4.1.11

MAP-39 PASS 22 MODE 1 DAS-3

AUTOCORRELATION FUNCTION

POINTING =  $.6^\circ$

(FILTERED)

FIGURE 4.1.12

## AUTOREGRESSIVE MODEL

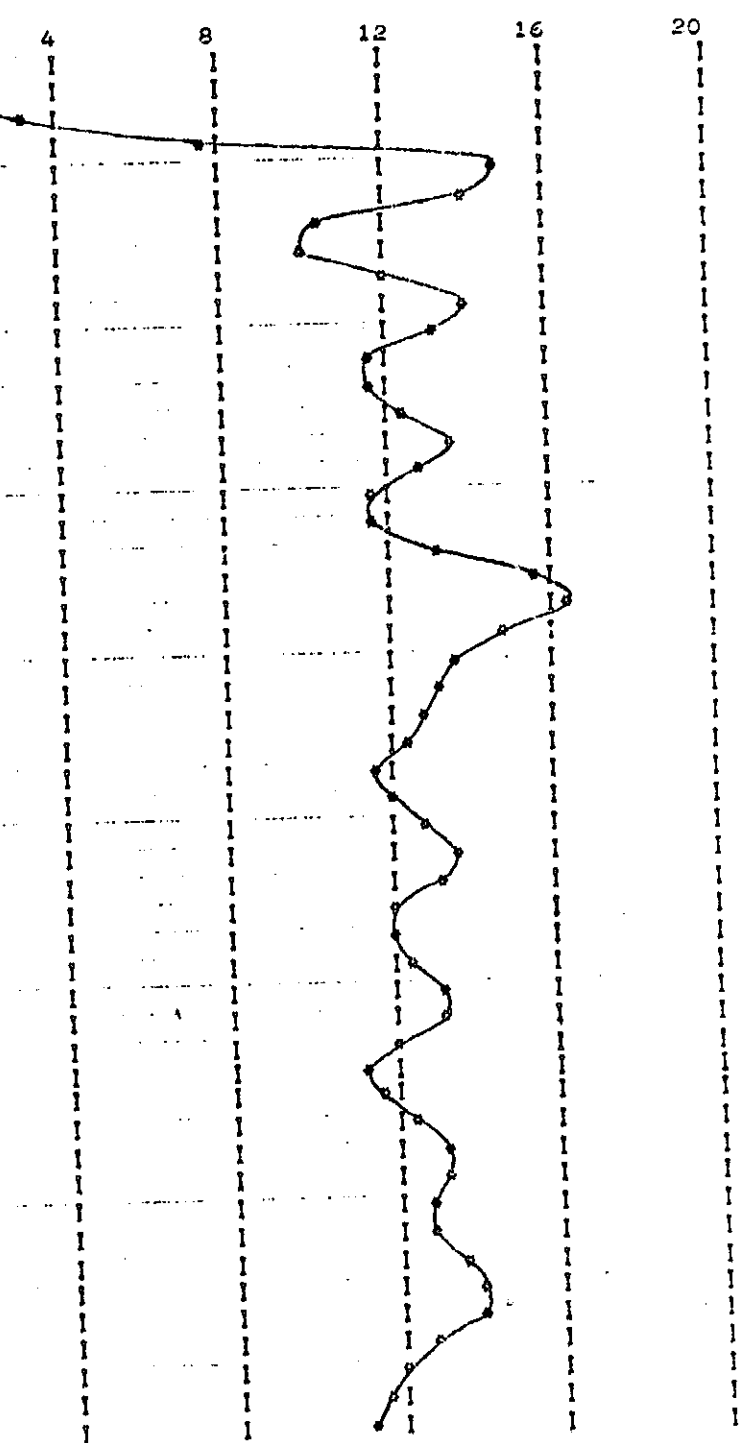
MAP-39 PASS-22 MODE-1 DAS-3

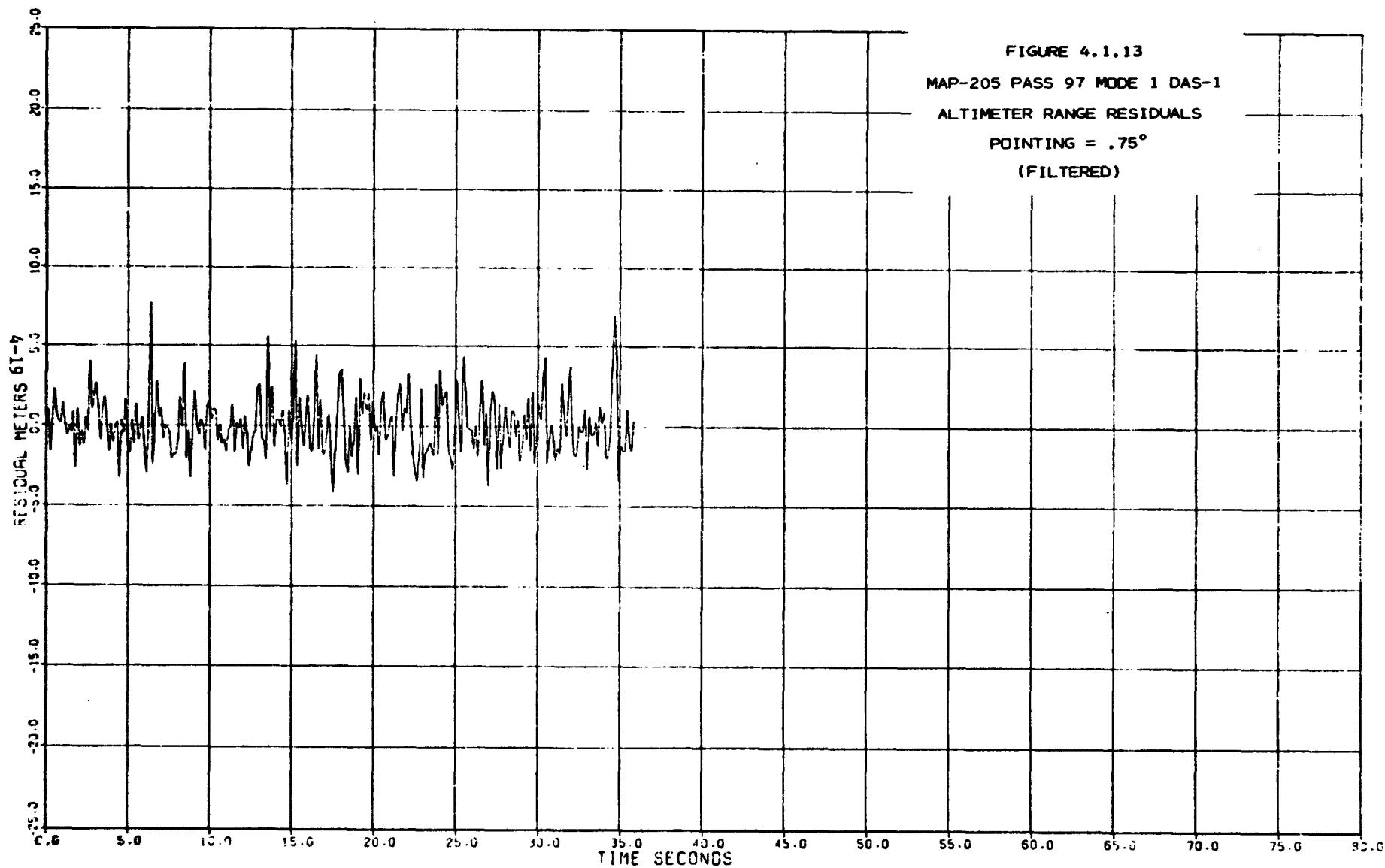
(FILTERED)

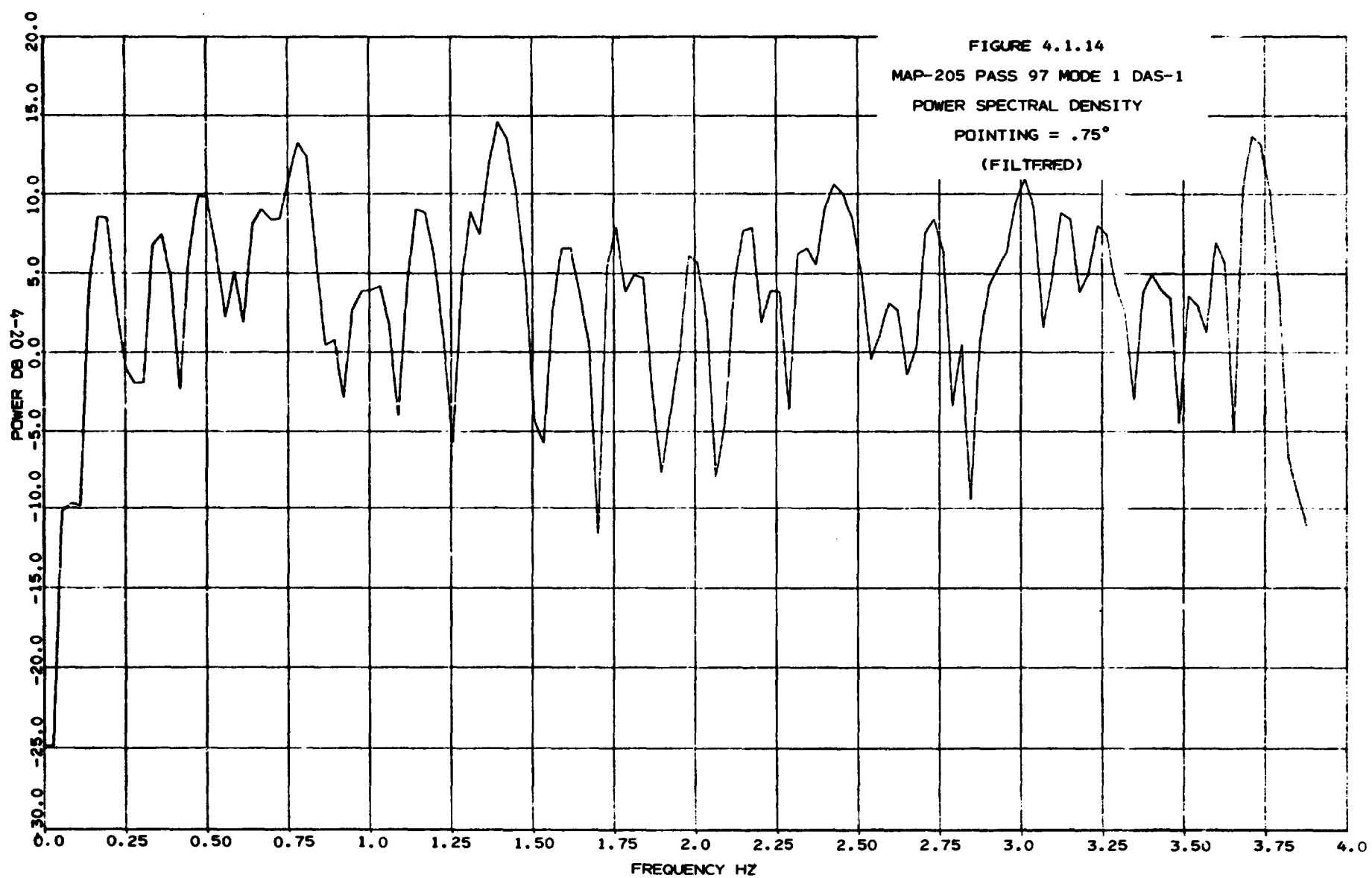
GAIN  
FREQUENCY (FRACTIONAL)

0,	0.66973102E-01
0,766E-01	0.78396428E-01
0,153E 00	0.12997618
0,230E 00	0.34717964
0,306E 00	1,7776574
0,383E 00	1,5648285
0,460E 00	0.69875690
0,536E 00	0.63600672
0,613E 00	0,95352429
0,689E 00	1,5589097
0,766E 00	1,2925901
0,843E 00	0.59819466
0,919E 00	0.66025808
0,996E 00	1,1022711
0,107E 01	1,3455384
0,115E 01	1,11,0246
0,123E 01	0.57867951
0,130E 01	0.90553807
0,138E 01	1,3102206
0,146E 01	2,3203524
0,153E 01	2,6459874
0,161E 01	1,8210084
0,169E 01	1,4060159
0,176E 01	1,2991104
0,184E 01	1,2028545
0,191E 01	1,0236745
0,199E 01	0.90946935
0,207E 01	0.95997937
0,214E 01	1,1979052
0,222E 01	1,4284756
0,230E 01	1,2692974
0,237E 01	1,0126642
0,245E 01	0.94552538
0,253E 01	1,0861984
0,260E 01	1,3195536
0,268E 01	1,2659644
0,276E 01	0.98709608
0,283E 01	0.83075614
0,291E 01	0.85215970
0,299E 01	1,0337843
0,306E 01	1,2623063
0,314E 01	1,3090949
0,322E 01	1,2075378
0,329E 01	1,1980255
0,337E 01	1,3540298
0,345E 01	1,5634918
0,352E 01	1,5101753
0,360E 01	1,2151519
0,368E 01	0.97596747
0,375E 01	0.86296541
0,383E 01	0.83483116

PLOT OF  
POWER TRANSFER FUNCTION DB







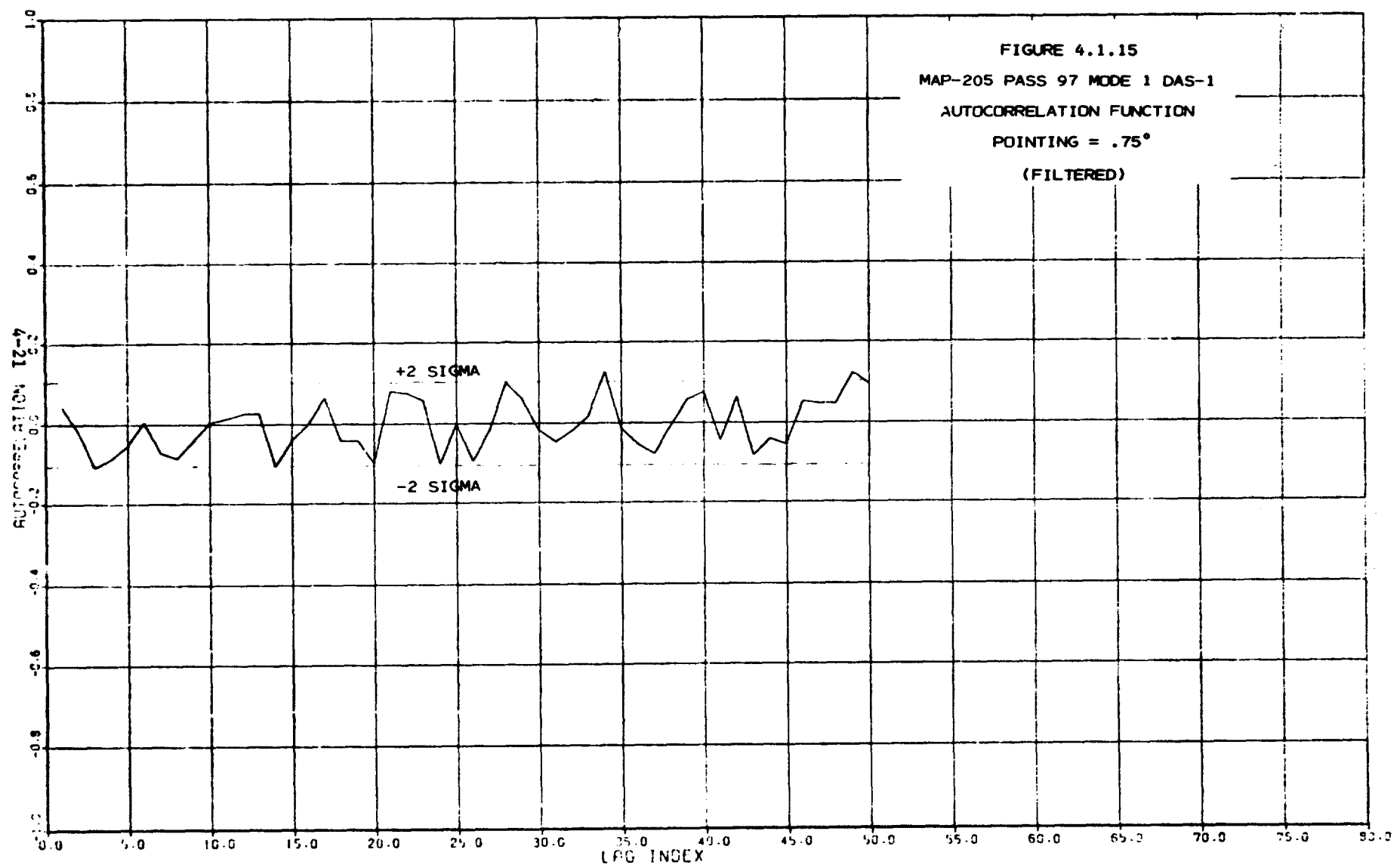
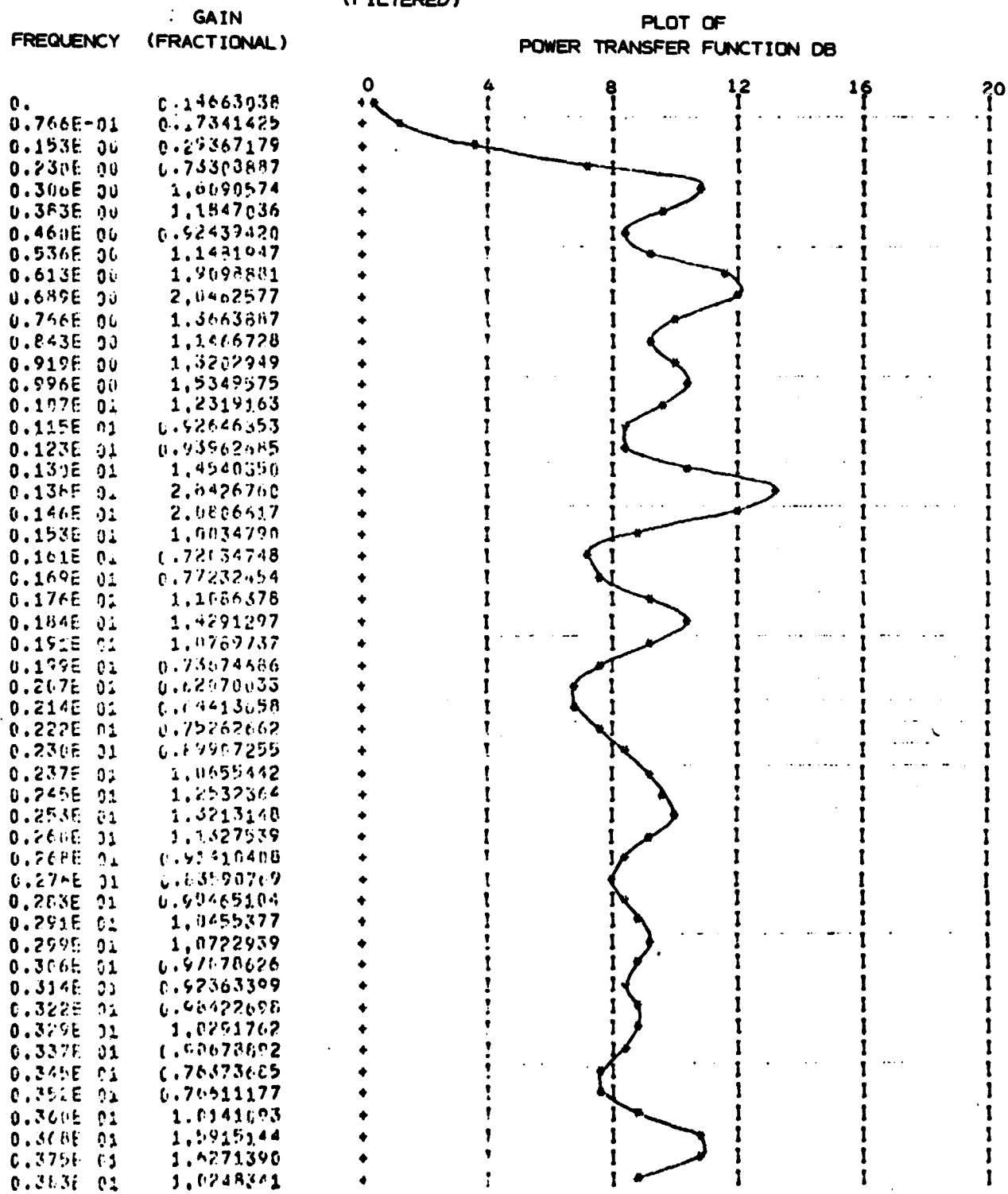
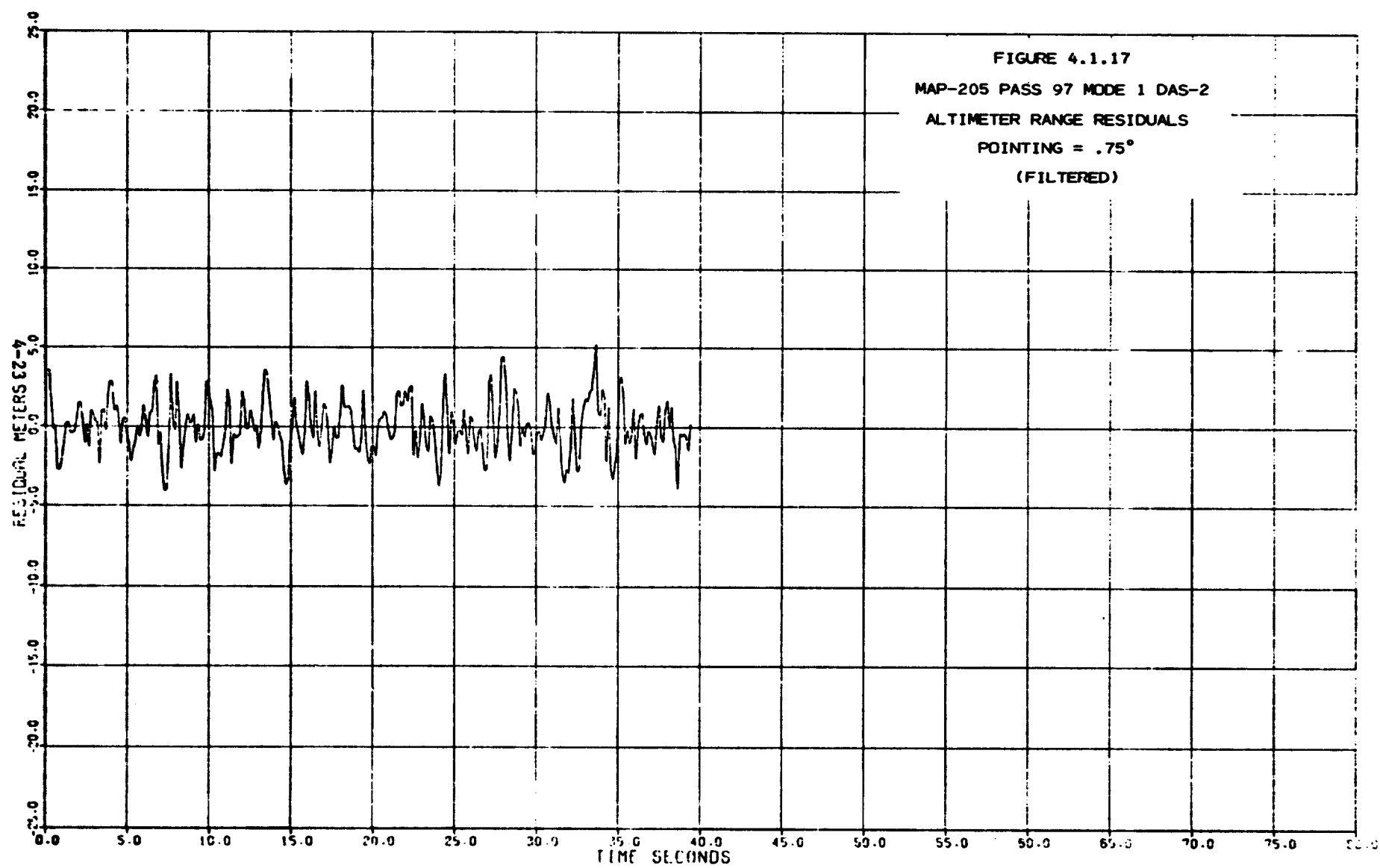


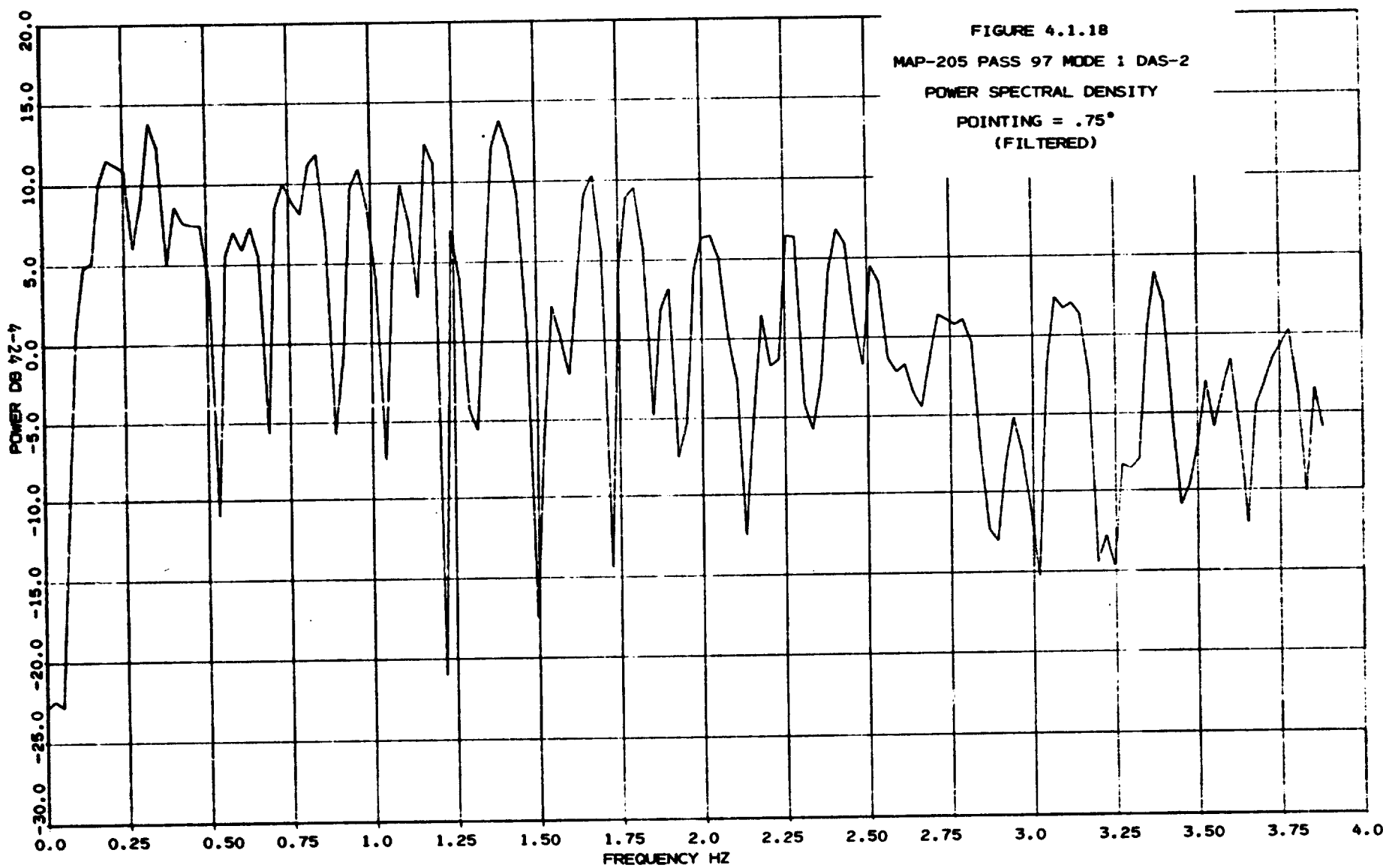
FIGURE 4.1.16  
AUTOREGRESSIVE MODEL

MAP-205 PASS-97 MODE-1 DAS-1  
(FILTERED)



ORIGINAL PAGE IS  
OF POOR QUALITY





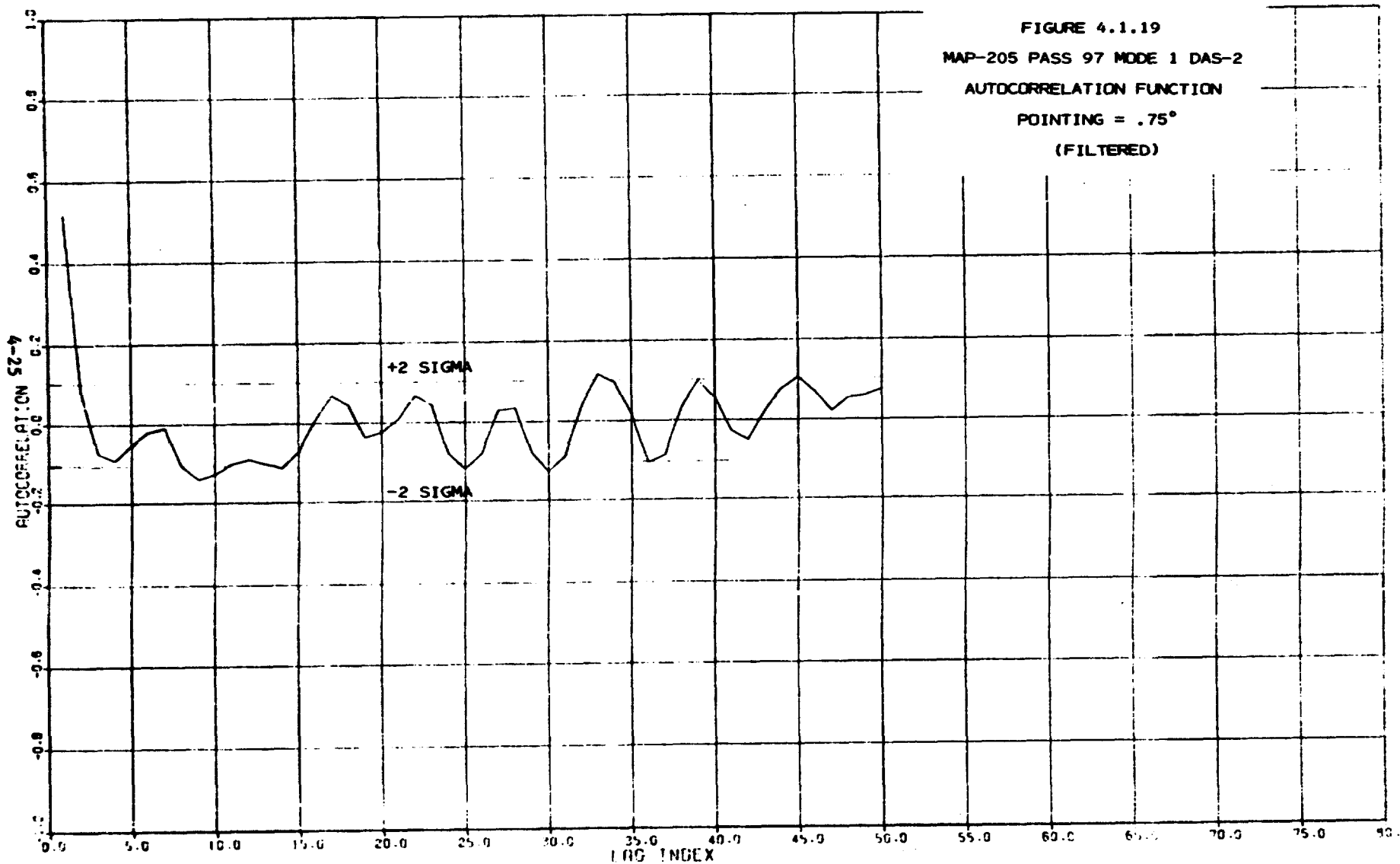


FIGURE 4.1.20A

## AUTOREGRESSIVE MODEL.

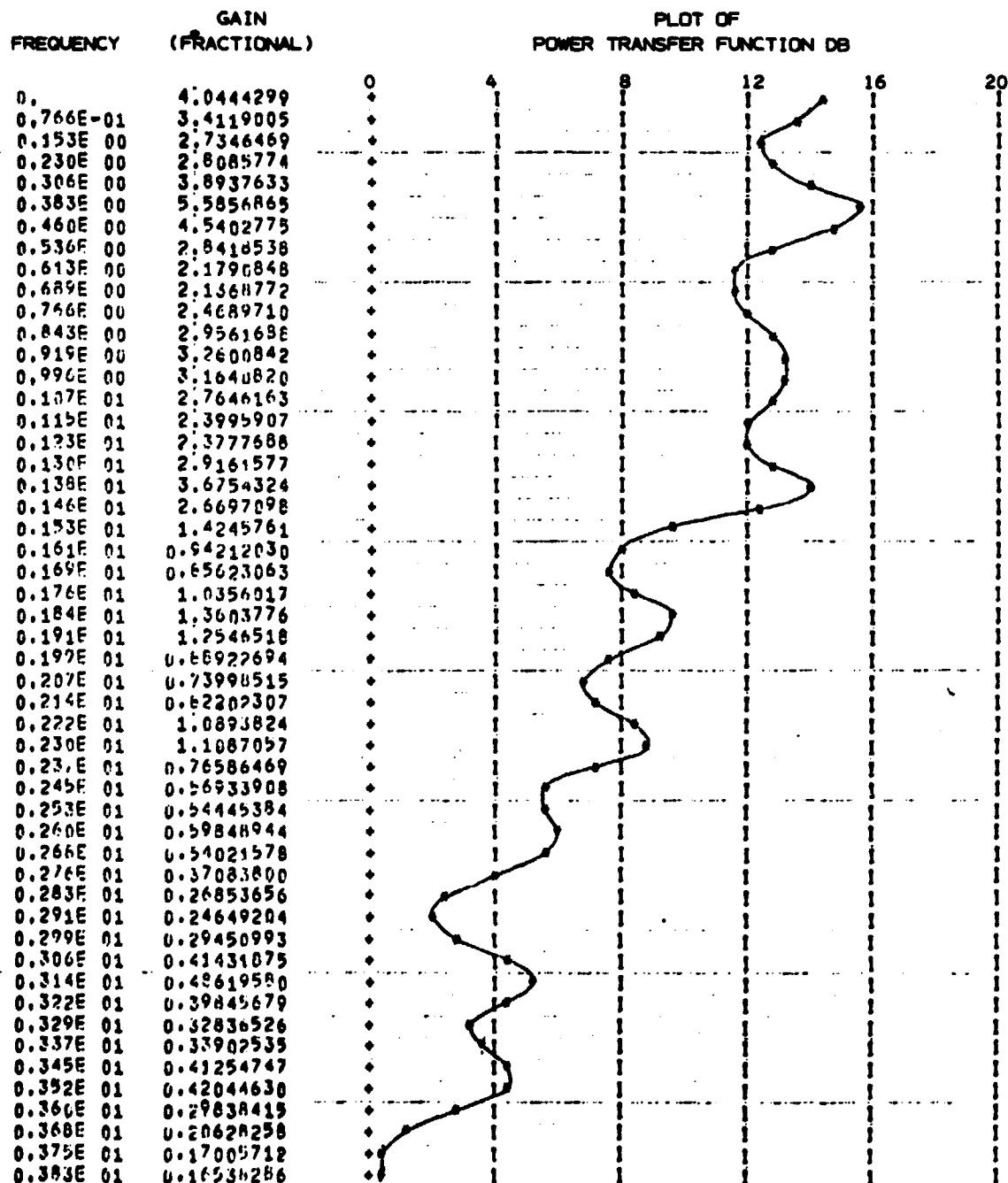
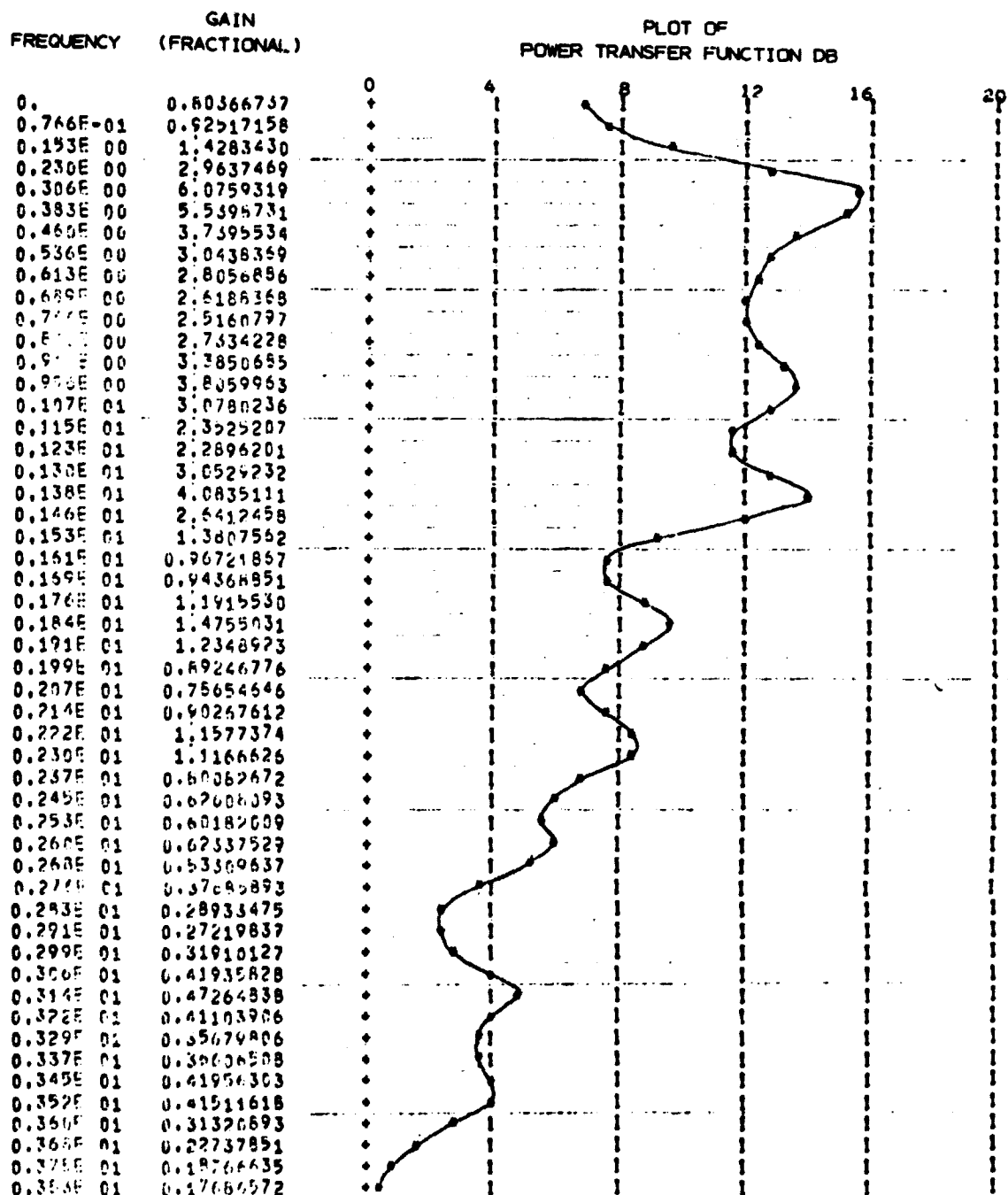
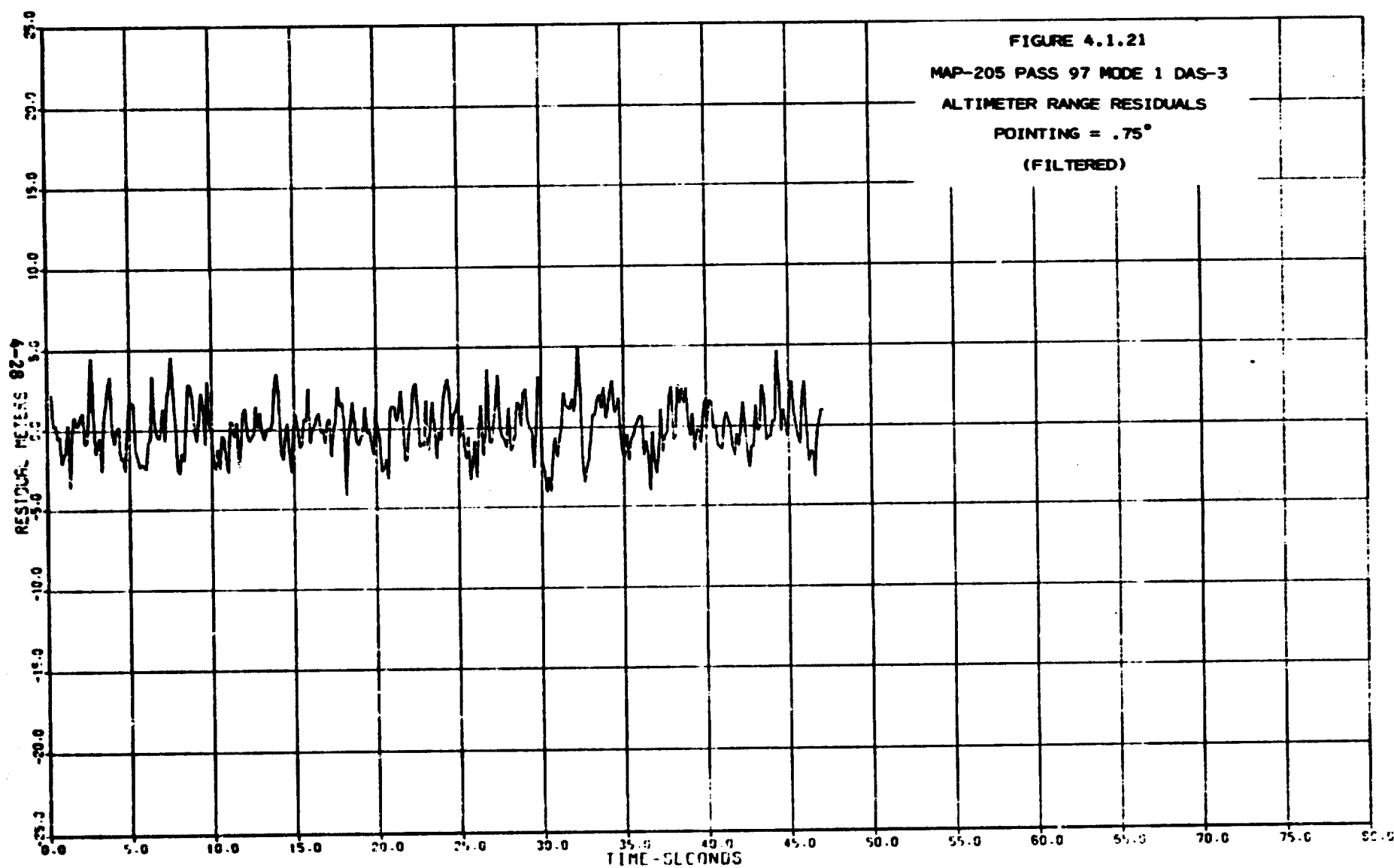
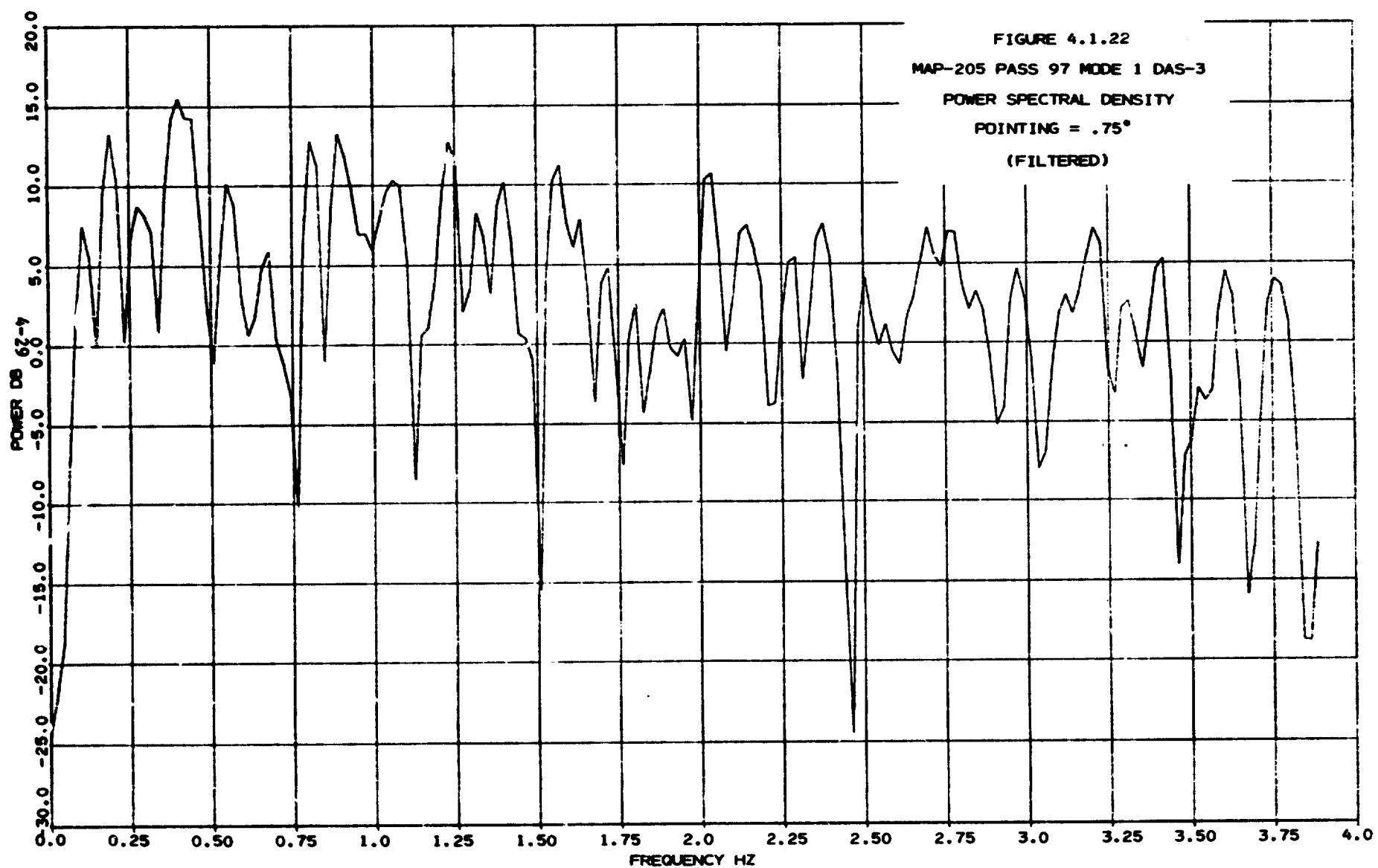
MAP-205 PASS-97 MODE-1 DAS-2  
(UNFILTERED)

FIGURE 4.1.208  
AUTOREGRESSIVE MODEL  
MAP-205 PASS-97 MODE-1 DAS-2  
(FILTERED)







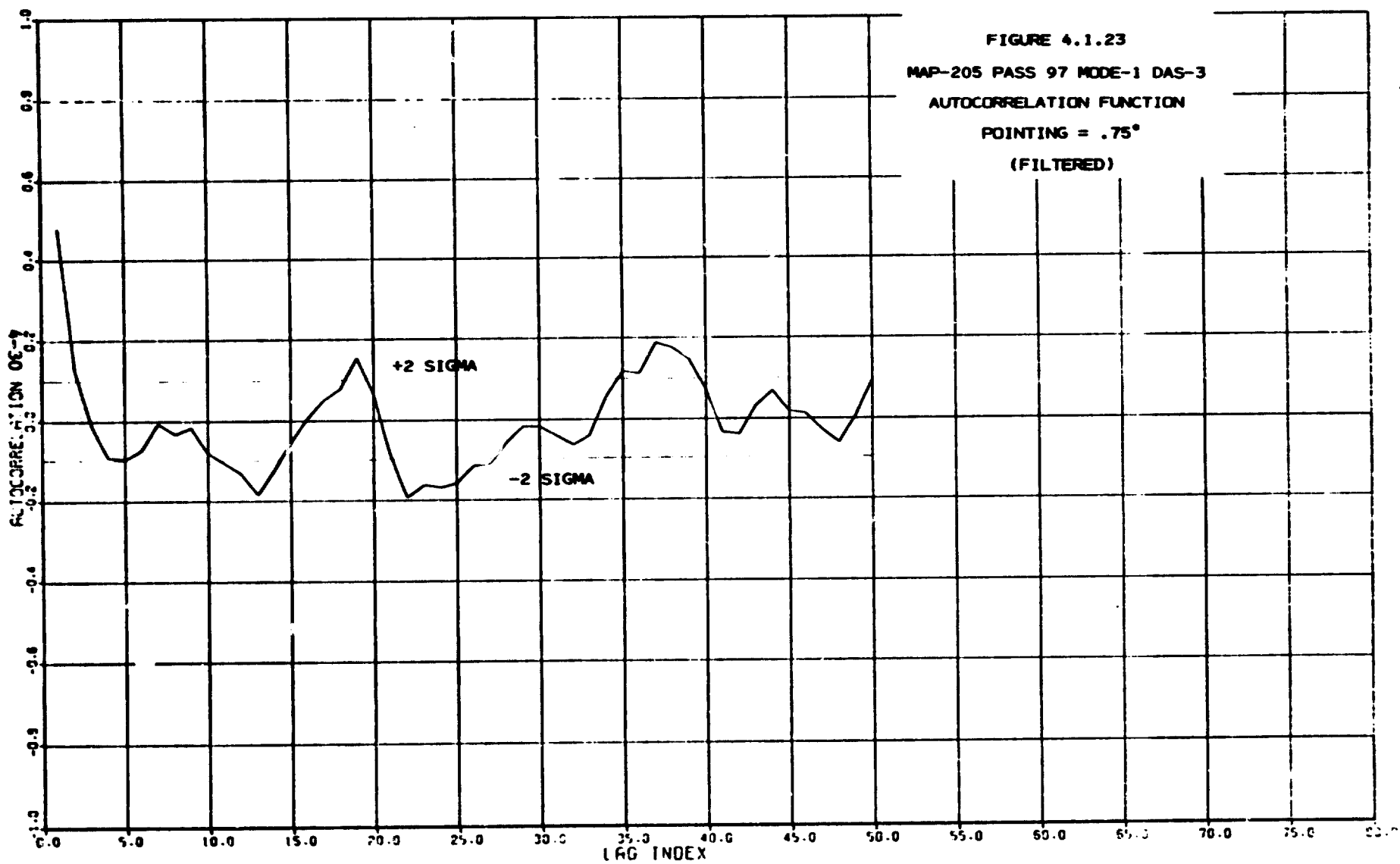
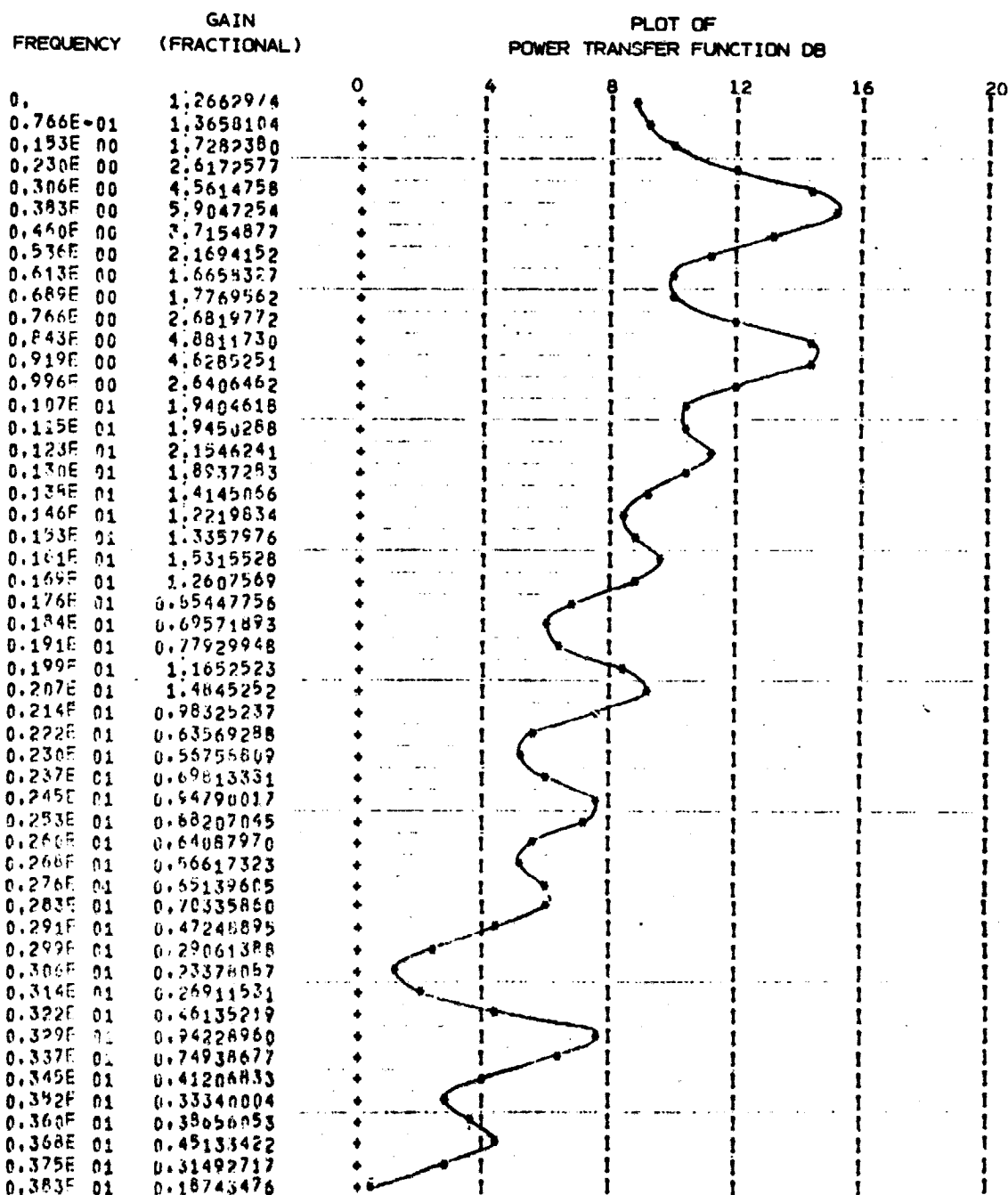
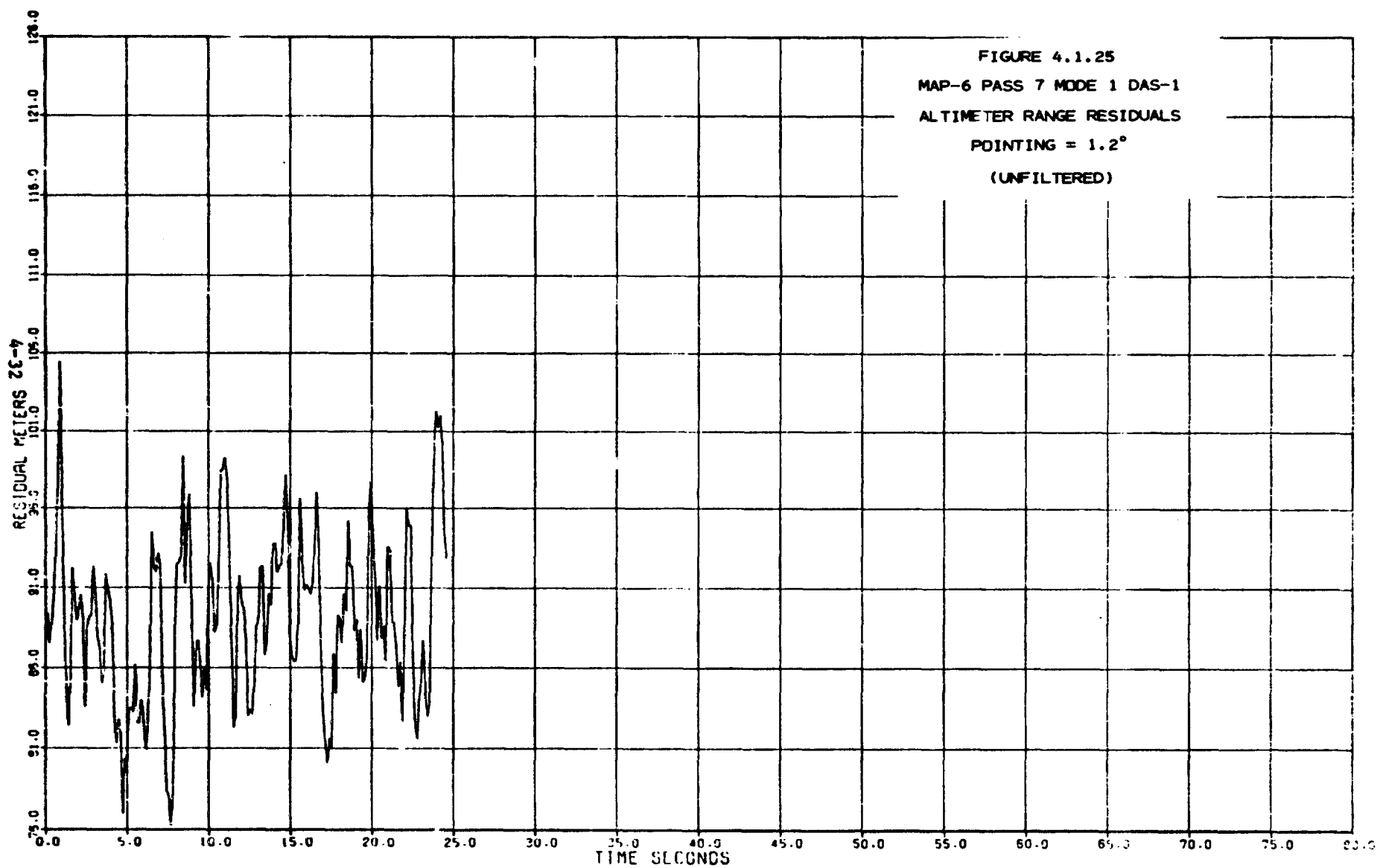
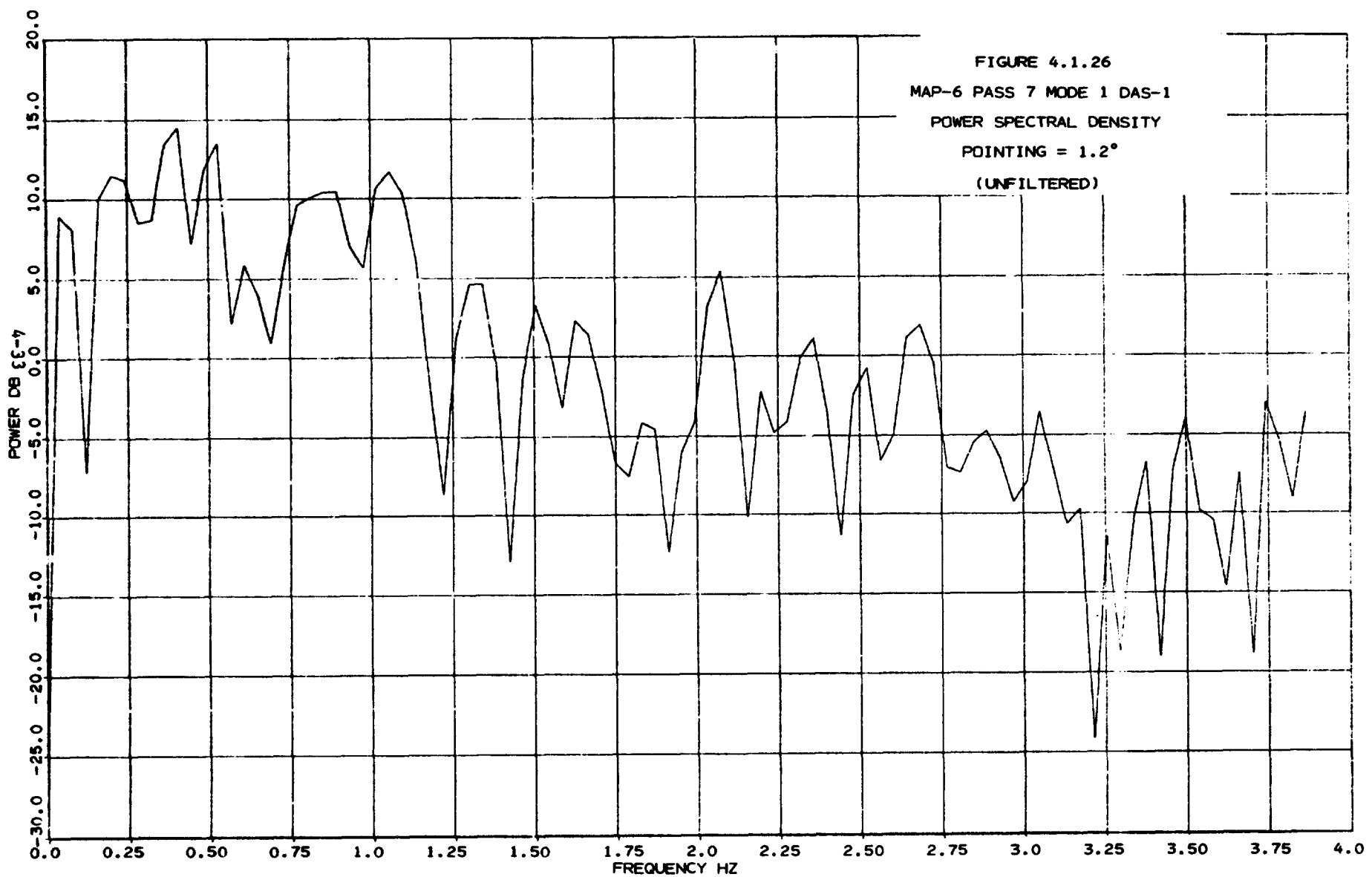


FIGURE 4.1.24  
AUTOREGRESSIVE MODEL

MAP-205 PASS-97 MODE-1 DAS-3  
(FILTERED)







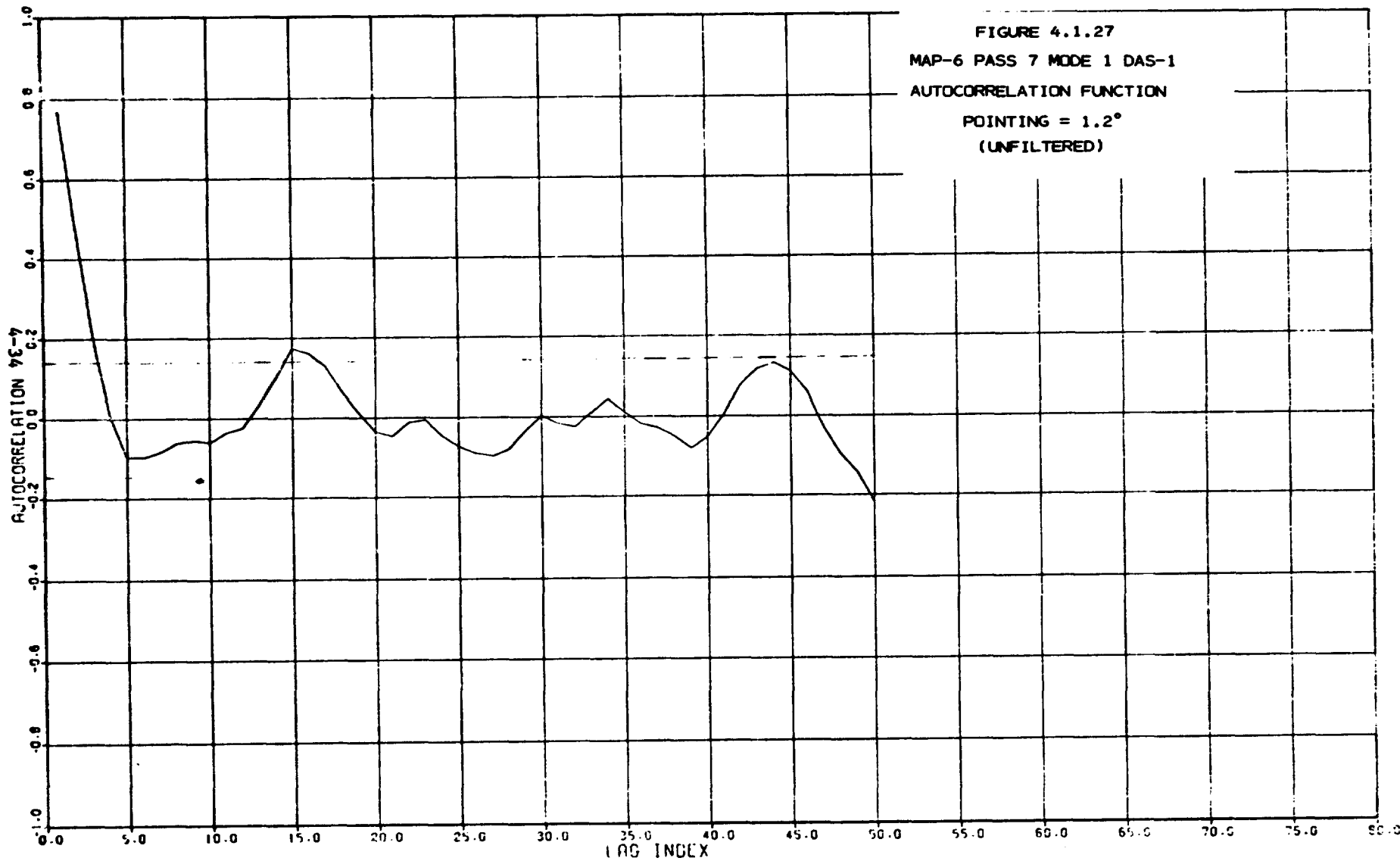


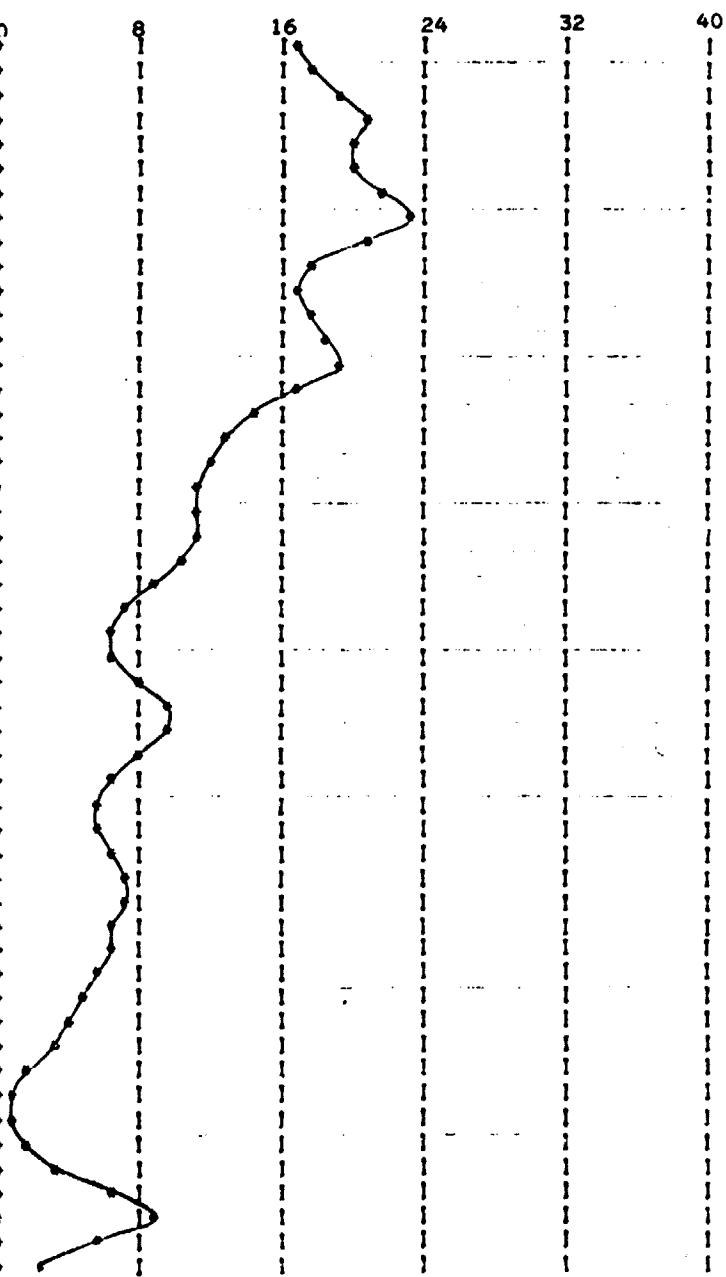
FIGURE 4.1.28  
AUTOREGRESSIVE MODEL

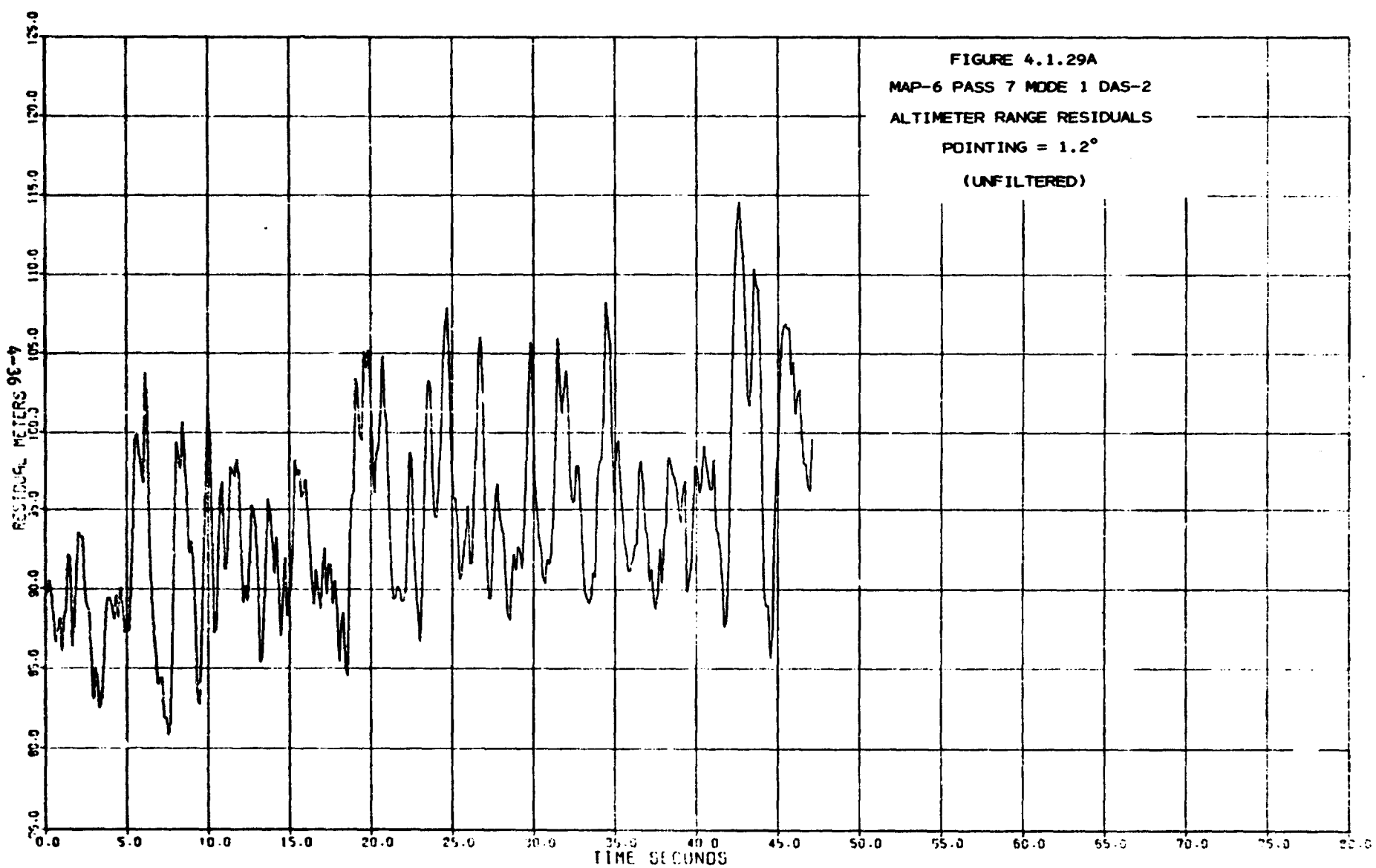
MAP-6 PASS-7 MODE-1 DAS-1  
(UNFILTERED)

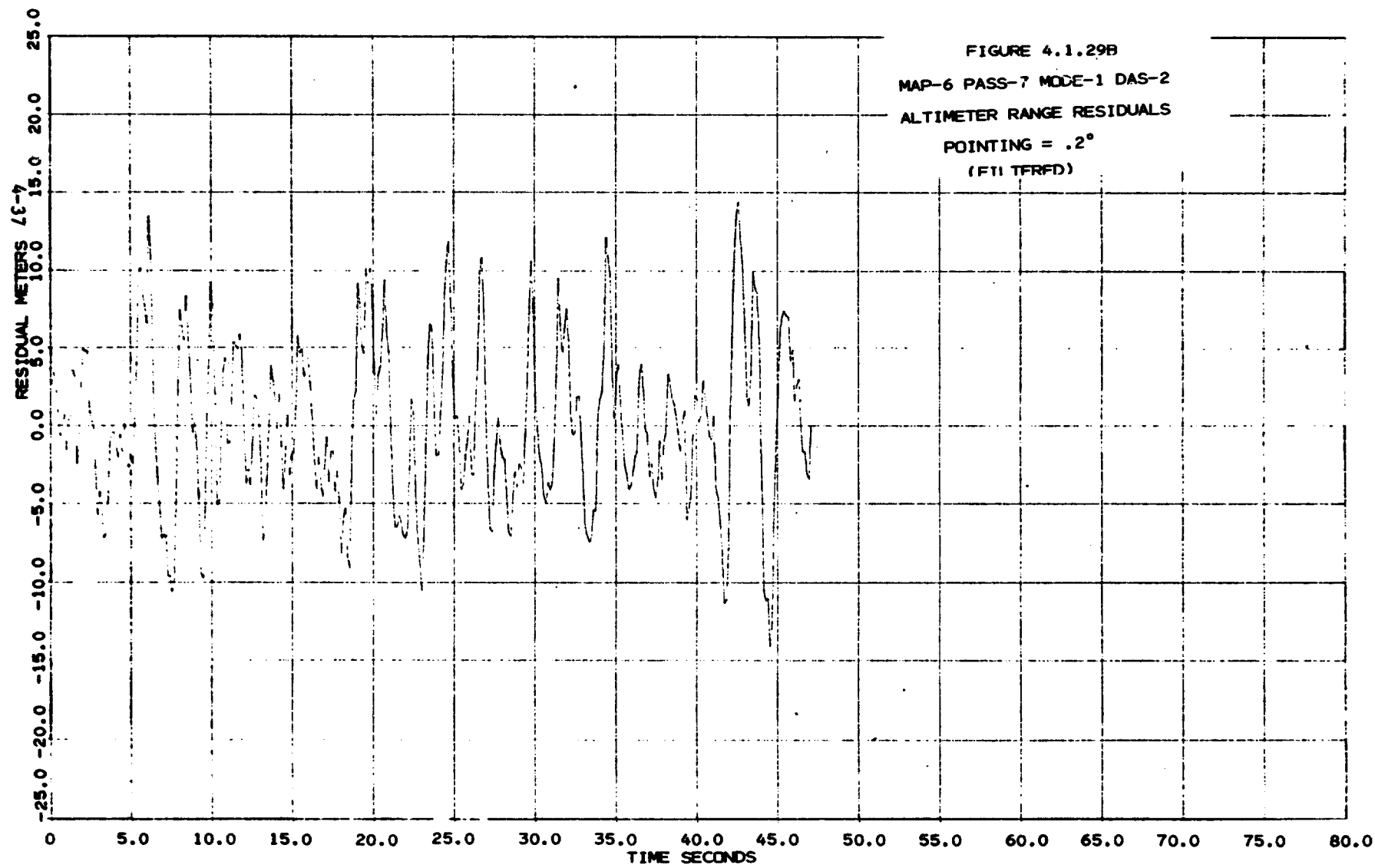
GAIN  
(FRACTIONAL)

FREQUENCY	GAIN (FRACTIONAL)
0.	4.8050004
0.766E-01	5.6246243
0.153E 00	6.2992423
0.230E 00	10.830091
0.306E 00	10.032124
0.383E 00	10.013123
0.460E 00	13.917347
0.536E 00	16.376155
0.613E 00	10.610059
0.689E 00	5.7576314
0.766E 00	4.5301813
0.843E 00	5.1370037
0.919E 00	7.2297671
0.996E 00	7.5102232
0.107E 01	4.5626549
0.115E 01	2.7109540
0.123E 01	1.8602163
0.130E 01	1.4627974
0.138E 01	1.2796416
0.146E 01	1.2733655
0.153E 01	1.2516606
0.161E 01	1.0093136
0.169E 01	0.67907534
0.176E 01	0.47550572
0.184E 01	0.40057313
0.191E 01	0.42915162
0.199E 01	0.56247542
0.207E 01	0.65083243
0.214E 01	0.63320961
0.222E 01	0.55462774
0.230E 01	0.39430960
0.237E 01	0.35441644
0.245E 01	0.37903769
0.253E 01	0.44545063
0.260E 01	0.50061356
0.268E 01	0.49972006
0.276E 01	0.45537301
0.283E 01	0.39226070
0.291E 01	0.32522205
0.299E 01	0.26677007
0.306E 01	0.22156790
0.314E 01	0.18435391
0.322E 01	0.15104631
0.329E 01	0.12264339
0.337E 01	0.11478720
0.345E 01	0.12597587
0.352E 01	0.16250050
0.360E 01	0.36689197
0.368E 01	0.75114817
0.375E 01	0.35296166
0.383E 01	0.16498679

PLOT OF  
POWER TRANSFER FUNCTION DB







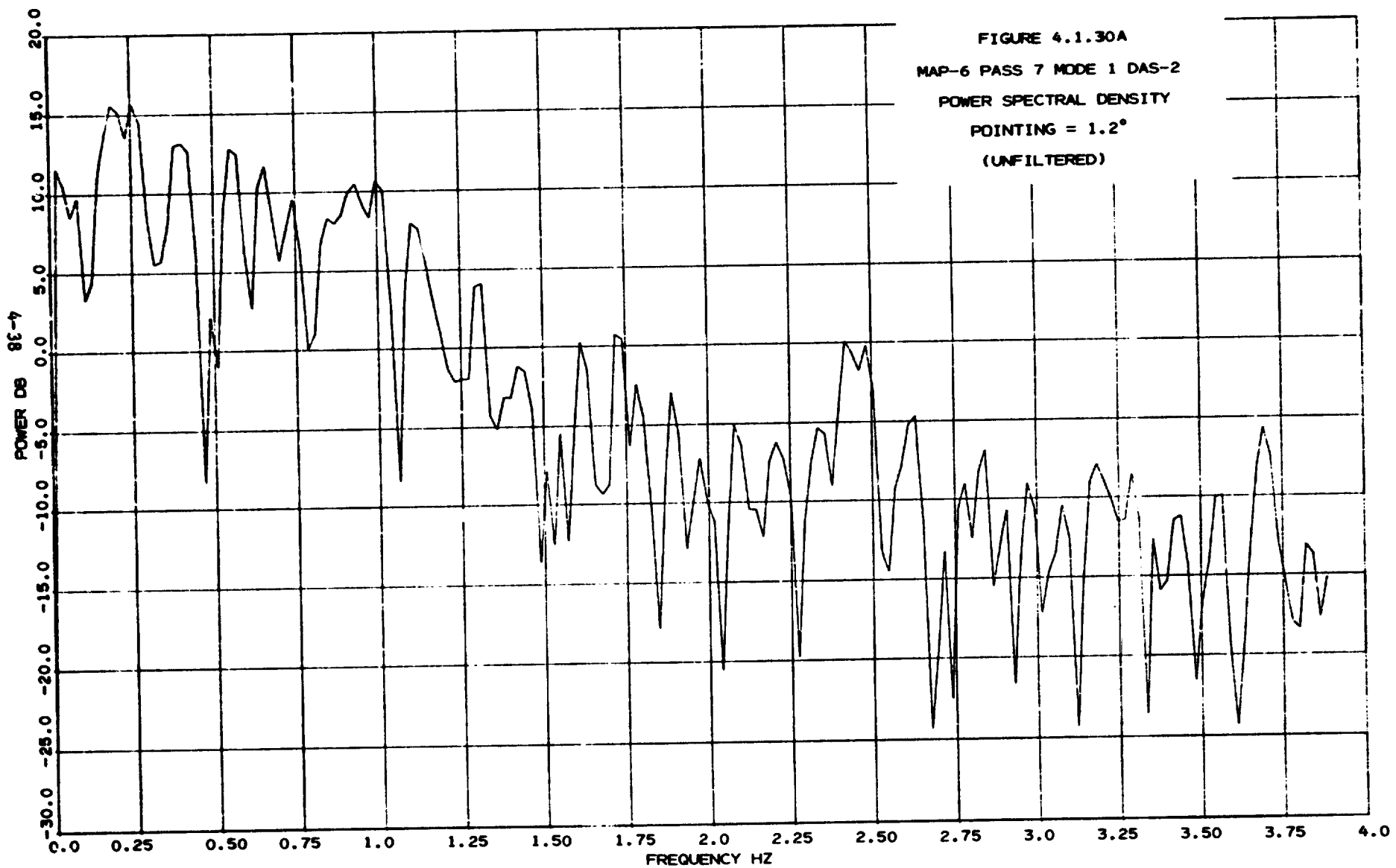
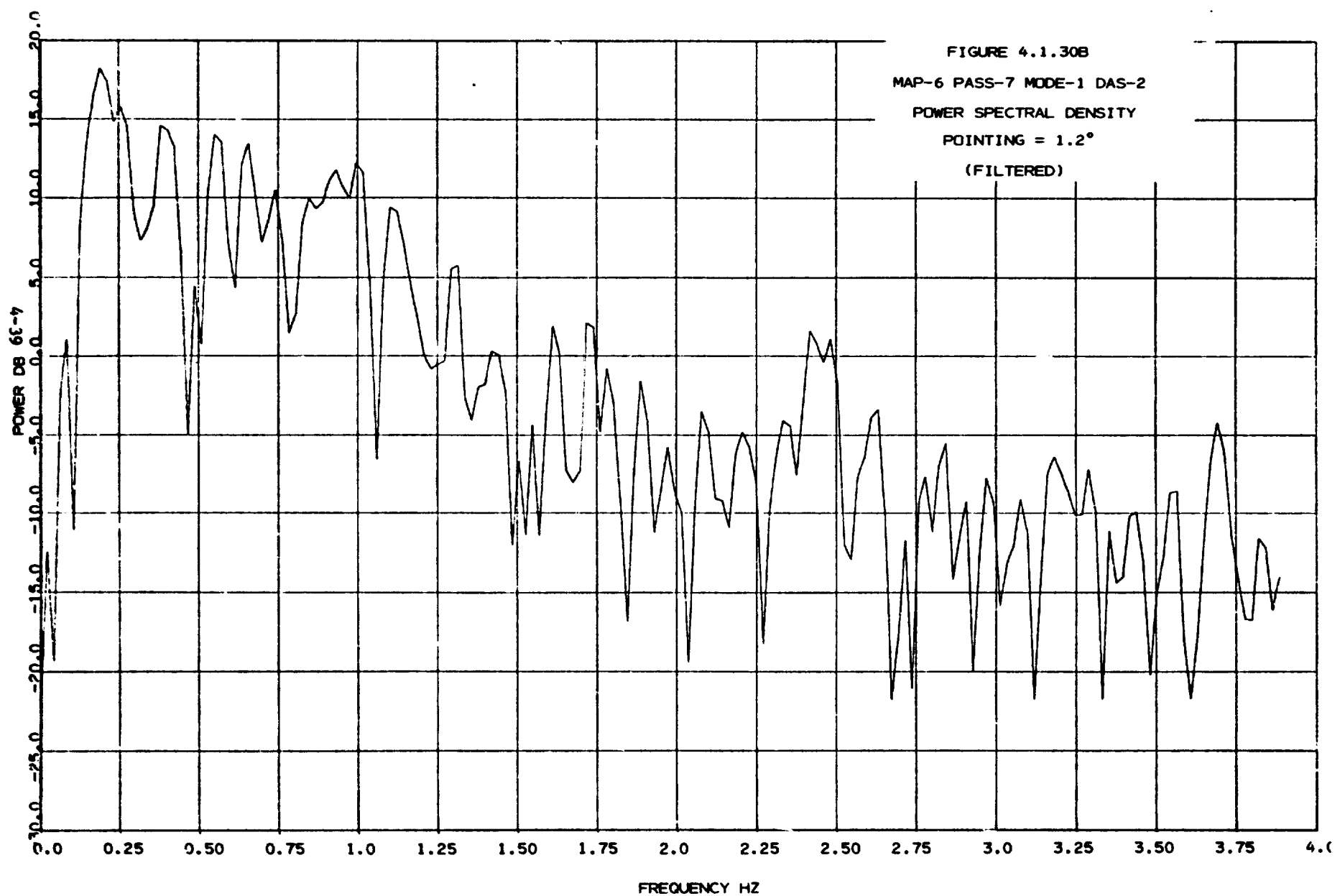
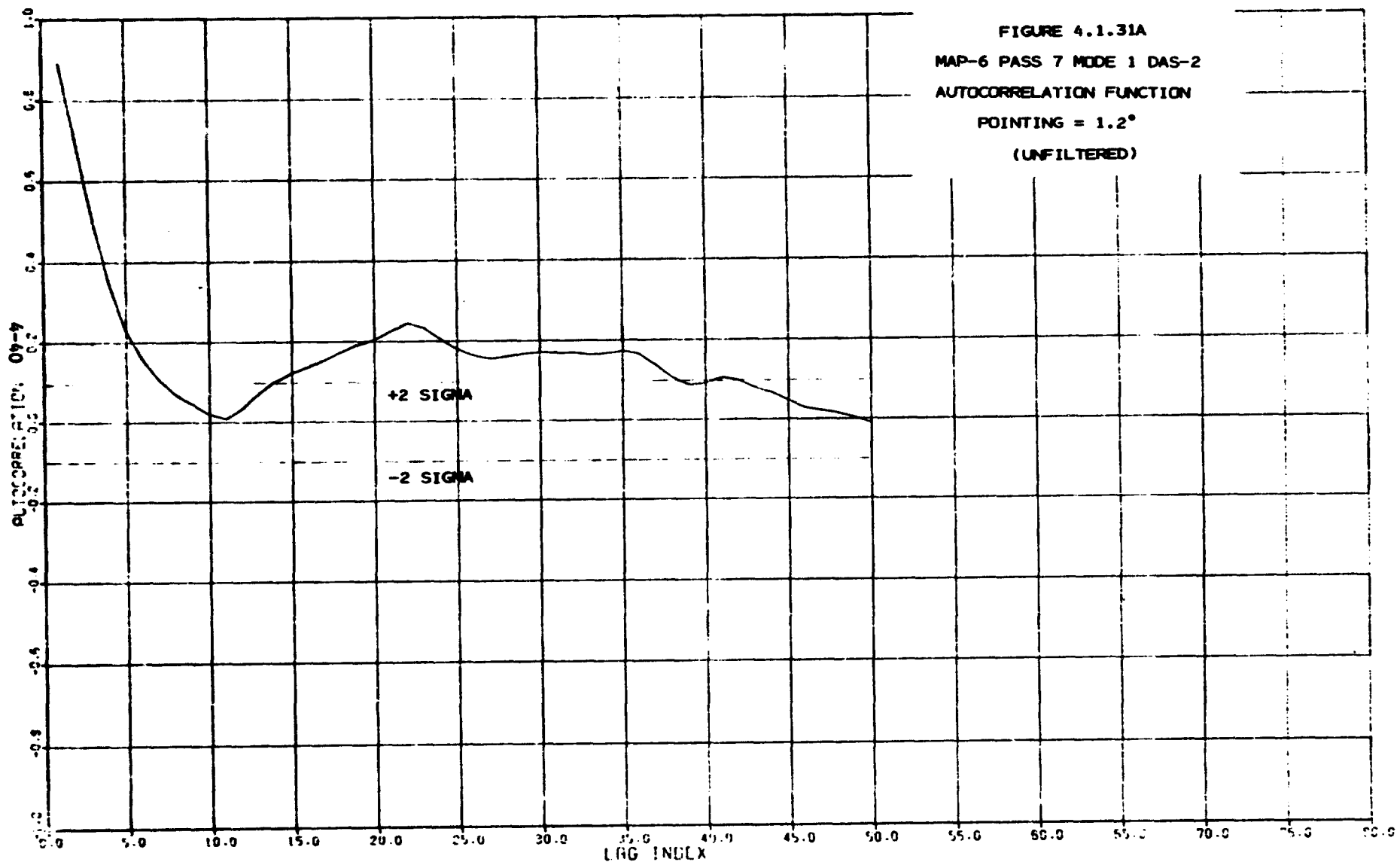


FIGURE 4.1.30A  
MAP-6 PASS 7 MODE 1 DAS-2  
POWER SPECTRAL DENSITY  
POINTING =  $1.2^\circ$   
(UNFILTERED)





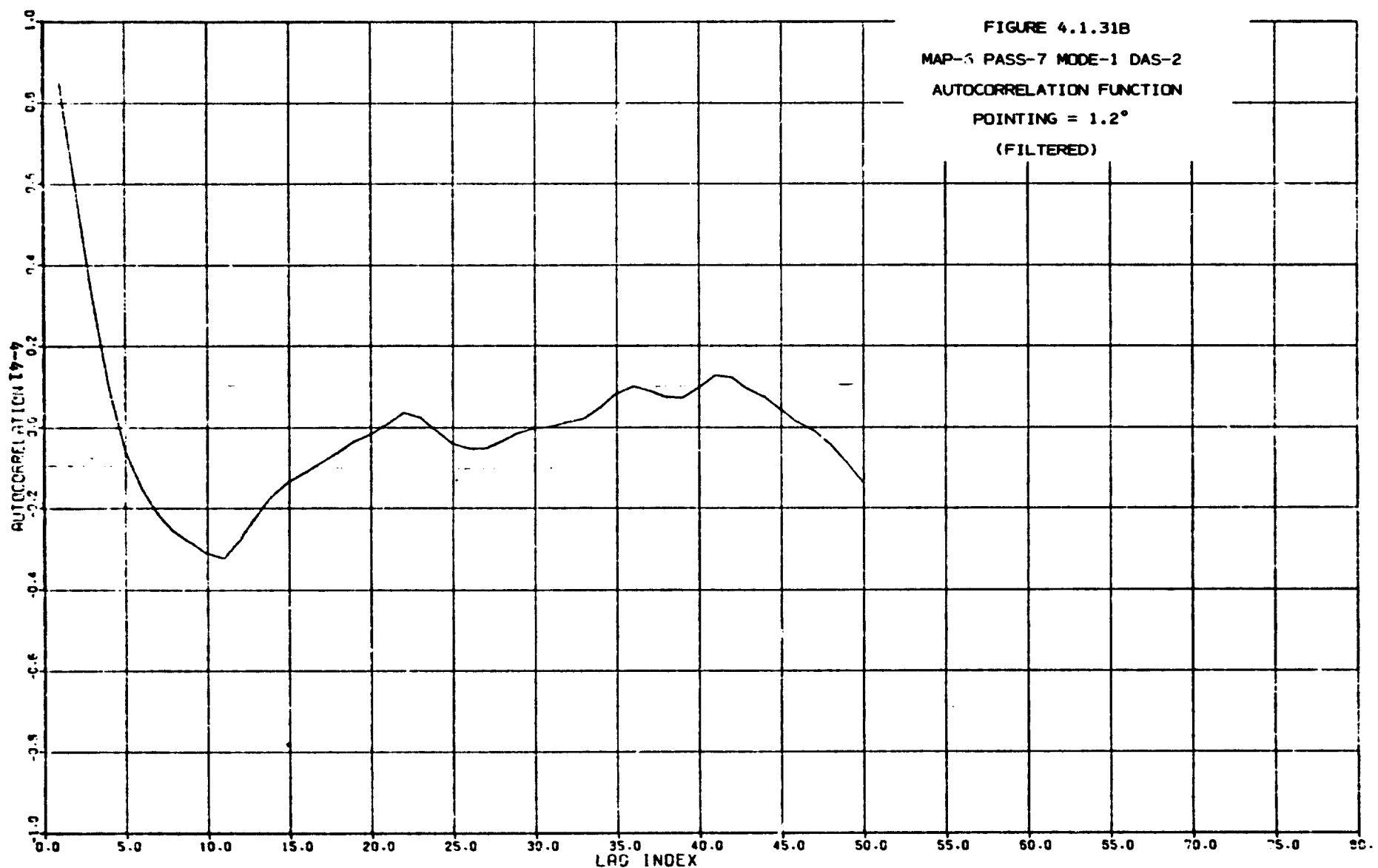
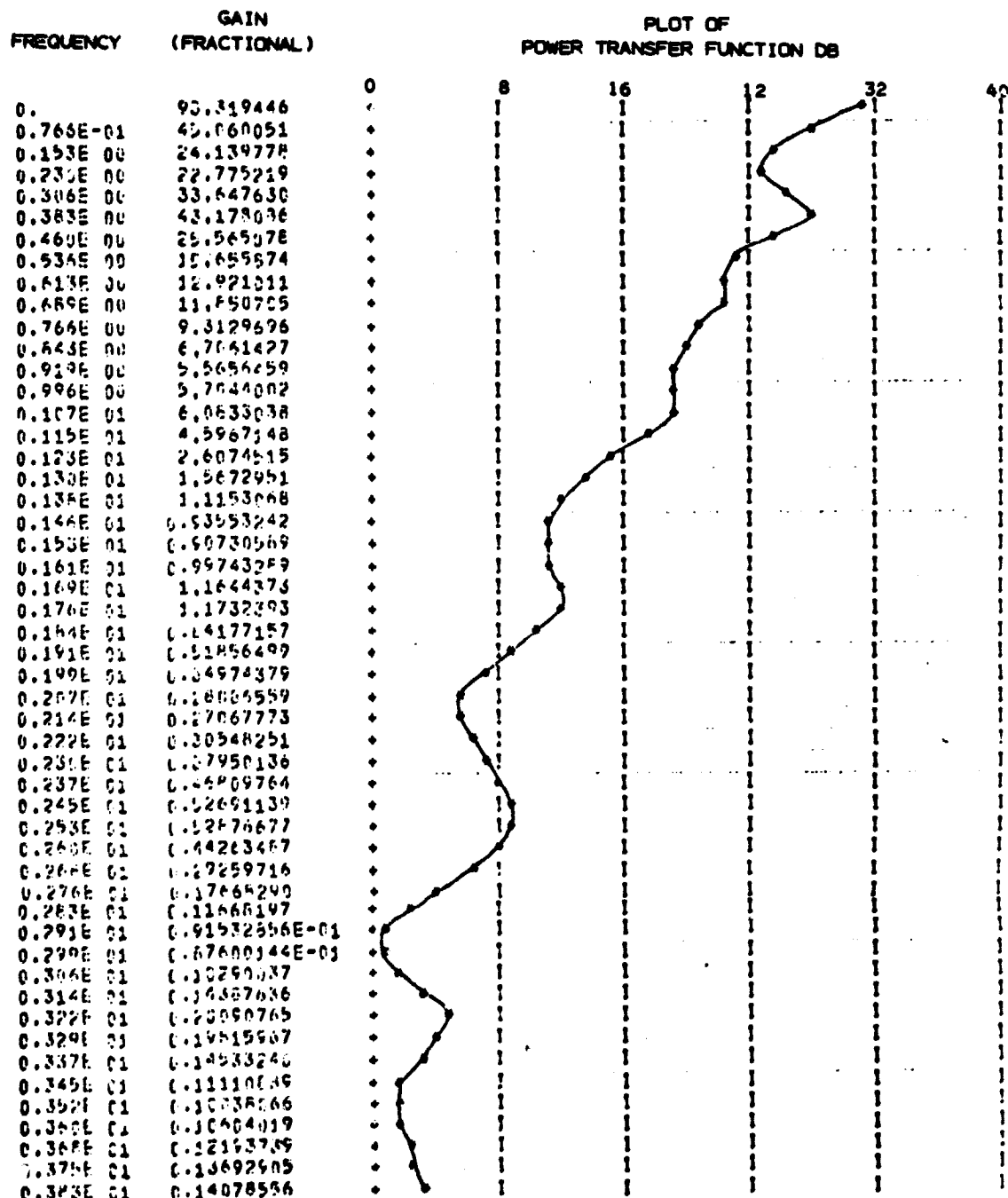


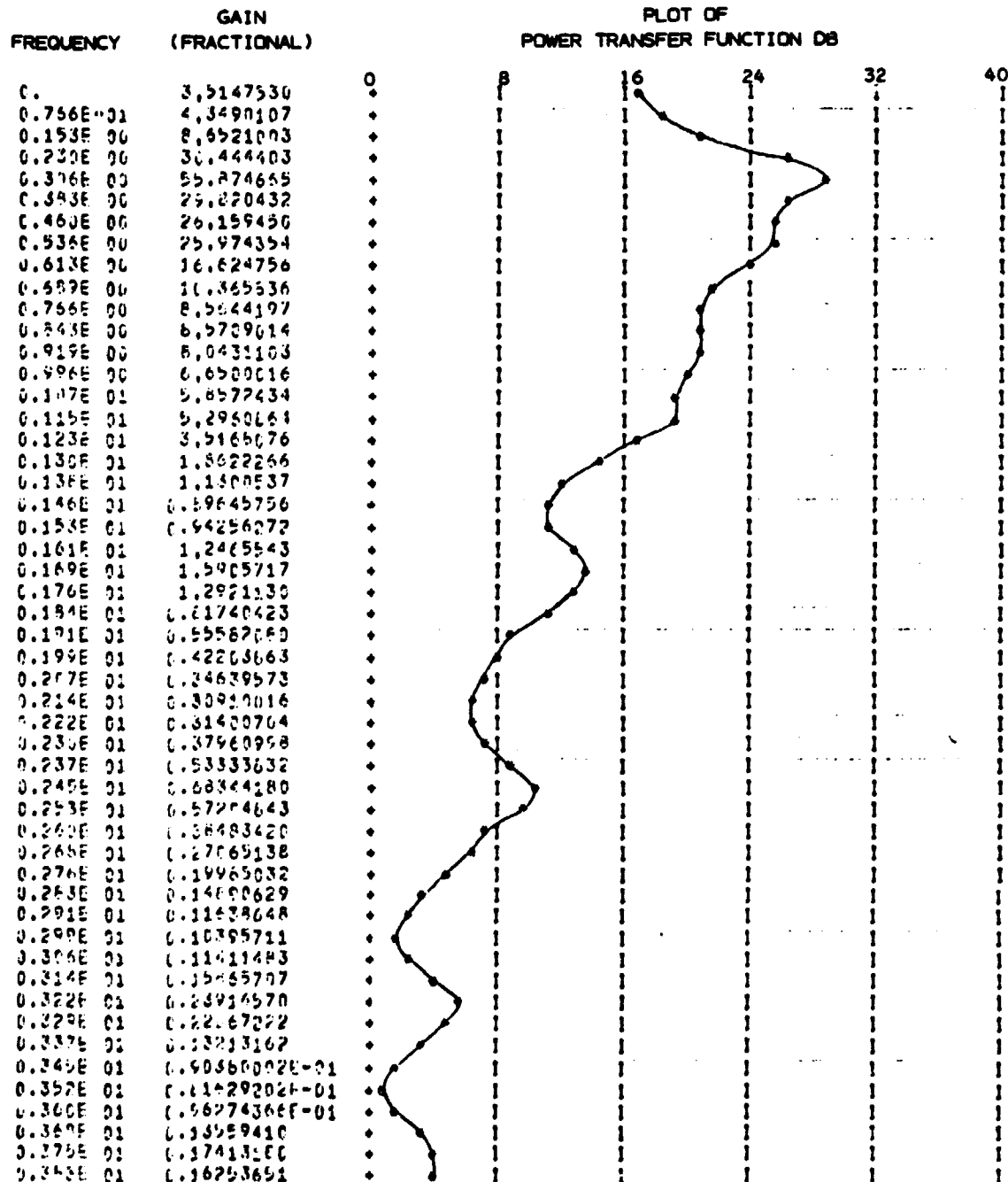
FIGURE 4.1.32A  
AUTOREGRESSIVE MODEL

MAP-6 PASS-7 MODE-1 DAS-2  
(UNFILTERED)

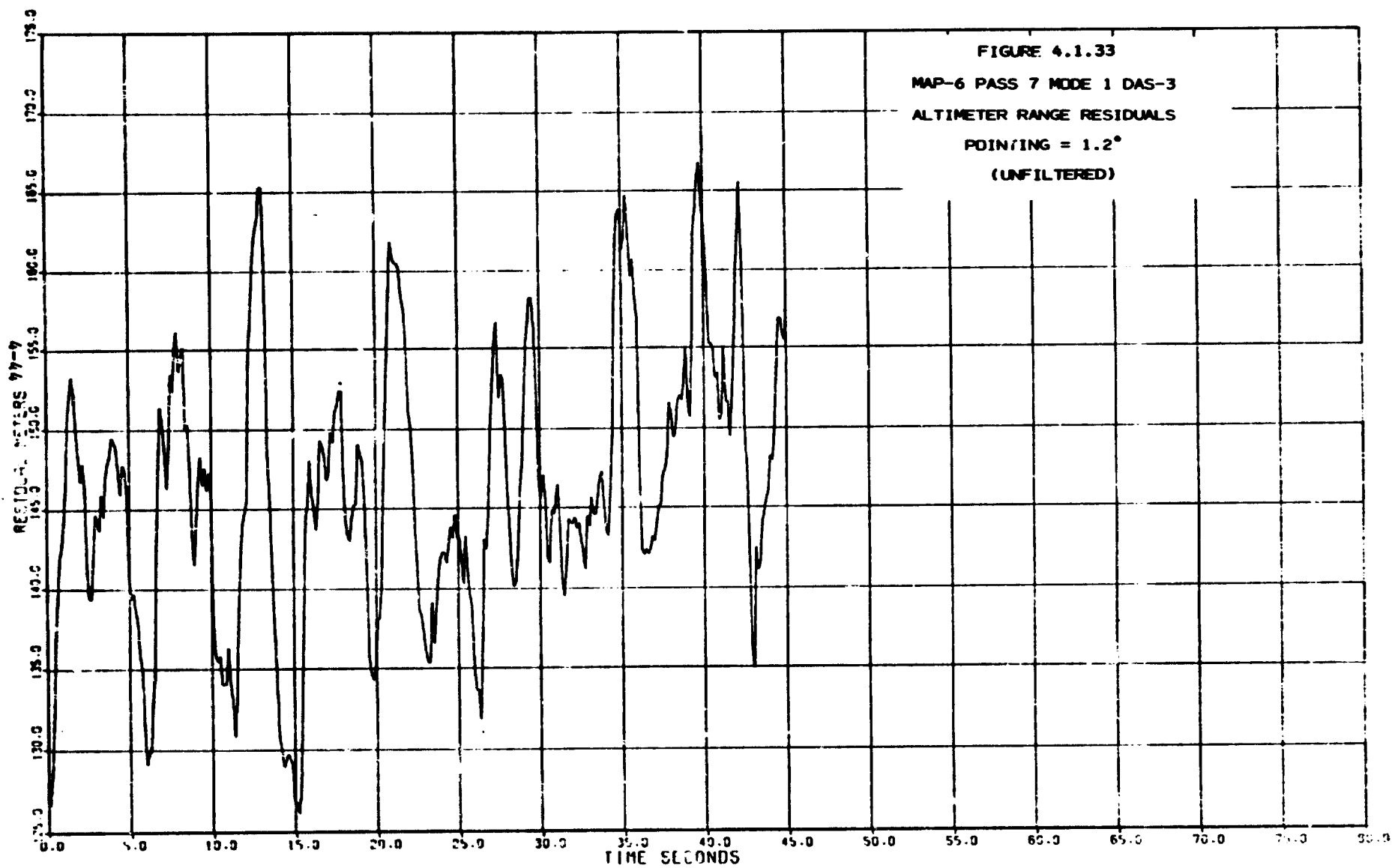


ORIGINAL PAGE IS  
OF POOR QUALITY

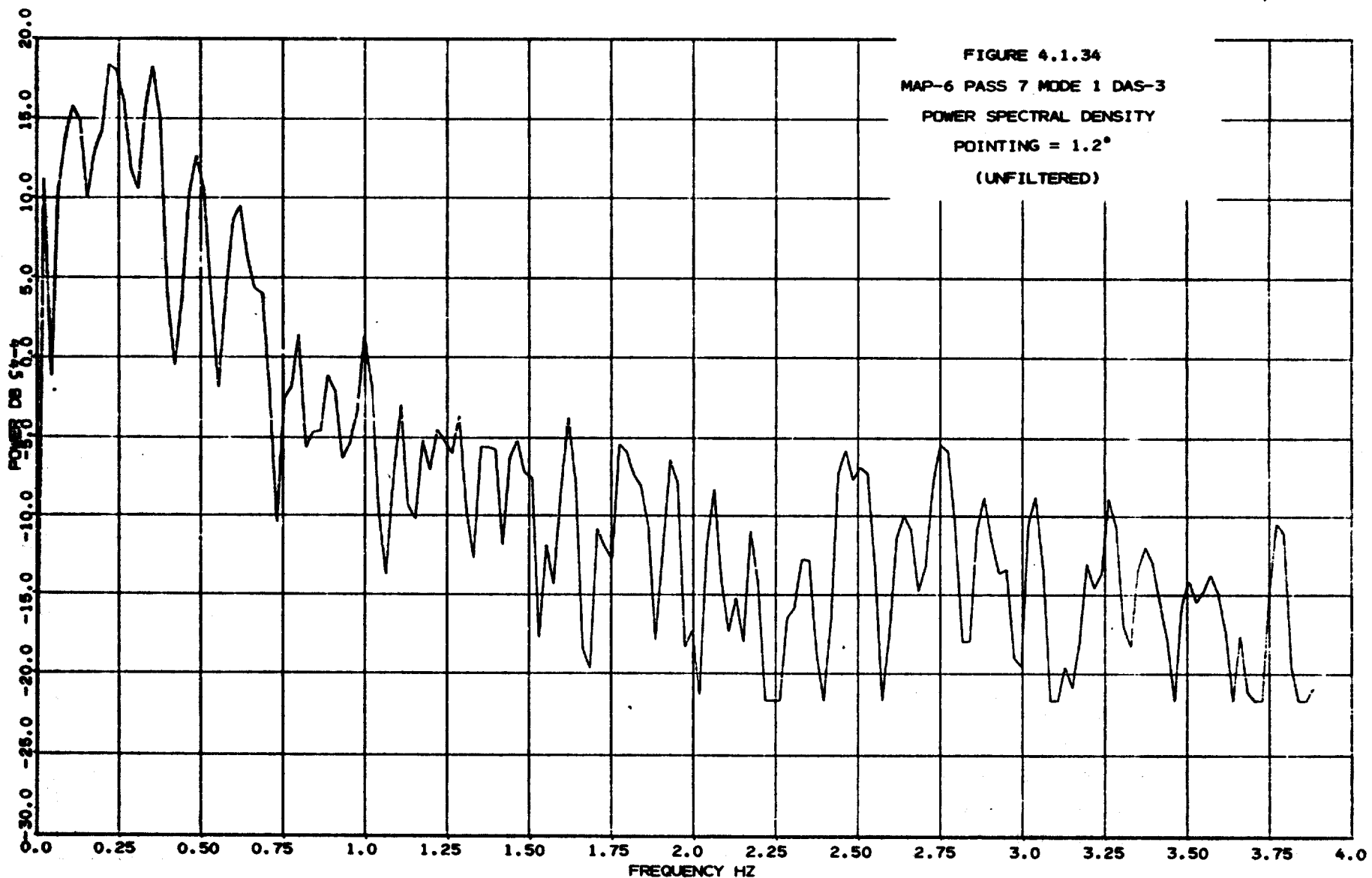
FIGURE 4.1.32B  
AUTOREGRESSIVE MODEL  
MAP-6 PASS-7 MODE-1 DAS-2  
(FILTERED)



ORIGINAL PAGE IS  
OF POOR QUALITY



C.2



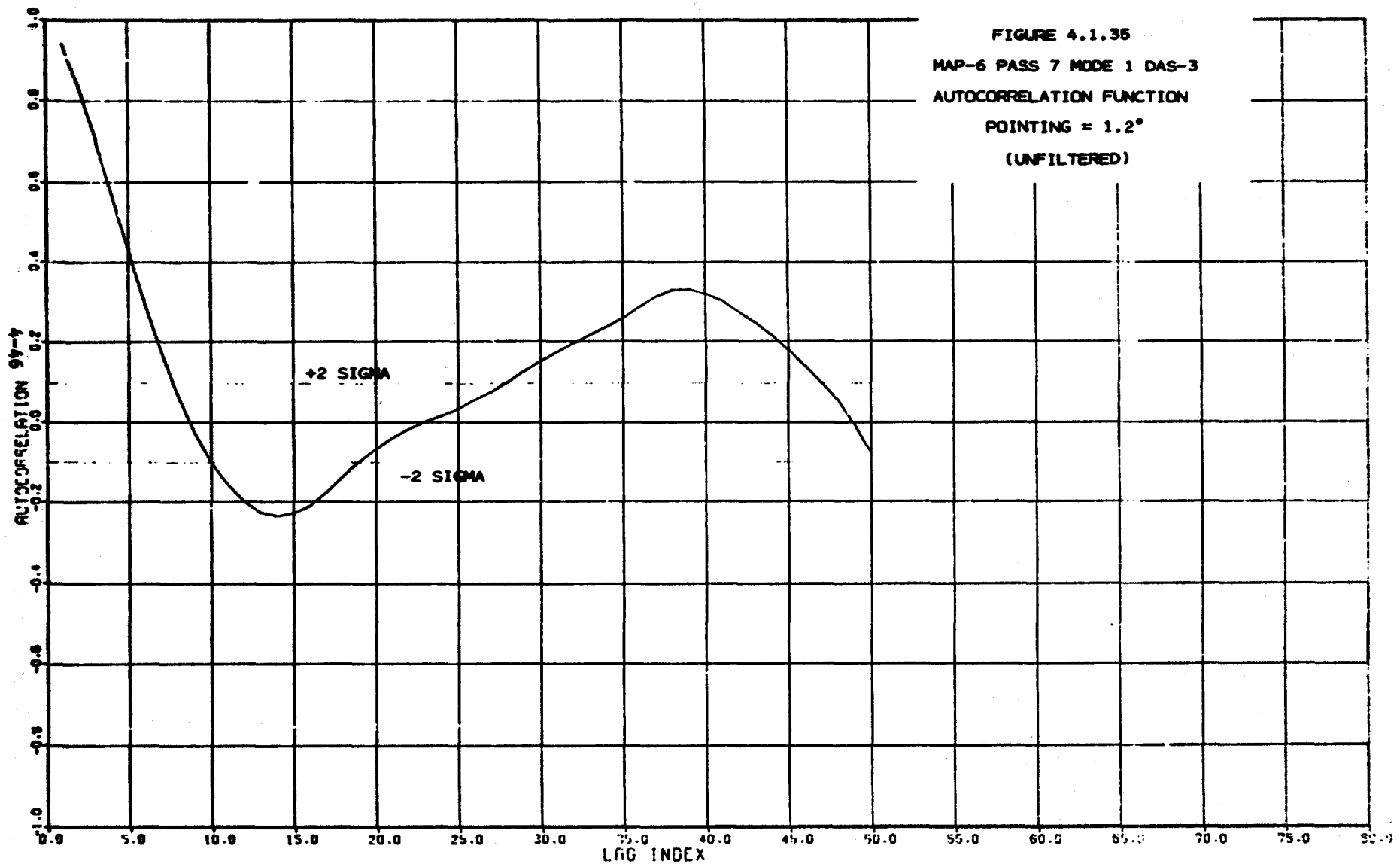
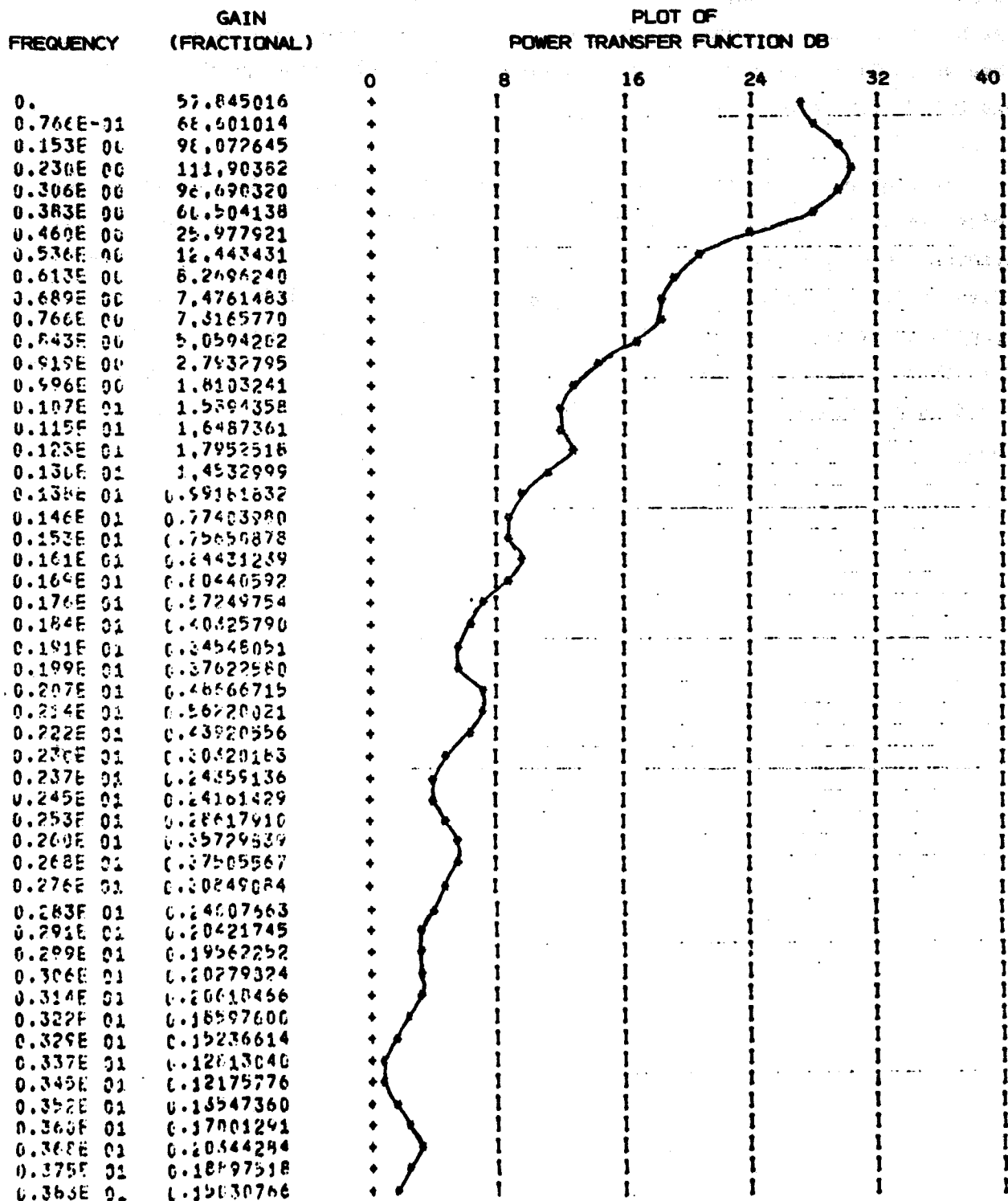


FIGURE 4.1.36  
AUTOREGRESSIVE MODEL  
MAP-6 PASS-7 MODE-1 DAS-3  
(UNFILTERED)



#### 4.2 Mode 3 Results

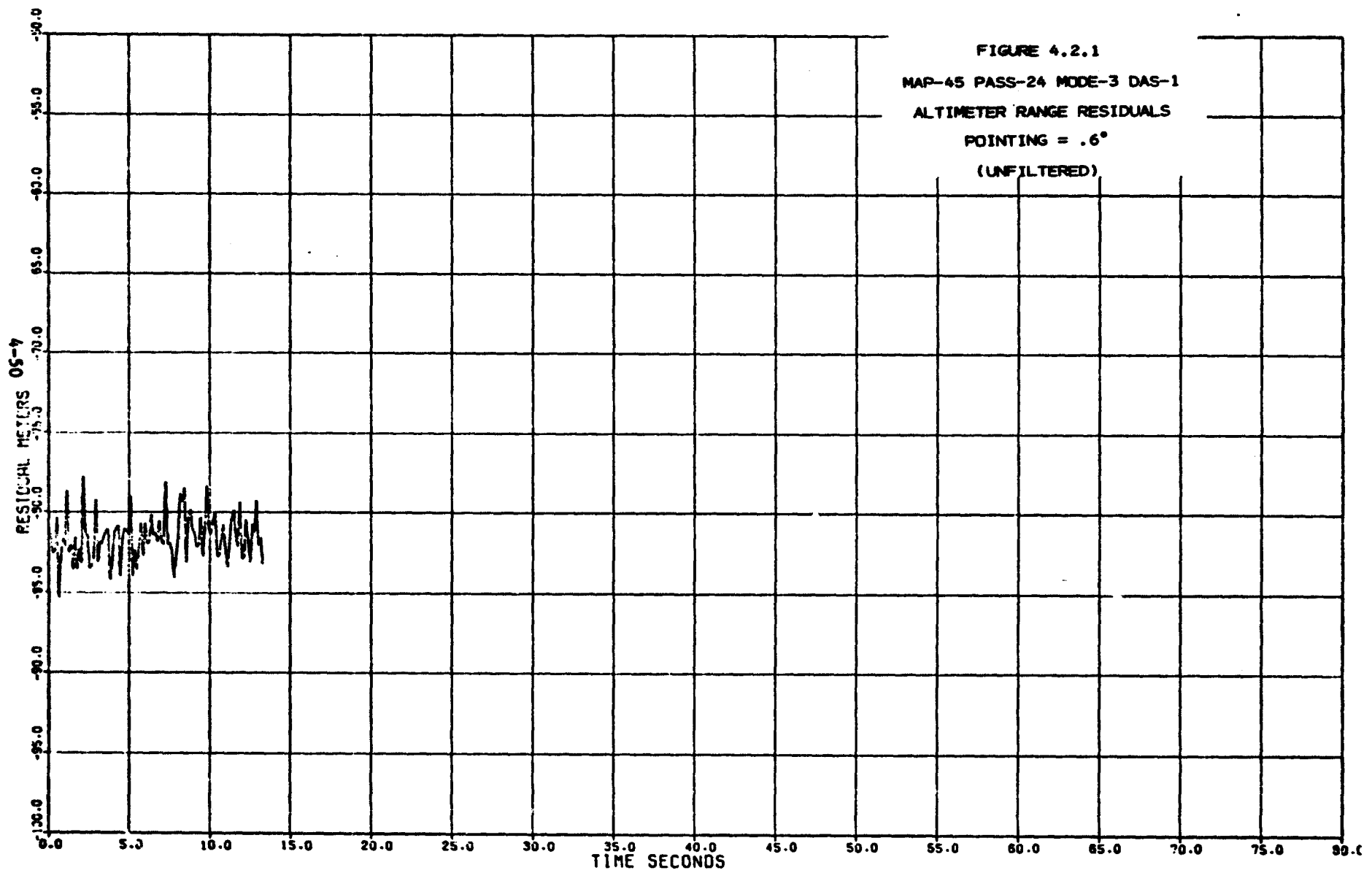
From Table 2.1 the three Mode 3 data acquisition submodes are 16.64 seconds, 26.0 seconds and 101.92 seconds long. Submode DAS-1 is a shortened replication of Mode 1 DAS-1. During DAS-2 only one of the transmitted pulse pairs is used for deriving range information making the measurement process essentially the same as in DAS-1. DAS-3 features a narrower pulse (20 nanoseconds) than DAS-1 and DAS-2 (100 nanoseconds).

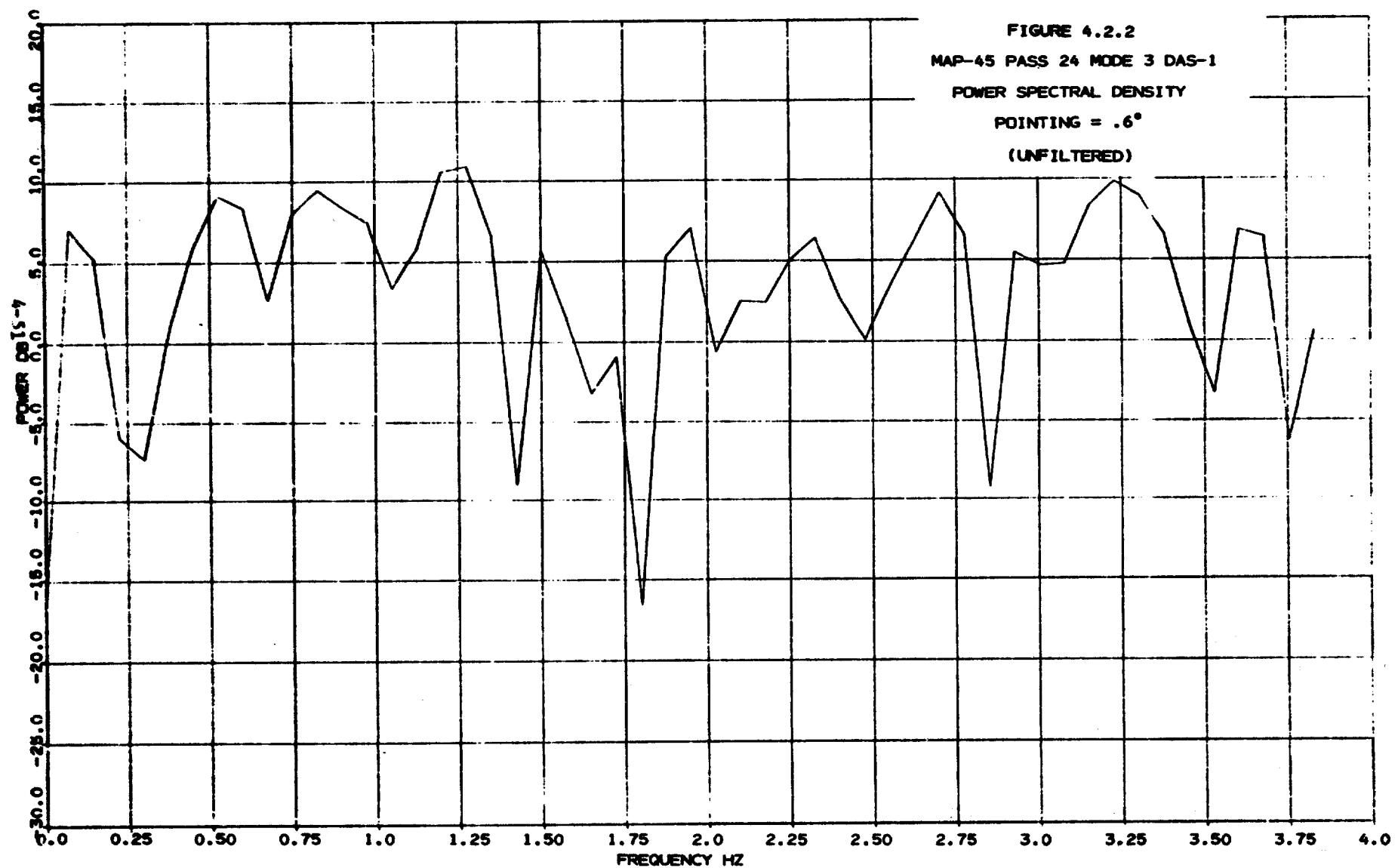
Tabulation of the Mode 3 statistics (Table 4.3) shows little change in the noise sigmas for successive submodes at low, moderate and high pointing angles. Examination of the power spectral plots for low and moderate pointing angles (Figures 4.4.2, 4.4.6, 4.4.10, 4.4.14, 4.4.18 and 4.4.22) shows that the power spectra are relatively flat with occasional peaks which are several Db above the ambient level. The high pointing angle (Map 12) power spectra (Figures 4.2.26, 4.2.30 and 4.2.34) do not appear to have as much attenuation of the higher frequencies as do the high pointing angle spectra from Mode 1 and Mode 3.

TABLE 4.3  
MODE 3 DETAIL ANALYSIS

MAP	PASS	SUB-MODE	POINT (DEGS)	SAMP. SIZE	MEAN (MTRS)	SIGMA (MTRS)	F STATISTIC	NORM. TEST	SIG. FREQ. BANDS (HZ)	SIGNIFICANT AUTOCORRELATION COEFFICIENTS
45	24	DAS-1	<.6°	104	-81.6	1.45	.952	.990	NONE	18
		DAS-2		114	-70.4	1.44	1.59	.182	.0685	1,2,6,7
		*DAS-3		435	-85.7	1.40	.869	.929	.723-.778	2,15
10	8	DAS-1	.75°	112	-29.8	1.44	.581	.704	.349	NONE
		DAS-2		170	-30.2	1.42	.621	.836	1.65	1,14
		*DAS-3		198	-31.7	1.40	.318	.624	NONE	5,13
12	9	DAS-1	1.1°	108	50.4	2.79	4.28	.926	.940	1
		DAS-2		176	50.9	2.25	.100	.451	.133 .488	1
		DAS-3		526	52.0	2.69	1.30	.972	0-.061 .458-.569 .687-.742	1,2,11,12

\*INDICATES DATA WAS FILTERED WITH 99 POINT QUADRATIC MIDPOINT HIGH PASS FILTER.





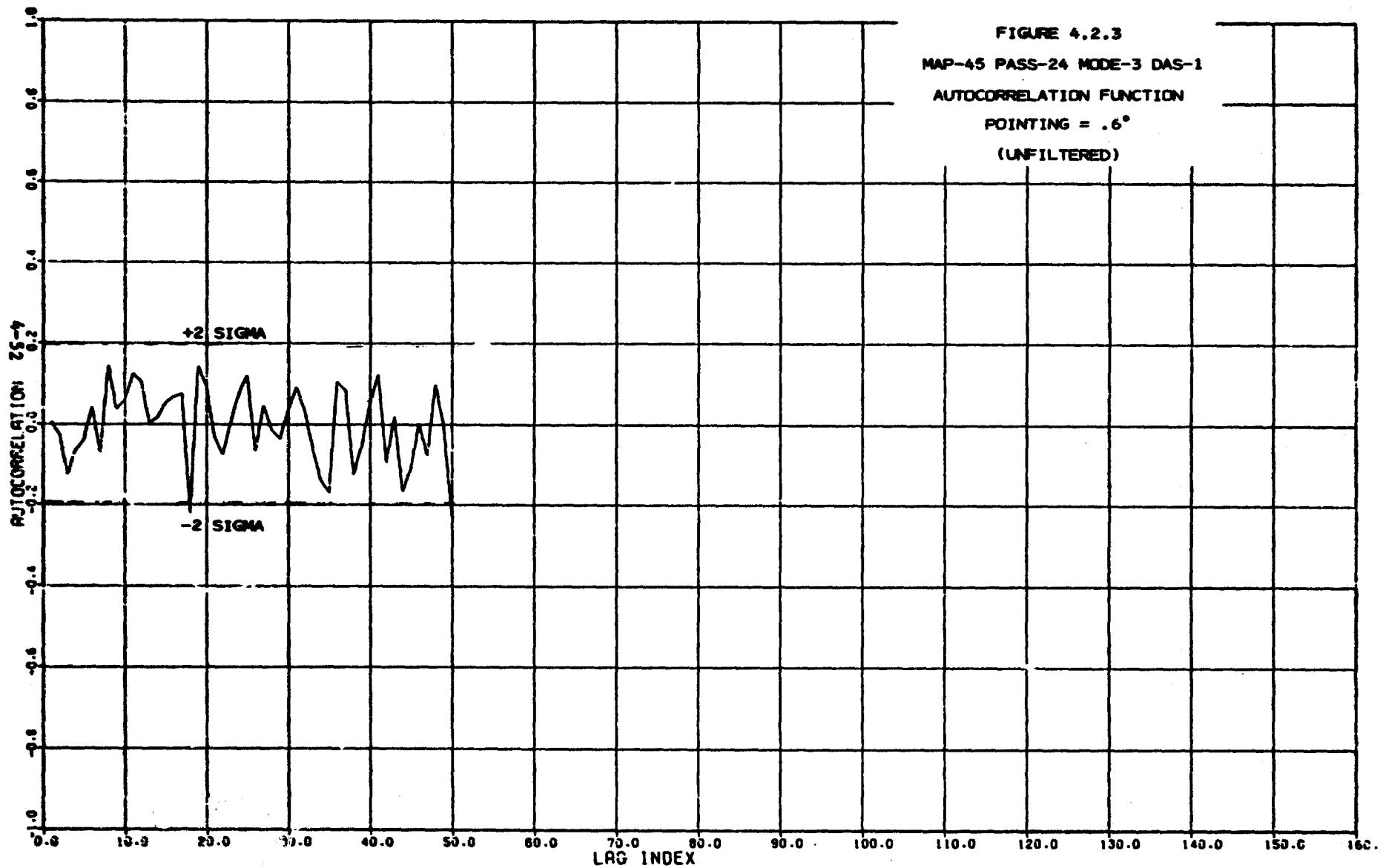


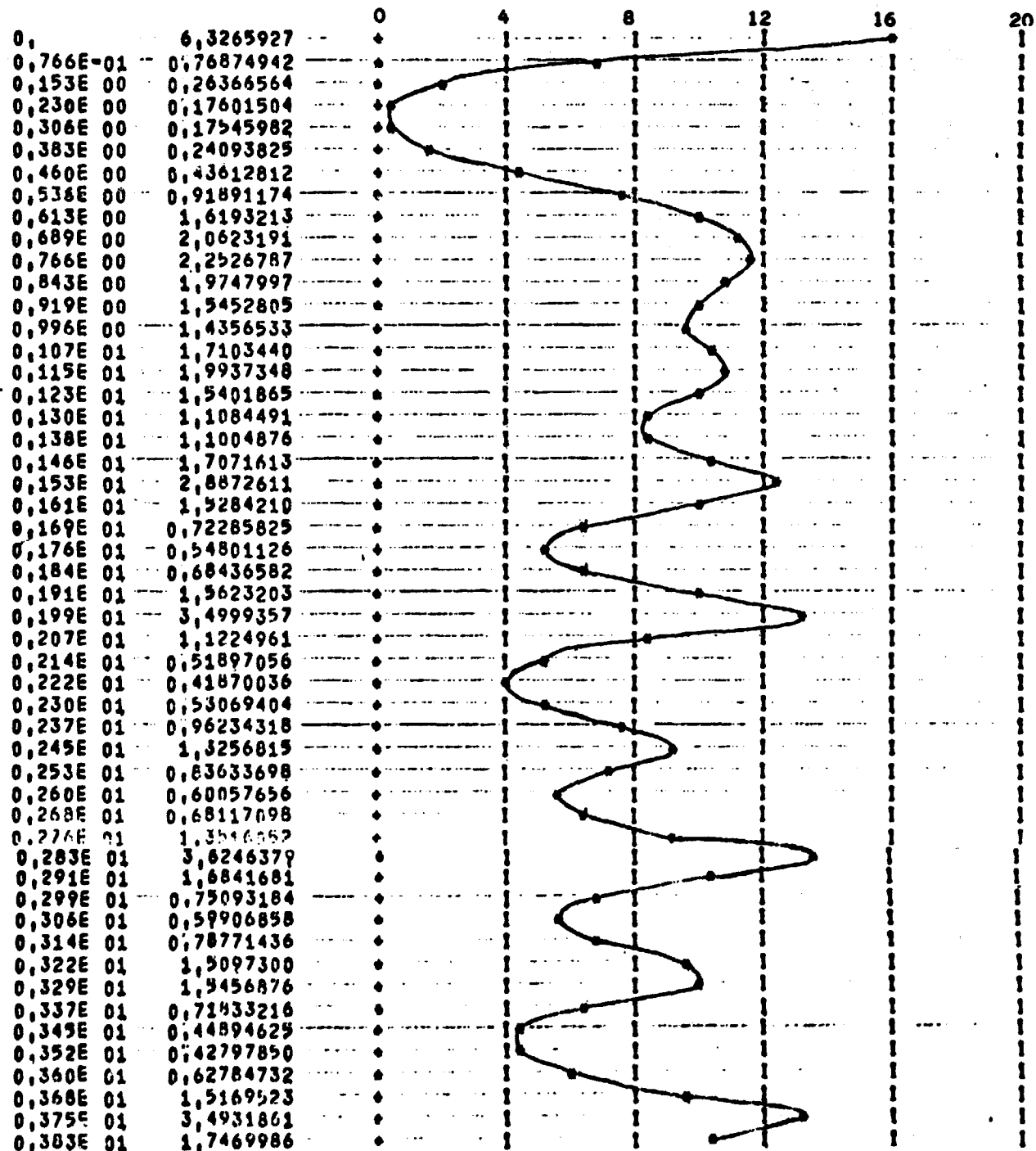
FIGURE 4.2.4  
AUTOREGRESSIVE MODEL

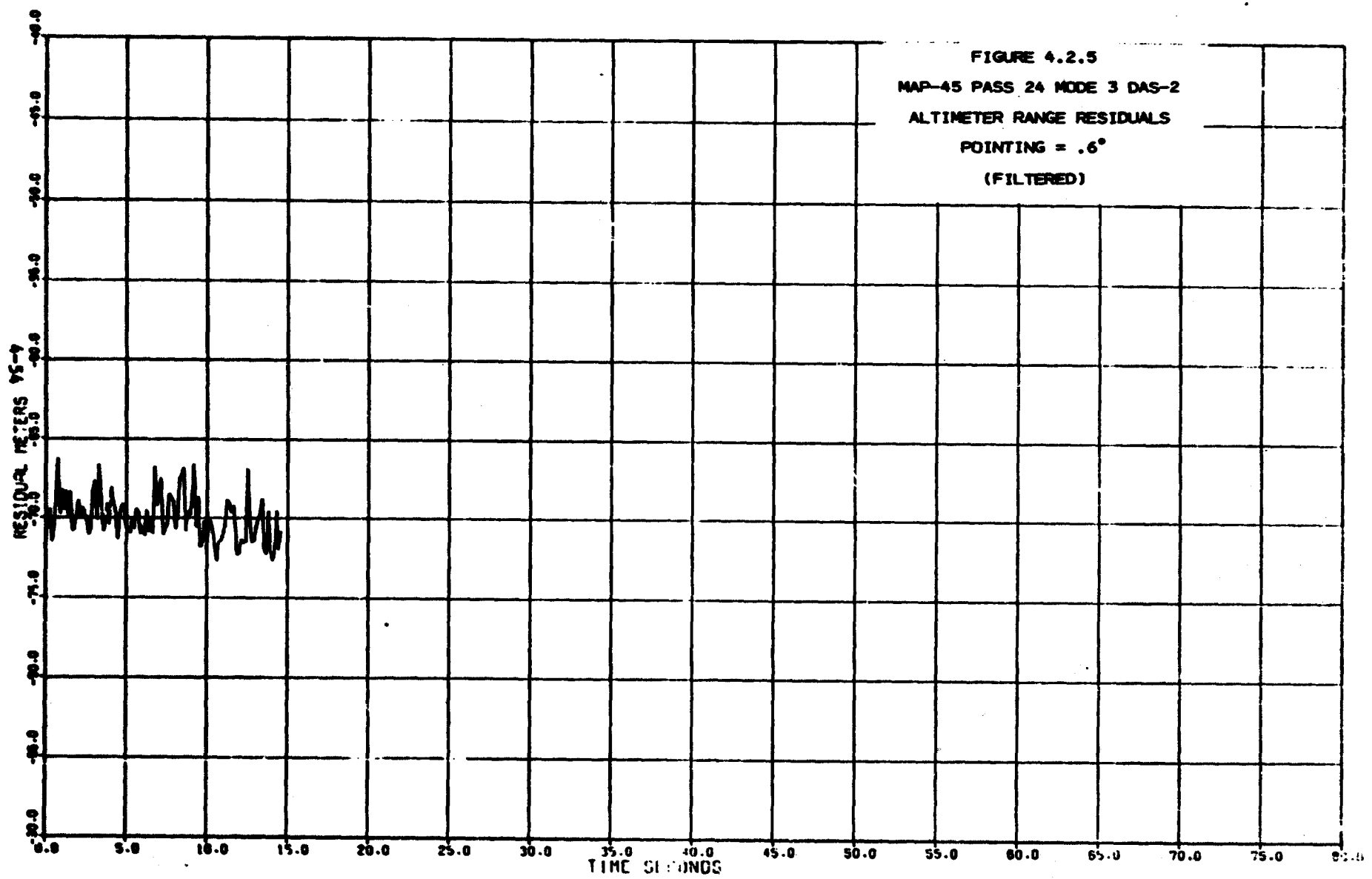
MAP-45 PASS-24 MODE-3 DAS-1

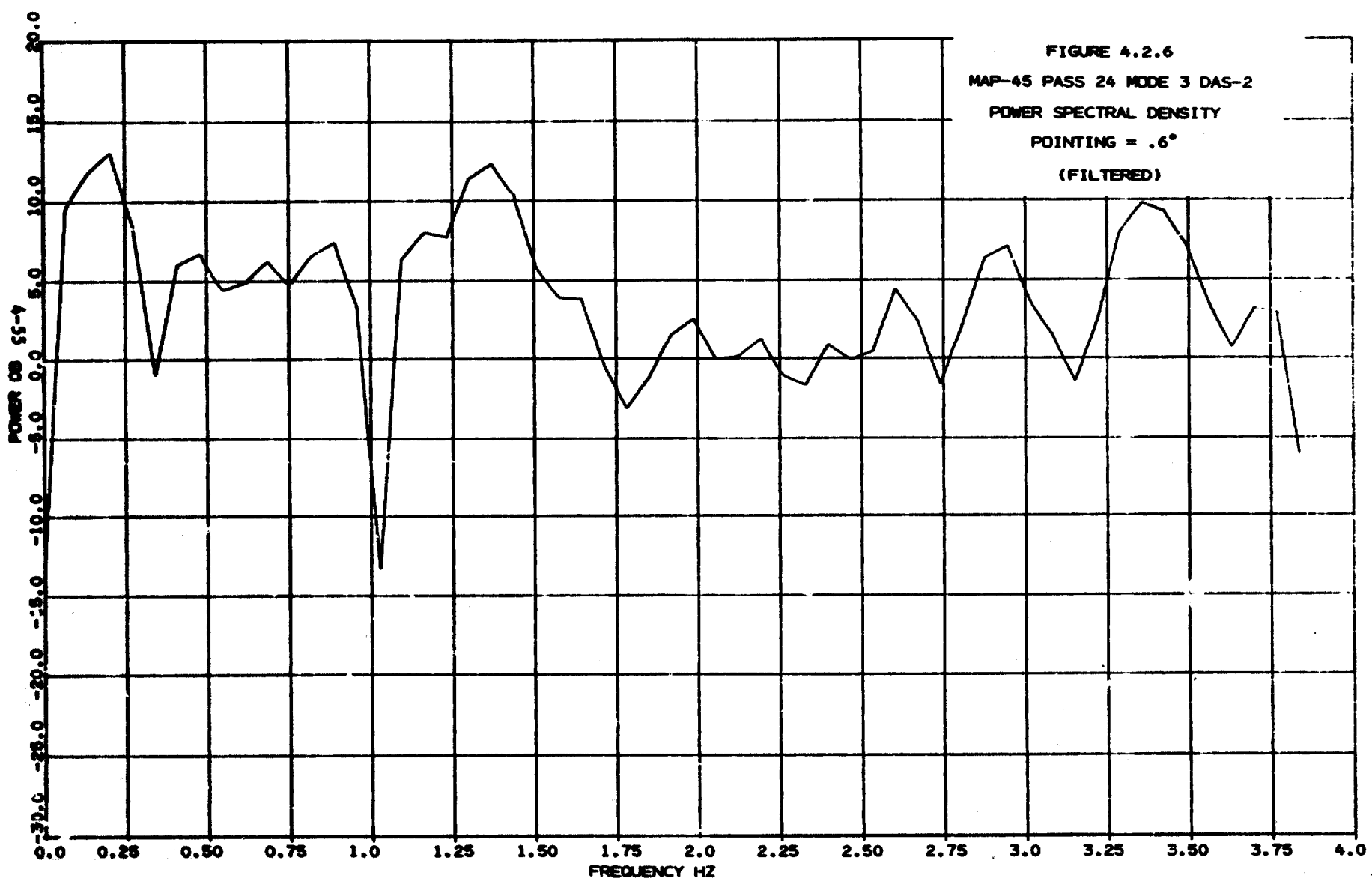
(UNFILTERED)

GAIN  
FREQUENCY (FRACTIONAL)

PLOT OF  
POWER TRANSFER FUNCTION DB







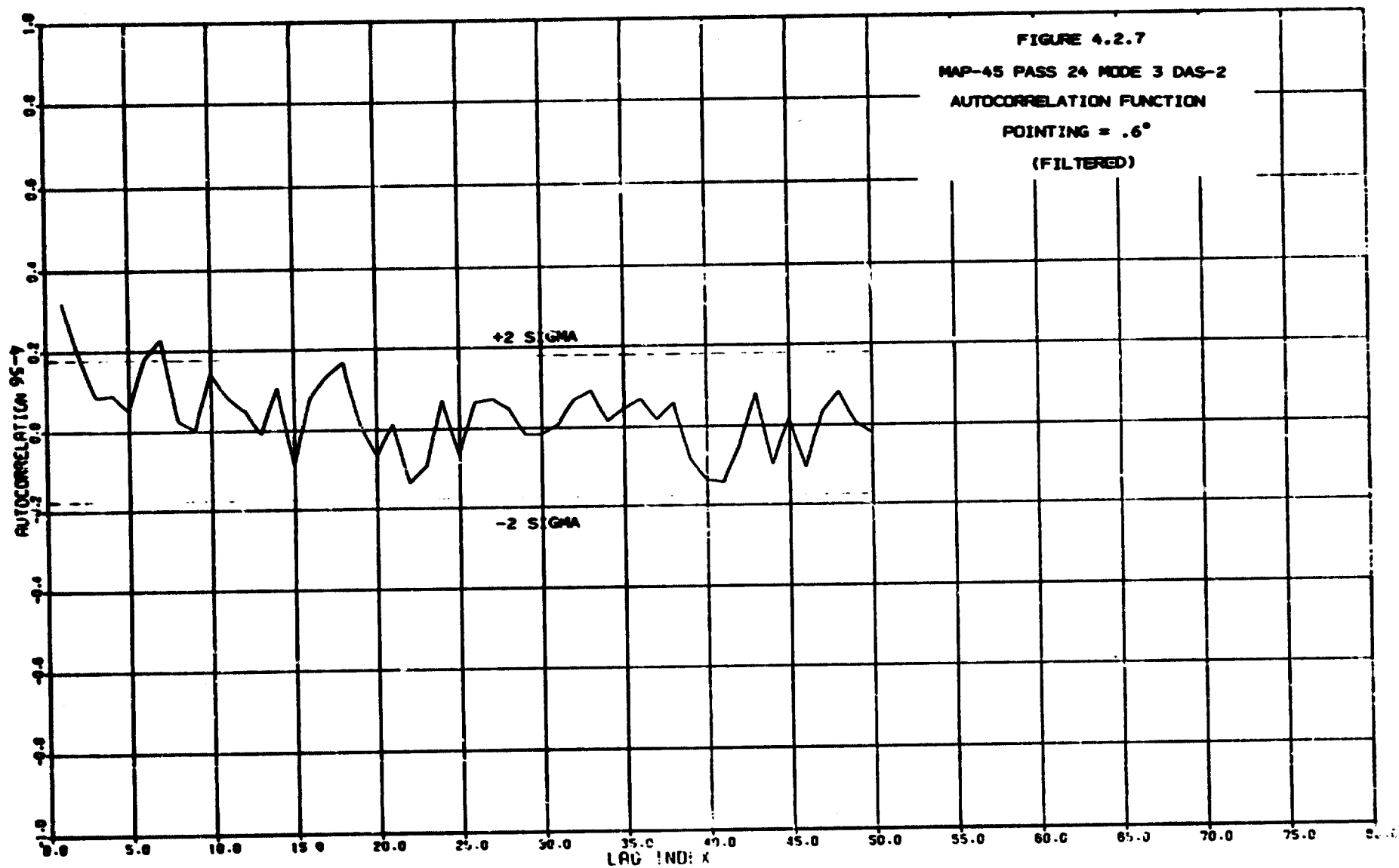
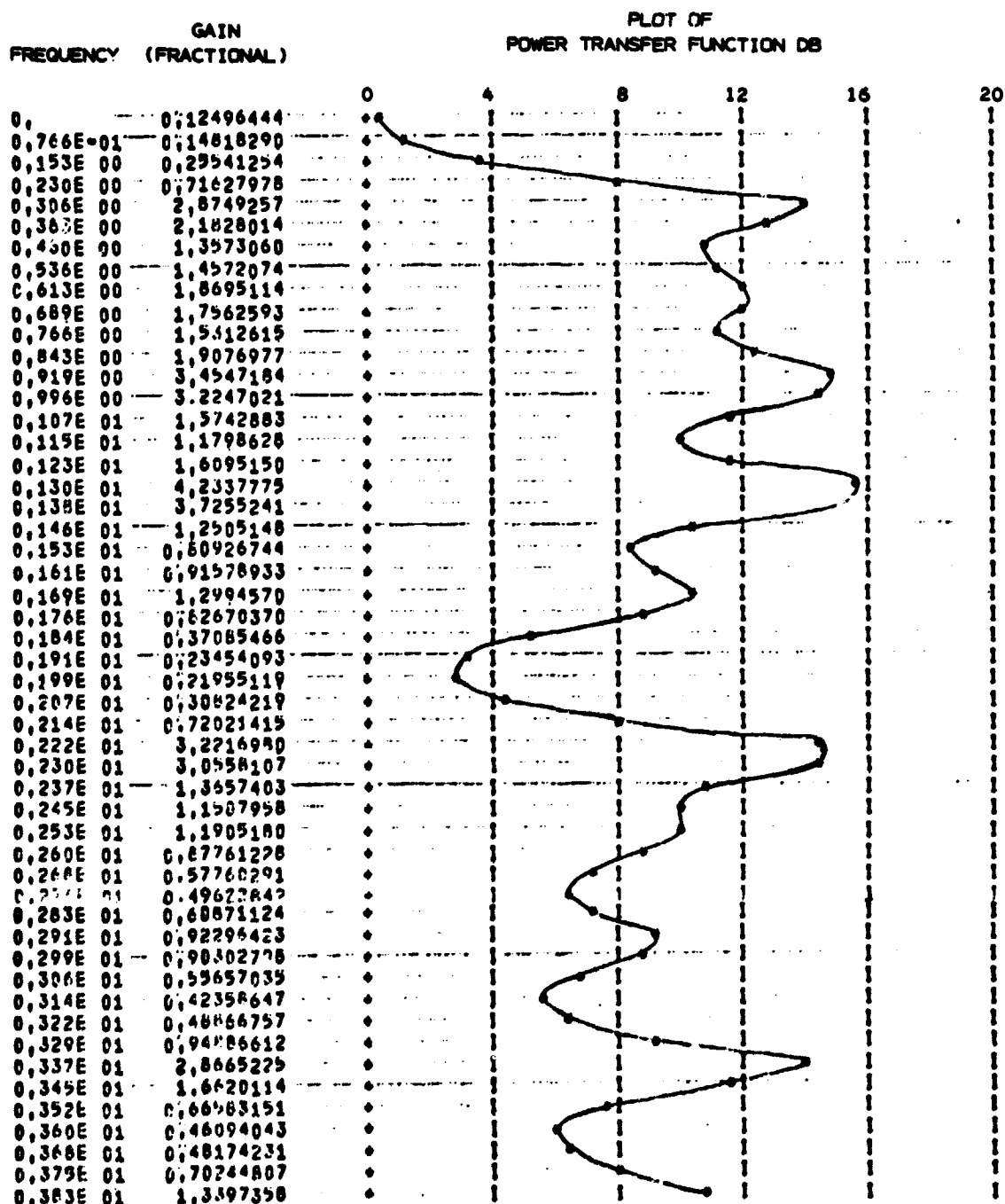
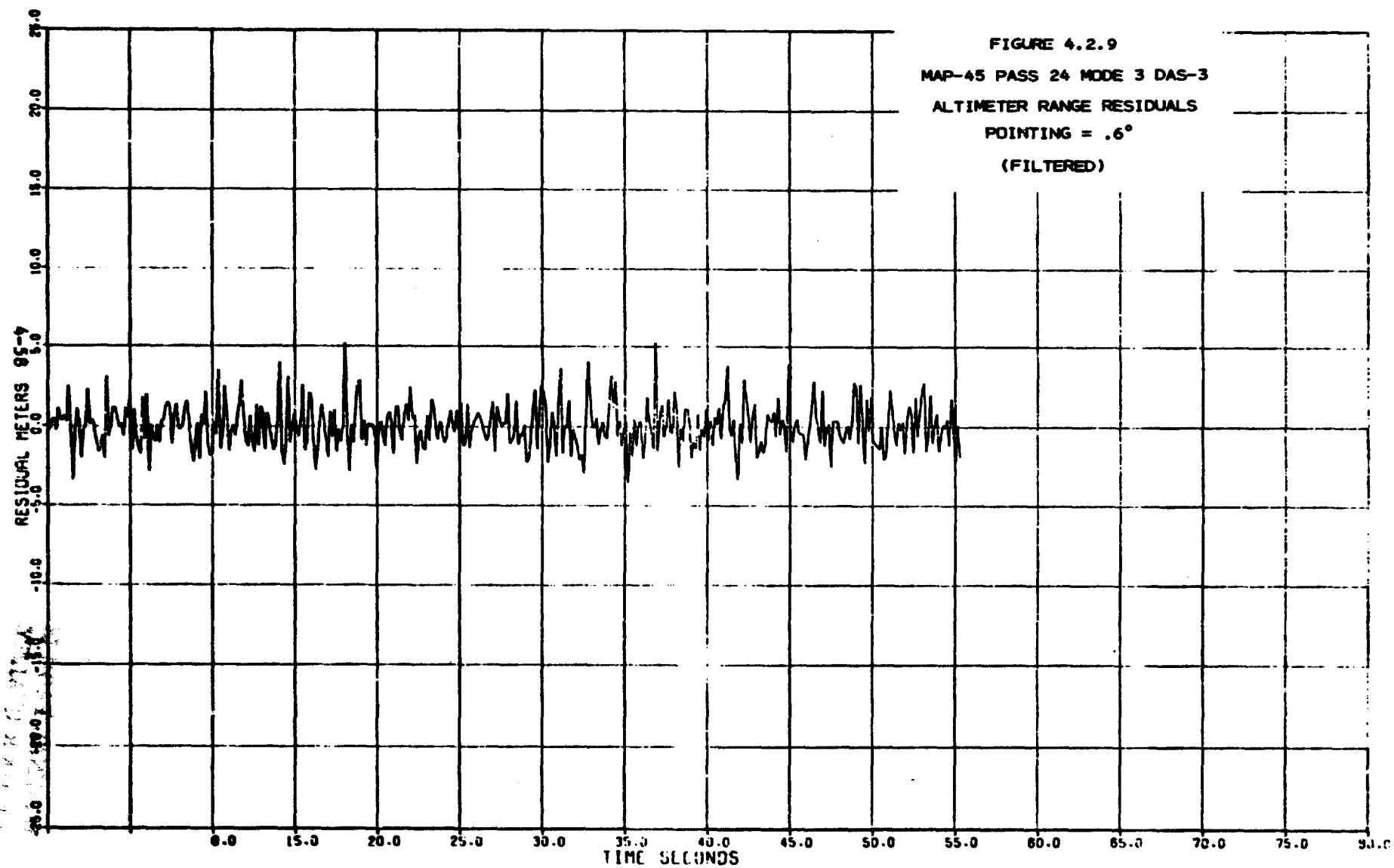


FIGURE 4.2.8  
AUTOREGRESSIVE MODEL

MAP-45 PASS-24 MODE-3 DAS-2  
(FILTERED)





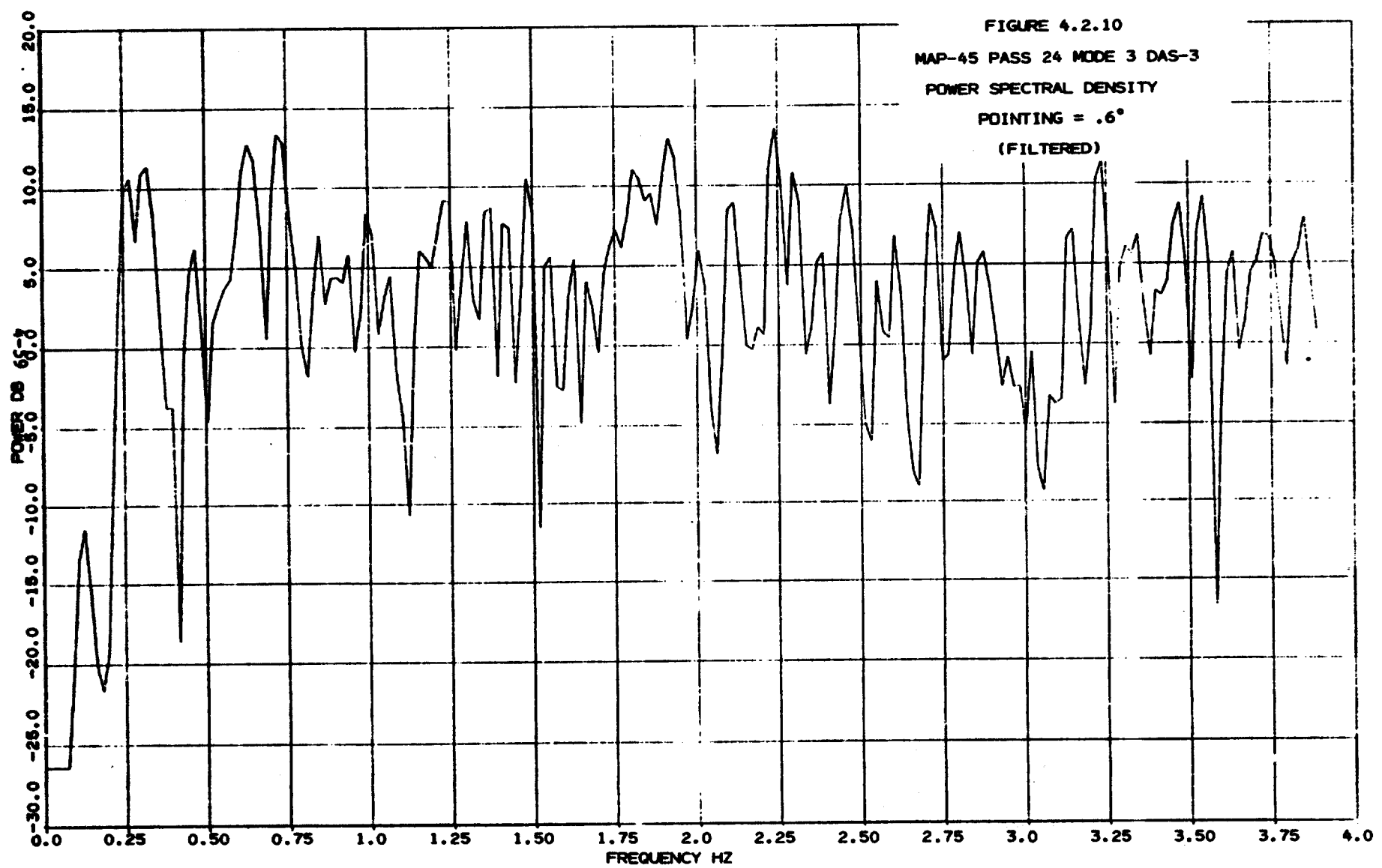


FIGURE 4.2.11

MAP-45 PASS 24 MODE 3 DAS-3  
AUTOCORRELATION FUNCTION  
POINTING =  $.6^\circ$   
(FILTERED)

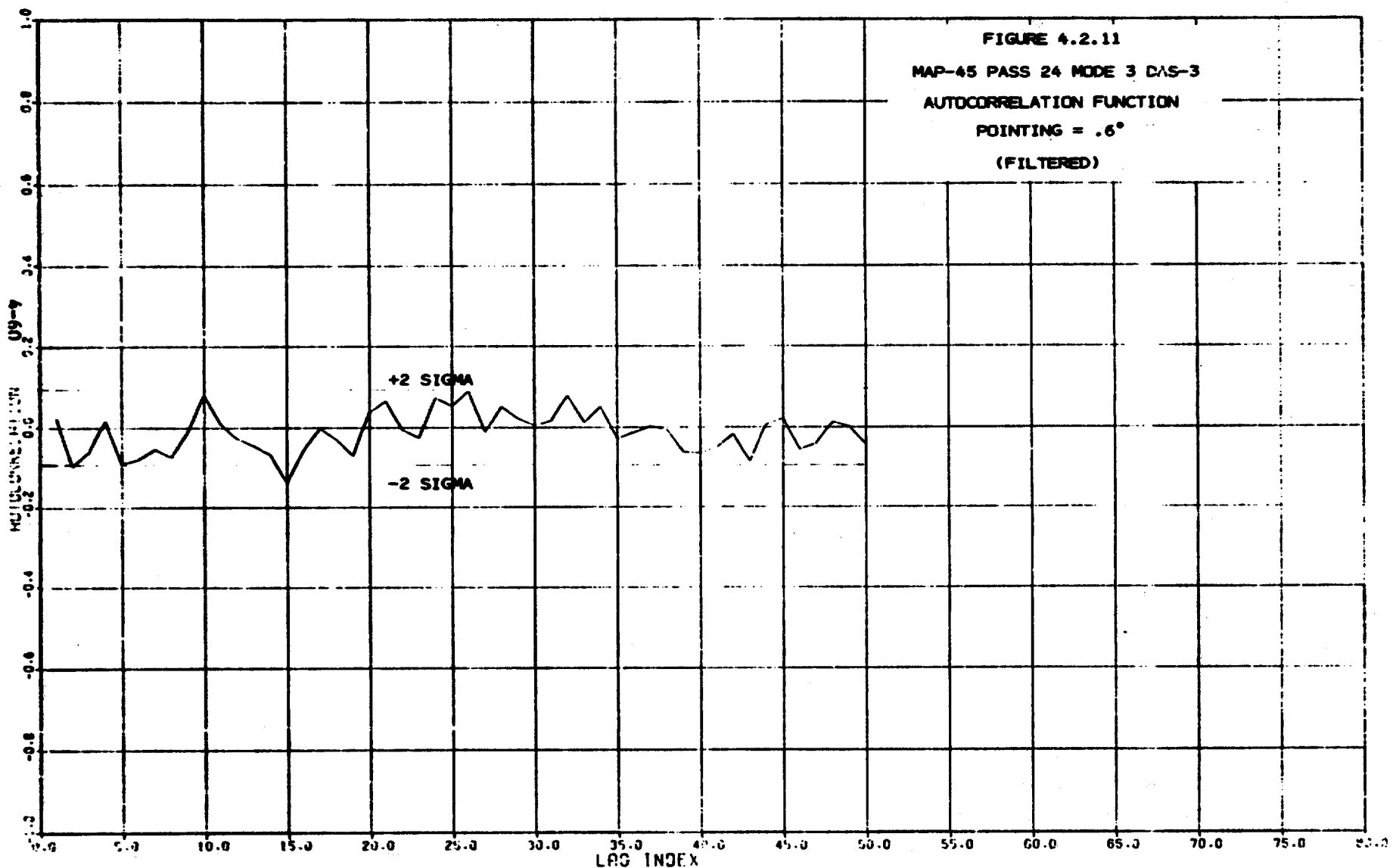


FIGURE 4.2.12  
AUTOREGRESSIVE MODEL

MAP-45 PASS-24 MODE-3 DAS-3  
(FILTERED)

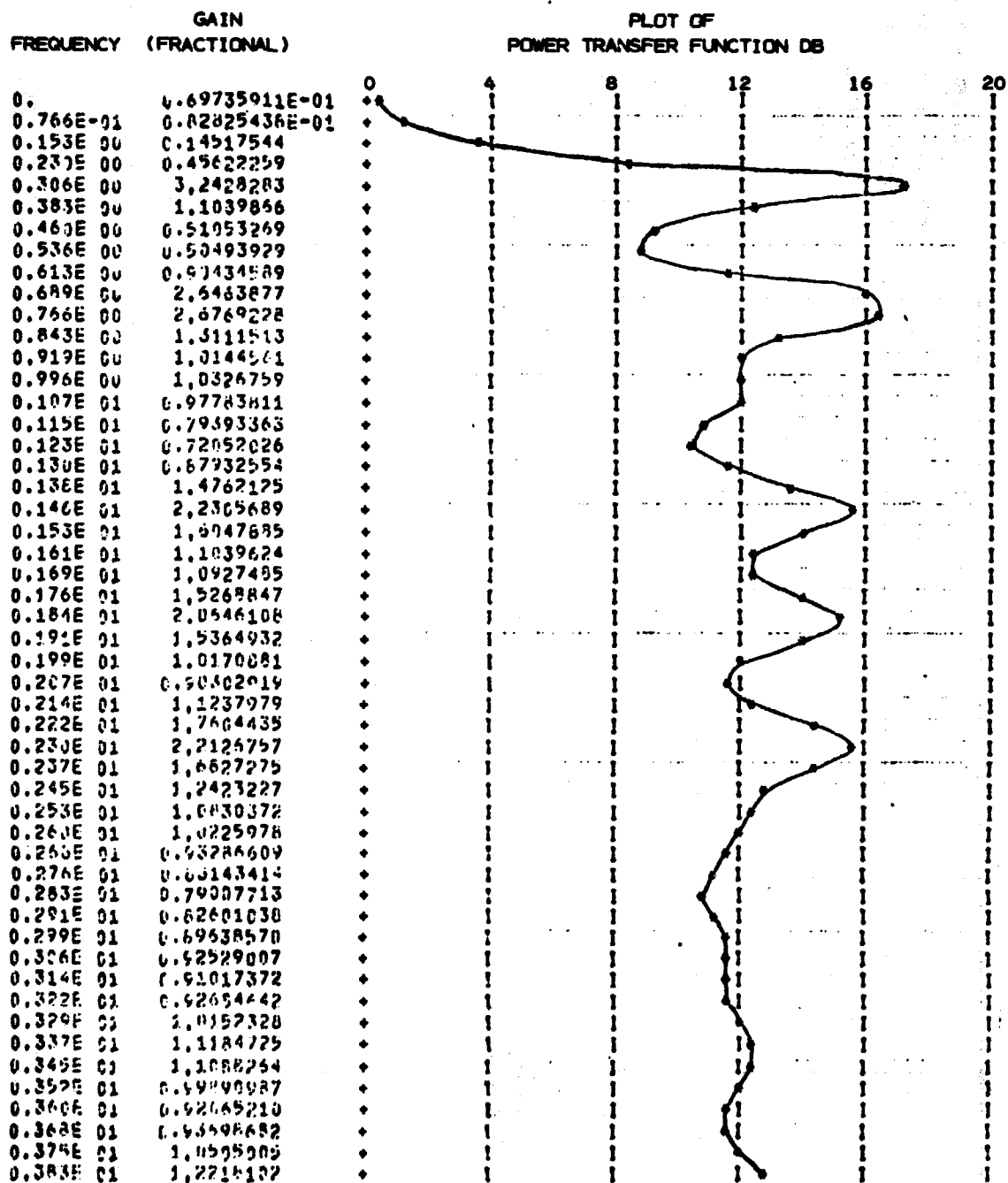


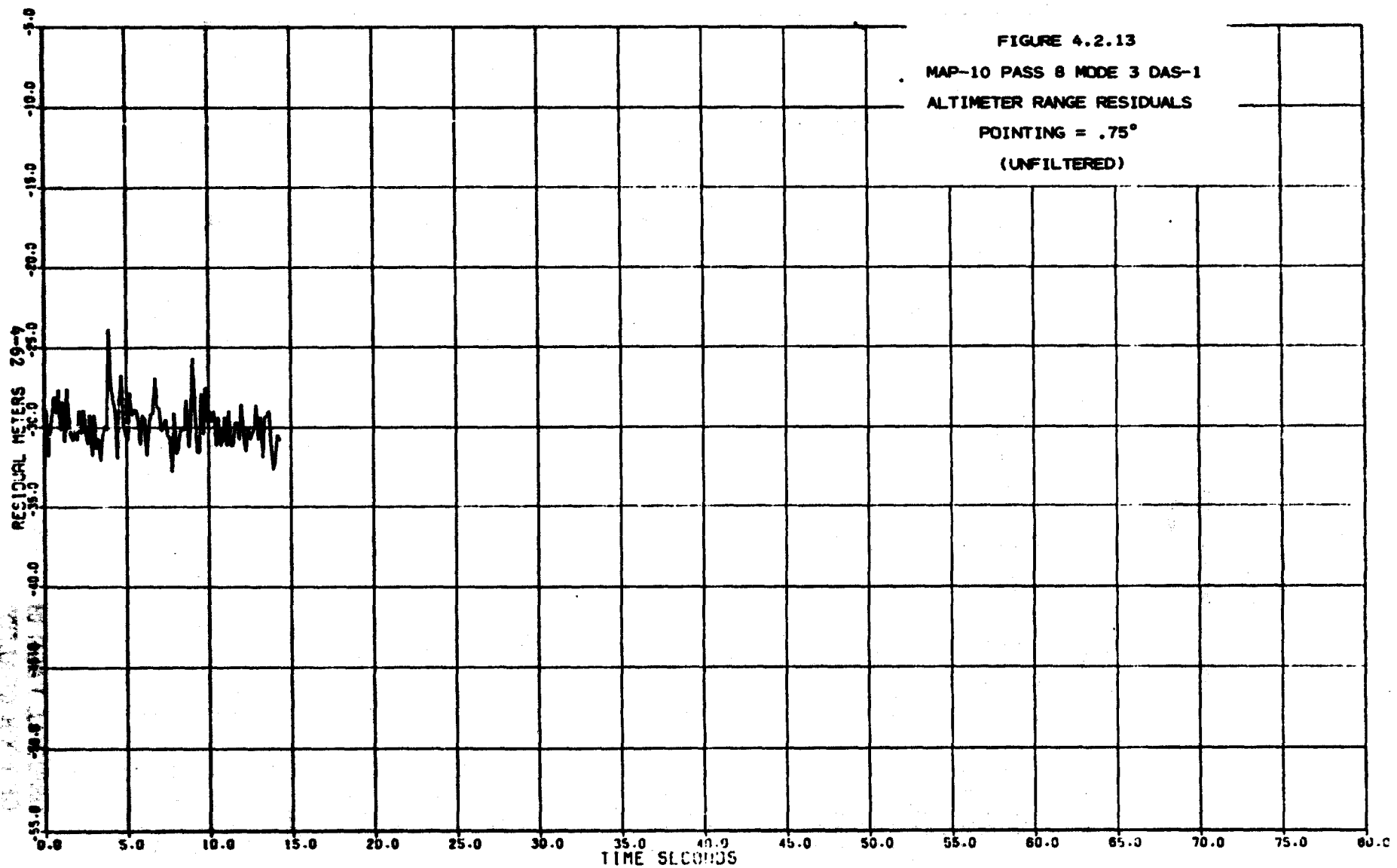
FIGURE 4.2.13

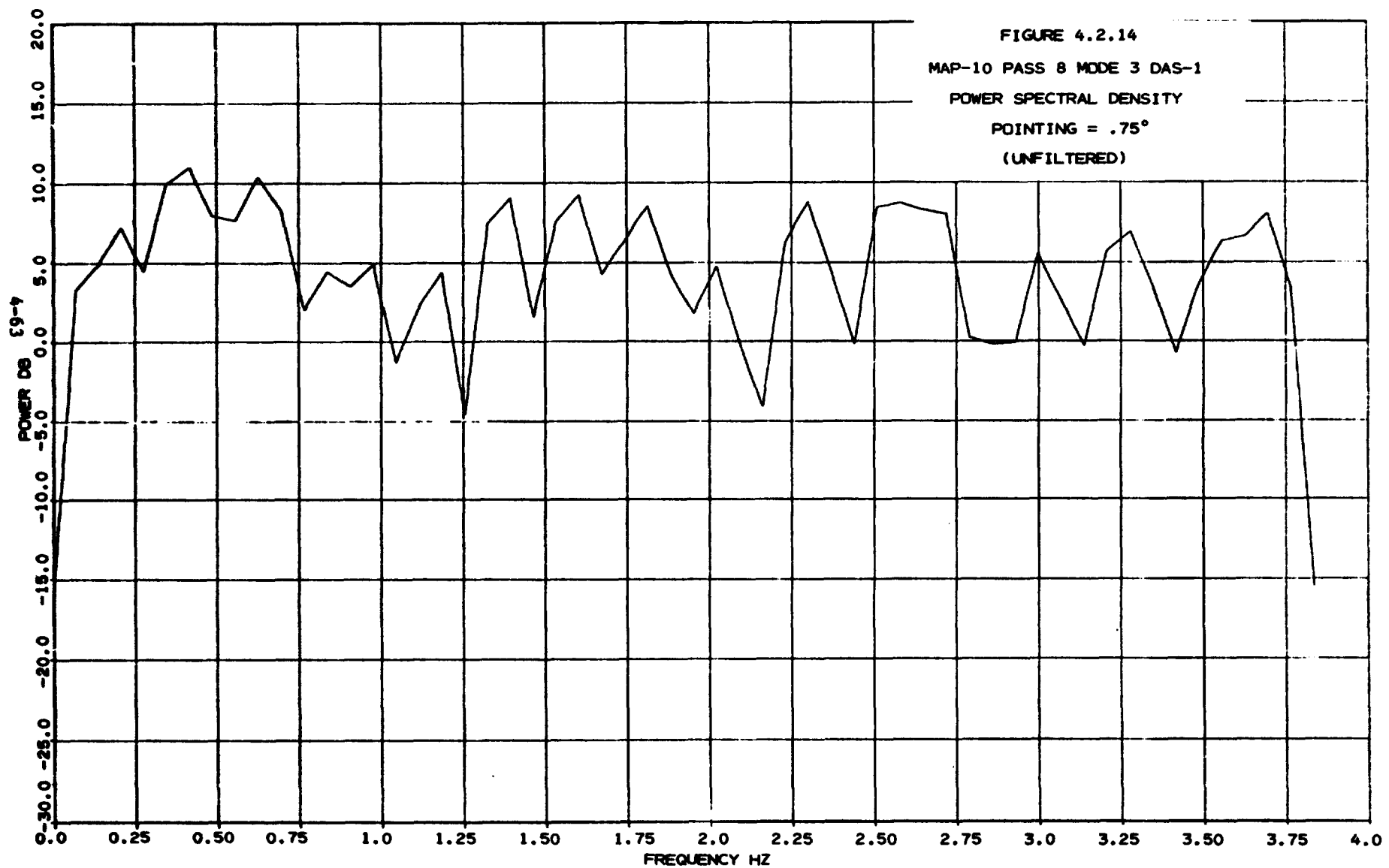
MAP-10 PASS 8 MODE 3 DAS-1

ALTIMETER RANGE RESIDUALS

POINTING =  $.75^\circ$

(UNFILTERED)





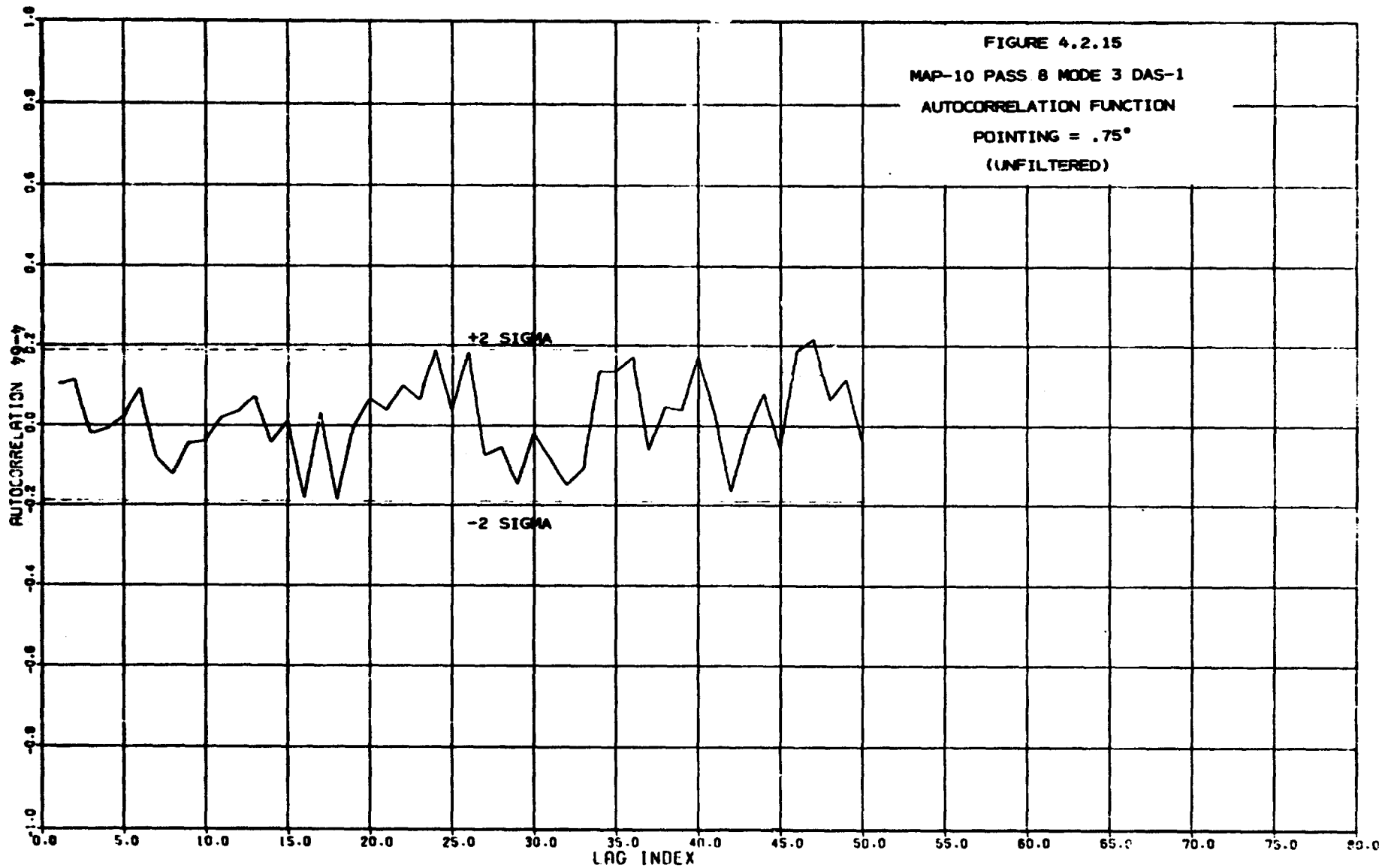
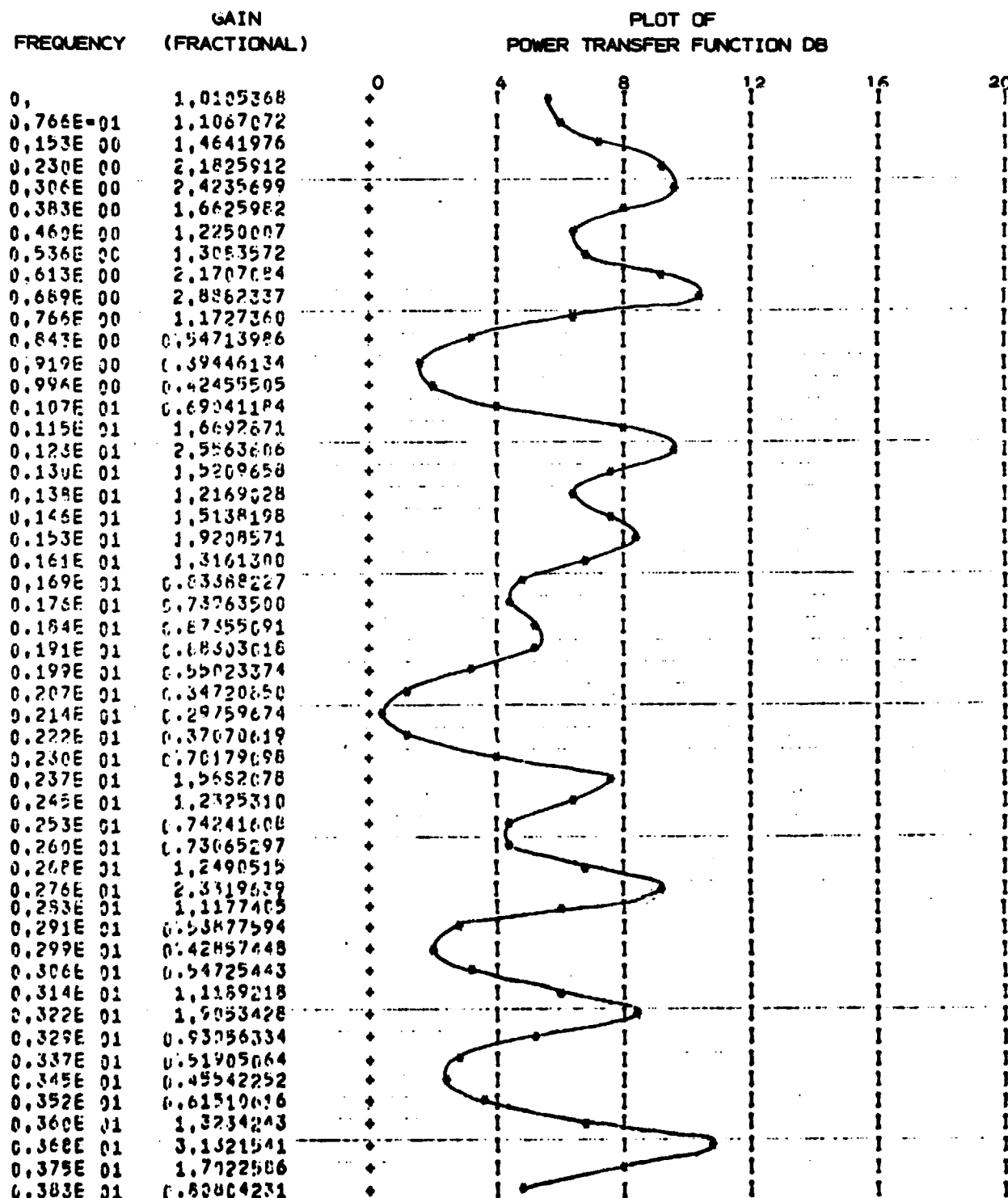
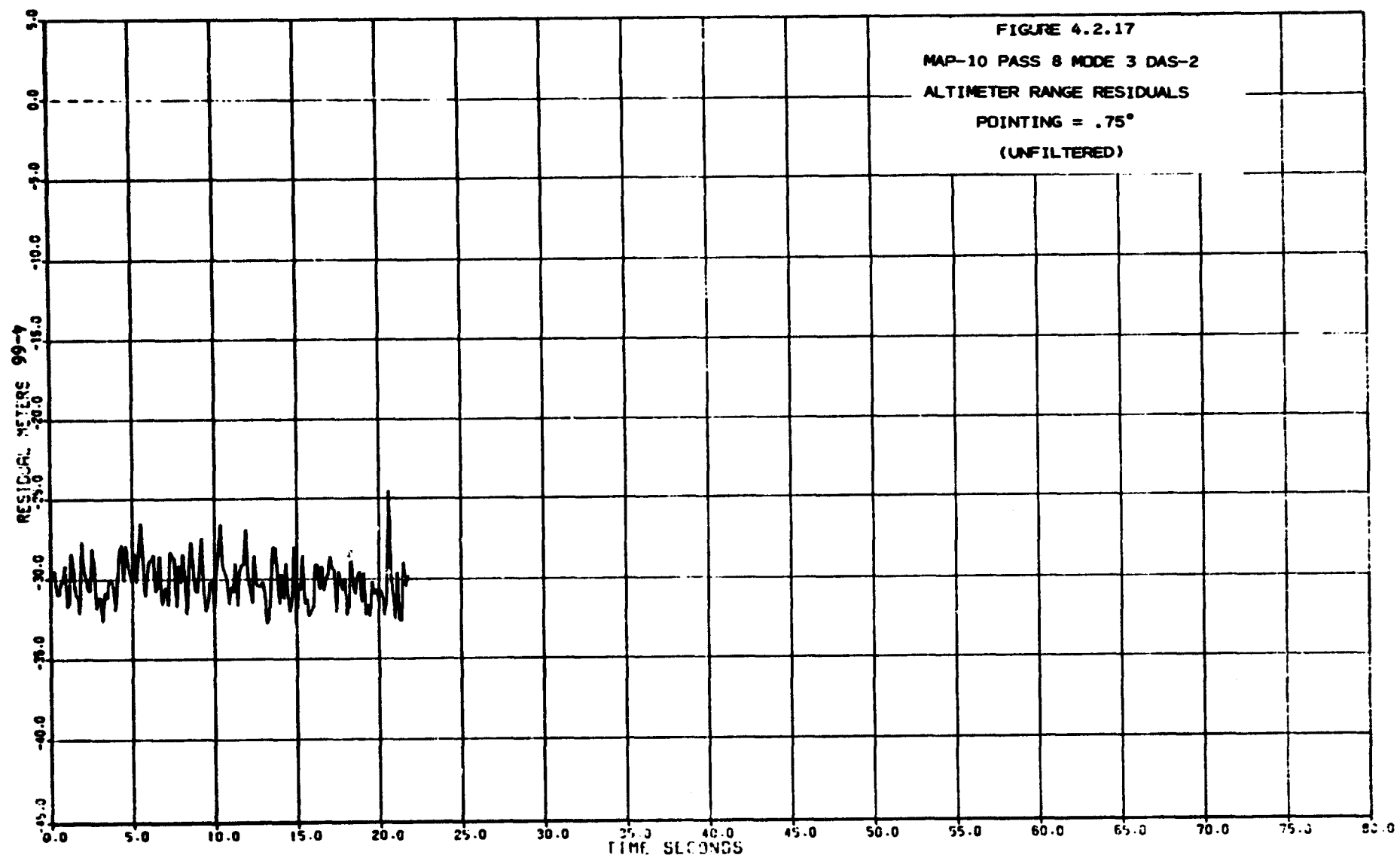
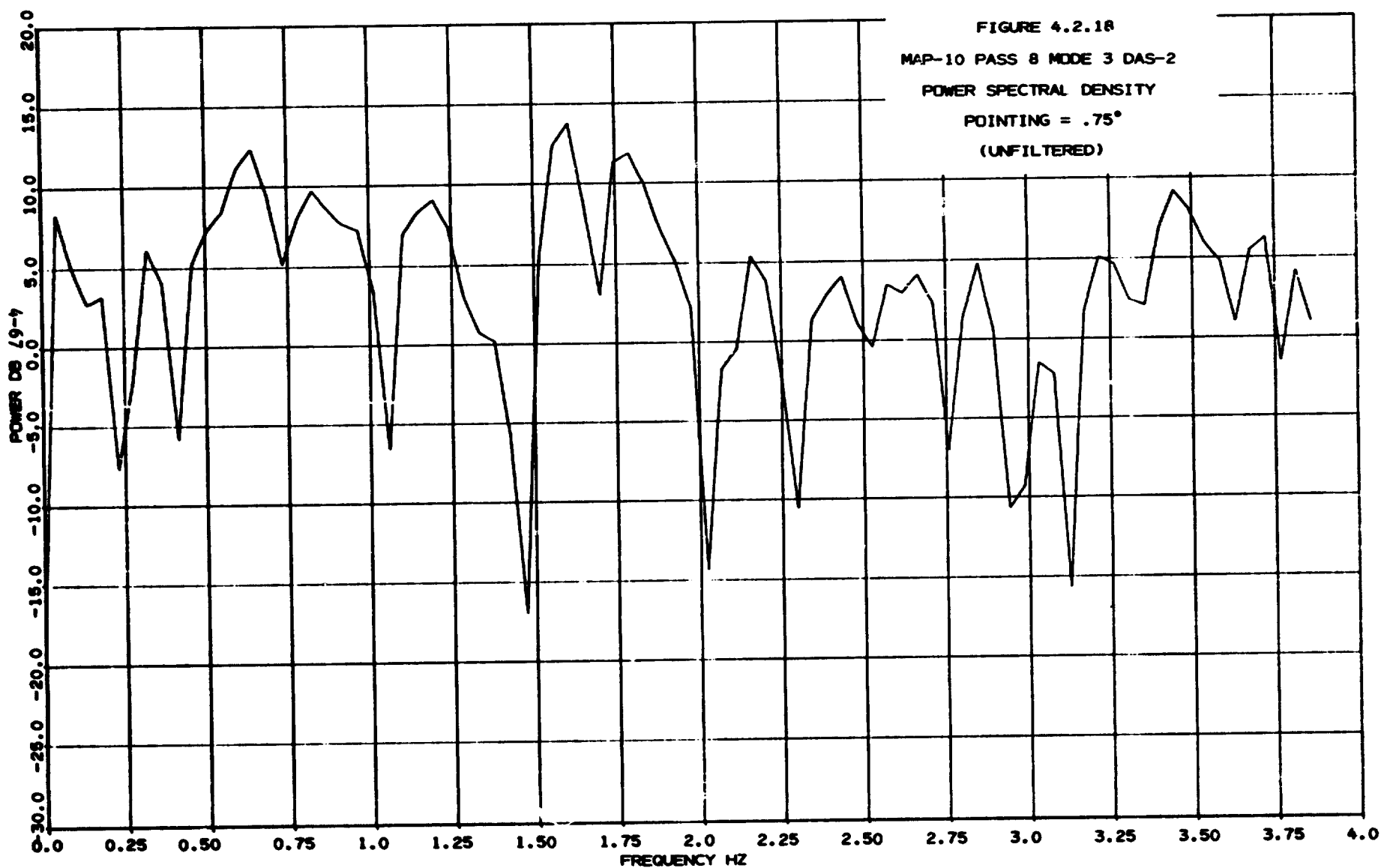


FIGURE 4.2.16  
AUTOREGRESSIVE MODEL  
MAP-10 PASS-8 MODE-3 DAS-1  
(UNFILTERED)







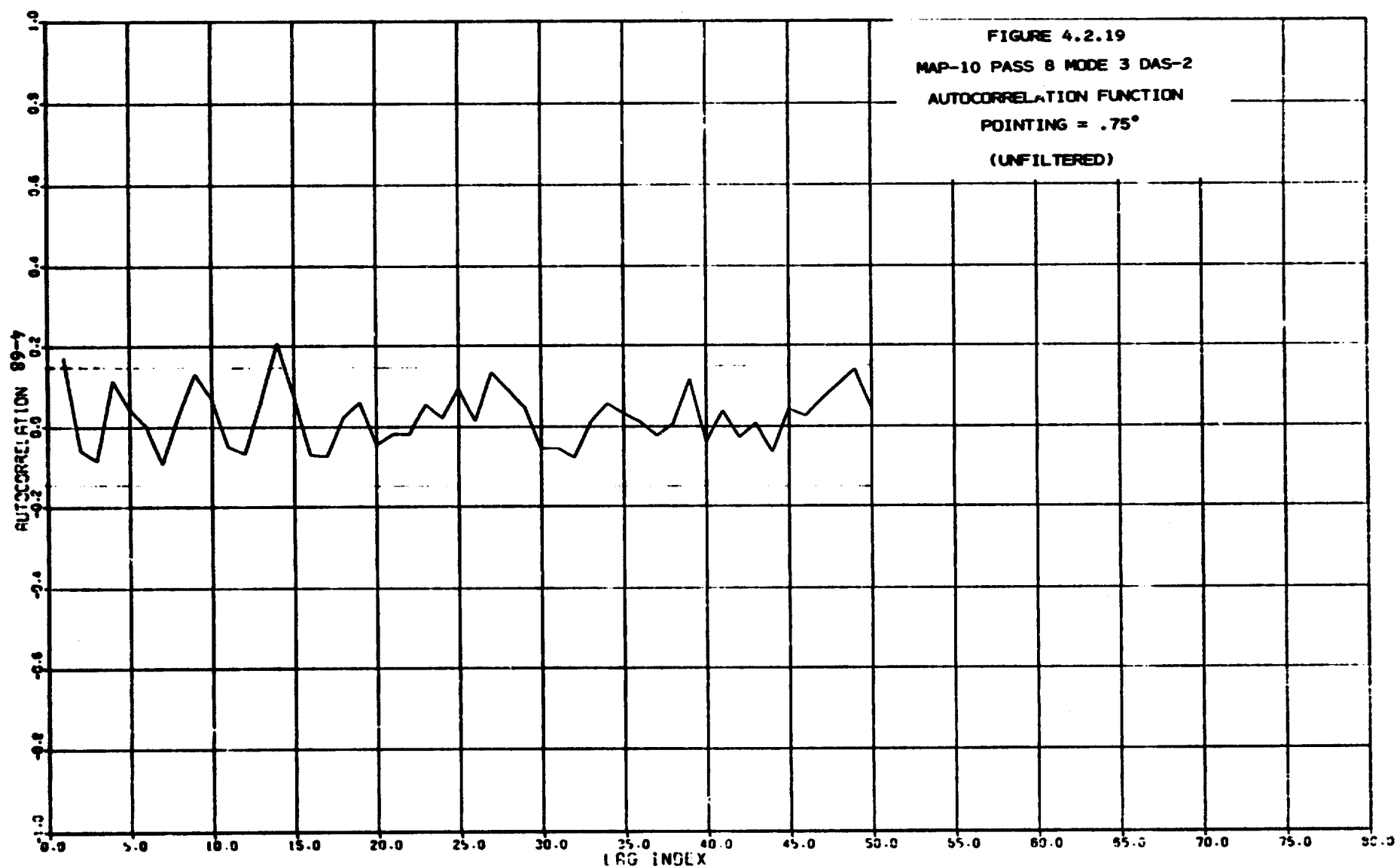


FIGURE 4.2.19

MAP-10 PASS 8 MODE 3 DAS-2

AUTOCORRELATION FUNCTION

POINTING =  $.75^\circ$

(UNFILTERED)

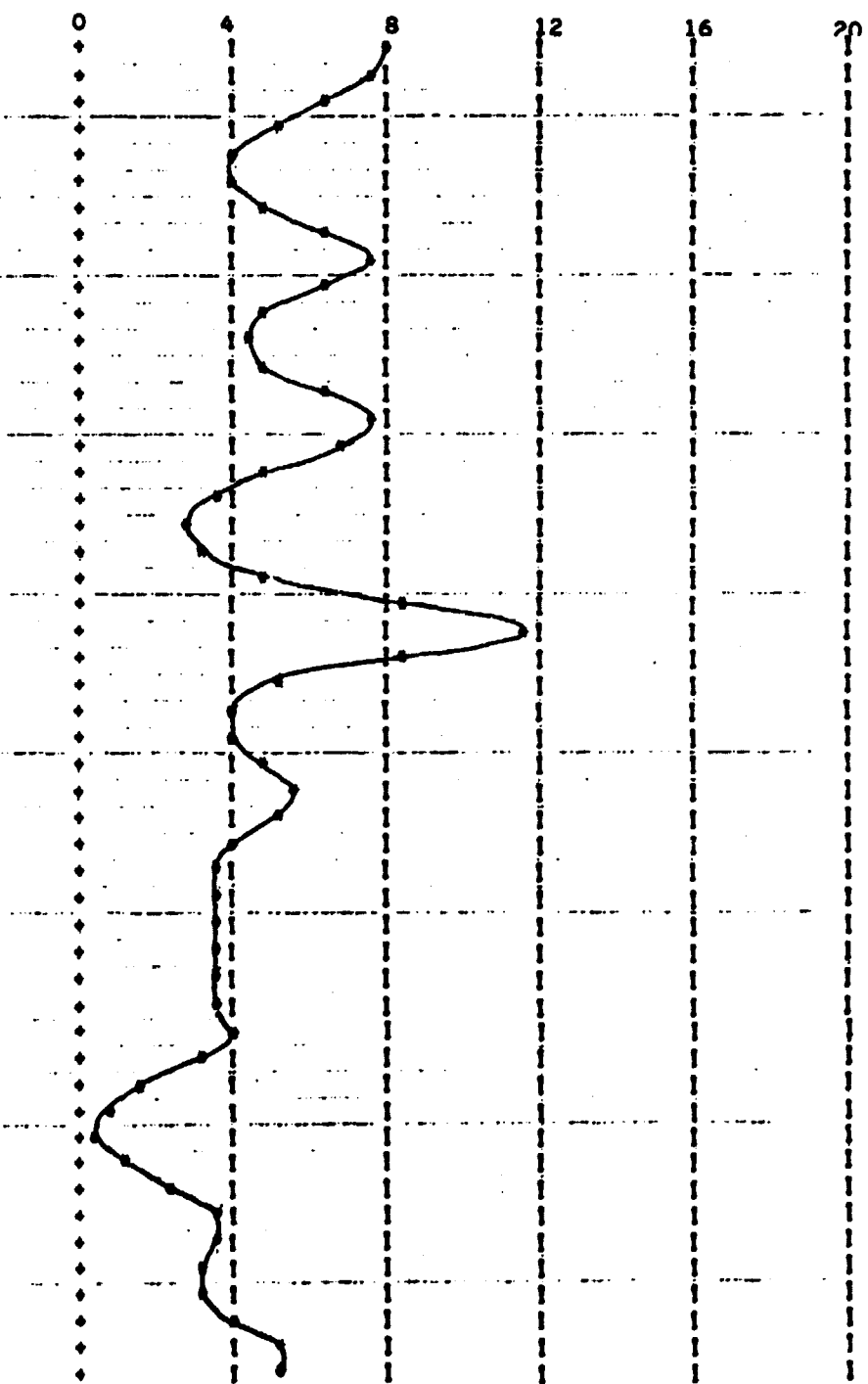
FIGURE 4.2.20  
AUTOREGRESSIVE MODEL

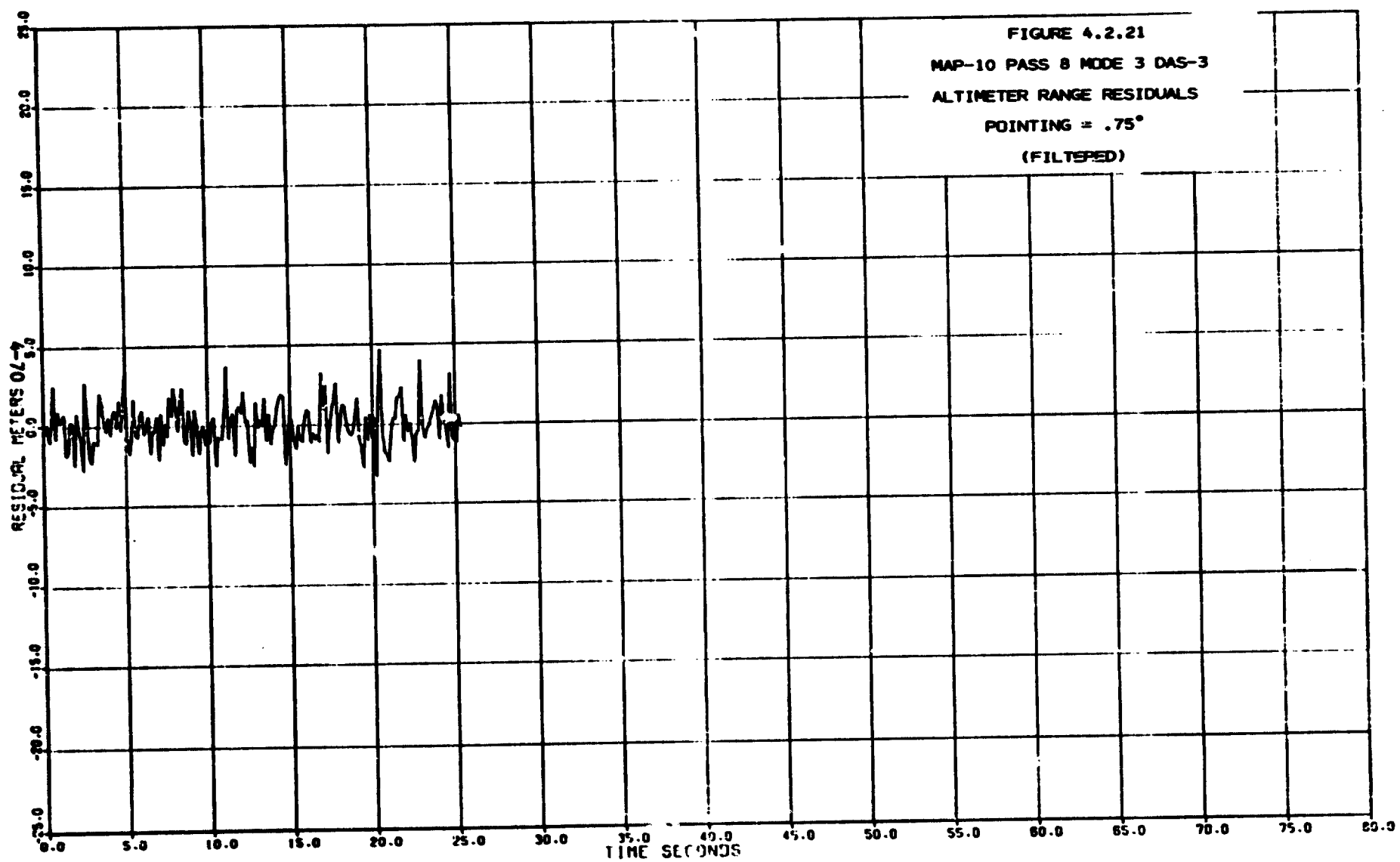
MAP-10 PASS-8 MODE-3 DAS-2  
(UNFILTERED)

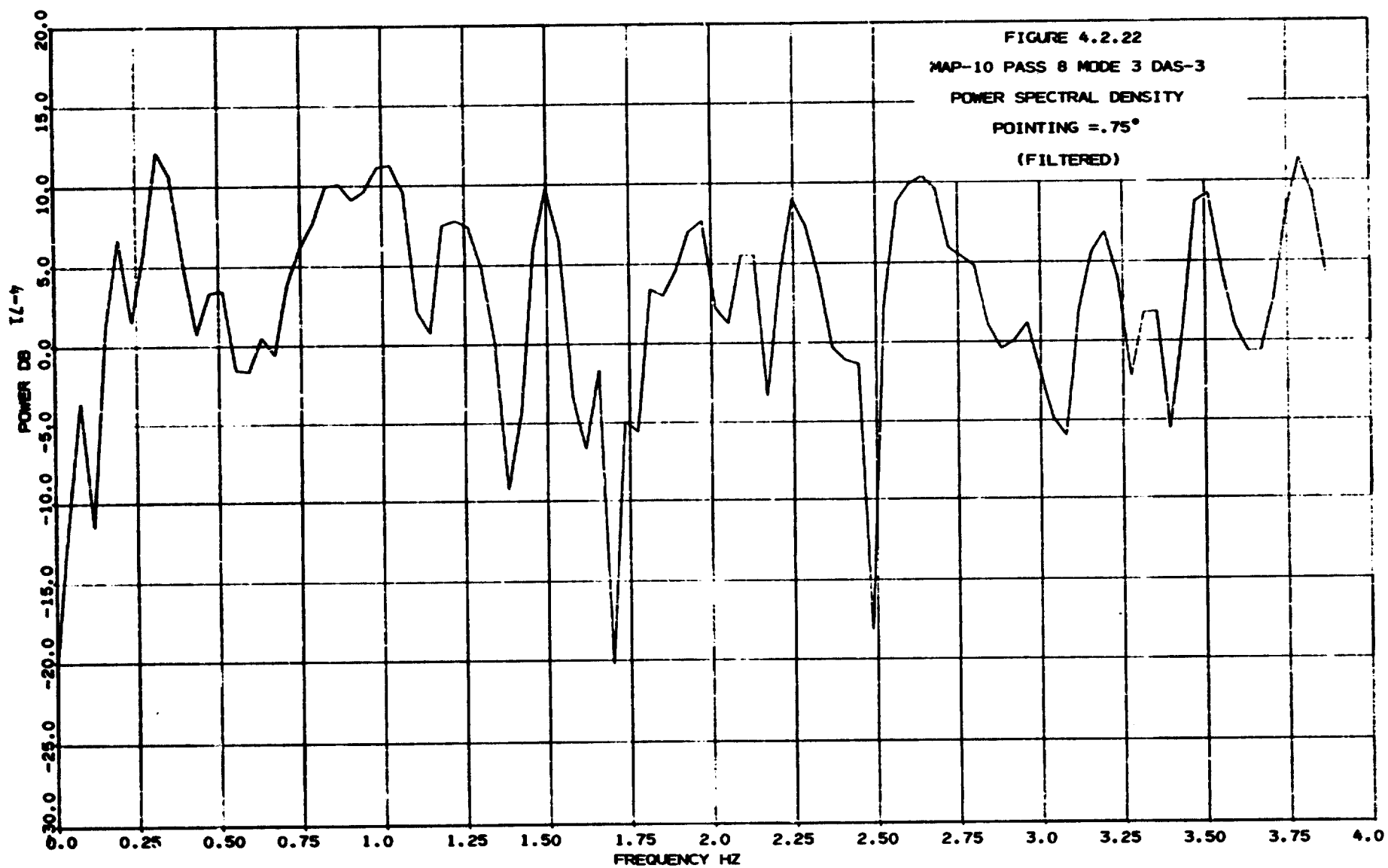
GAIN  
(FRACTIONAL)

PLOT OF  
POWER TRANSFER FUNCTION DB

FREQUENCY	GAIN (FRACTIONAL)
0.	2.1694376
0.766E-01	1.9685978
0.153E 00	1.5087603
0.230E 00	1.0994191
0.306E 00	0.88632512
0.383E 00	0.86857620
0.460E 00	1.0701532
0.536E 00	1.5556476
0.613E 00	1.9144147
0.689E 00	1.4973201
0.766E 00	1.0744906
0.843F 00	0.94043324
0.919E 00	1.0532730
0.996E 00	1.4377652
0.107E 01	1.9024607
0.115E 01	1.6586573
0.123E 01	1.0833259
0.130F 01	0.75803253
0.138E 01	0.64657454
0.146E 01	0.70381793
0.153E 01	1.0394656
0.161E 01	2.2927987
0.169E 01	5.0893694
0.176E 01	2.4656031
0.184E 01	1.1555162
0.191E 01	0.82806005
0.199F 01	0.82955968
0.207E 01	1.0224749
0.214E 01	1.2108283
0.222E 01	1.1021941
0.230E 01	0.90019063
0.237E 01	0.60742226
0.245E 01	0.80364373
0.253E 01	0.50796835
0.260E 01	0.77667053
0.268E 01	0.76594806
0.276F 01	0.81285827
0.283E 01	0.84530048
0.291F 01	0.71054574
0.299E 01	0.51186176
0.306F 01	0.39799832
0.314E 01	0.37649665
0.322E 01	0.44132113
0.329F 01	0.59893347
0.337F 01	0.76249798
0.345E 01	0.75856643
0.352E 01	0.69639123
0.360E 01	0.72828519
0.368F 01	0.68957056
0.375F 01	1.0954658
0.383E 01	1.1384738







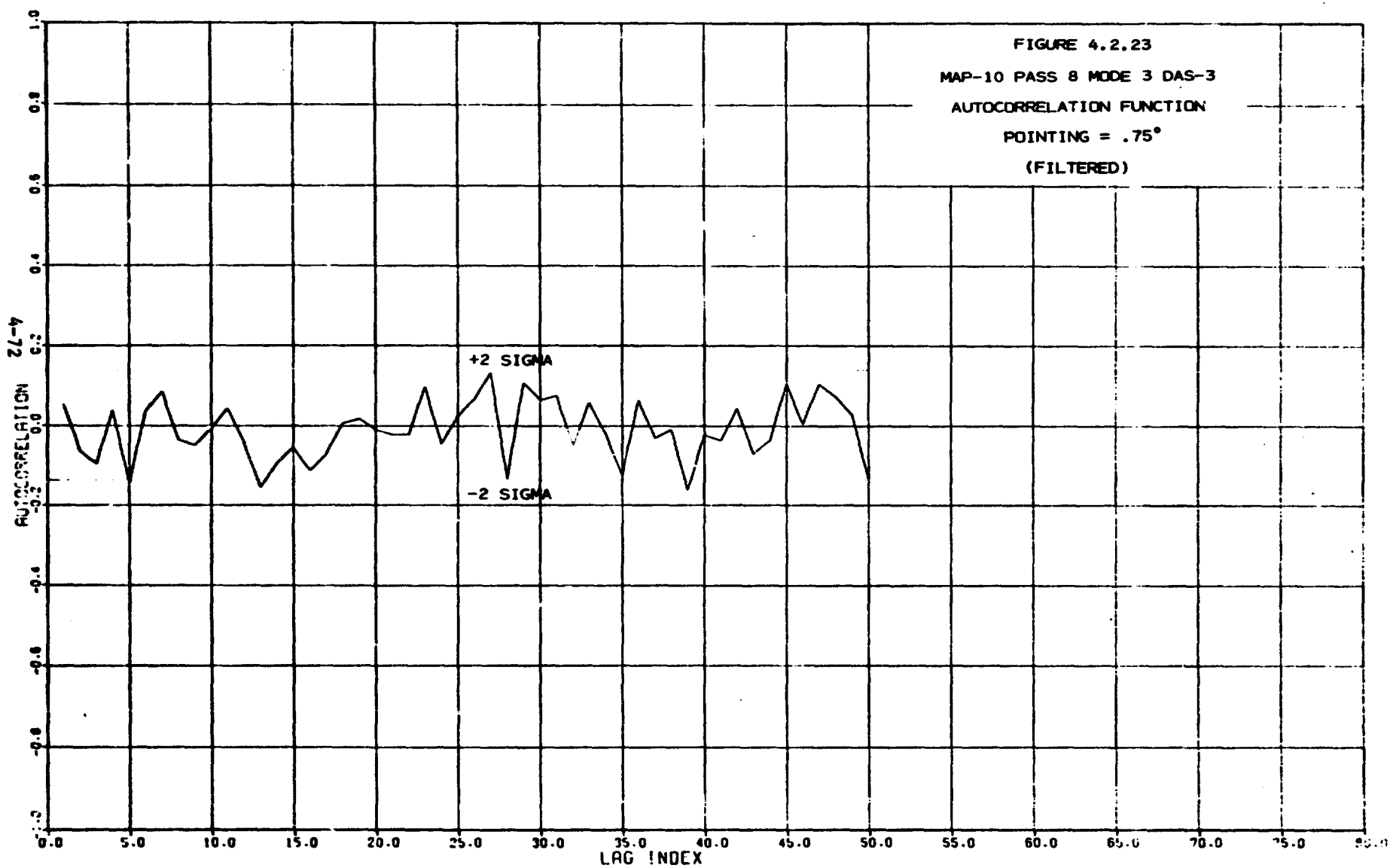
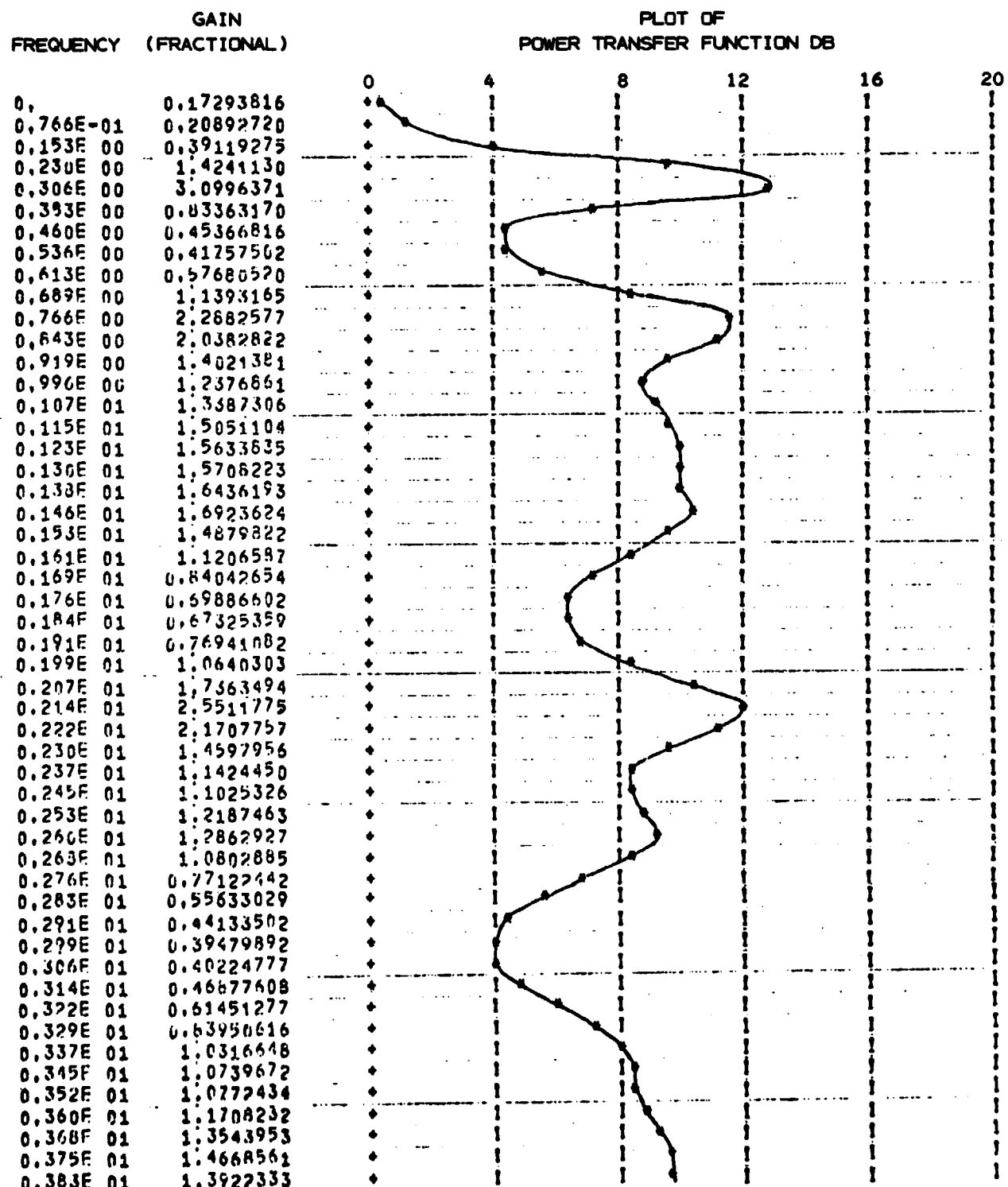
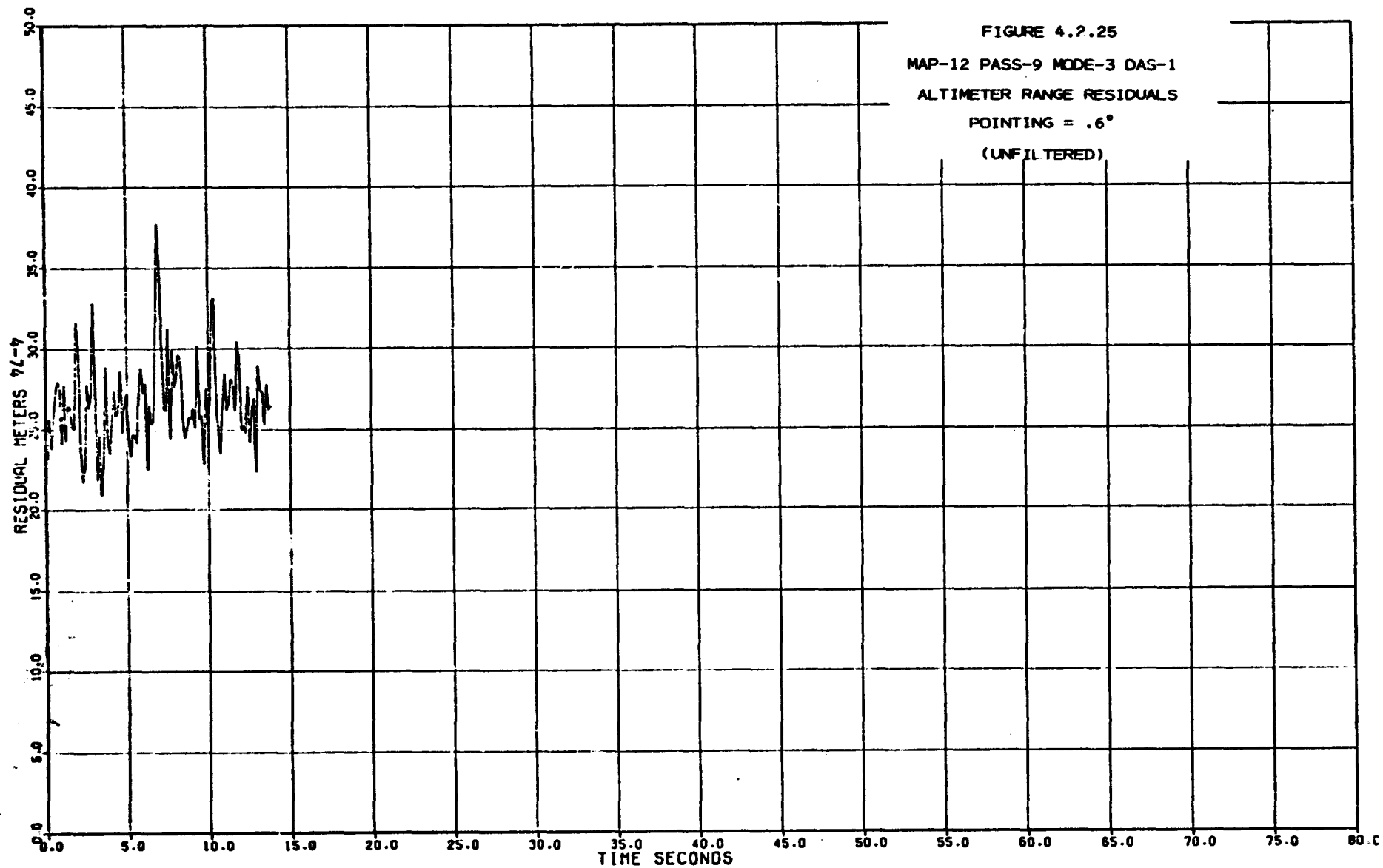
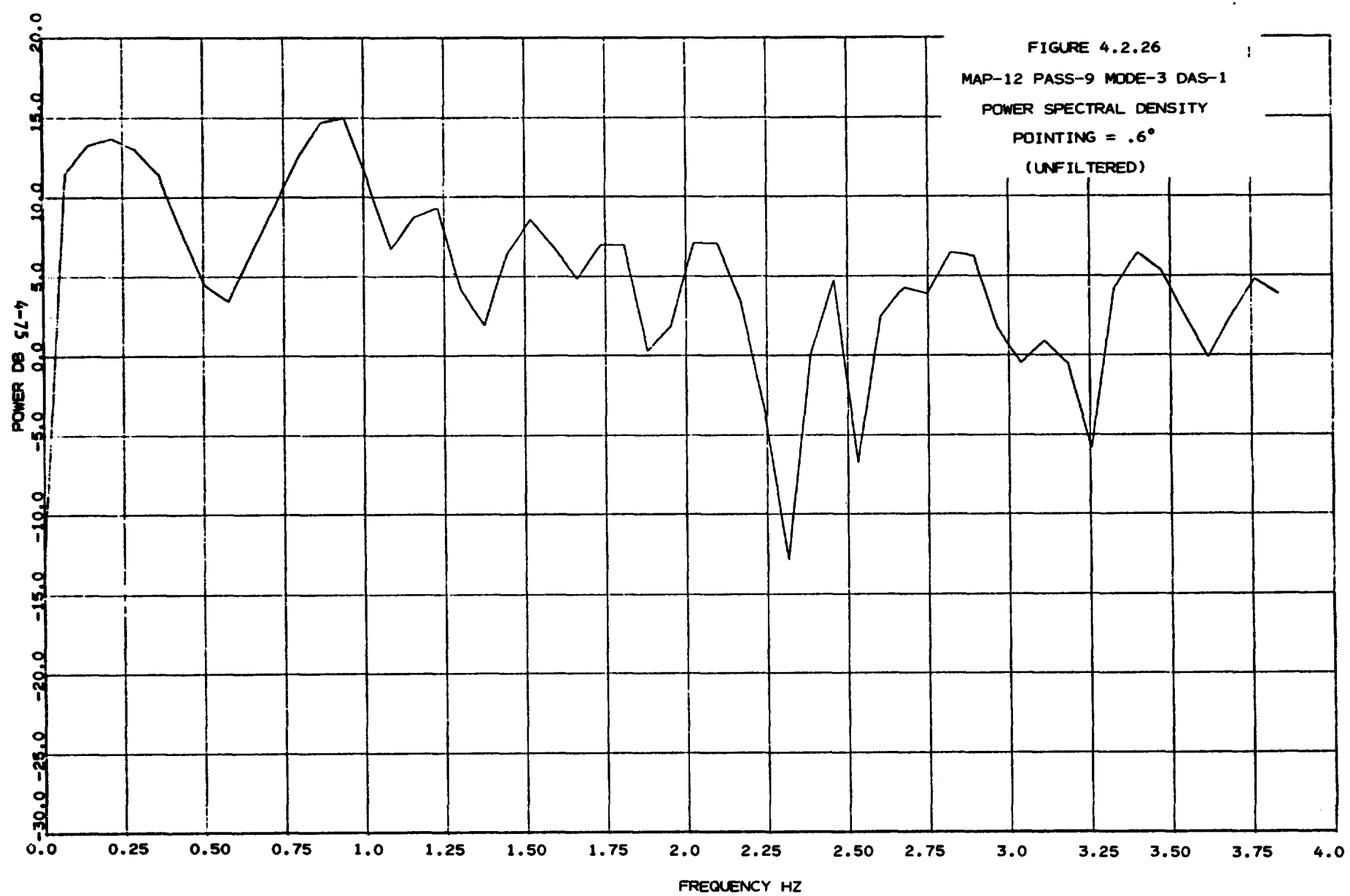


FIGURE 4.2.24  
AUTOREGRESSIVE MODEL  
MAP-10 PASS-8 MODE-3 DAS-3  
(FILTERED)







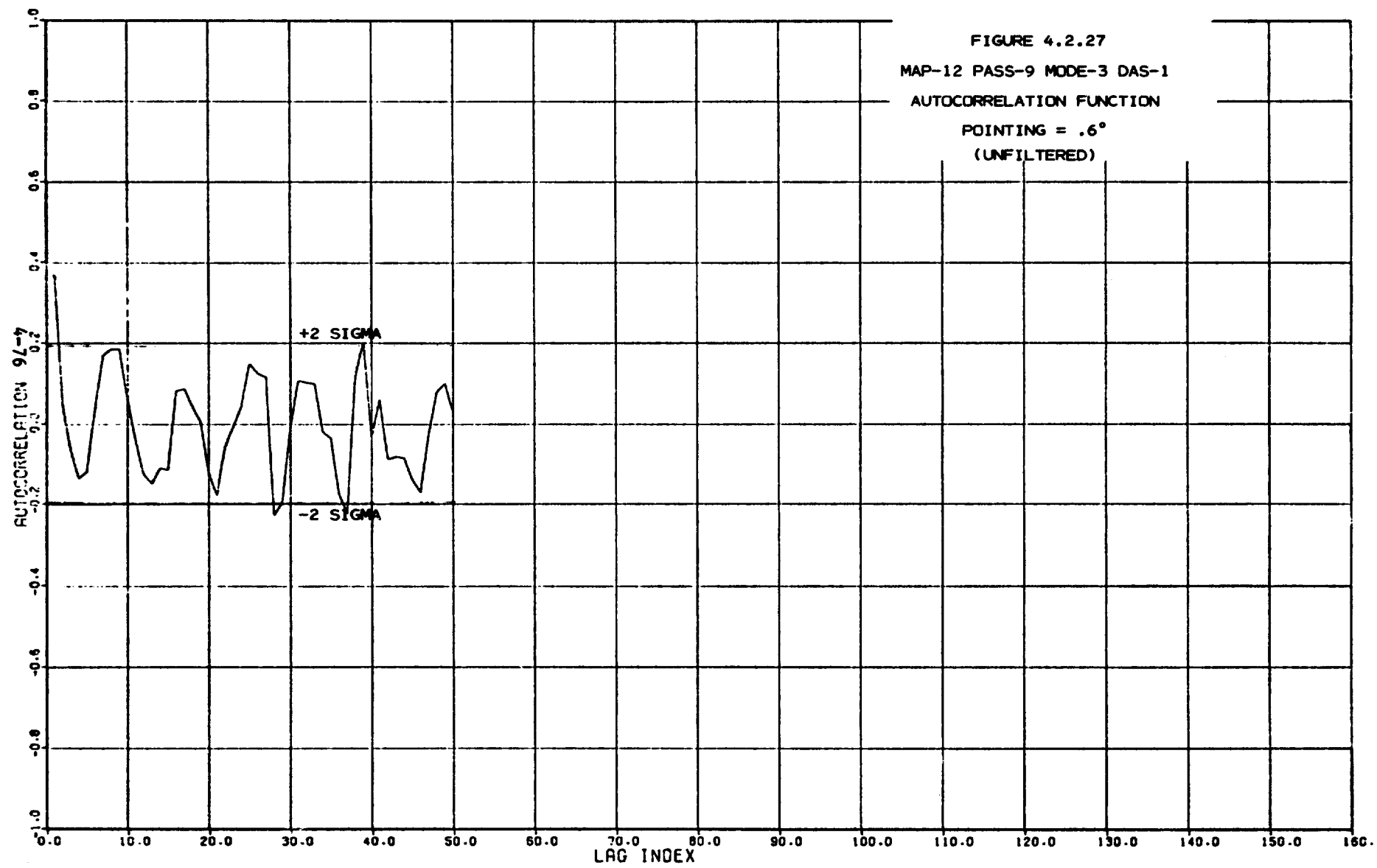
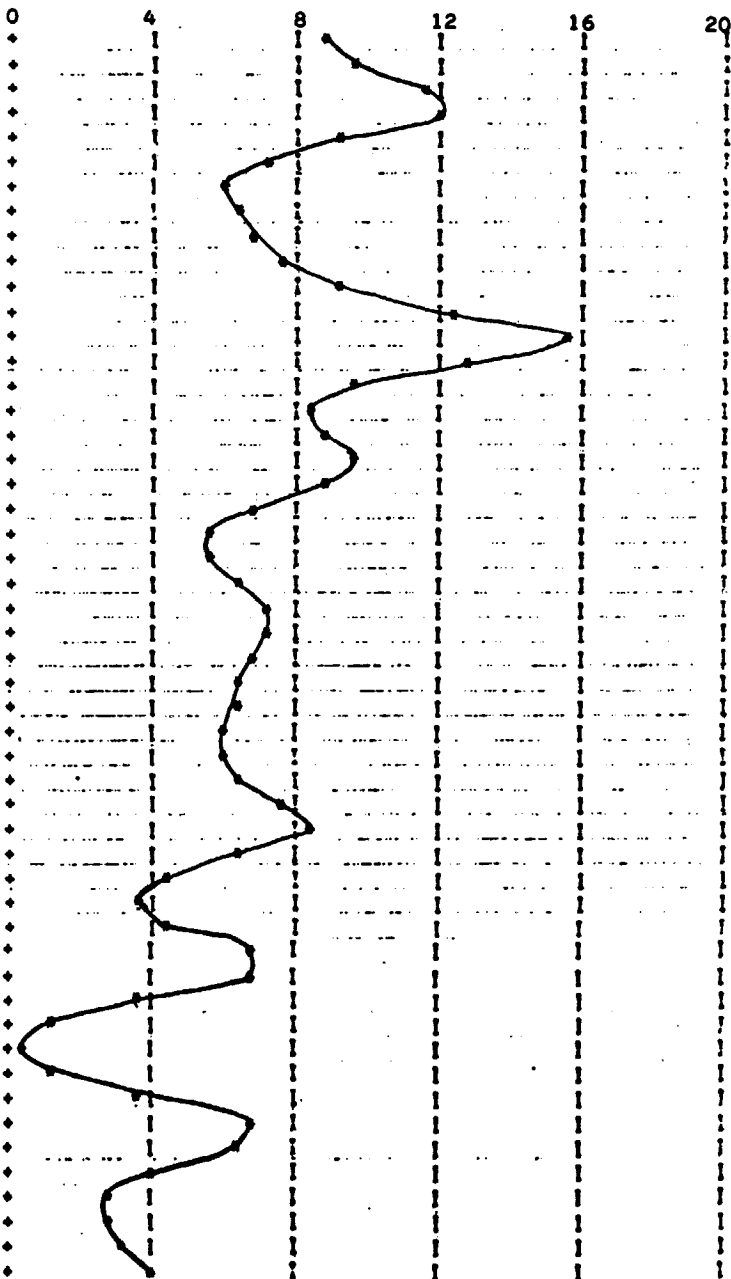


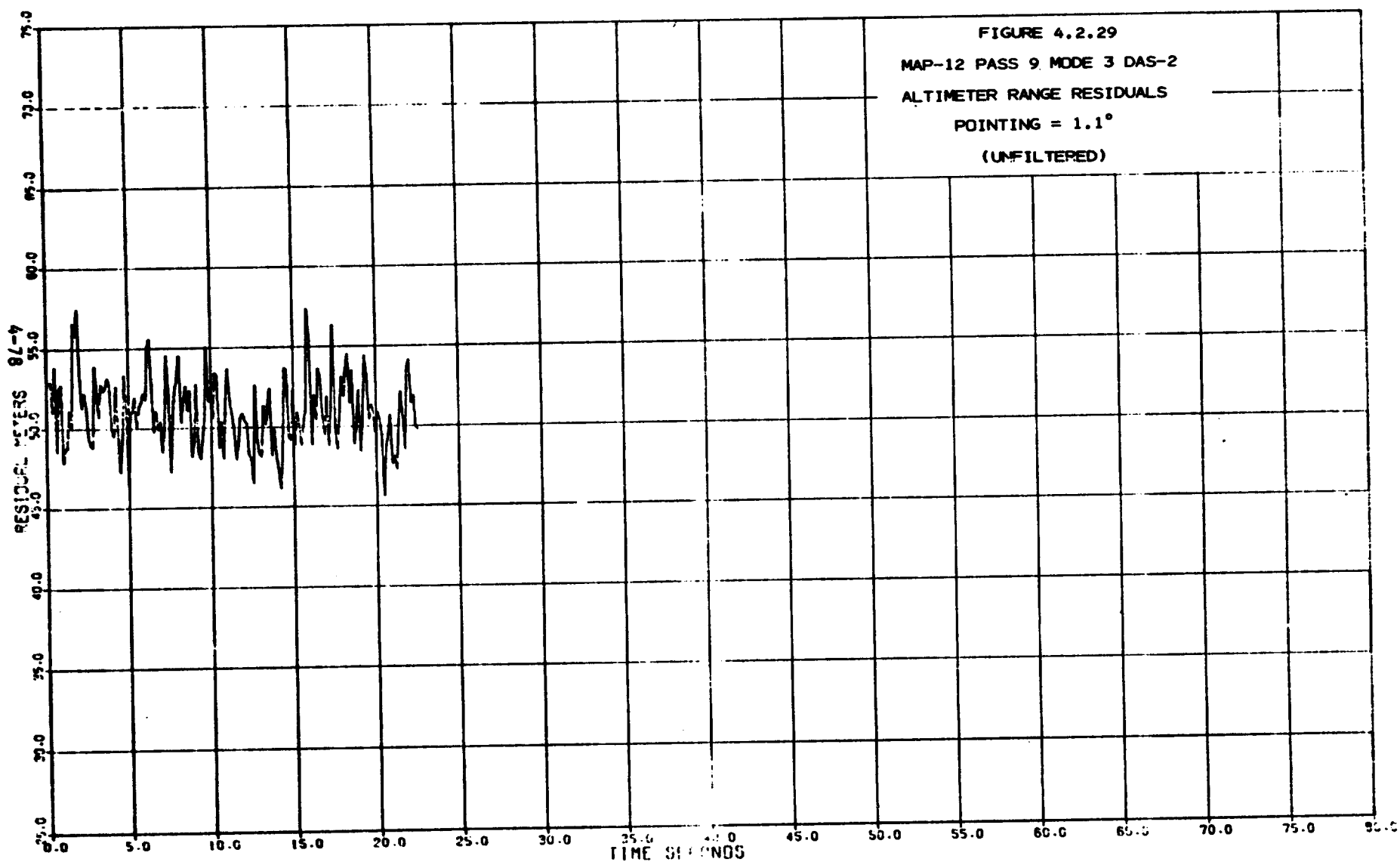
FIGURE 4.2.28  
 AUTOREGRESSIVE MODEL  
 MAP-12 PASS-9 MODE-3 DAS-1  
 (UNFILTERED)

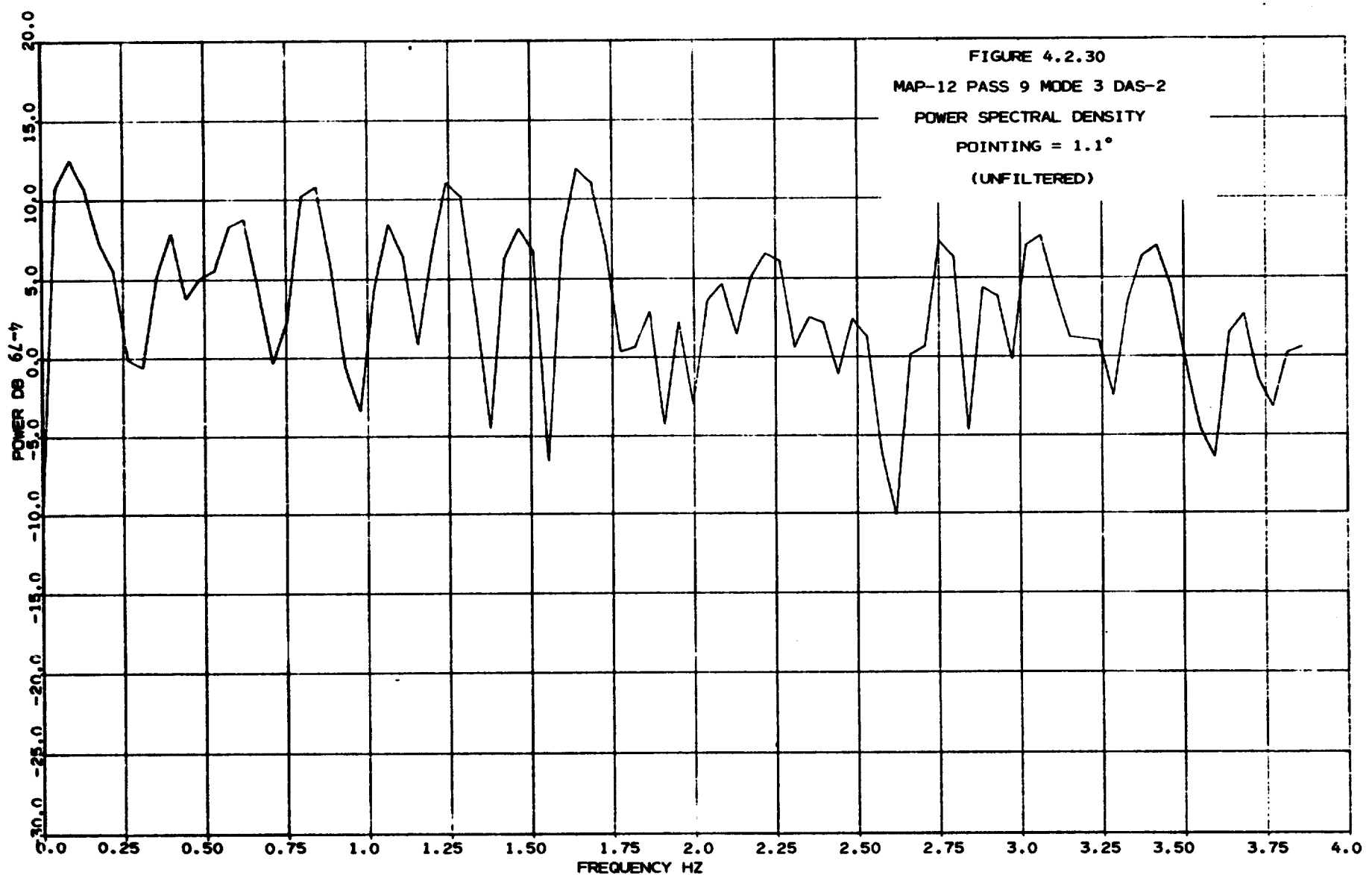
FREQUENCY  
 (HZ) GAIN  
 (FRACTIONAL)

FREQUENCY (HZ)	GAIN (FRACTIONAL)
0.	1.5572871
0.766E=01	1.9090528
0.153E 00	3.1214798
0.230E 00	3.2511334
0.306E 00	1.7566493
0.383E 00	1.0890182
0.460E 00	0.69281406
0.536E 00	0.89588023
0.613E 00	1.0056858
0.689E 00	1.2305630
0.766E 00	1.7949303
0.843E 00	3.6666642
0.919E 00	7.9710416
0.996E 00	4.1326739
0.107E 01	1.9296257
0.115E 01	1.4495126
0.123E 01	1.5840729
0.130E 01	1.9307054
0.138E 01	1.6092385
0.146E 01	1.0326497
0.153E 01	0.77651993
0.161E 01	0.75817363
0.169E 01	0.90825483
0.176E 01	1.1154949
0.184E 01	1.1444813
0.191E 01	1.0394193
0.199E 01	0.97474932
0.207E 01	0.43909922
0.214E 01	0.87169117
0.222E 01	0.42756688
0.230E 01	0.92395929
0.237E 01	1.2605173
0.245E 01	1.4685495
0.253E 01	0.94613616
0.260E 01	0.56053990
0.268E 01	0.48734179
0.276E 01	0.60181959
0.283E 01	1.0056120
0.291E 01	1.0062841
0.299E 01	0.47869130
0.306E 01	0.27849642
0.314E 01	0.23526632
0.322E 01	0.28653744
0.329E 01	0.50698577
0.337E 01	1.0587211
0.345E 01	0.95580325
0.352E 01	0.53995099
0.360E 01	0.40116737
0.368E 01	0.39363704
0.375E 01	0.45035459
0.383E 01	0.51710384

PLOT OF  
 POWER TRANSFER FUNCTION DB







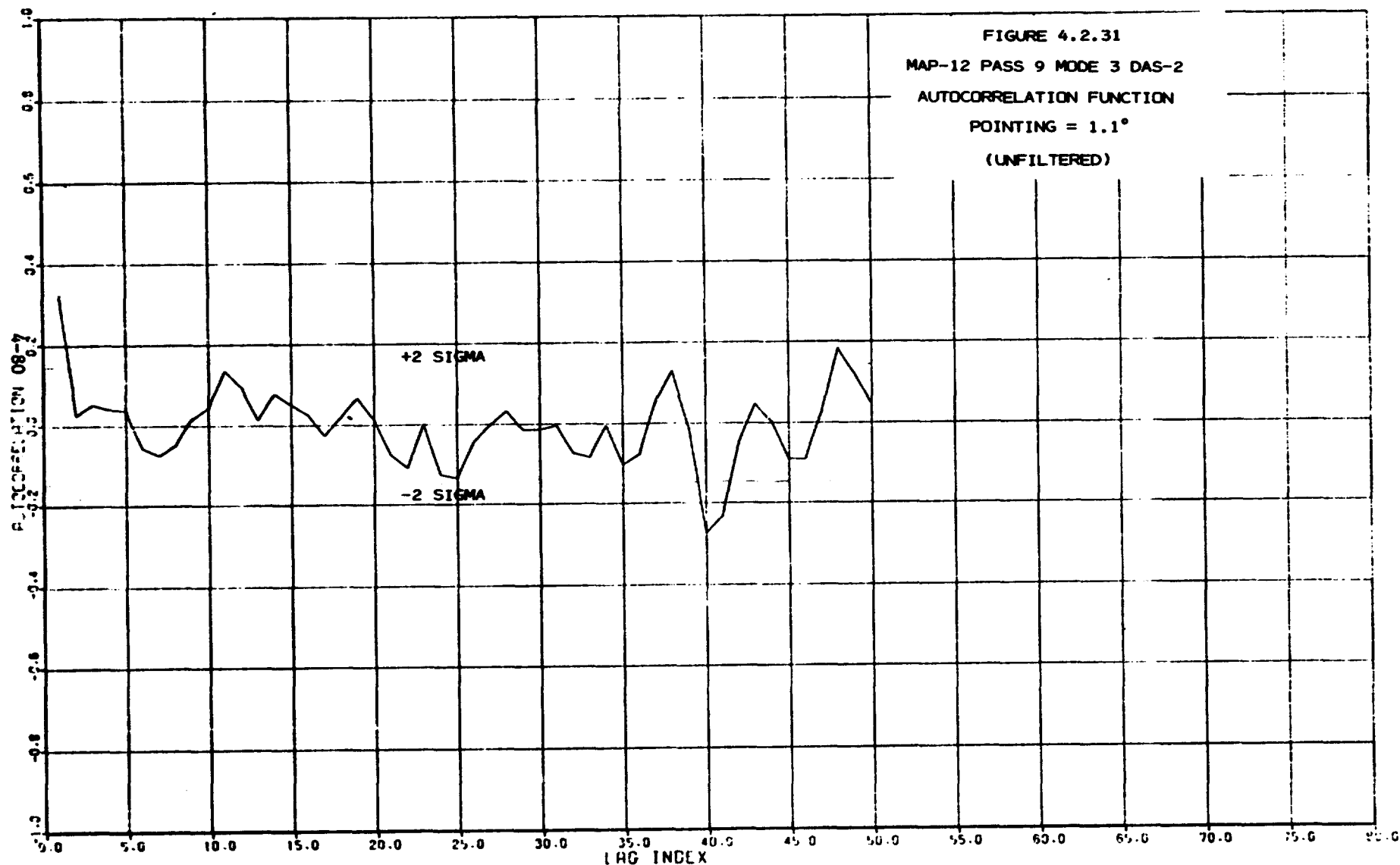
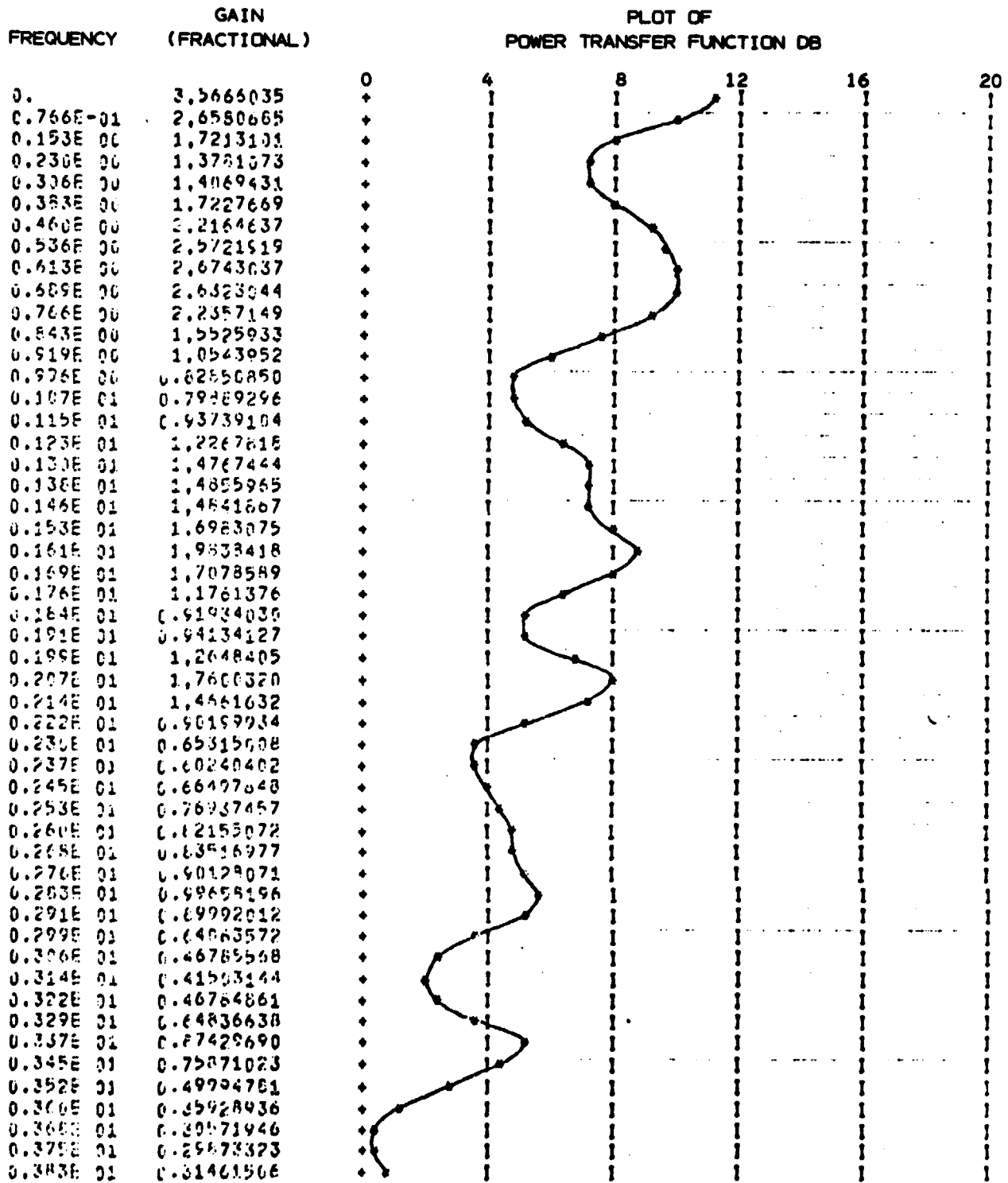
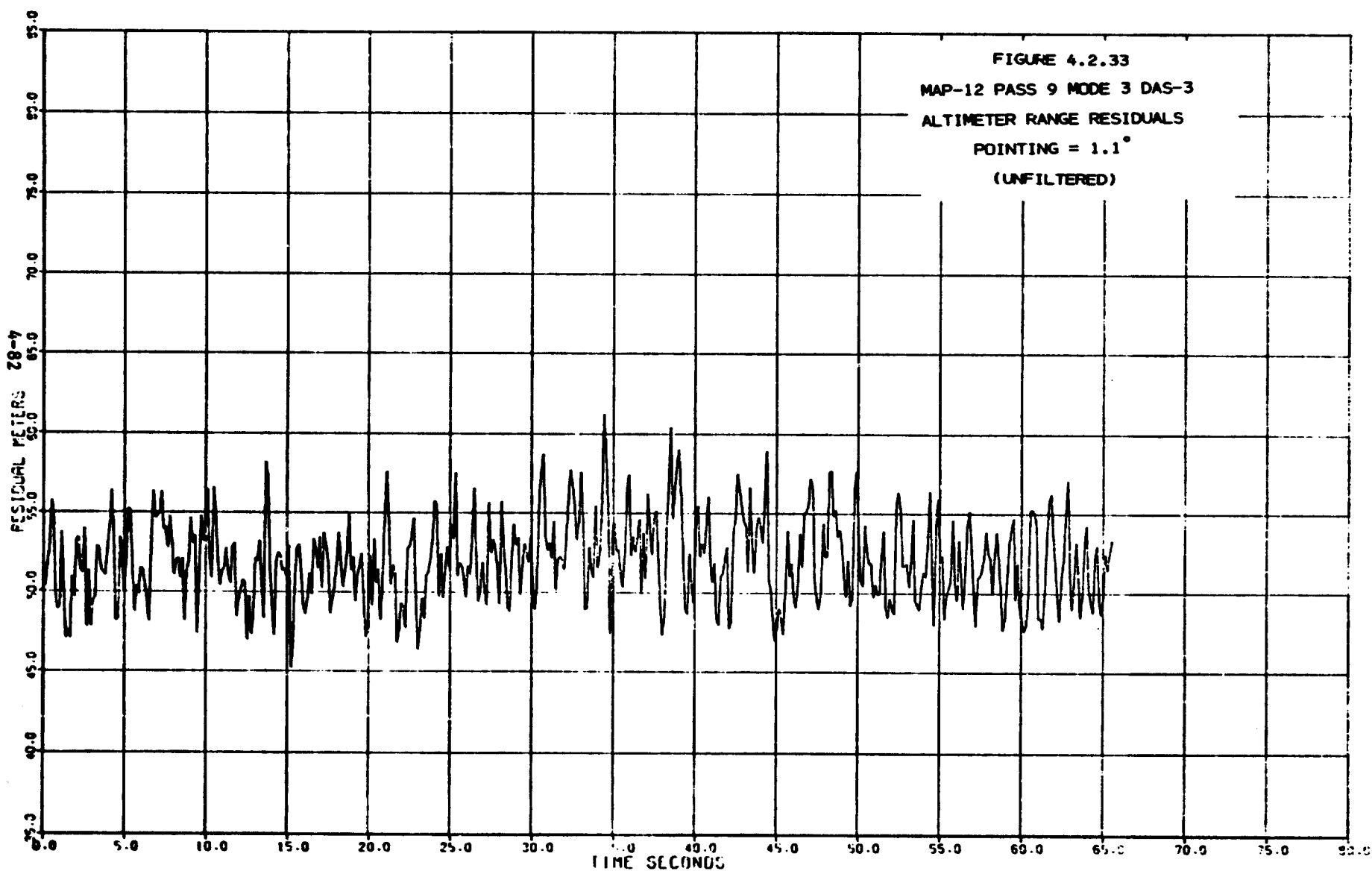
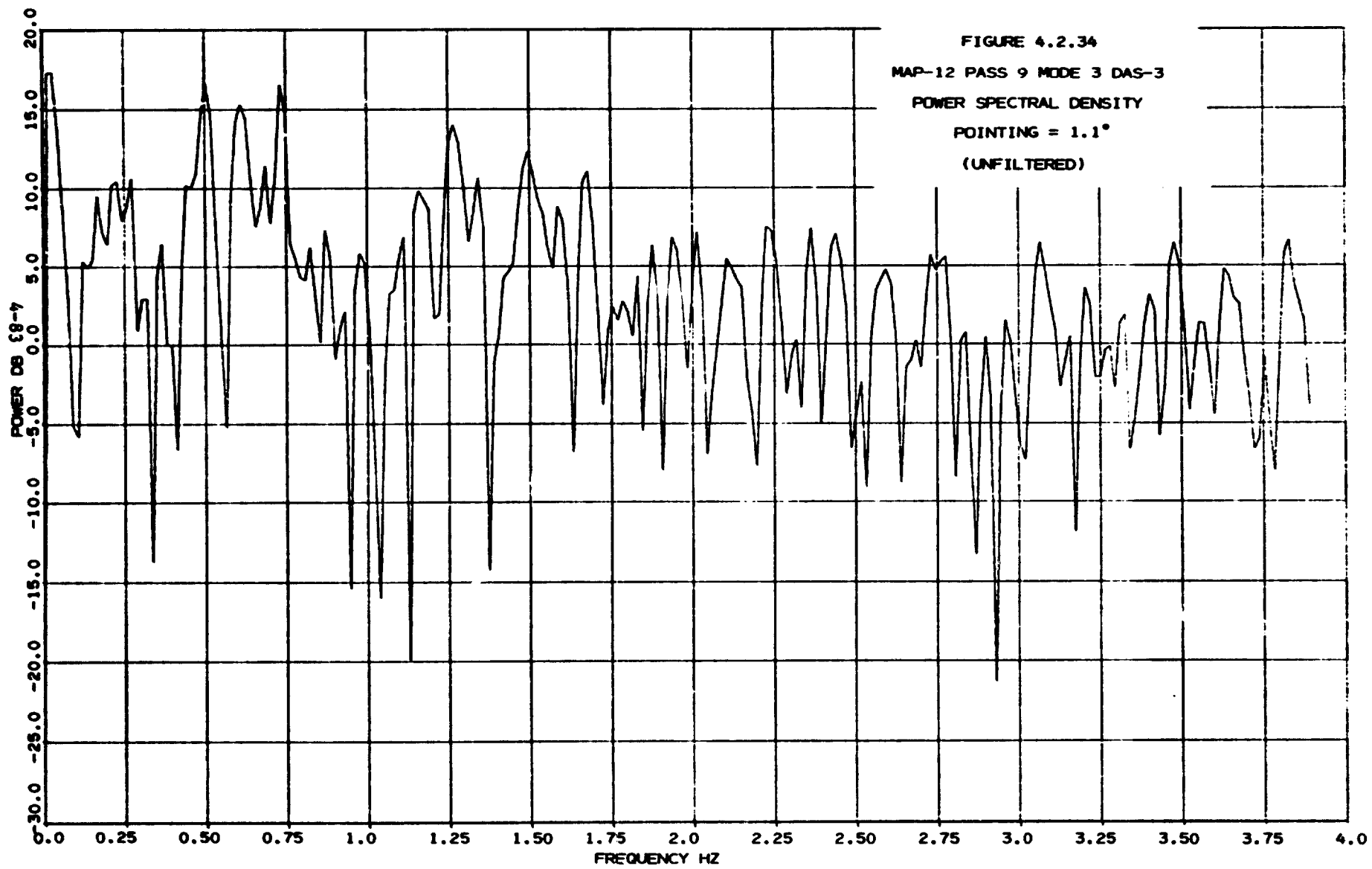


FIGURE 4.2.32  
AUTOREGRESSIVE MODEL

MAP-12 PASS-9 MODE-3 DAS-2  
(UNFILTERED)







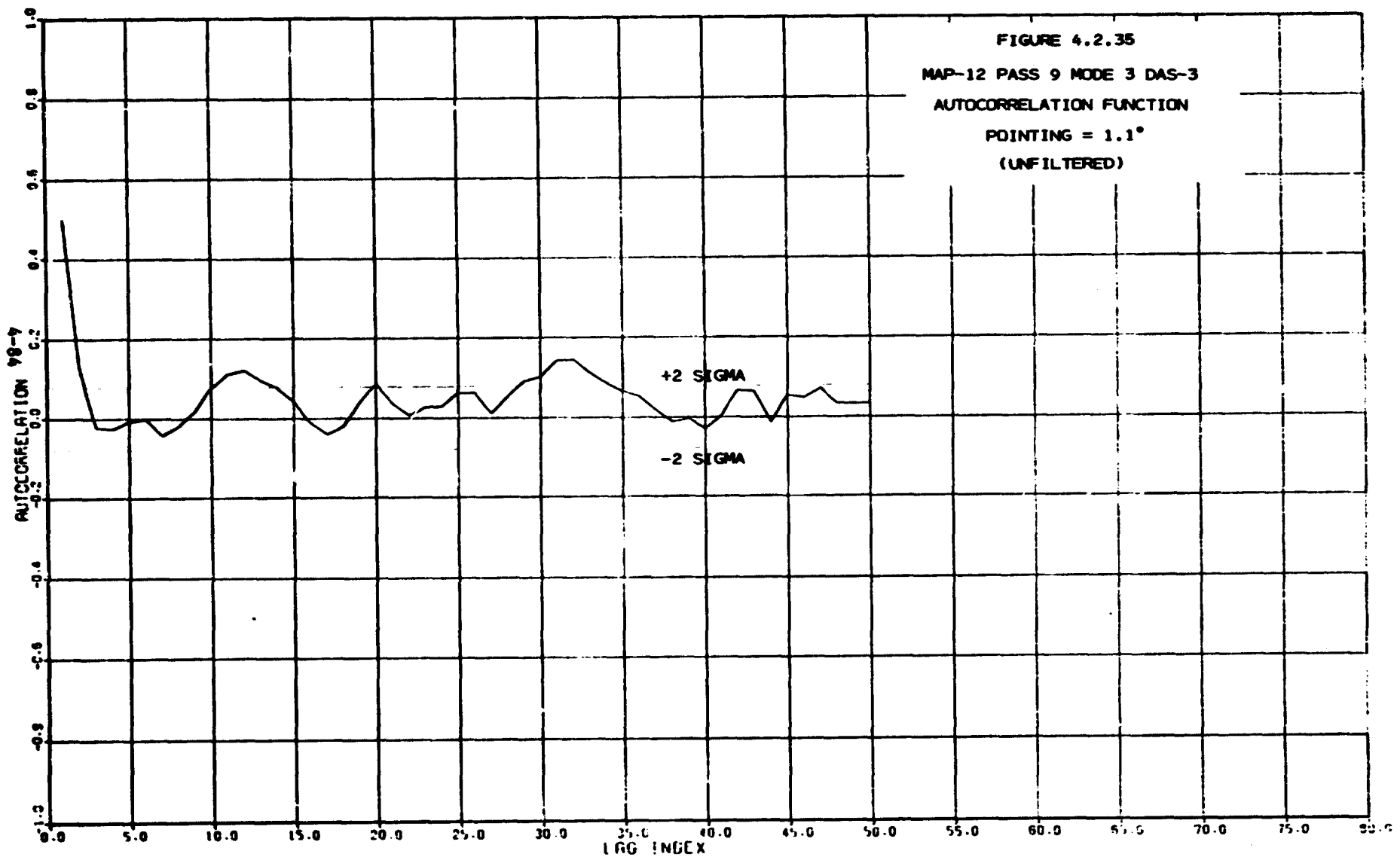
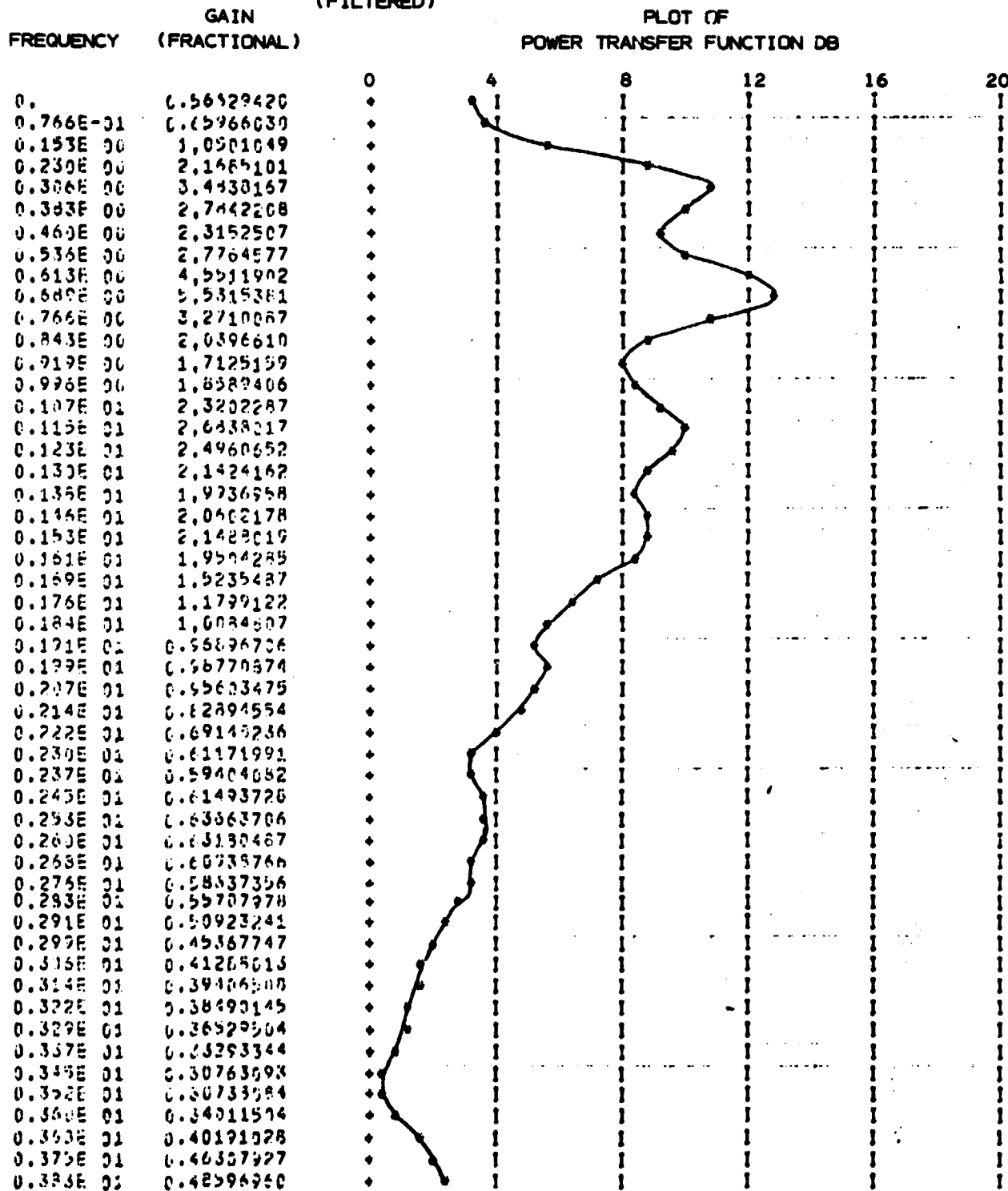


FIGURE 4.2.36B  
AUTOREGRESSIVE MODEL

MAP-12 PASS-9 MODE-3 DAS-3  
(FILTERED)



#### 4.3 Mode-5 Results

From Table 2.1 the three Mode 5 data acquisition submodes (DAS-1, DAS-2 and DAS-3) are 16.64 seconds, 102.96 seconds and 53.04 seconds long. DAS-1 is a shortened replication of Mode 1 DAS-1. DAS-2 uses pulse compression techniques to increase range measurement accuracy. DAS-3 transmits a 20 nanosecond pulse for comparison with the DAS-2 pulse compression results. Discussions with NASA/Wallops have indicated that, out of the three Mode 5 data sets (Maps 47, 74 and 66) selected for detailed analysis the pulse compression was operating only during Map 74.

Examination of Table 4.4 shows that for low, moderate and high pointing angles (Maps 47, 74 and 66, respectively) the noise sigma is largest for sub-mode DAS-1 followed by DAS-2 and DAS-3. Table 4.5 shows the ratios of the DAS-1 and DAS-2 sigmas to the DAS-3 sigma. Note that for DAS-1 this ratio increases from 1.58 for low pointing angles to 2.67 for high pointing angles (Map 66) while for DAS-2 this ratio is constant at about 1.3 for all pointing angles.

At low pointing angles (Map 47) the DAS-1 power spectrum (Figure 4.3.2) and autocorrelation function (Figure 4.3.3) do not indicate any significant deviation from a white noise process. The DAS-2 power spectrum (Figure 4.3.6) shows considerable attenuation of frequencies higher than 1.25 Hz. The autocorrelation function (Figure 4.3.7) shows 8 of the first 20 autocorrelation coefficients exceed the plus or minus two sigma limits for a white noise process. The DAS-3 power spectrum (Figure 4.3.10) also shows some attenuation of the higher frequencies and 5 of the first 20 autocorrelation coefficients exceed the two sigma limits for a white noise process.

At moderate pointing angles (Map 74) the DAS-1 power spectrum (Figure 4.3.14) is relatively flat and only two of the first twenty autocorrelation coefficients (Figure 4.3.15) exceed the two sigma limits for a white noise process. The DAS-2 power spectrum (Figure 4.3.18B) shows 10 to 15 db attenuation at frequencies higher than 1.25 Hz and the DAS-3 power spectrum (Figure 4.3.22) shows a similar attenuation at frequencies higher than 1.0 Hz. Comparison of the DAS-2 and DAS-3 autocorrelation functions (Figures 4.3.19 and 4.3.23) show that the DAS-3 has a higher degree of serial correlation.

TABLE 4.5  
MODE 5  
RATIO OF SUBMODE  
NOISE SIGMAS TO DAS-3 NOISE SIGMA

MAP	SUBMODE	SIGMA/ DAS-3 SIGMA
47	DAS-1	1.58
	(1)DAS-2 (2)	1.36
74	DAS-1	1.93
	(1)DAS-2	1.30
66	DAS-1	2.67
	(2)DAS-2	1.30

(1) DATA FILTERED BY 99 POINT QUADRATIC  
MIDPOINT HIGH PASS FILTER

(2) PULSE COMPRESSION INOPERATIVE

The effect of high pass filtering on the Map 74 DAS-2 data is shown by comparing the unfiltered and filtered time series plots (Figures 4.3.17A and 4.3.17B) and power spectra (Figures 4.3.18A and 4.3.18B). The unfiltered time series plot shows a well defined slope of about .2 meters per second for the first 35 seconds of data. This produces a large low frequency (0 to .10 Hz) spike in the corresponding power spectrum (Figure 4.3.18A). Comparison of the unfiltered data power spectrum (Figure 4.3.18A) and the filtered data power spectrum (Figure 4.3.18B) shows that filtering had no appreciable effect on the spectral coefficients for frequencies greater than .2 Hz.

At high pointing angles (Map 66) the time series plots (Figures 4.3.25, 4.3.29 and 4.3.33) show that the measurement noise is dominated by low frequency (.2 Hz) oscillations. The power spectra (Figures 4.3.26, 4.3.30, 4.3.34) show considerable attenuation of spectral coefficients at frequencies greater than .25 to .5 Hz. Note that the DAS-2 and DAS-3 spectra are plotted at 10 Db per division instead of the 5 Db per division used for all other power spectral plots. The autocorrelation function (Figures 4.3.27, 4.3.31 and 4.3.35) are smooth damped oscillation type curves.

TABLE 4.4  
MODE 5 DETAIL ANALYSIS

MAP	PASS	SUB-MODE	POINTING	SAMP. SIZE	MEAN (MTRS)	SIGMA (MTRS)	F STATISTIC	NORM. TEST	SIG. FREQ. BANDS (HZ)	SIGNIFICANT AUTOCORRELATION COEFFICIENTS
47	25	DAS-1	<.5°	92	-32.3	1.10	.768	.931	NONE	16
		+*DAS-2		704	-39.6	.95	3.87	1.0	.155-.300 .621-1.08	1,2,3-6,8,13,14
		*DAS-3		324	-49.4	.697	.671	.242	.072-.121	1,4-7
74	39	DAS-1	.85°	100	-93.2	1.85	.648	.606	.148	8,20
		+*DAS-2		686	-89.8	1.25	.793	.999	.273-.330 .410-.467 .547-.604 .688-.740 .888-.945 1.09-1.22	1,3-6,17
		*DAS-3		342	-100.3	.955	8.23	.999	.343-.457 .548-.731 .822-.936 1.17-1.21	1,2,4-9
66	37	DAS-1	1.4°	110	70.4	11.94	2.54	.969	0-.213	ALL
		+DAS-2		640	76.8	5.81	23.2	1.0	0-.354	ALL
		DAS-3		294	84.6	4.46	10.6	1.0	0-.239	ALL

\*DATA FILTERED WITH 99 POINT QUADRATIC MIDPOINT HIGH PASS FILTER

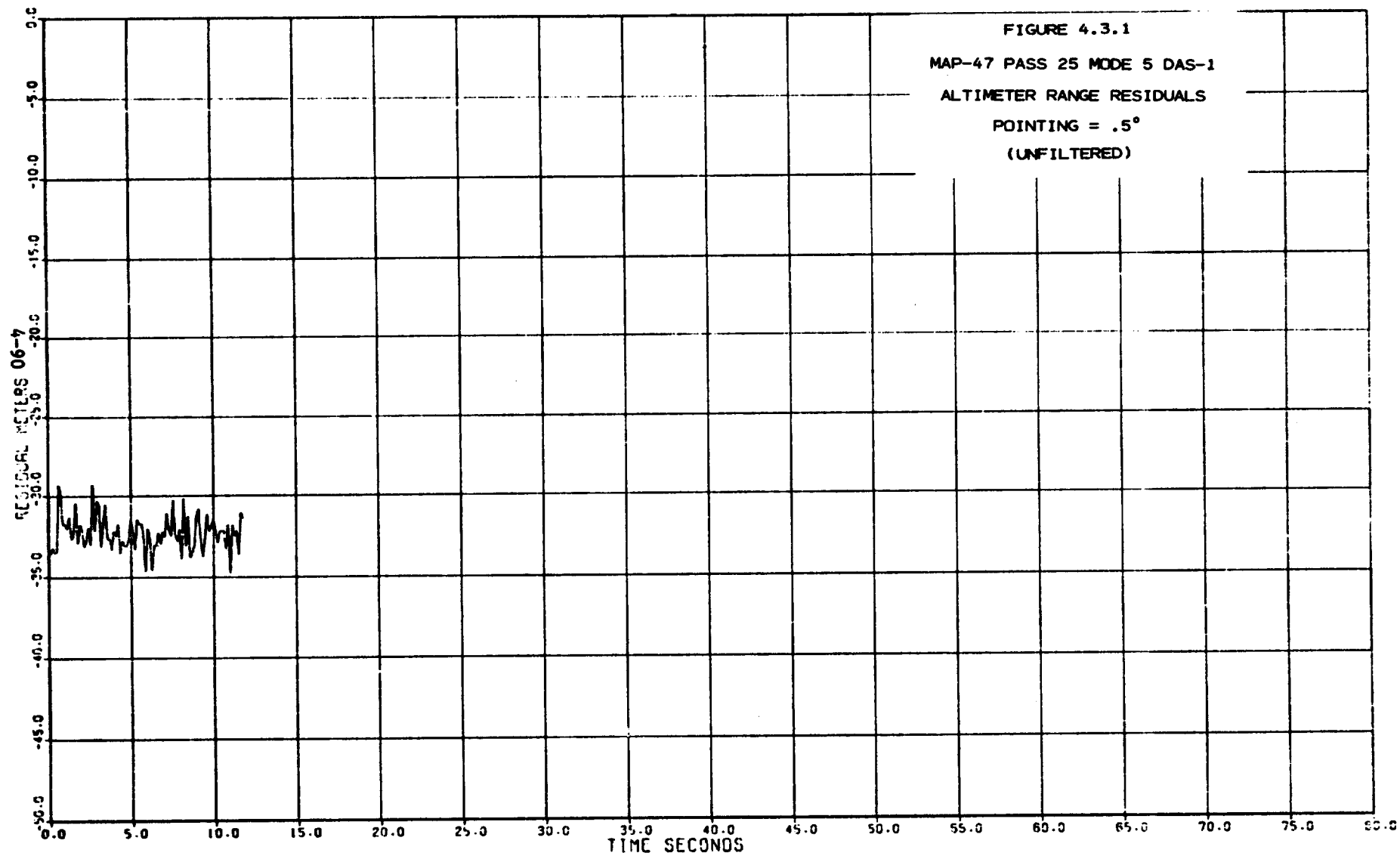
+PULSE COMPRESSION INOPERATIVE

TABLE 4.5  
 MODE 5  
 RATIO OF SUBMODE  
 NOISE SIGMAS TO DAS-3 NOISE SIGMA

MAP	SUBMODE	SIGMA/ DAS-3 SIGMA
47	DAS-1	1.58
	(1) DAS-2 (2)	1.36
74	DAS-1	1.93
	(1) DAS-2	1.30
66	DAS-1	2.67
	(2) DAS-2	1.30

(1) DATA FILTERED BY 99 POINT QUADRATIC  
 MIDPOINT HIGH PASS FILTER

(2) PULSE COMPRESSION INOPERATIVE



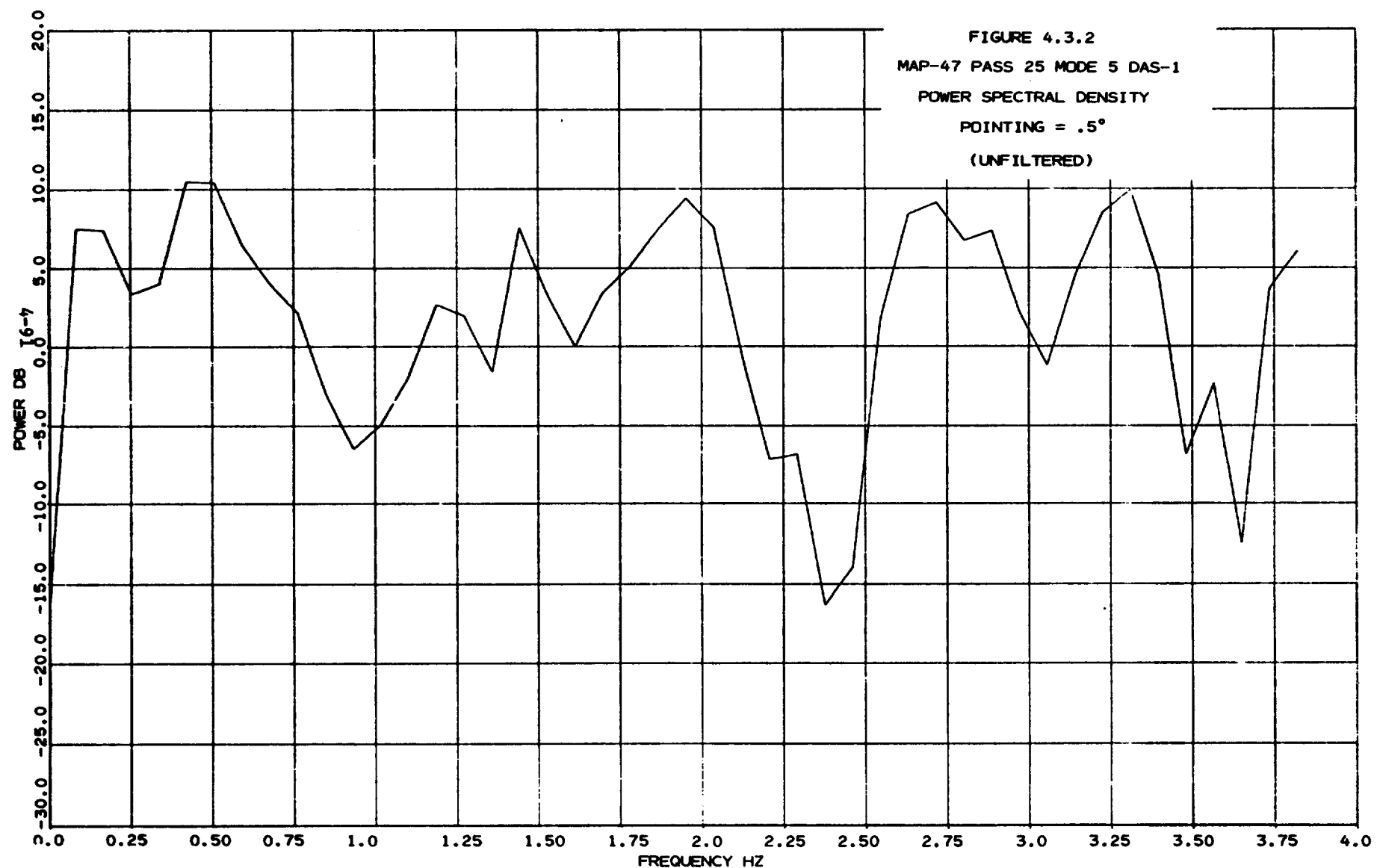


FIGURE 4.3.3

MAP-47 PASS 25 MODE 5 DAS-1

AUTOCORRELATION FUNCTION

POINTING =  $.5^\circ$

(UNFILTERED)

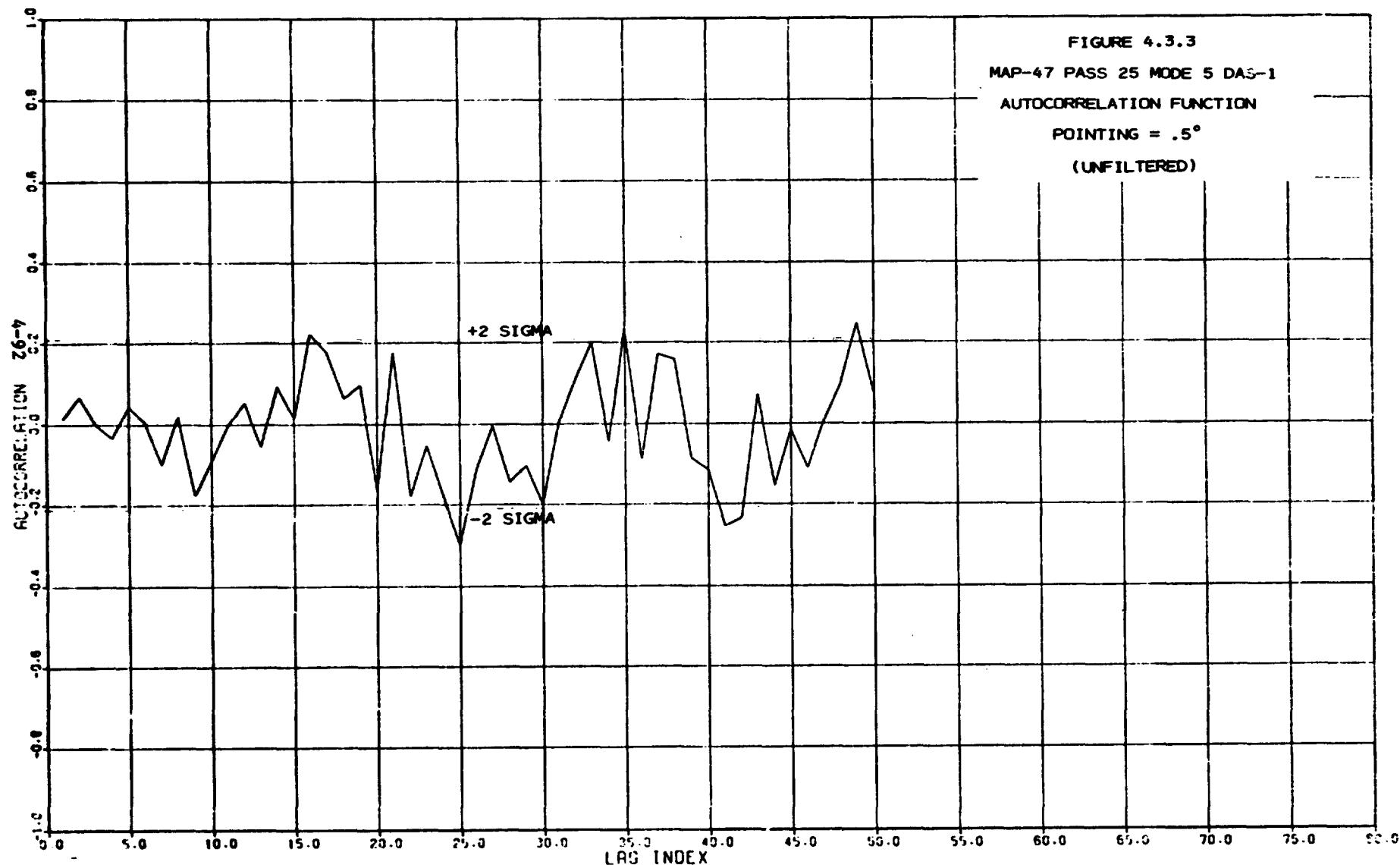


FIGURE 4.3.4  
AUTOREGRESSIVE MODEL

MAP-47 PASS-25 MODE-5 DAS-1  
(UNFILTERED)

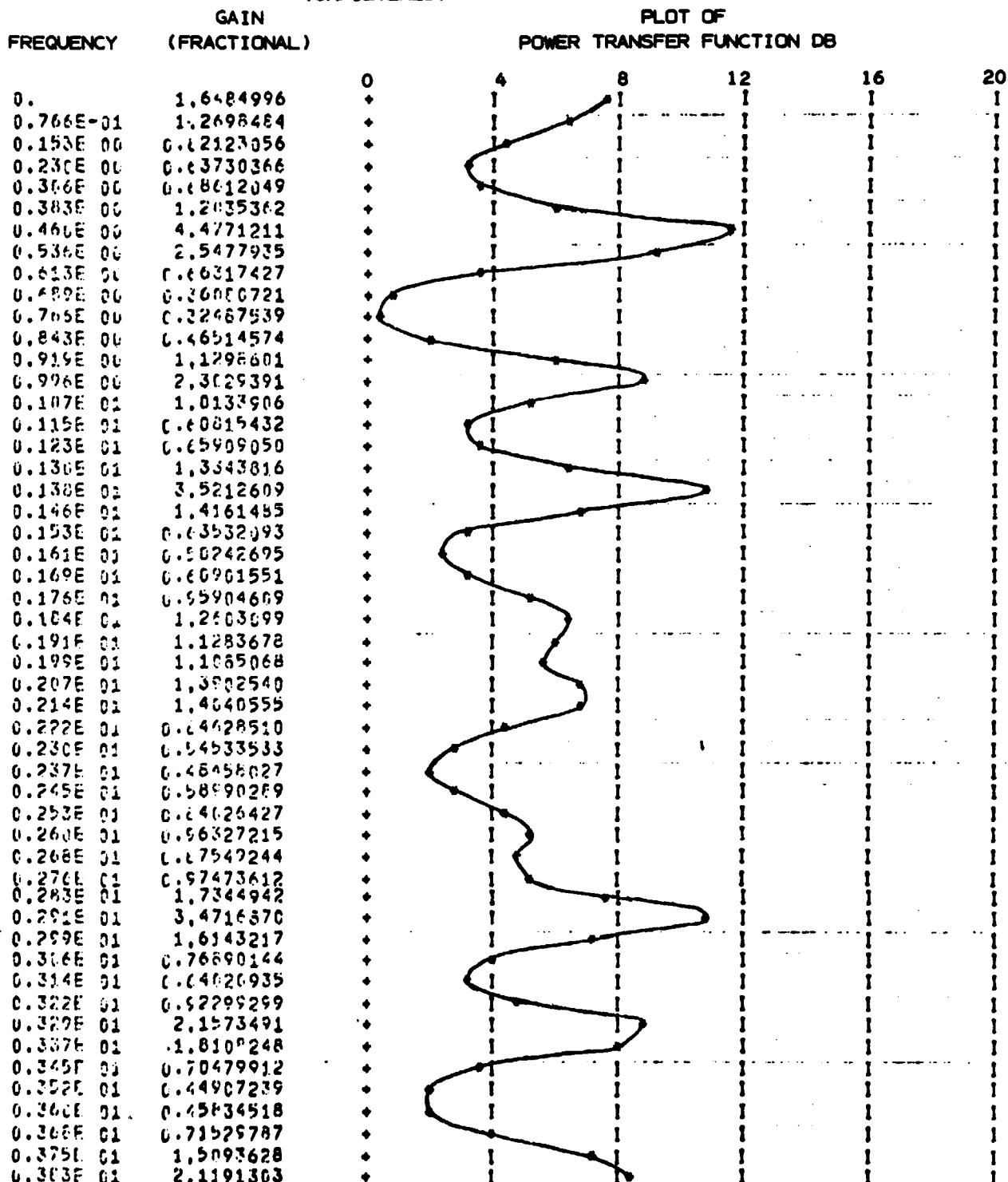


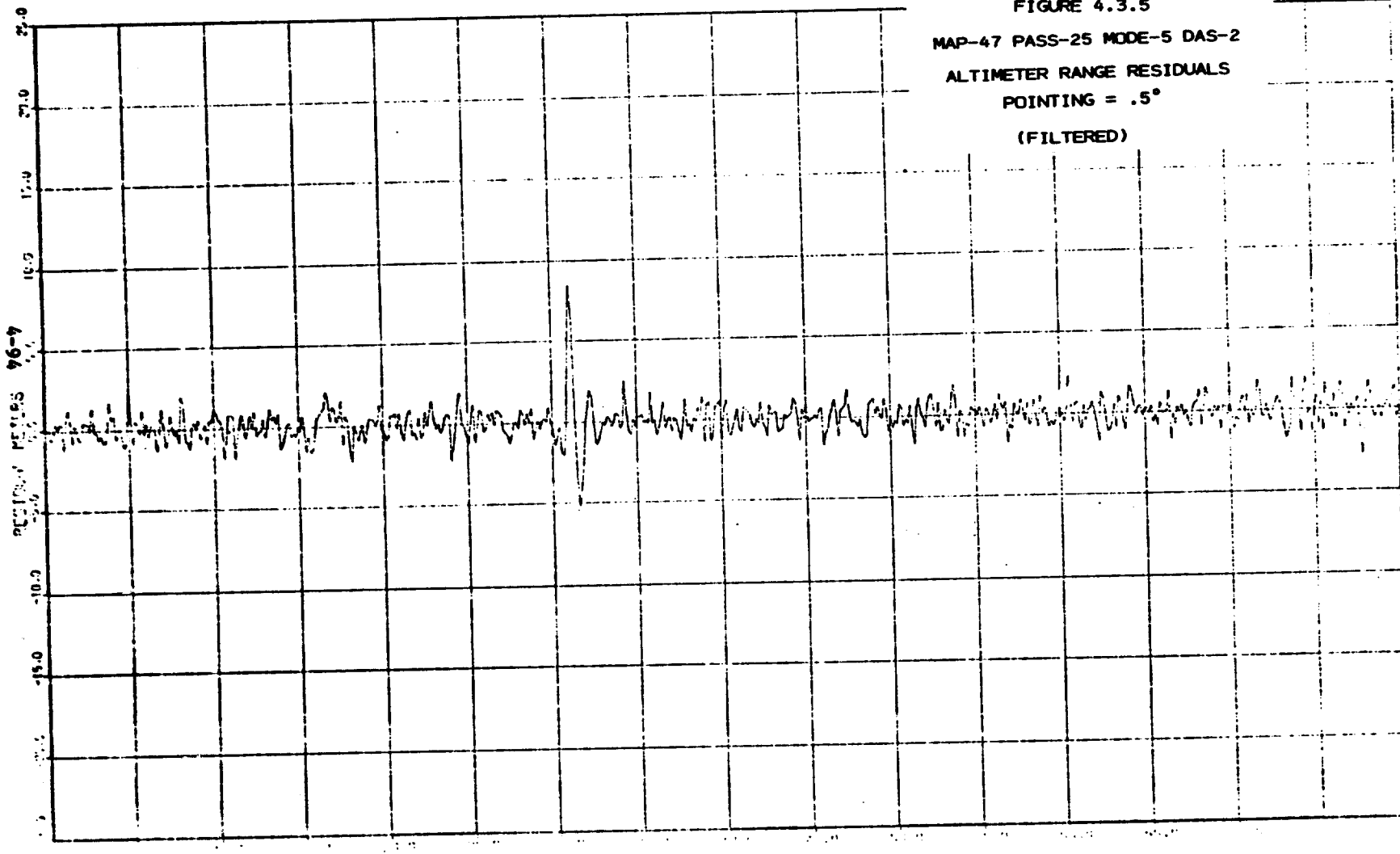
FIGURE 4.3.5

MAP-47 PASS-25 MODE-5 DAS-2

ALTIMETER RANGE RESIDUALS

POINTING =  $.5^\circ$

(FILTERED)



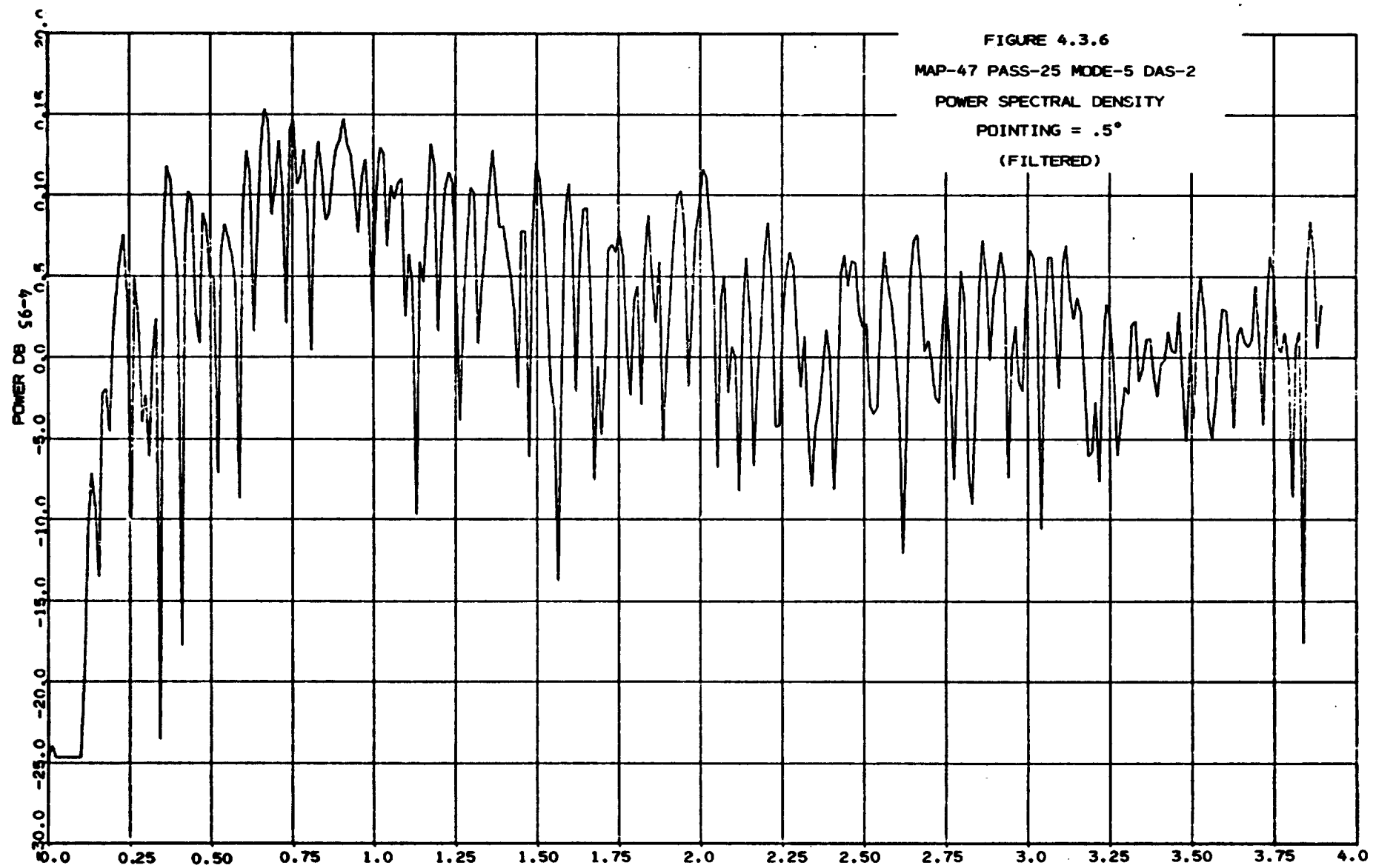


FIGURE 4.3.7

MAP-47 PASS-25 MODE-5 DAS-2

AUTOCORRELATION FUNCTION

POINTING =  $.5^\circ$

(FILTERED)

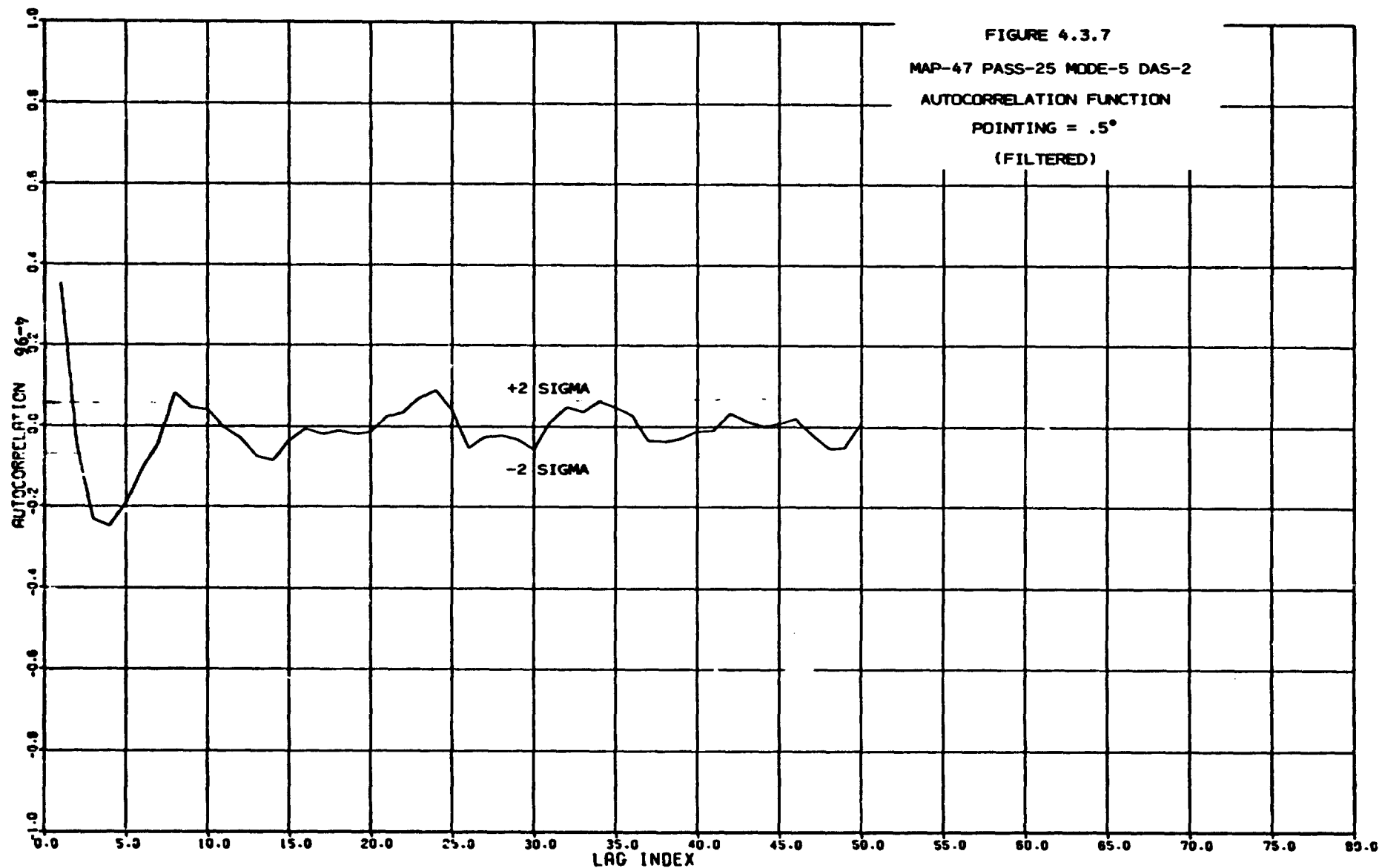
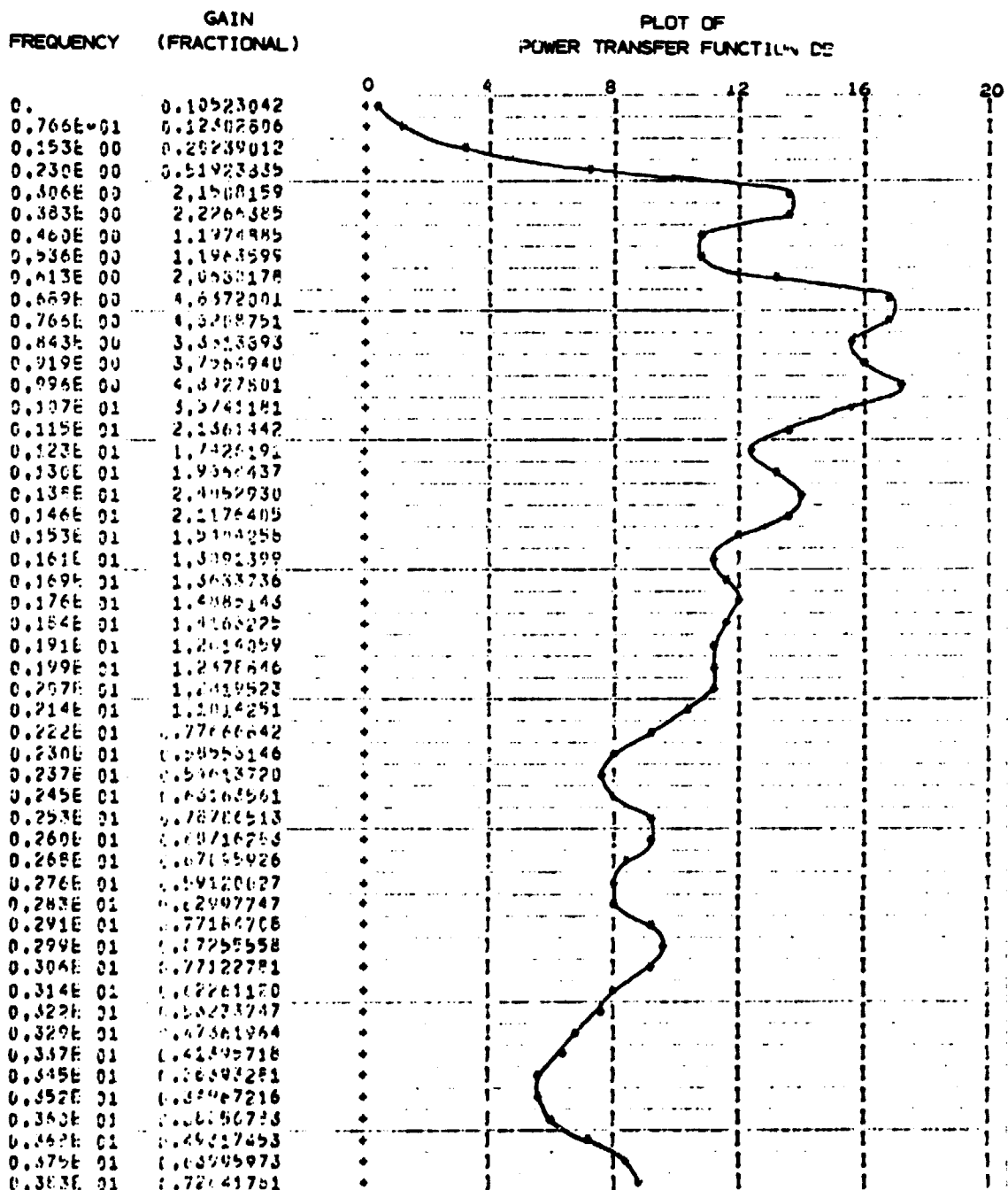
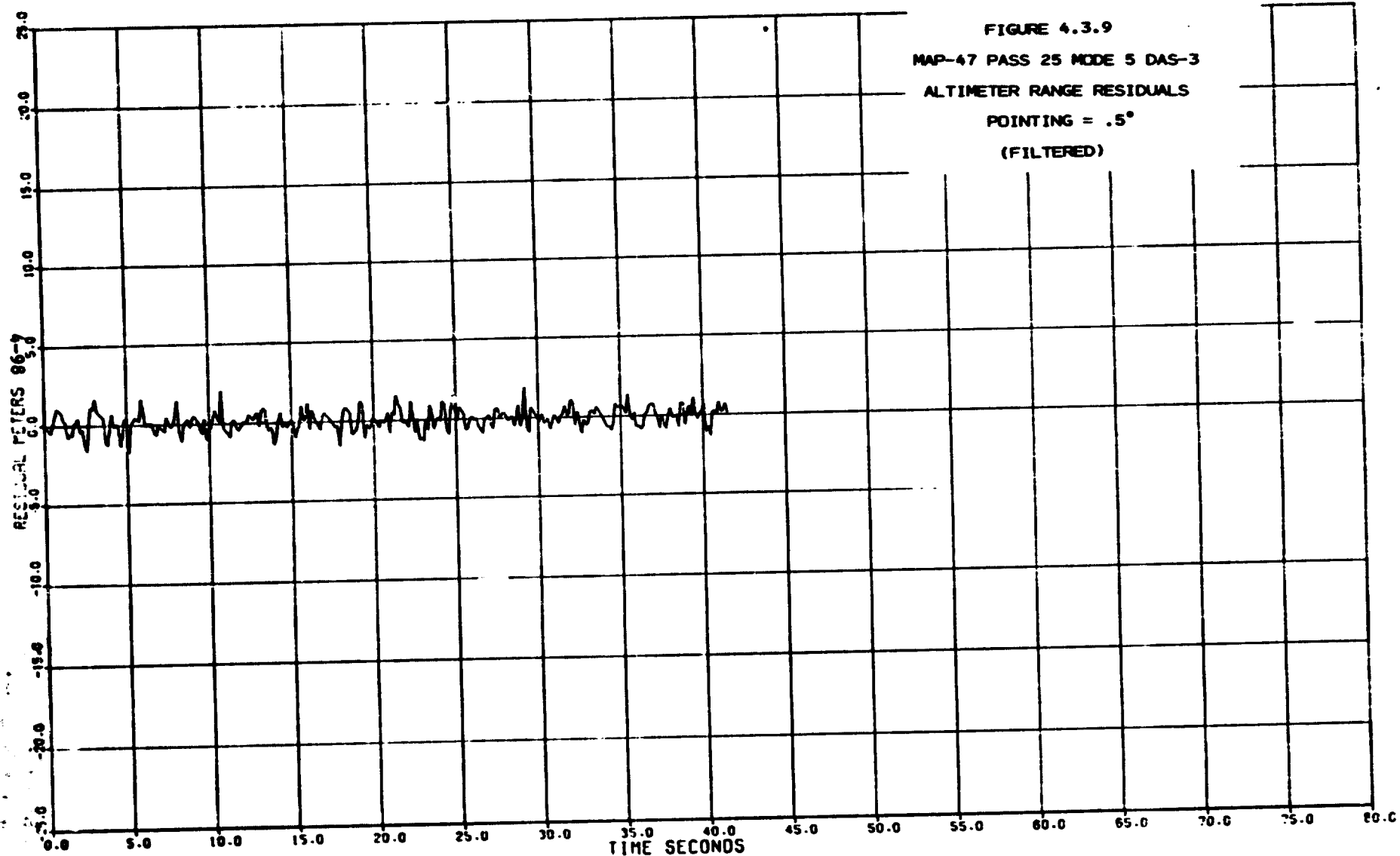


FIGURE 4.3.8  
AUTOREGRESSIVE MODEL  
MAP-47 PASS-25 MODE-5 DAS-2  
(FILTERED)





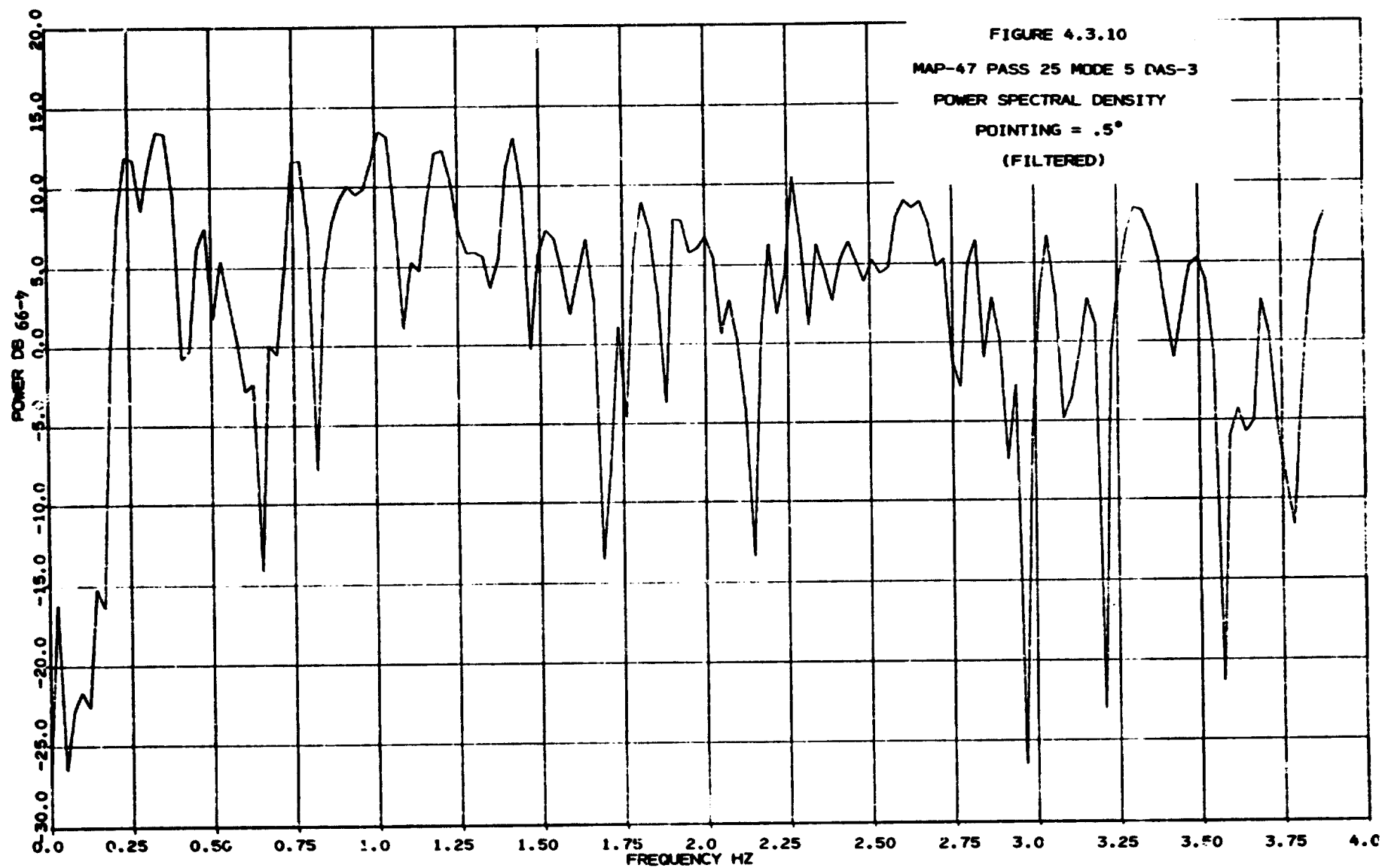


FIGURE 4.3.11

MAP-47 PASS 25 MODE 5 DAS-3

AUTOCORRELATION FUNCTION

POINTING =  $.5^\circ$

(FILTERED)

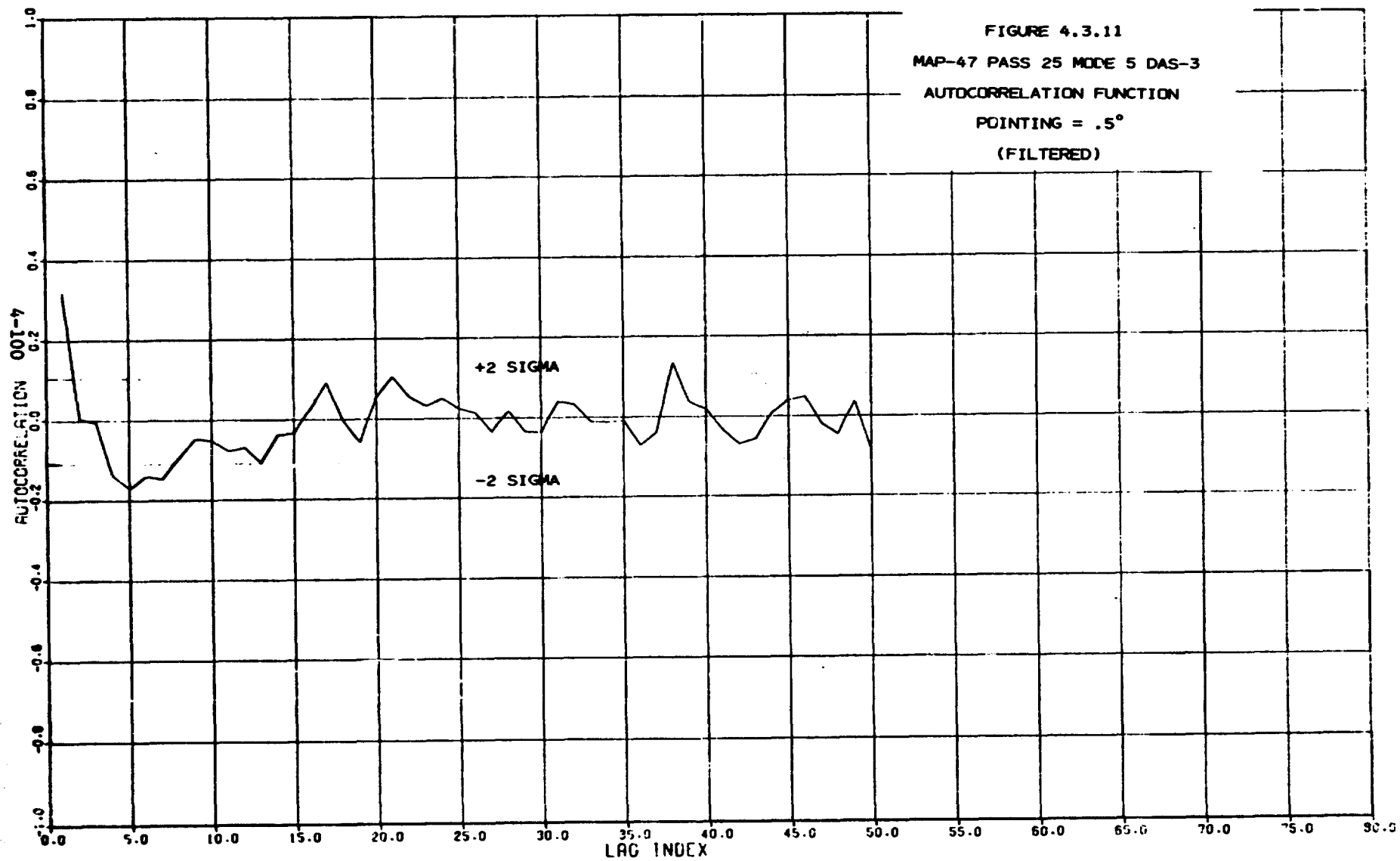
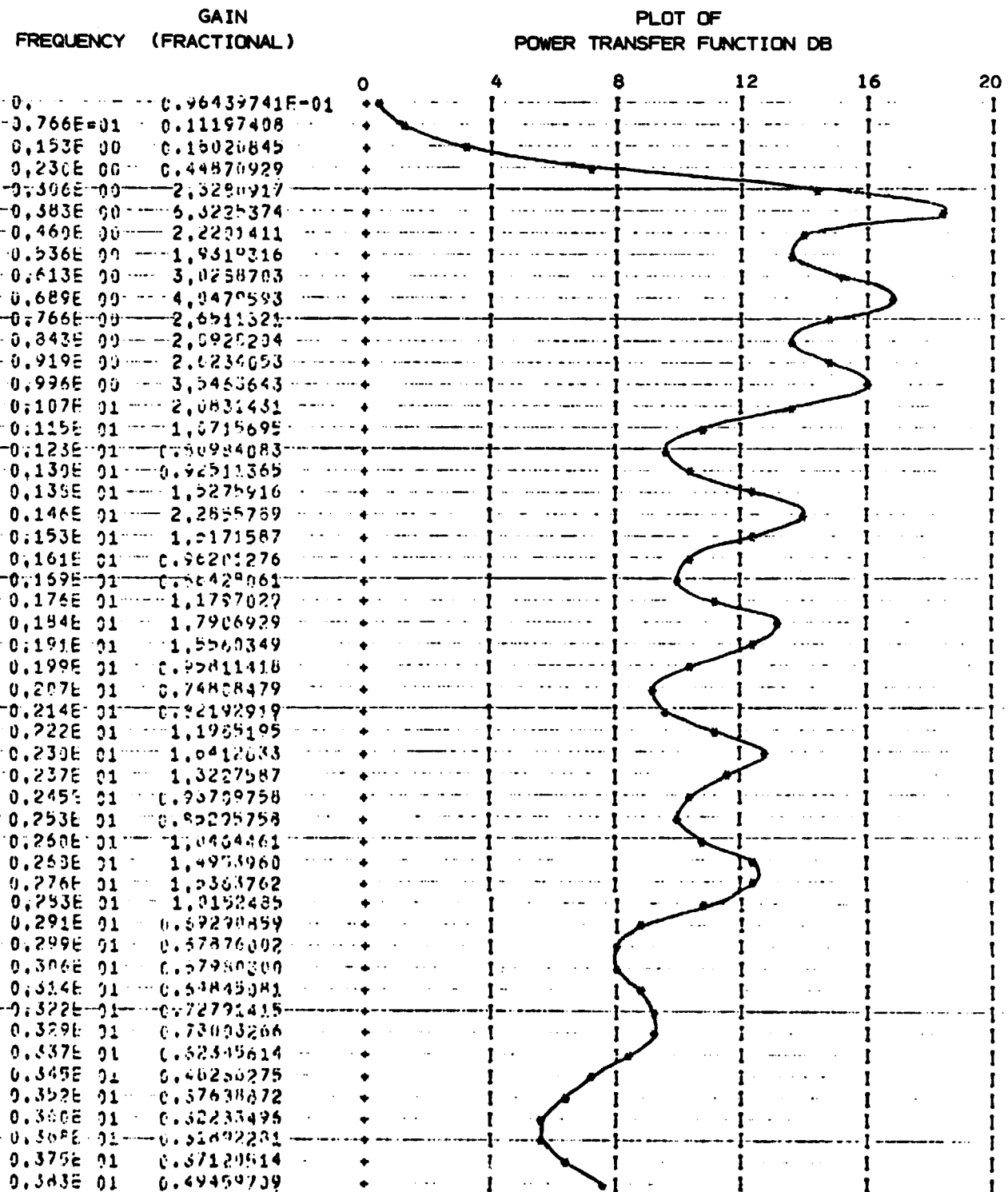
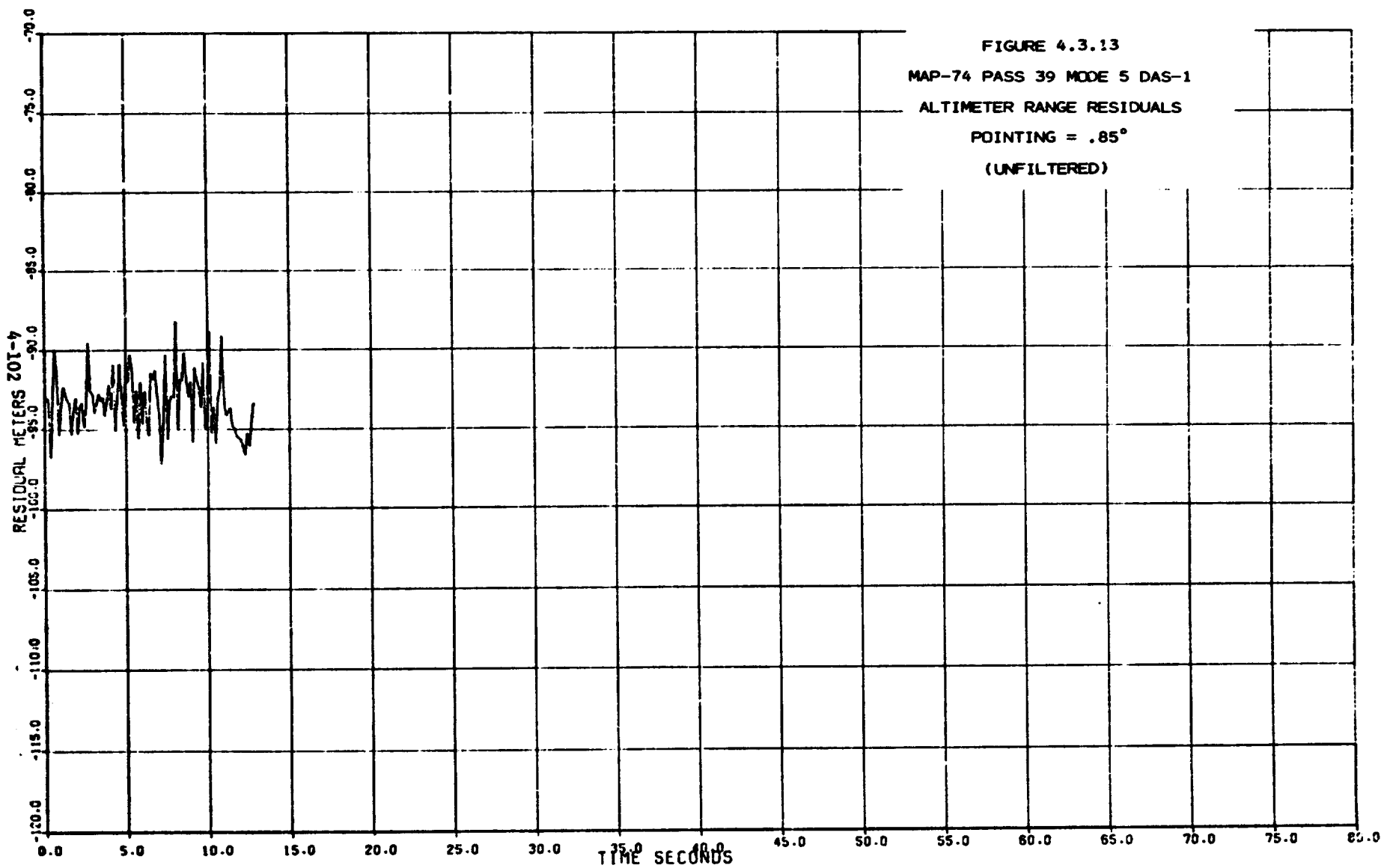
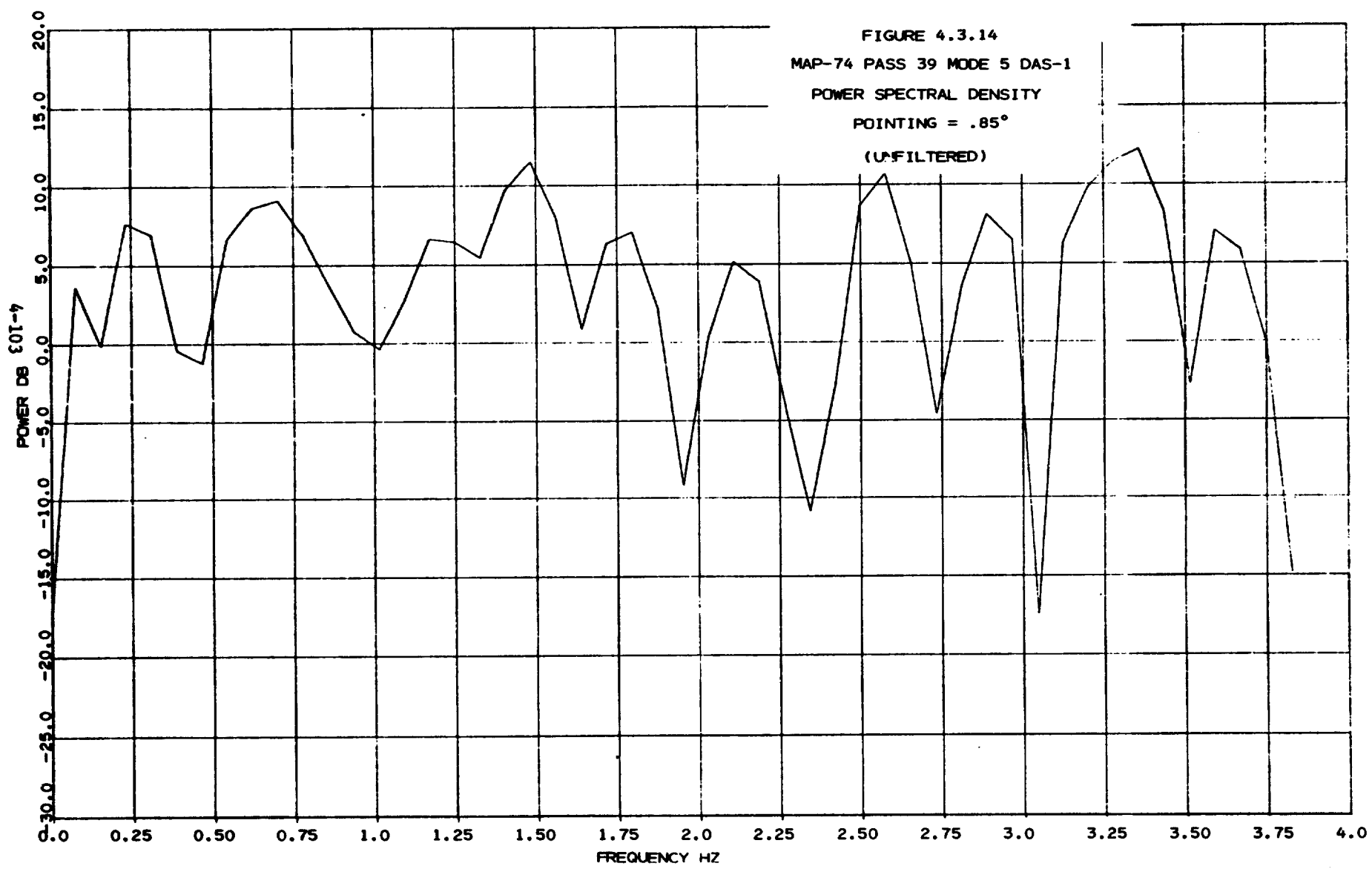


FIGURE 4.3.12  
AUTOREGRESSIVE MODEL

MAP-47 PASS-5 MODE-5 DAS-3  
(FILTERED)







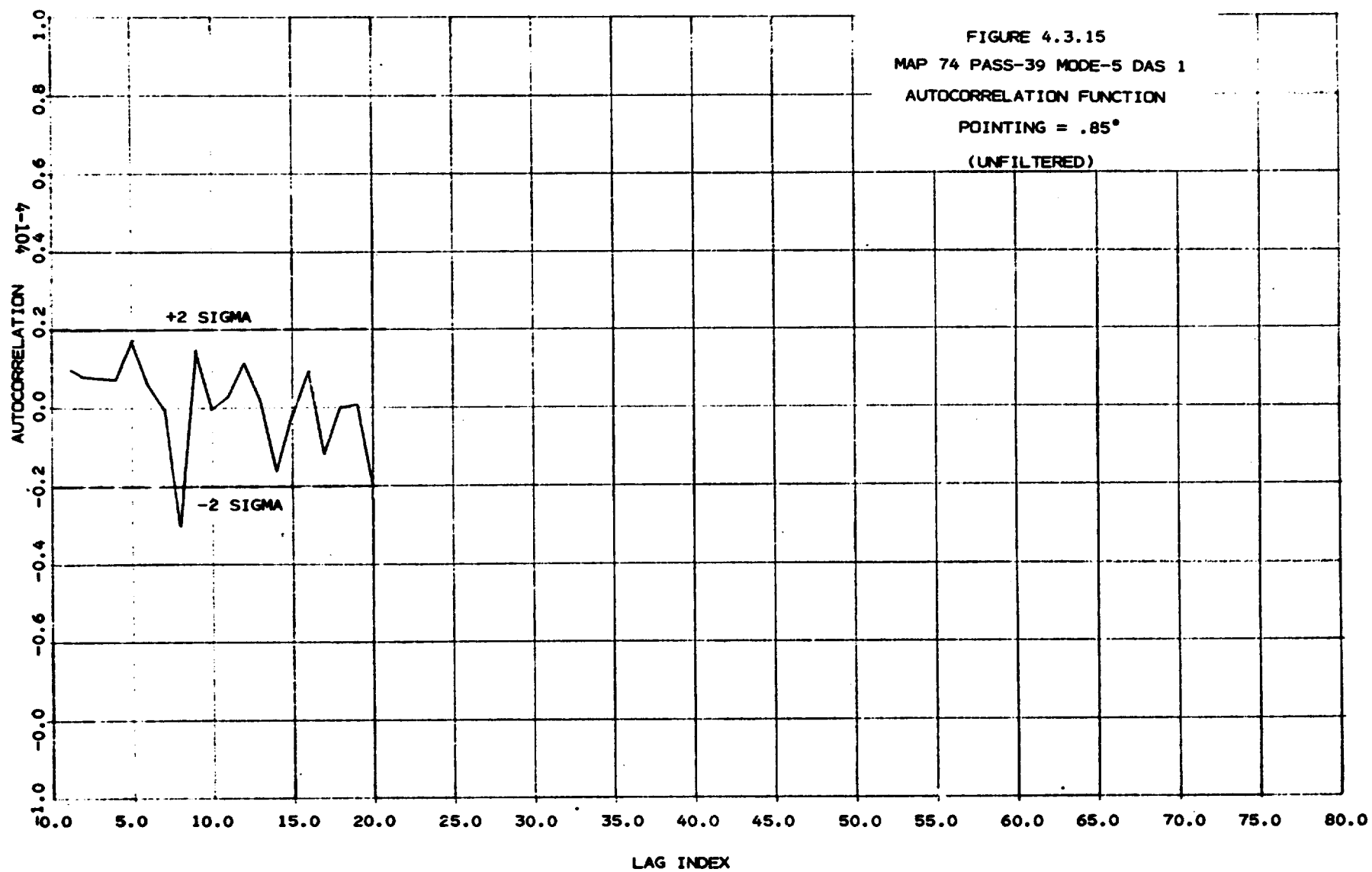
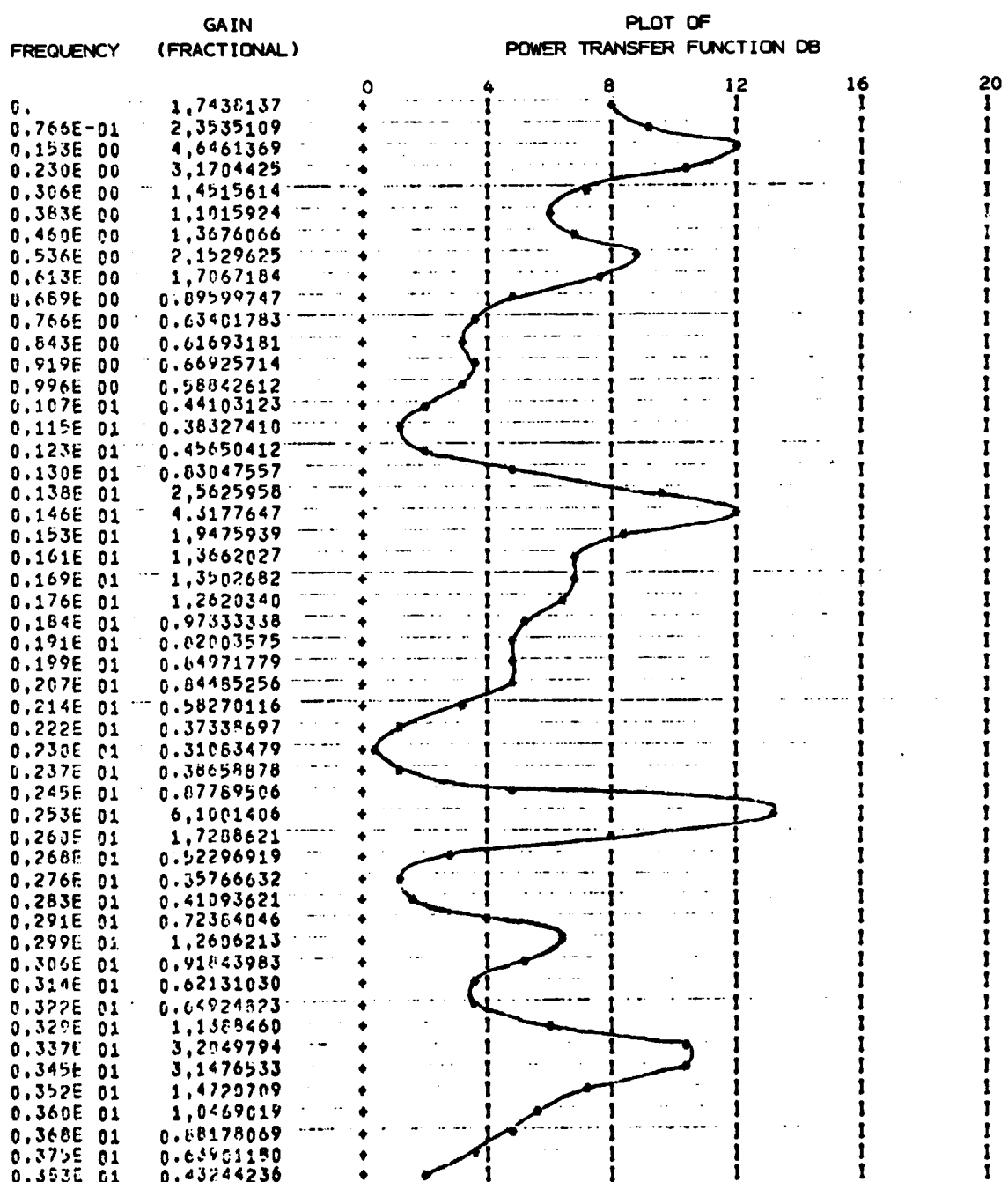
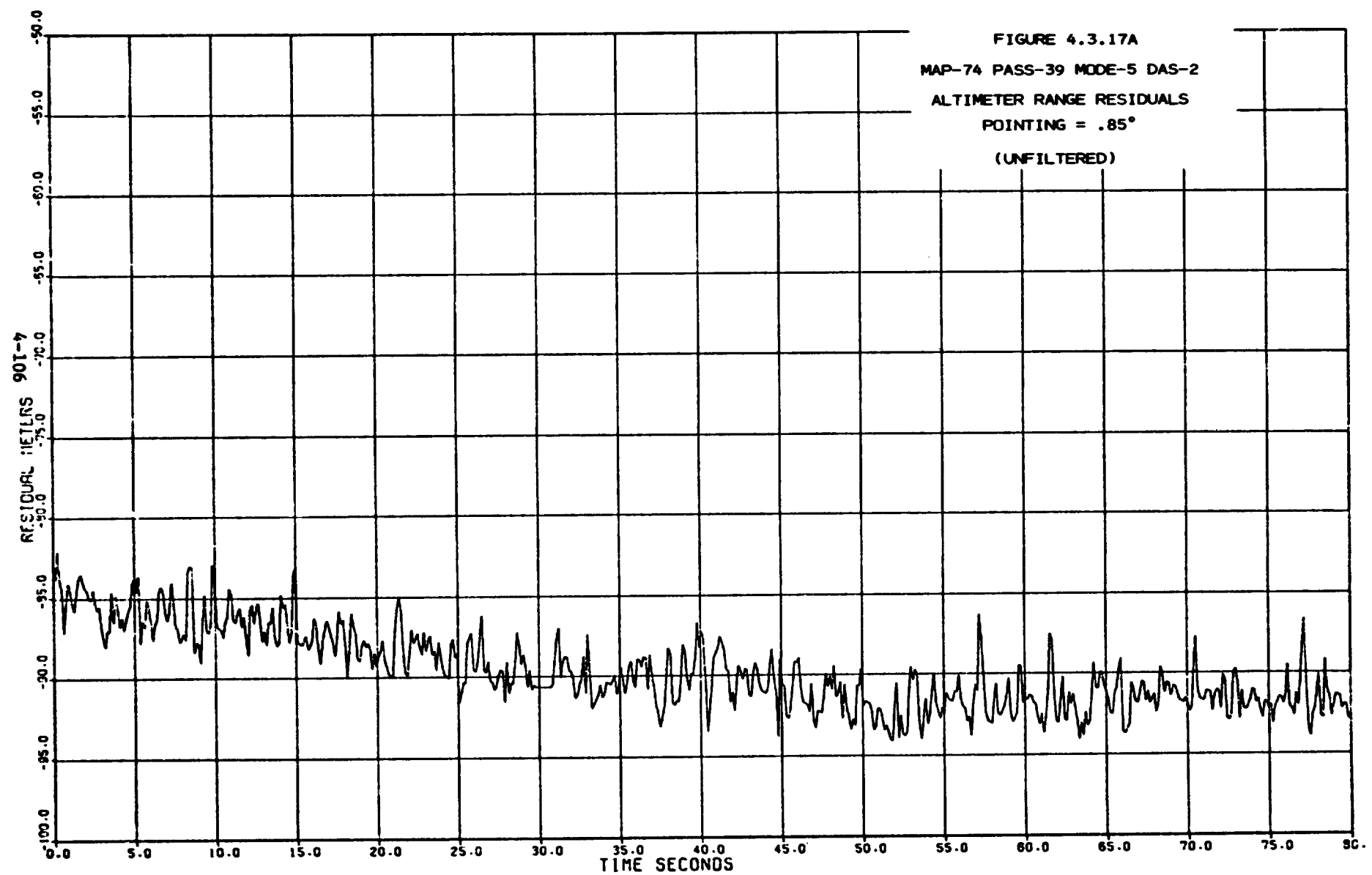
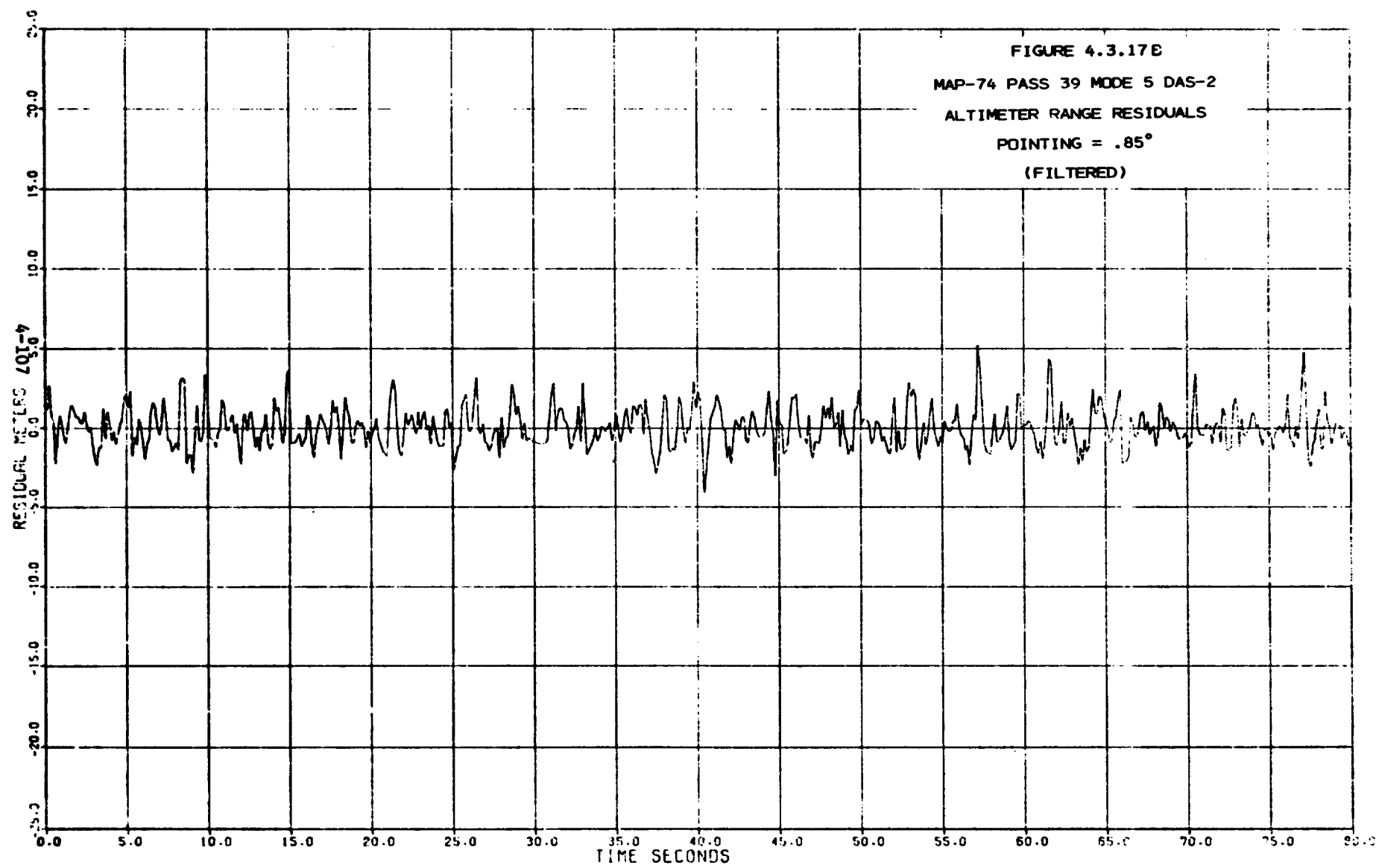
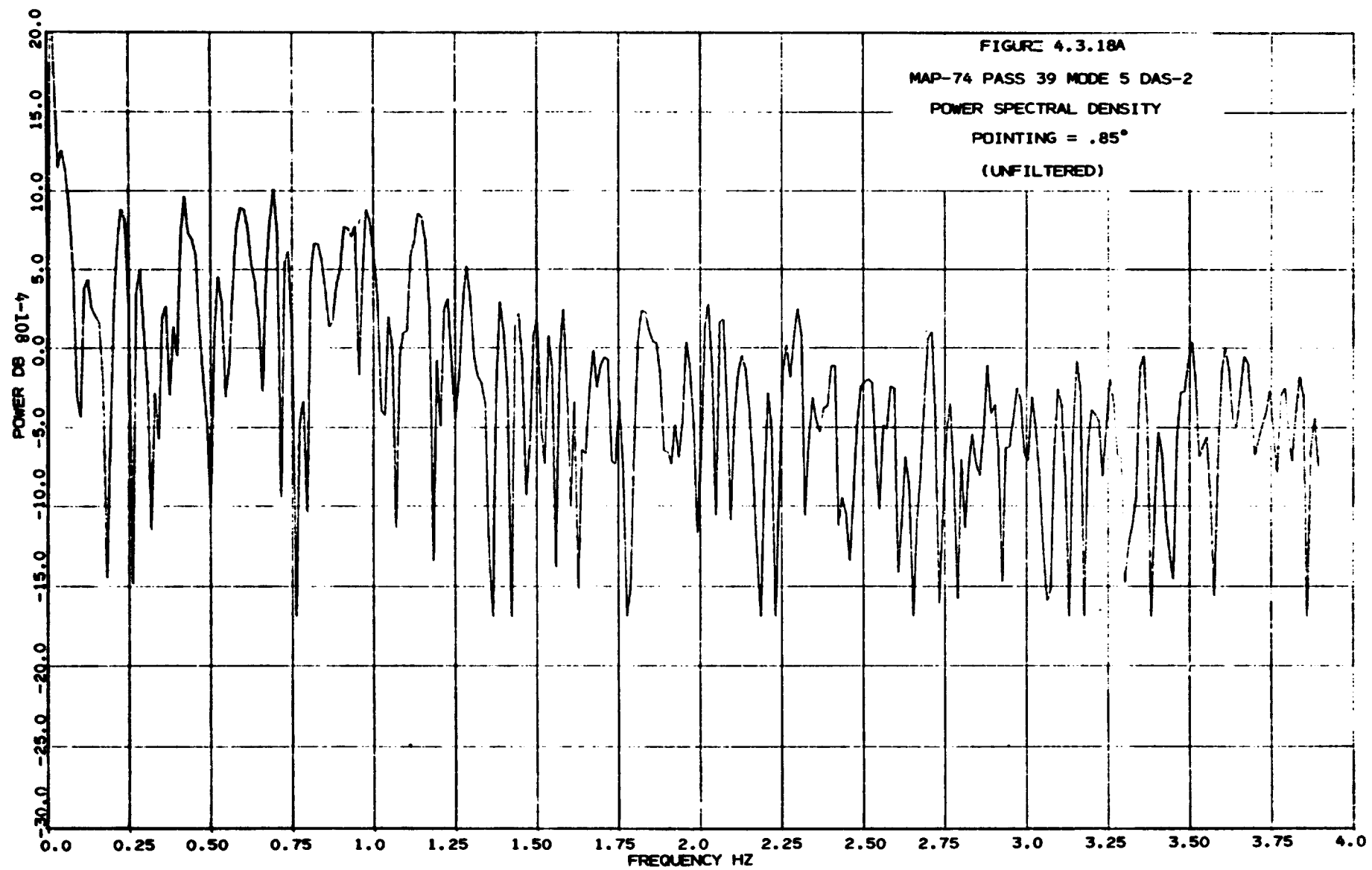


FIGURE 4.3.16  
AUTOREGRESSIVE MODEL  
MAP-74 PASS-39 MODE-5 DAS-1  
(UNFILTERED)









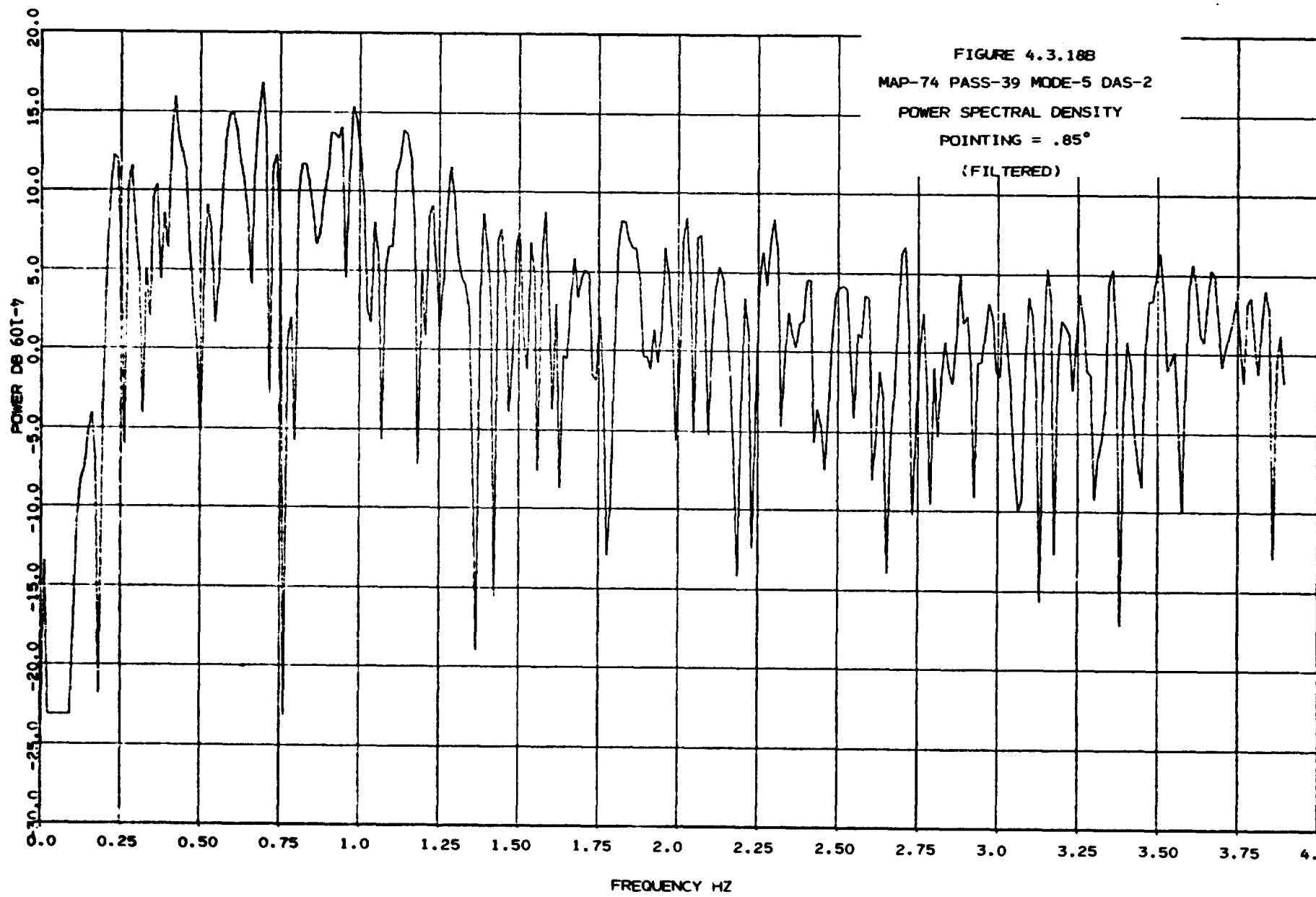


FIGURE 4.3.19

MAP-74 PASS 39 MODE 5 DAS-2

AUTOCORRELATION FUNCTION

POINTING =  $.85^\circ$

(FILTERED)

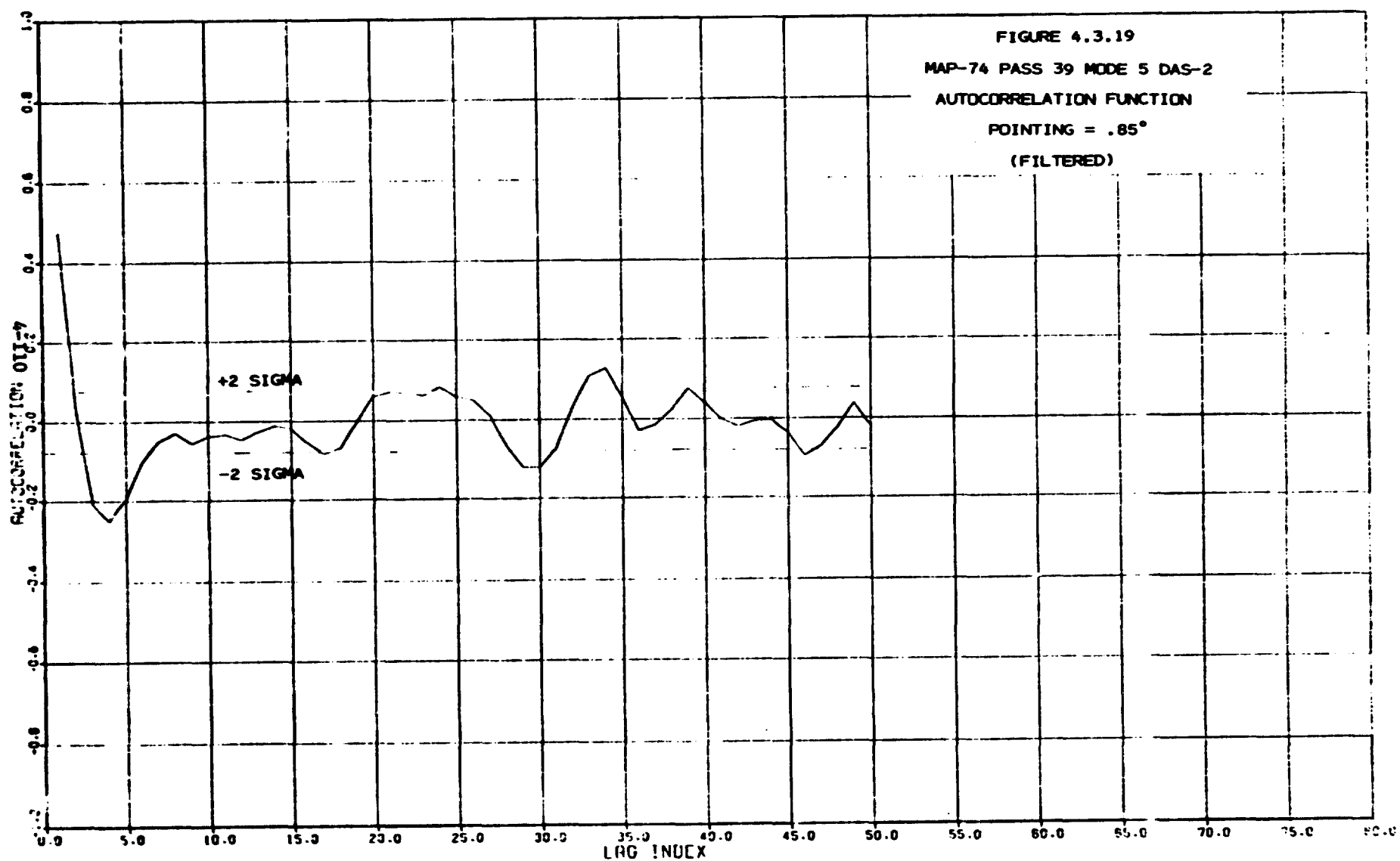
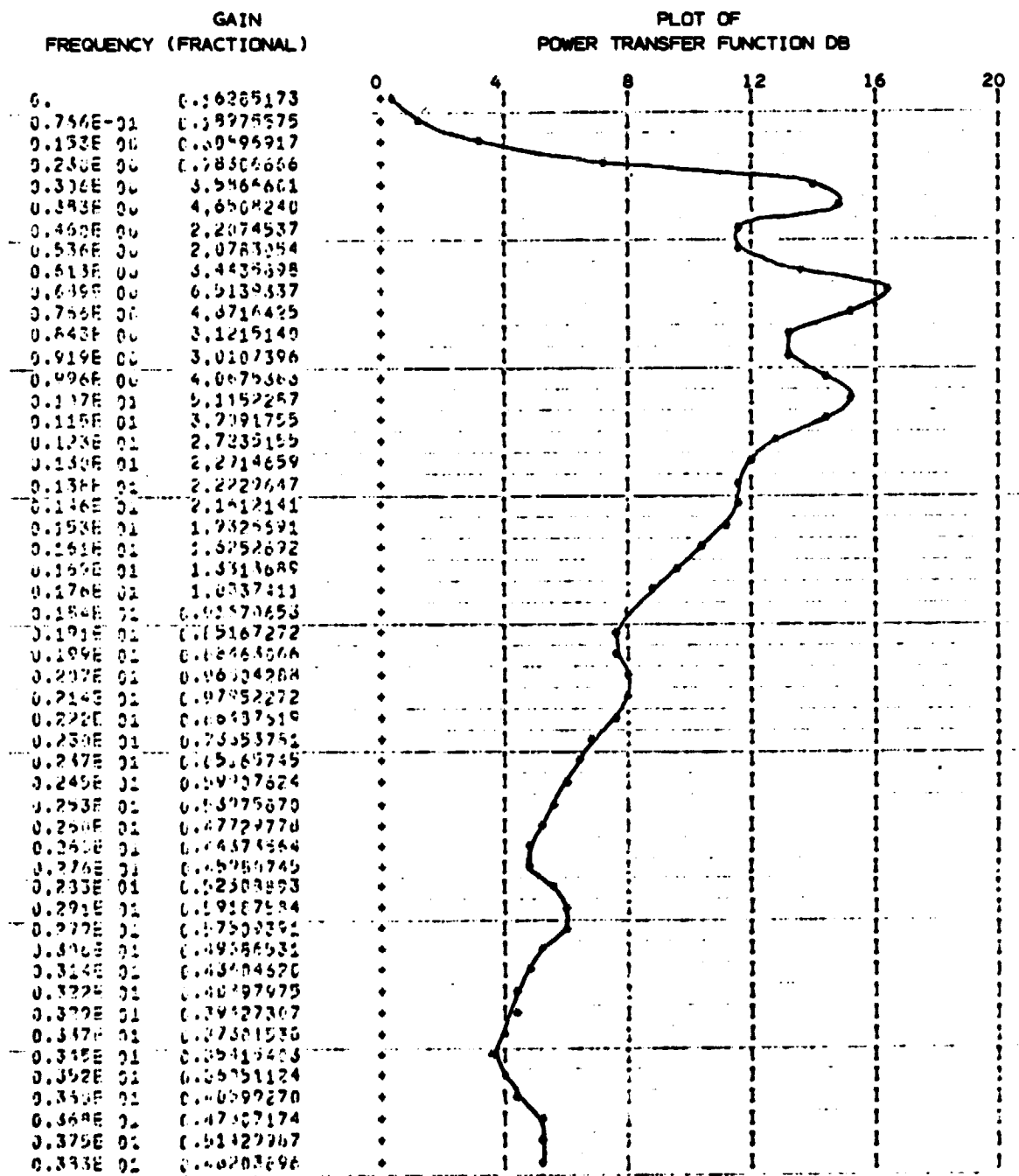
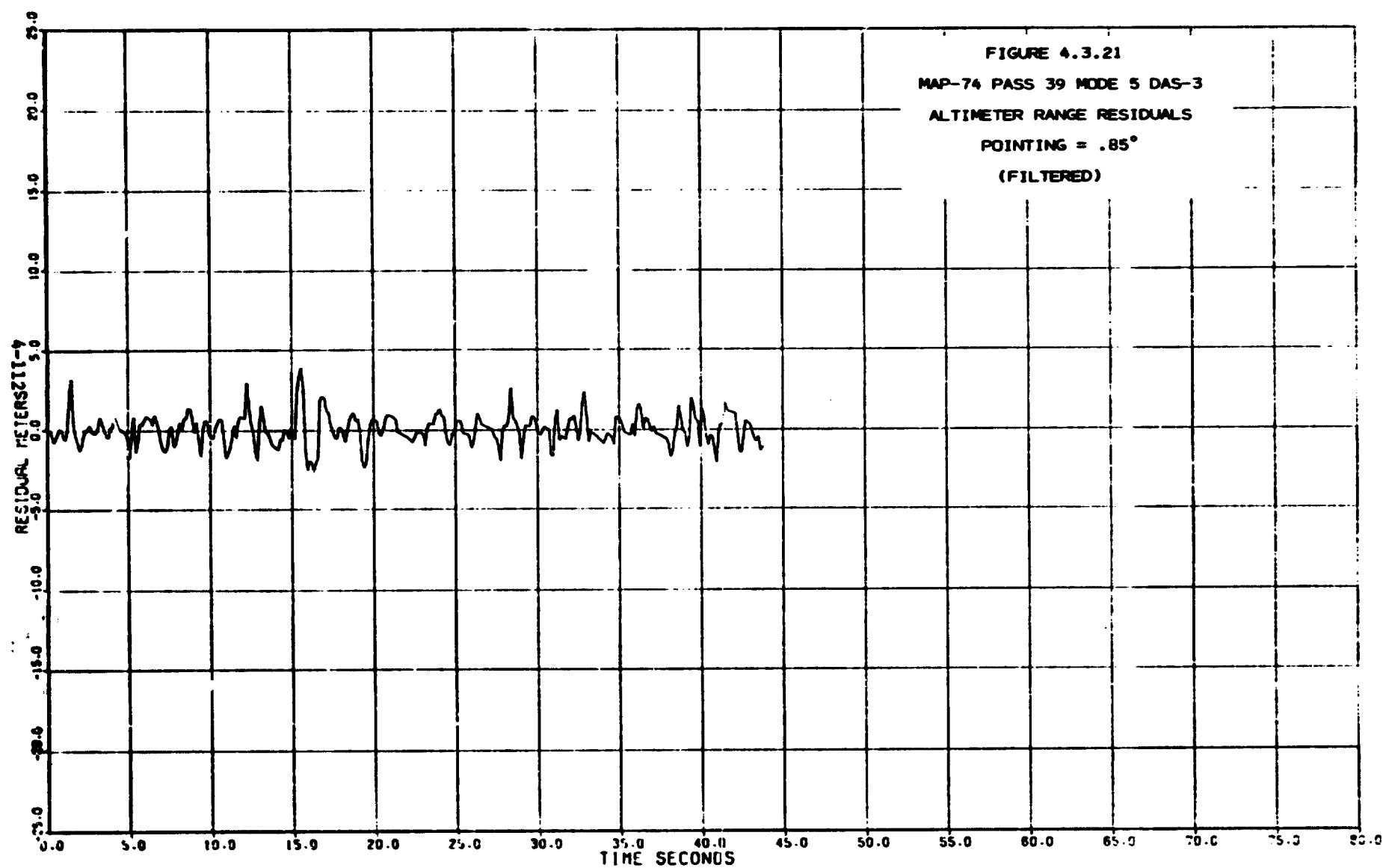


FIGURE 4.3.20  
AUTOREGRESSIVE MODEL

MAP-74 PASS-39 MODE-5 DAS-2  
(FILTERED)





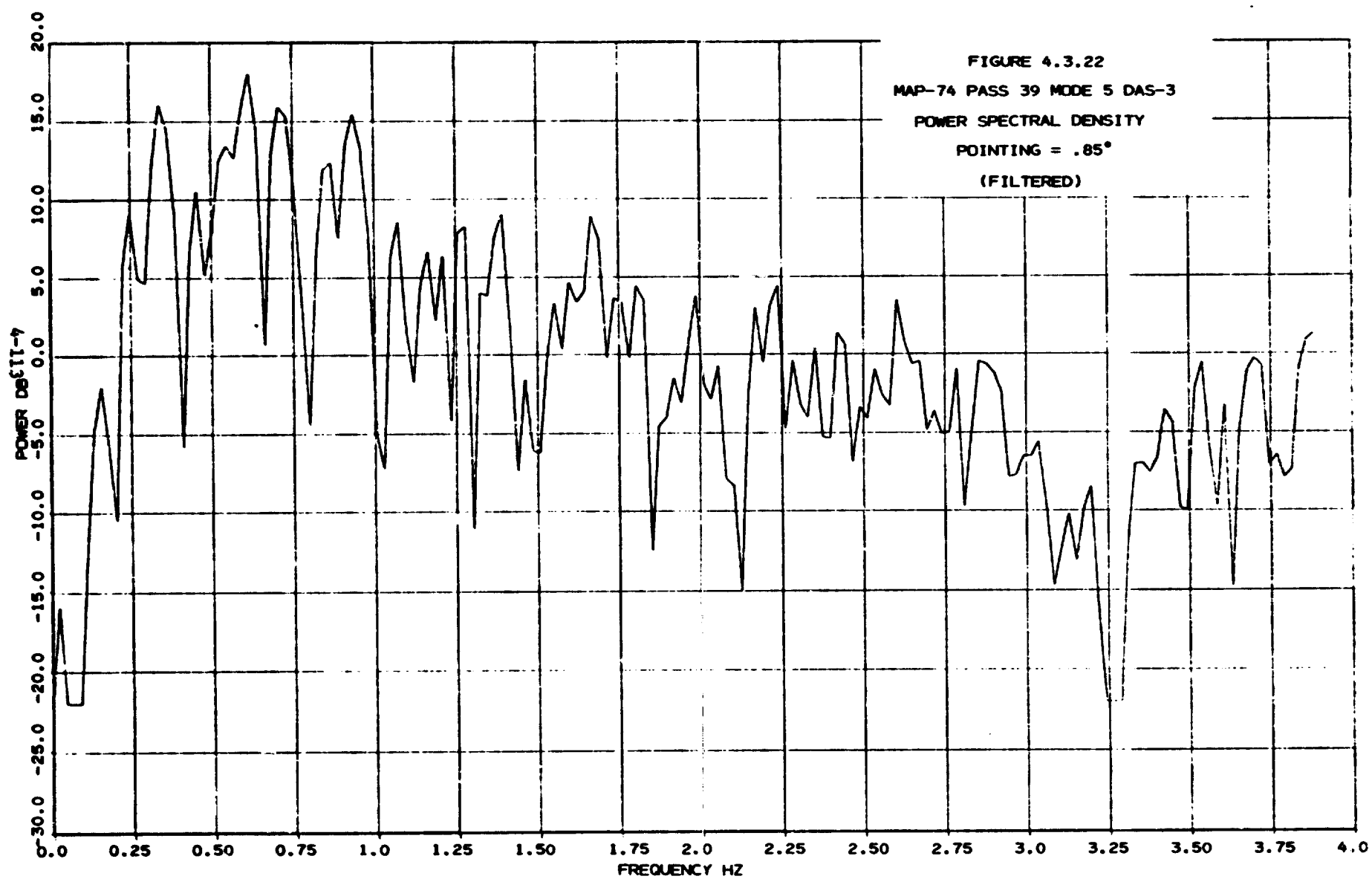


FIGURE 4.3.23  
MAP-74 PASS 39 MODE 5 DAS-3  
AUTOCORRELATION FUNCTION  
POINTING =  $.85^\circ$   
(FILTERED)

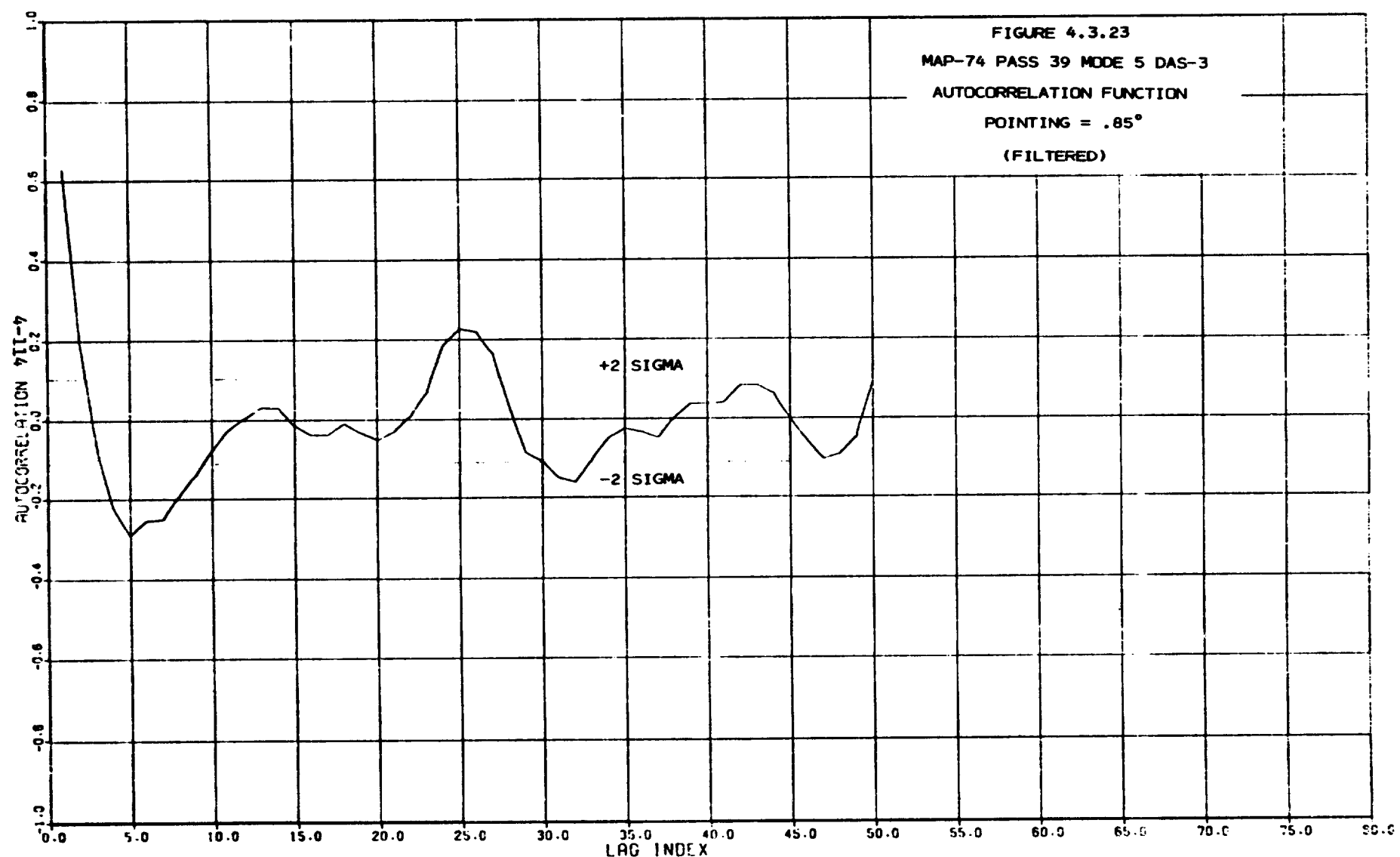


FIGURE 4.3.24  
AUTOREGRESSIVE MODEL

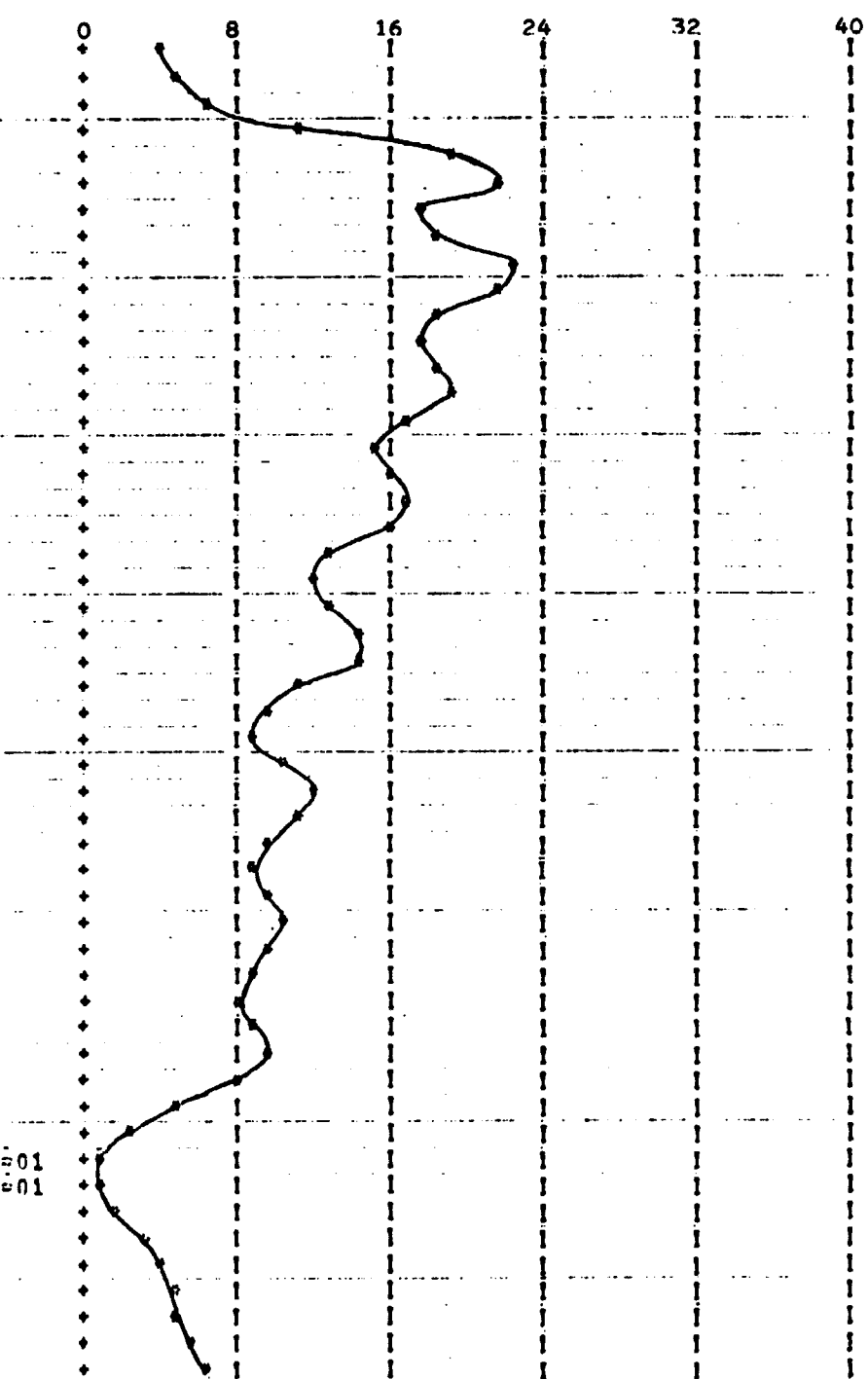
MAP-74 PASS-39 MODE-5 DAS-3

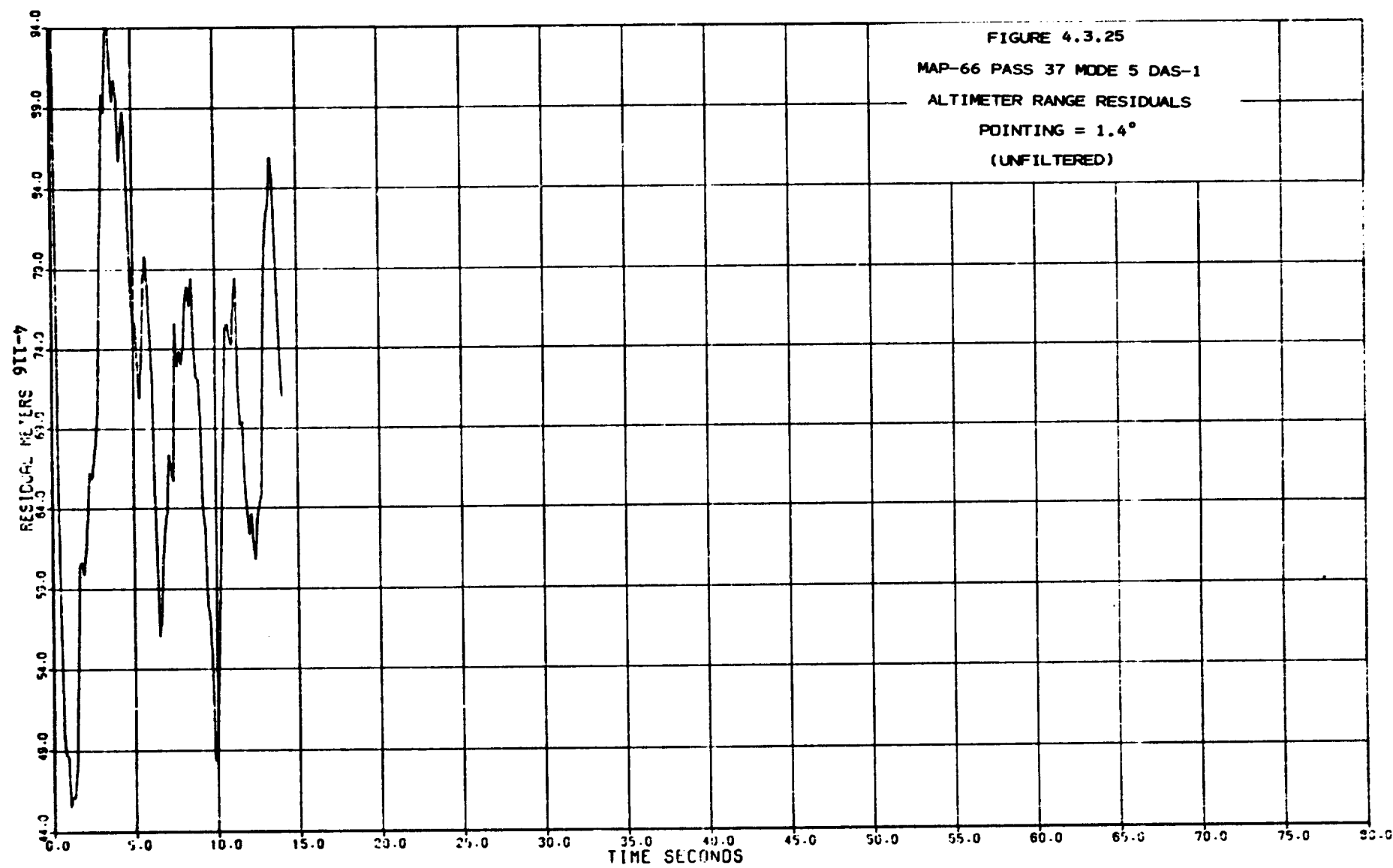
(FILTERED)

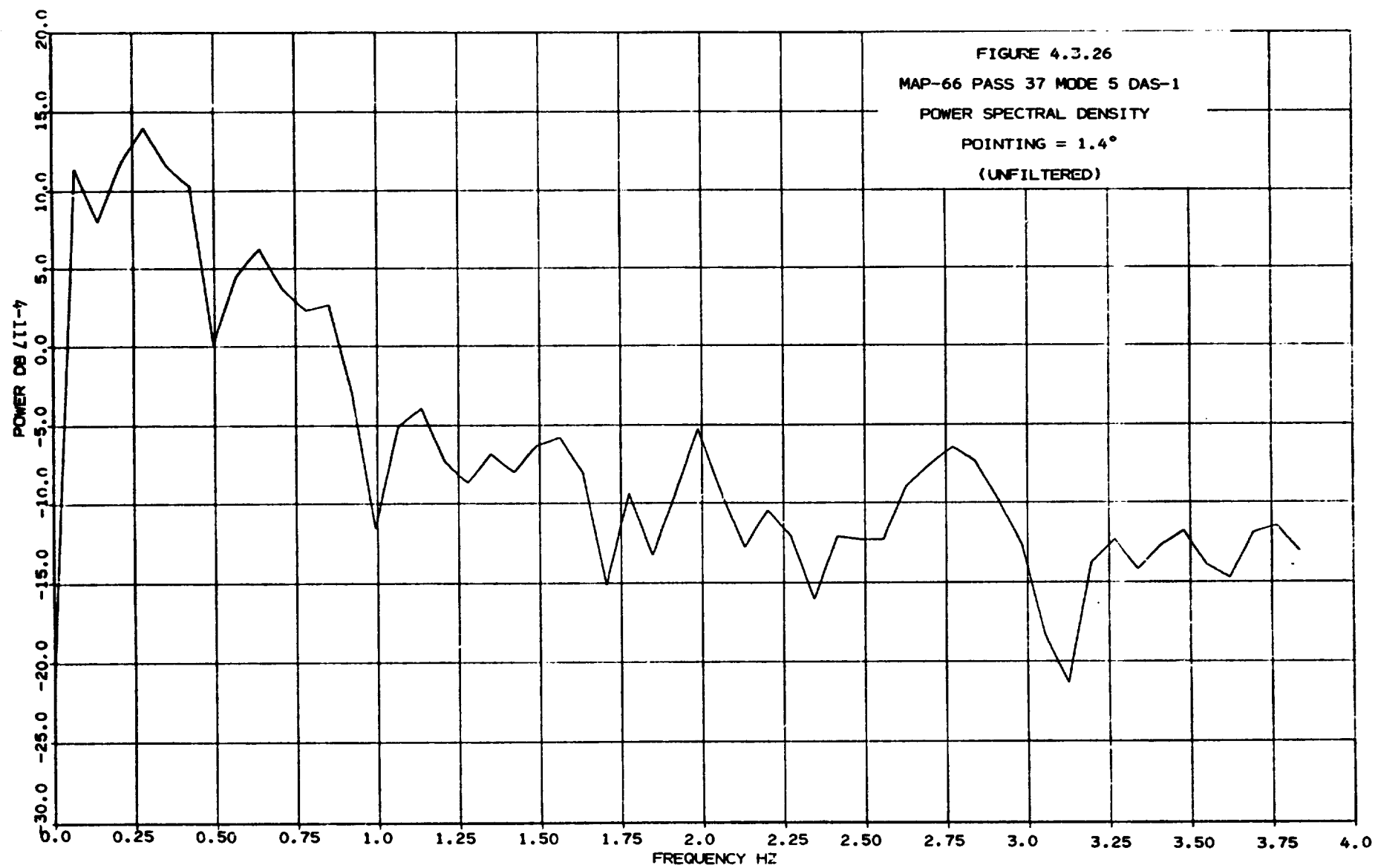
GAIN  
FREQUENCY (FRACTIONAL)

0,	0.18978398
0.766E-01	0.22283731
0.153E 00	0.37228591
0.230E 00	1.0045366
0.306E 00	6.1584156
0.383E 00	11.925826
0.460E 00	5.0051292
0.536E 00	6.0000977
0.613E 00	14.806592
0.689E 00	11.411397
0.766E 00	5.0505692
0.843E 00	4.2246234
0.919E 00	5.6179621
0.996E 00	6.1133021
0.107E 01	3.7312100
0.115E 01	2.7078932
0.123E 01	2.9920817
0.130E 01	4.0222930
0.138E 01	3.0284959
0.146E 01	1.5483108
0.153E 01	1.2263917
0.161E 01	1.3831472
0.169E 01	2.0912151
0.176E 01	2.0169522
0.184E 01	1.0565130
0.191E 01	0.67529567
0.199E 01	0.62990099
0.207E 01	0.83295122
0.214E 01	1.2378088
0.222E 01	1.1232908
0.230E 01	0.73977754
0.237E 01	0.60610903
0.245E 01	0.67491619
0.253E 01	0.85202871
0.260E 01	0.79279018
0.268E 01	0.56766849
0.276E 01	0.47976611
0.283E 01	0.55516046
0.291E 01	0.71421687
0.299E 01	0.49034423
0.306E 01	0.22013494
0.314E 01	0.13001926
0.321E 01	0.95135476E-01
0.328E 01	0.95385473E-01
0.337E 01	0.11506076
0.345E 01	0.16029731
0.352E 01	0.21767290
0.360E 01	0.24273639
0.368E 01	0.24496743
0.376E 01	0.27567051
0.383E 01	0.37235376

PLOT OF  
POWER TRANSFER FUNCTION DB







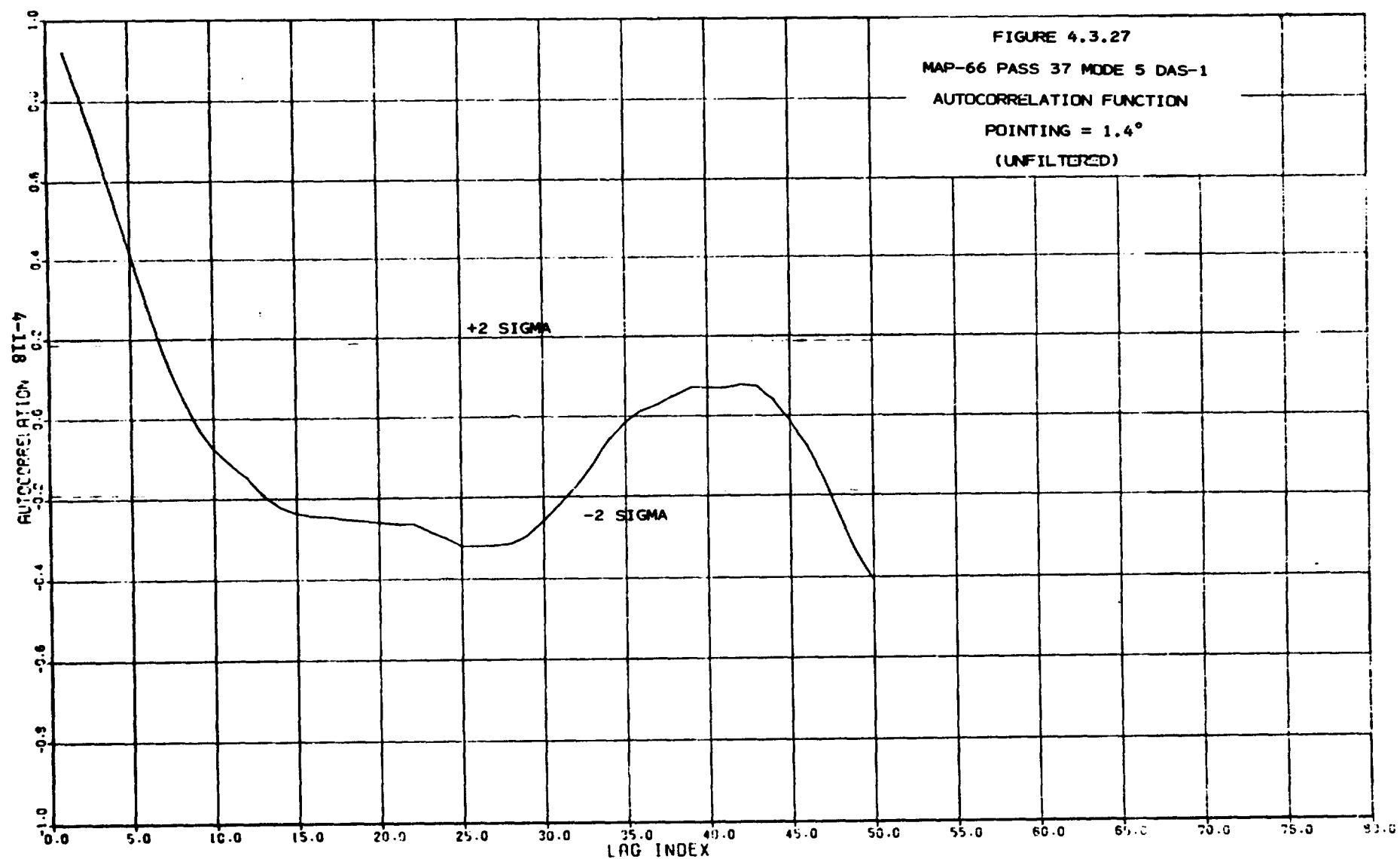
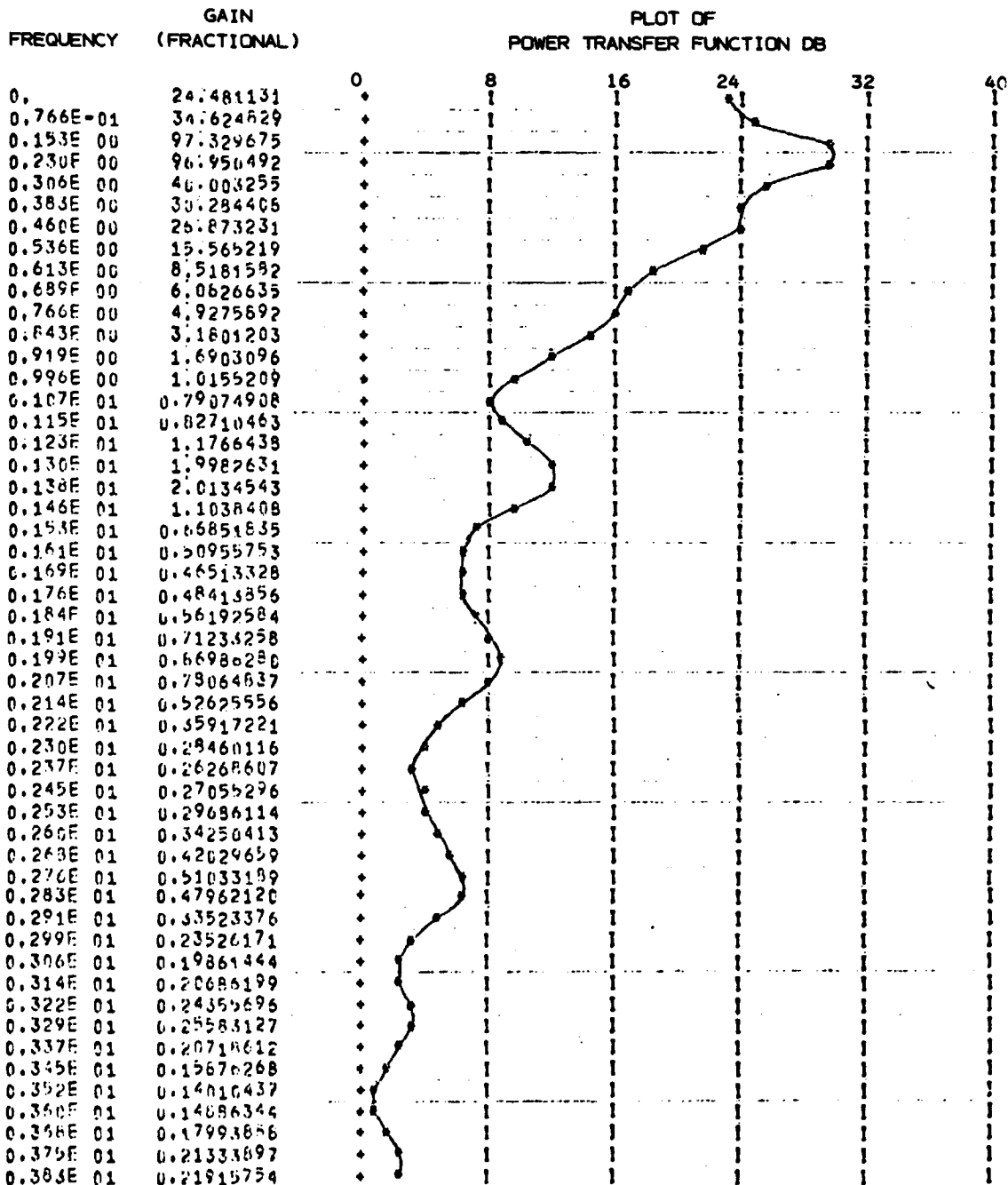
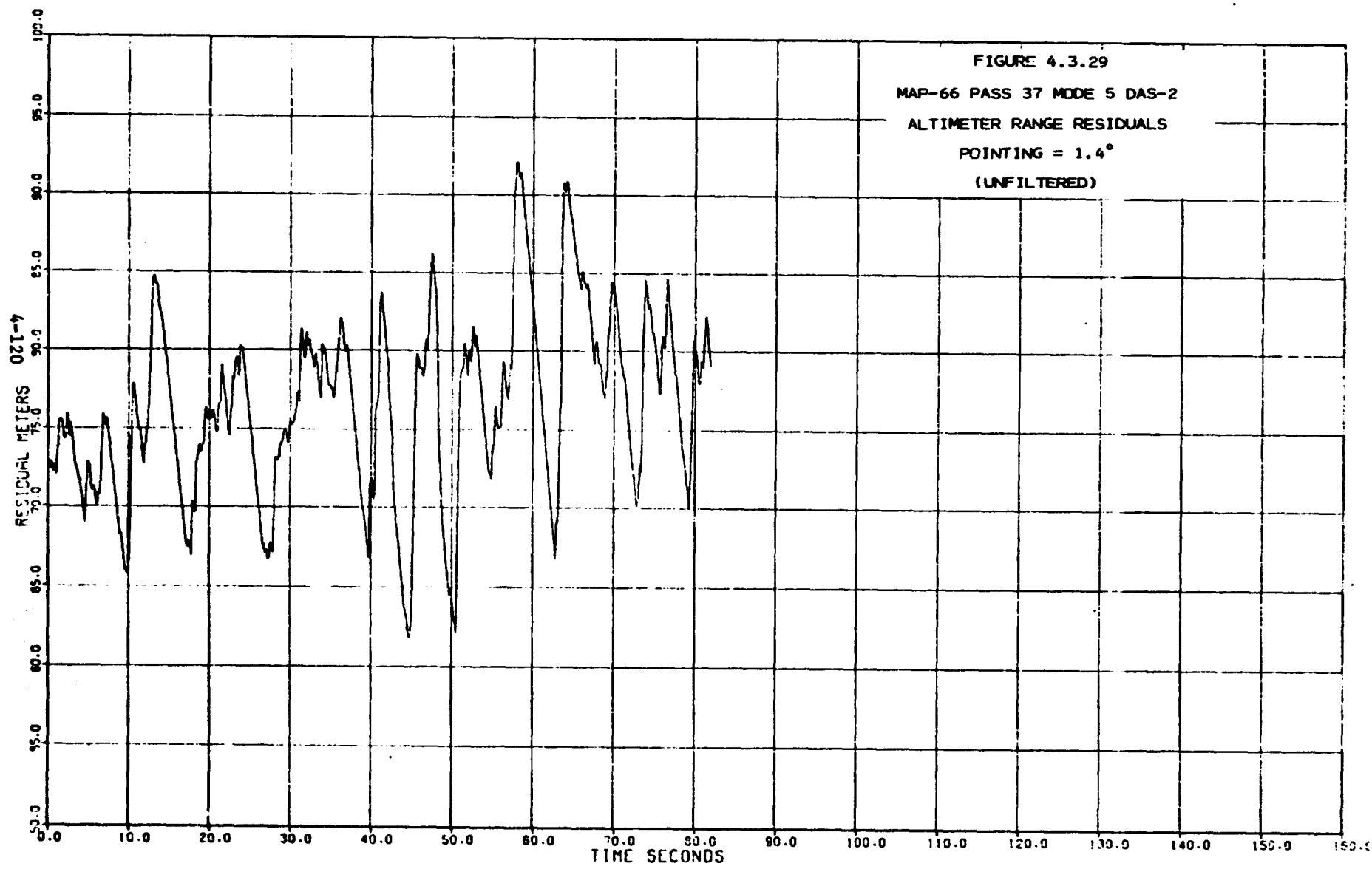


FIGURE 4.3.28  
AUTOREGRESSIVE MODEL  
MAP-66 PASS-37 MODE-5 DAS-1  
(UNFILTERED)





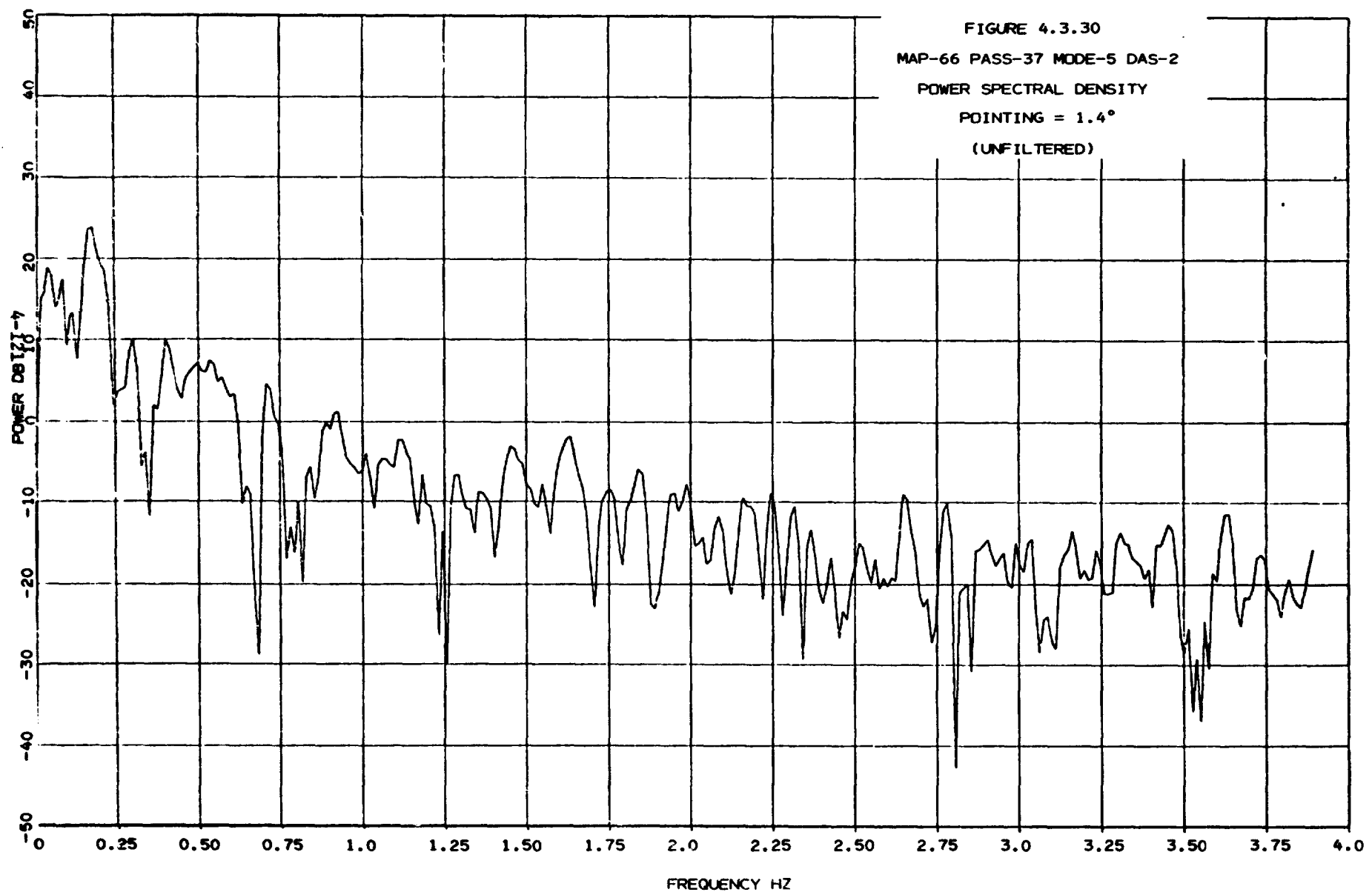


FIGURE 4.3.30  
MAP-66 PASS-37 MODE-5 DAS-2  
POWER SPECTRAL DENSITY  
POINTING =  $1.4^\circ$   
(UNFILTERED)

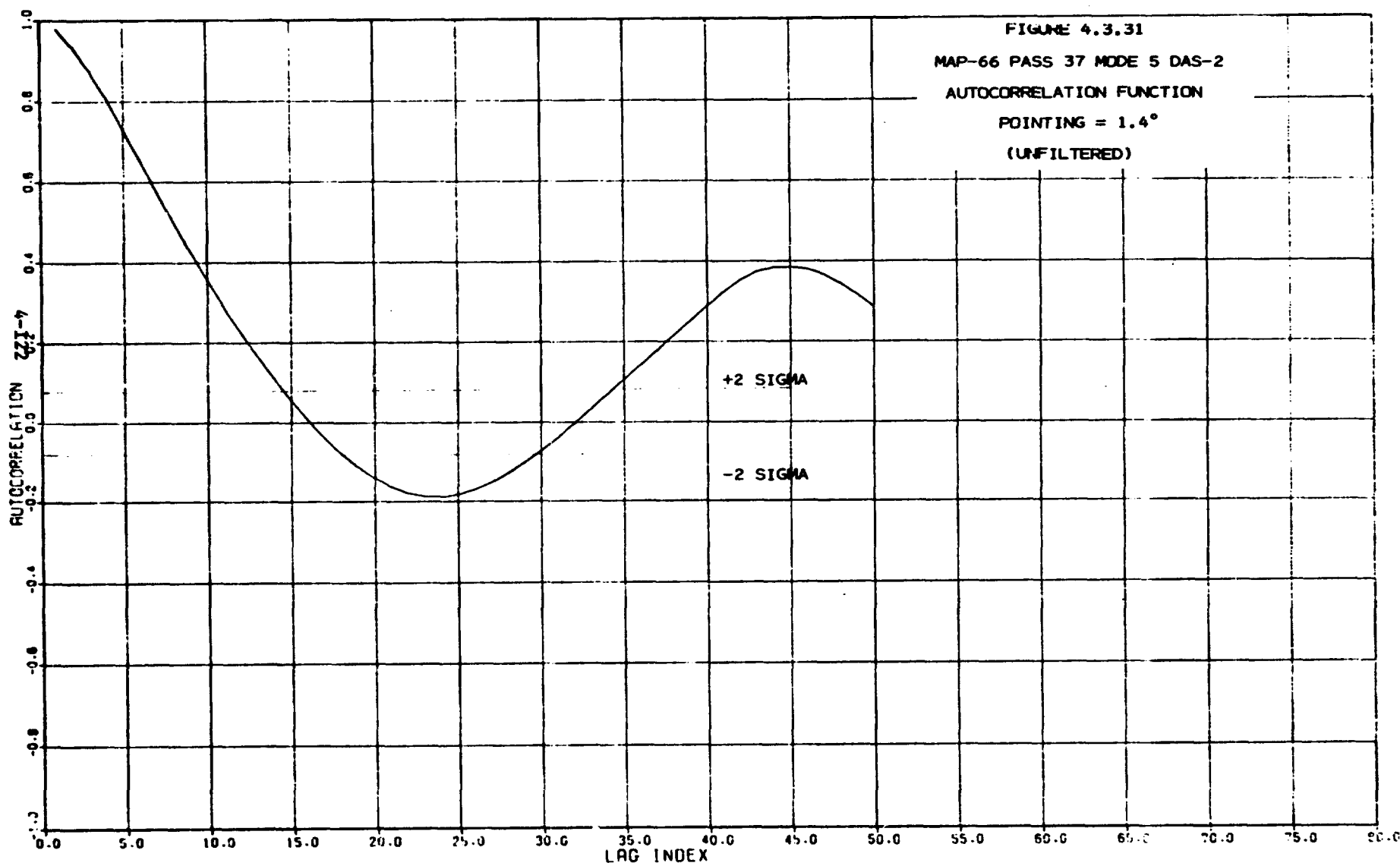
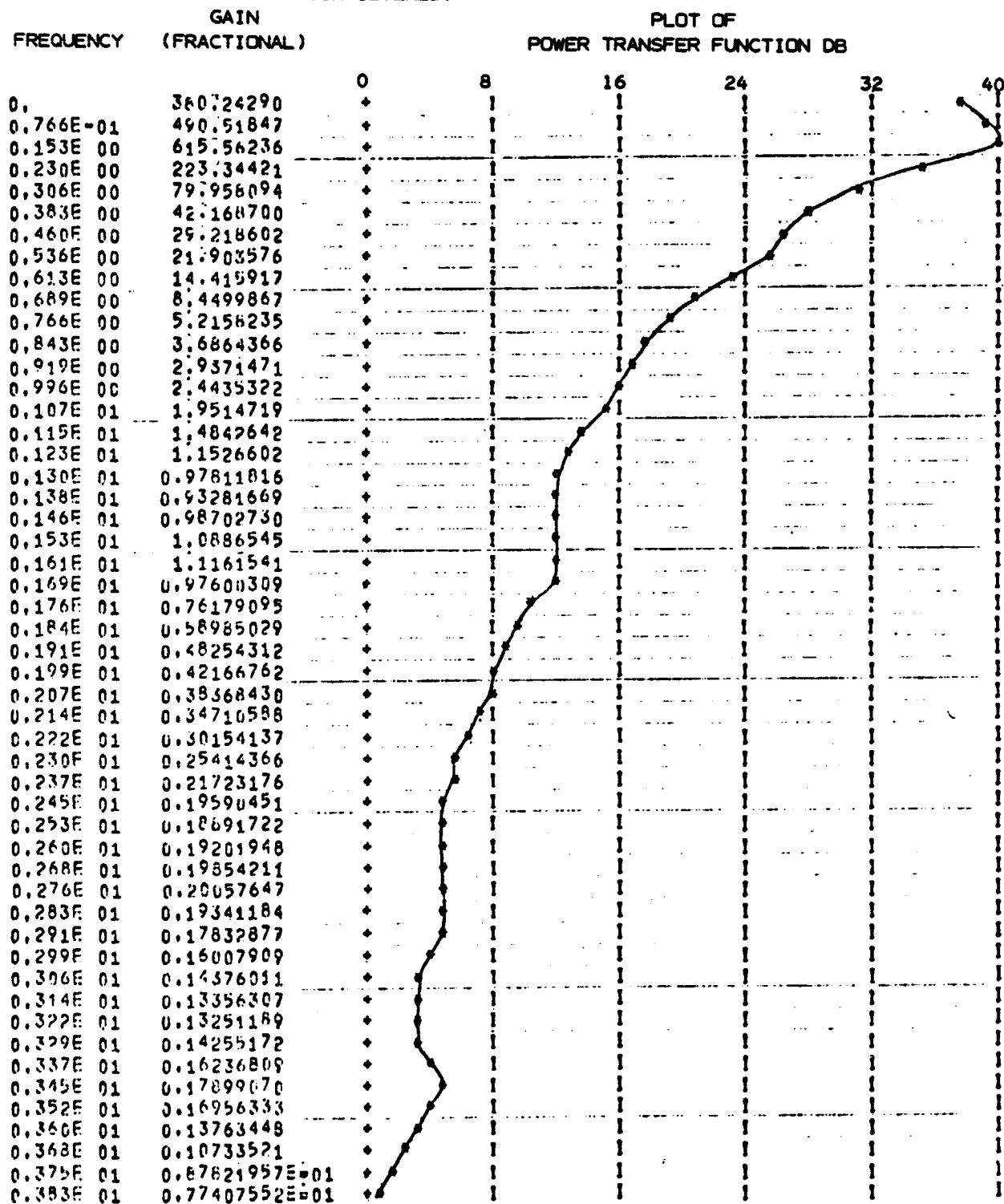


FIGURE 4.3.32  
AUTOREGRESSIVE MODEL

MAP-66 PASS-37 MODE-5 DAS-2  
(UNFILTERED)



ORIGINAL PAGE IS  
OF POOR QUALITY

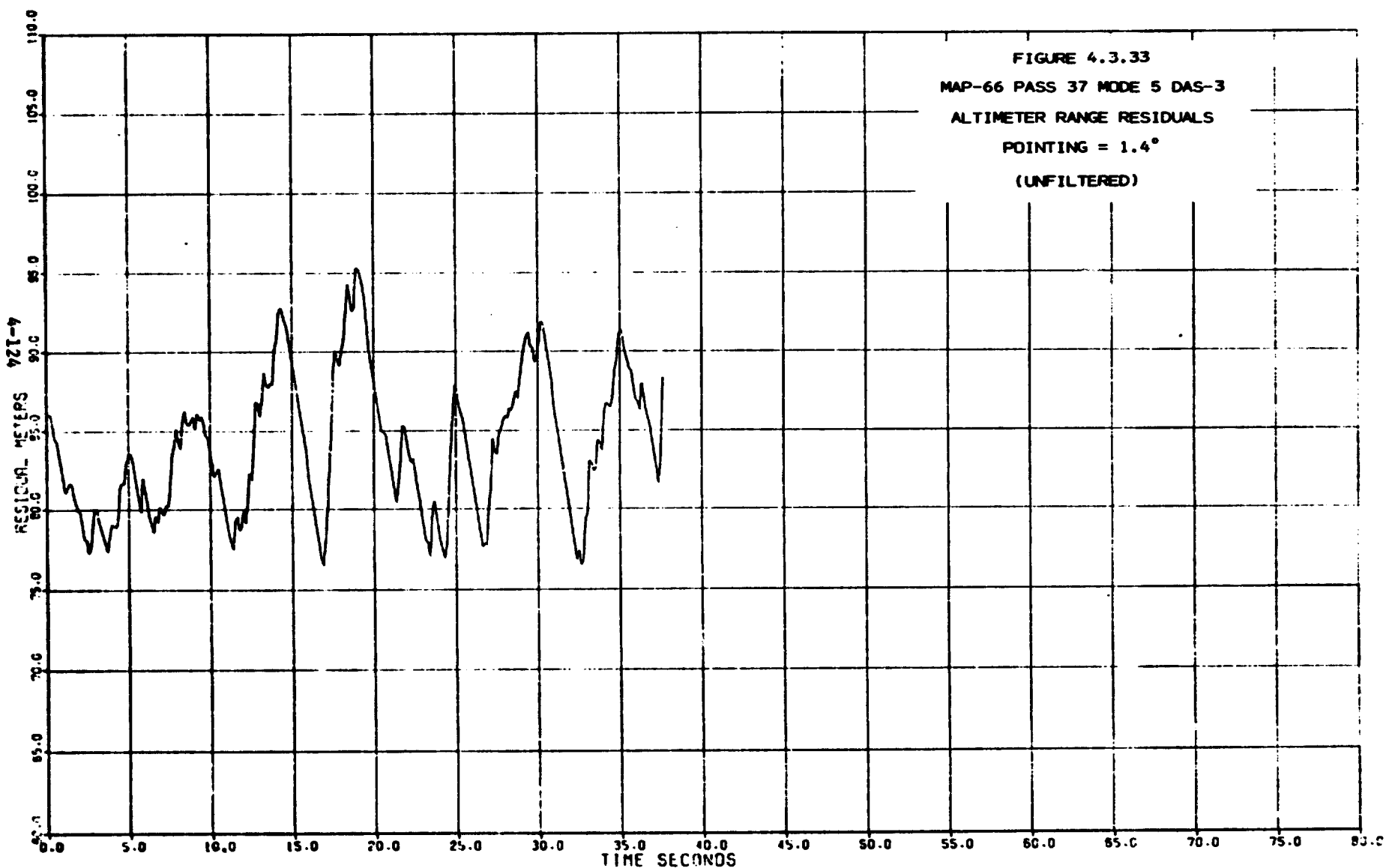
FIGURE 4.3.33

MAP-66 PASS 37 MODE 5 DAS-3

ALTIMETER RANGE RESIDUALS

POINTING = 1.4°

(UNFILTERED)



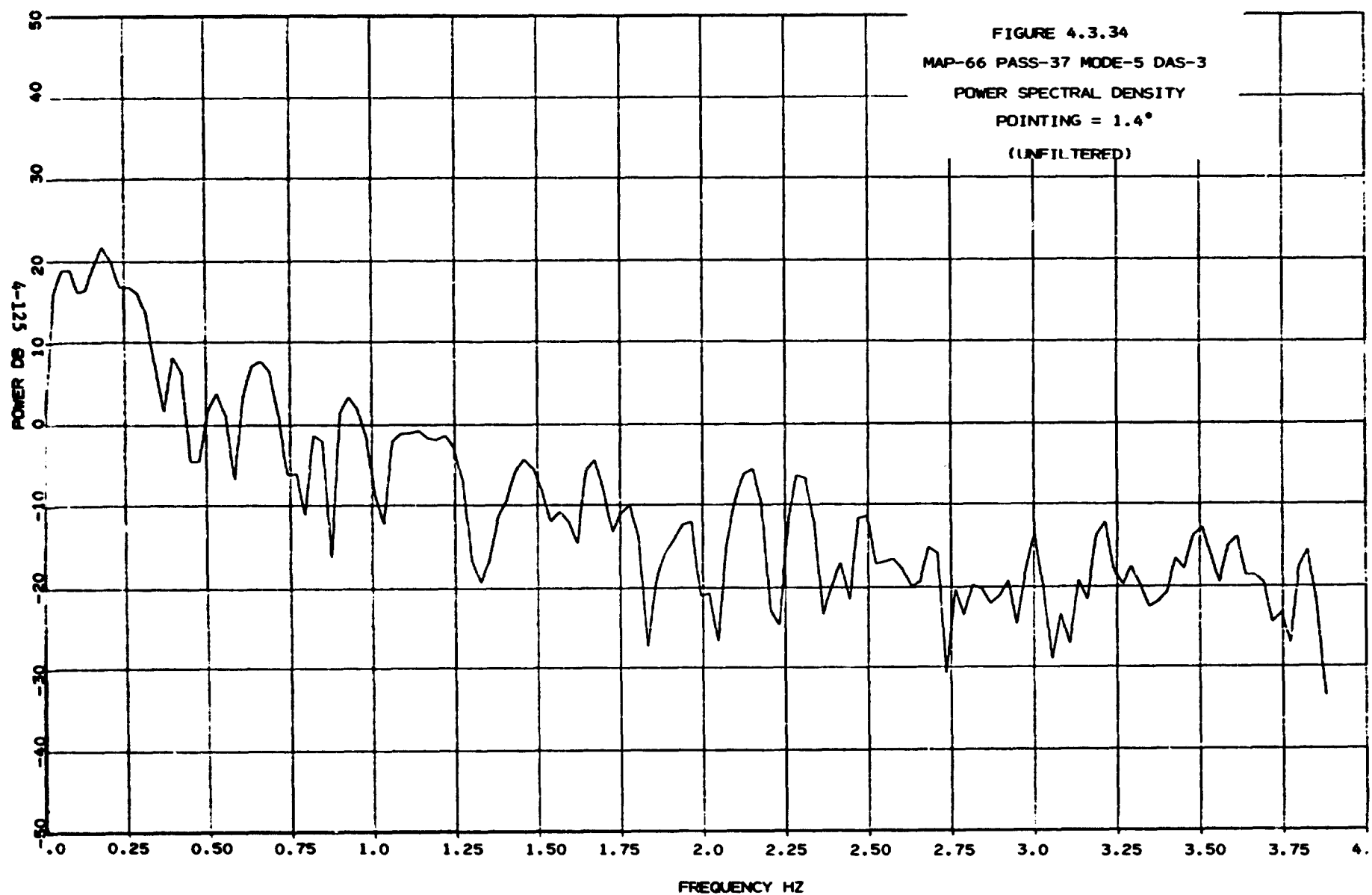


FIGURE 4.3.35

MAP-66 PASS 37 MODE 5 DAS-3  
AUTOCORRELATION FUNCTION  
POINTING =  $1.4^\circ$   
(UNFILTERED)

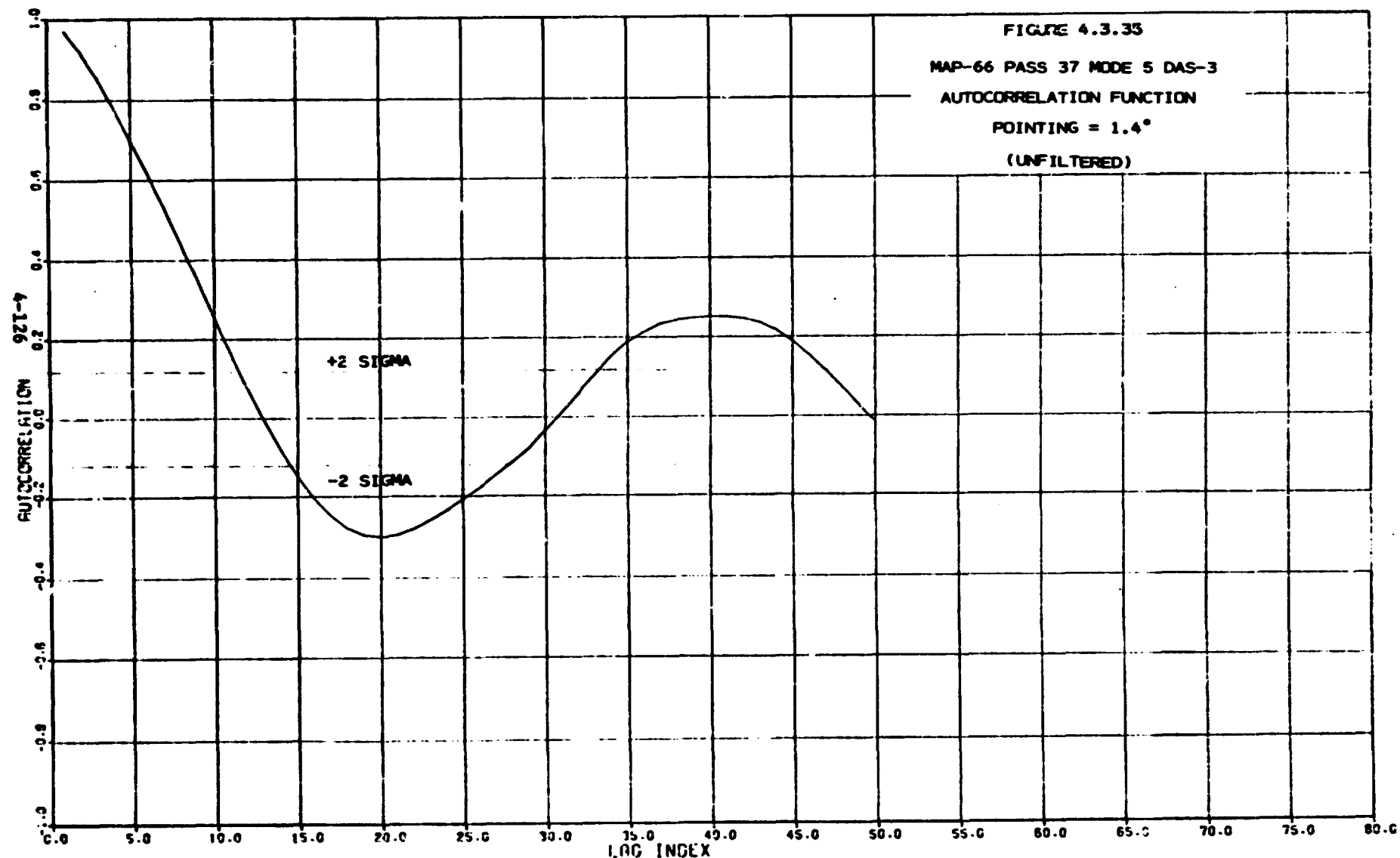
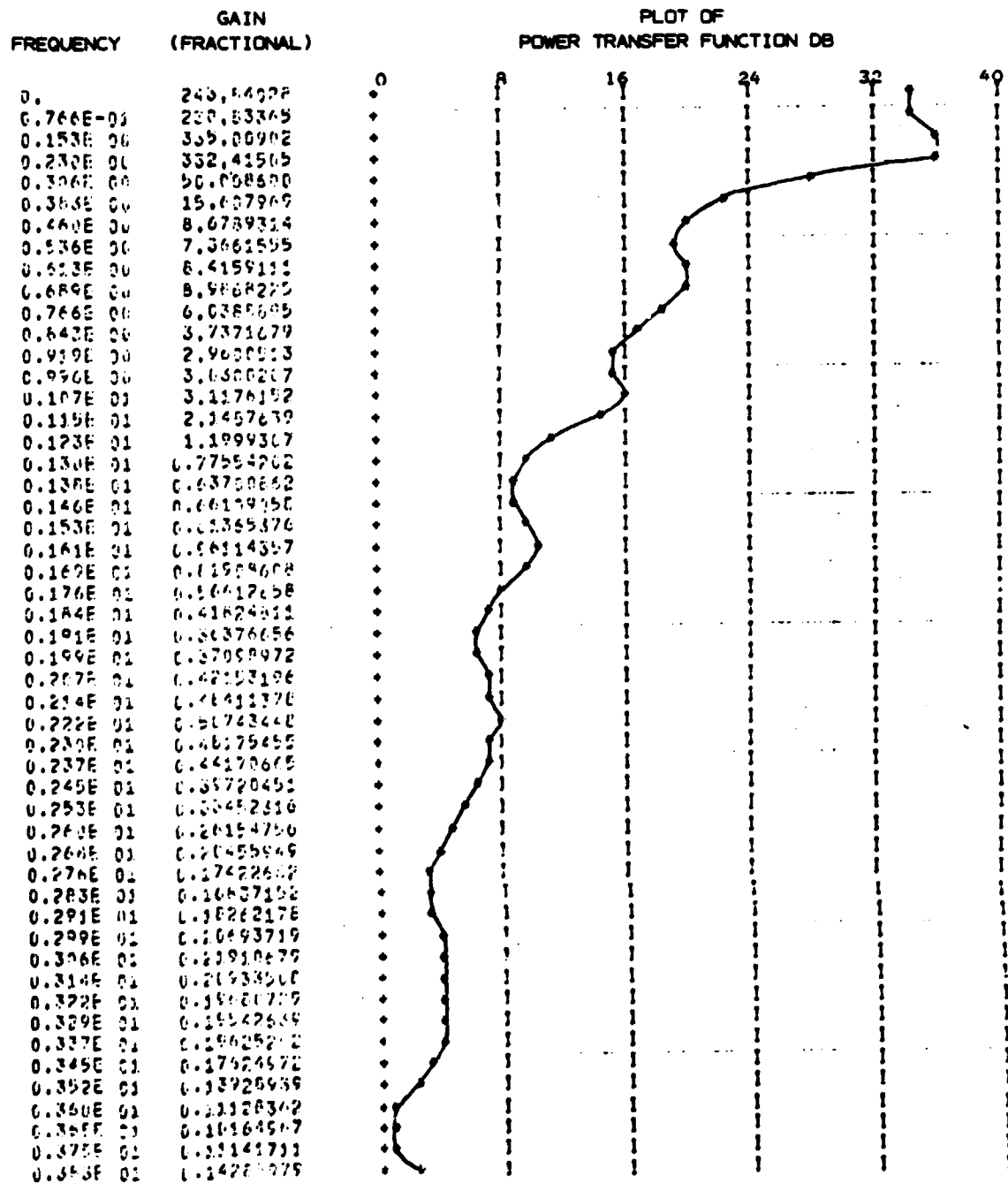


FIGURE 4.3.36  
AUTOREGRESSIVE MODEL  
MAP-66 PASS-37 MODE-5 DAS-3  
(UNFILTERED)



#### 4.4 Comparison of Power Spectrum with Autoregressive Model Transfer Function

As discussed in Section 2.2, the coefficients for an autoregressive model of order 20 are computed from the autocorrelation function. This model is useful in that it describes the serial correlation structure of the time series with a small set of parameters. The analytical power transfer function computed from the autoregressive model is actually a smoothed representation of the power spectral density of the original time series.

For Map 39 DAS-1 comparison of the power spectrum (Figure 4.1.2) and the autoregressive model power transfer function (Figure 4.1.4) shows that both curves have the same overall shape although the power spectrum, which has 108 coefficients, shows more detail than the power transfer function, which was derived from 20 autoregressive coefficients. Table 4.4.1 compares the frequencies of major power spectrum peaks with peak frequencies of the power transfer function. Peaks in the power spectrum separated by less than .15 Hz were merged into one peak in the power transfer function. Power spectrum peaks separated by .3 Hz are well defined in the power transfer function.

For Map 45 DAS-3 Table 4.4.2 shows a similar comparison of peak frequencies for the power spectrum (Figure 4.2.10) and the autoregressive model power transfer function. Again, the power spectrum, which in this case has 215 coefficients, shows much greater detail than the power transfer function which is derived from 20 parameters. Peaks separated by less than .12 Hz were combined into a single peak in the power transfer function.

Overall qualitative evaluation indicates that with 20 autoregressive coefficients the autoregressive model power transfer function provides a smoothed representation of overall power spectrum shape and will reproduce individual peaks which are separated by at least .3 Hz.

TABLE 4.2.2  
MAP 45 DAS-3  
LOCATION OF POWER SPECTRUM PEAKS

POWER SPECTRUM (FIGURE 4.2.10)	AUTOREGRESSIVE MODEL TRANSFER FUNCTION (FIGURE 4.2.12)
.271 Hz	{ .306 Hz
.326 Hz	
.633 Hz	{ .766 Hz
.723 Hz	
1.48 Hz	1.46 Hz
1.81 Hz	{ 1.84 Hz
1.92 Hz	
2.24 Hz	2.30 Hz
3.24 Hz	3.37 Hz

TABLE 4.4.1  
MAP 39 DAS-1  
LOCATION OF POWER SPECTRUM PEAKS

POWER SPECTRUM (FIGURE 4.1.2)	AUTOREGRESSIVE MODEL TRANSFER FUNCTION (FIGURE 4.1.4)
.338 Hz	.306 Hz
.676 Hz	.613 Hz
1.01 Hz	1.07 Hz
1.43 Hz	{ 1.46 Hz
1.58 Hz	{ 1.84 Hz
1.84 Hz	2.22 Hz
1.95 Hz	{ 3.45 - 3.60 Hz
2.44 Hz	
3.38 Hz	
3.57 Hz	
3.87 Hz	3.75 Hz

**APPENDIX A**

## RESIDUAL ANALYSIS PROGRAM MATHEMATICAL DESCRIPTION

### TABLE OF CONTENTS

	Page
1.0 INTRODUCTION.....	A-3
2.0 DESCRIPTIVE STATISTICS.....	A-4
2.1 Time Series Plot.....	A-4
2.2 Histogram.....	A-4
2.3 Sample Mean.....	A-4
2.4 Sample Standard Deviation.....	A-4
2.5 Standardized Variates.....	A-5
2.6 Power Spectral Density.....	A-6
2.7 Autocorrelation Coefficients.....	A-8
2.8 Cross Spectral Coefficients.....	A-10
2.9 Cross Correlation Coefficients.....	A-11
2.10 Autoregressive Model.....	A-12
2.11 References.....	A-13
3.0 TESTS FOR STATIONARITY AND NORMALITY.....	A-14
3.1 Chi Square Test for Distribution Normality.....	A-14
3.2 "t" Statistic to Test for Zero Residual Mean.....	A-15
3.3 F Test for Homogeneity of Variances.....	A-15
3.4 F Test for Homogeneity of Means.....	A-17
3.5 Kolmogorov-Smirnov Test for Homogeneity of Sample Distribution Functions.....	A-17
3.6 References.....	A-19

## 1.0 INTRODUCTION

The Residual Analysis Program (RAP) is designed to perform a statistical analysis of altimeter residual data. The program performs data screening, displays various descriptive statistics and plots, tests for stationarity and normality and computes the power spectral density and autocorrelogram. Each input data set is assumed to contain 3 columns of data which are:

- Column 1 - Altimeter Residual data
- Column 2 - Other time series data sequence
- Column 3 - Time labels corresponding to entries in Columns 1, 2.

The specific operations performed by RAP on Columns 1 and 2 of the data array include the following:

1. Computation of overall mean, standard deviation, maximum, minimum, range and "t" statistic;
2. Time series and histogram plots;
3. Partitioning of each column into subgroups and computation of subgroup means and standard deviations;
4. Computation of statistics to assess the homogeneity of subgroup variances, means and the underlying probability distributions;
5. Computation of statistics to test the hypothesis that the residuals follow a normal probability distribution;
6. For each column, computation of the power spectral density and autocorrelation function and autoregressive model coefficients.
7. Computation of the cross correlation function and cross spectral density for columns 1 and 2 of the data array.

RAP contains logic for the extraction of data from an input tape between given start and stop dates and times. Outlying observations in either Column 1 or Column 2 of the data set can be deleted if the absolute value exceeds a user specified edit threshold. Deleted data points are replaced with the error code - 7777. and are ignored except in the computations of power spectral density, autocorrelation coefficients, cross correlation coefficients and cross spectral density. For these computations the deleted data points (error code - 7777.) are replaced with a local average.

## 2.0 DESCRIPTIVE STATISTICS

RAP outputs various descriptive statistics and plots designed to give the user a feel for the underlying data structure. The sample size,  $N$ , for each data column is defined as the total number of data points minus the number of edited data points.

### 2.1 Time Series Plot

The time series plot is simply a display of the raw input data (after editing) in time order. The abscissa (x axis) contains the data time tags and the ordinate (y axis) is the value of the associated data point.

### 2.2 Histogram

The histogram is a means of graphically representing the sample probability density function. The abscissa is divided into equally spaced intervals and the ordinate is scaled to give the percentage of data values falling within each interval.

### 2.3 Sample Mean

The sample mean  $\bar{x}$ , of a variable  $x$ , is the average value of the  $N$  measurements of that variable. This statistic is a measure of the centrality or location of the distribution. It is calculated from the expression

$$\bar{x} = \frac{1}{N} \sum_{i=0}^{N-1} x_i . \quad (2.1)$$

### 2.4 Sample Standard Deviation

The sample standard deviation,  $s$ , is a measure of the dispersion of the  $N$  variable measurements about the sample mean value  $\bar{x}$ . As the mean  $\bar{x}$  corresponds to the center of gravity of the mass of the distribution,  $N$  times the moment of second order (variance) corresponds to the moment of inertia of the mass with respect to a perpendicular axis through the center of gravity. The standard deviation,  $s$ , corresponds to the positive square root of this

variance so as to keep the statistic in the units of the variable.

$$s^2 = \frac{1}{(N-1)} \sum_{i=0}^{N-1} (x_i - \bar{x})^2. \quad (2.2)$$

The reason for dividing by  $(N-1)$  is so that  $s^2$  is an unbiased estimator of the population variance.

## 2.5 Standardized Variates

Prior to computing the power spectrum, autocorrelation function, cross correlation function, cross spectrum and autoregressive coefficients described in Section 2.6-2.10, all edited data points are replaced by a local average defined as

$$a_i = \frac{1}{2}(f_i + f_{i-1}) \quad (2.3)$$

where  $f_i$  and  $f_{i-1}$  are those two non-edited data points directly preceding the edited data point. This replacement is necessary because the algorithms used in computing the power spectrum and autocorrellogram assume that the data points are all present and equi-spaced in time. After this replacement the mean and standard deviation are computed as

$$\bar{x} = \frac{1}{N} \sum_{i=0}^{N-1} x_i \quad (2.4)$$

$$\hat{s} = \sqrt{\frac{1}{N} \sum_{i=0}^{N-1} (x_i - \bar{x})^2} \quad (2.5)$$

Note that for these formulas  $N$  is the total number of time points in the data set since all edited points have been replaced with a local average. The mean, Eqn. (2.4), is exactly as defined in Eqn. (2.1) but the standard deviation, Eqn. (2.5), contains a divisor of  $N$  instead of  $N-1$  as in formula (2.2). This is done so that the computed autocorrelation coefficients will be as defined by Blackman and Tukey (Reference 1, pp. 53).

The standardized time series variates are computed as

$$\tilde{x}_i = \frac{x_i - \bar{x}}{s} \quad i=0,1,2 \dots N-1 \quad (2.6)$$

In the following descriptions of power spectrum and autocorrelation computations it is assumed that the edited data points have been replaced and the resultant time series standardized as per Eqn. (2.6).

## 2.6 Power Spectral Density

For the discrete time series  $\{x_j, j=0,1,2,\dots,N-1\}$  of  $N$  equi-spaced data points the Fourier transform is defined as

$$\alpha_k = \frac{1}{N} \sum_{j=0}^{N-1} x_j \exp\left(i \frac{2\pi j k}{N}\right) \quad k=0,1,2 \dots N-1 \quad (2.7)$$

where  $i = \sqrt{-1}$  and the  $\{\alpha_k\}$  are in general complex valued.

If  $\Delta t$  is defined as the time interval between data points then the total interval is given by

$$T = N\Delta t \quad (2.8)$$

The frequency resolution is inversely related to the total time interval as

$$\Delta f = \frac{1}{T} = \frac{1}{N\Delta t} \quad (2.9)$$

Thus the frequency associated with the Fourier coefficient  $\alpha_k$  is given by

$$f_k = k\Delta f \quad (2.10)$$

If the time series  $\{x_j\}$  is real valued, and  $N$  is even, as assumed in RAP, the Fourier coefficients  $\alpha_k$  and  $\alpha_{N-k}$  are complex conjugates. Thus

if  $a_k$  is expressed as

$$a_k = k^{+ib_k} \quad k=0,1,2,\dots,N-1 \quad (2.11)$$

Then  $a_{N-k}$  is given by

$$a_{N-k} = a_k^{-ib_k} = {}^*a_k \quad k=1,2\dots N/2-1 \quad (2.12)$$

where  ${}^*$  signifies complex conjugate. The coefficients  $a_{N/2}$  and  $a_0$  are unique.

In RAP the Singleton fast Fourier transform (FFT) algorithm, described in Reference 8, is used to compute the complex Fourier coefficients defined in Eqn. (2.11). The selection of this algorithm was based on the competitive evaluation published in Reference 5.

The power spectral coefficients are defined as

$$P_k = 2N(a_k^2 + b_k^2) \quad k=1,2\dots(N-1)/2 \quad (2.13)$$

$$P_{N/2} = N(a_{N/2}^2 + b_{N/2}^2)$$

Eqns. (2.11) and (2.12) demonstrate that the power spectral coefficients for  $k = N/2+1, \dots, N-1$  are mirror images of the spectral coefficients for  $k=1,2\dots N/2-1$ . Thus a time series containing  $N$  data points yield  $N/2+1$  unique spectral coefficients. From equation (2.10) the highest frequency for which a unique spectral coefficient can be computed is given by the nyquist frequency defined as

$$f_q = \left(\frac{N}{2}\right) \Delta f \quad (2.14)$$

This definition of the power spectral coefficients from reference 2 is programmed in RAP. If the time series,  $\{x_k\}$  is a white noise process (i.e. with no serial correlation) then each individual power spectral coefficient  $\{P_k, k=1,2\dots(N-1)/2\}$  will be distributed as a chi square variate with two degrees of freedom and the coefficients will be uncorrelated with each other. (Reference 1).

In general the discrete time series  $\{x_k\}$  will have been obtained by sampling a continuous process or by subsampling a much denser discrete time series. In either case, if the original data contained components at frequencies higher than  $f_q$ , the power spectrum computed for  $\{x_k\}$  will contain contributions due to these higher frequencies. The contributions will be folded such that the power spectral coefficient of the original series at frequency  $f_q + p\Delta f$  would appear in the spectral coefficients of  $\{x_k\}$  at frequency  $f_q - p\Delta f$ .

An option is available to smooth the Fourier coefficients with a Hanning window prior to computing the power spectral coefficients as defined in Eqn. (2.13). The smoothed coefficients are given by

$$\tilde{a}_k = -.25a_{k-1} + .5a_k - .25a_{k+1} \quad k=1, 2 \dots N/2-1 \quad (2.15)$$

The end coefficients  $a_0$  and  $a_{N/2}$  are smoothed as

$$\begin{aligned} \tilde{a}_0 &= .5 a_0 - .5 a_1 \\ \tilde{a}_{N/2} &= -.5 a_{N/2-1} + .5 a_{N/2} \end{aligned} \quad (2.16)$$

The power spectrum computed from the  $\{\tilde{a}_k\}$  is called a modified power spectrum or modified periodogram.

## 2.7 Autocorrelation Coefficients

For a data sequence  $\{x_j, j=0, 1, 2 \dots N-1\}$  the autocorrelation coefficients are defined as

$$r_k = \frac{1}{N-k} \sum_{j=0}^{N-k-1} x_j x_{j+k} \quad (2.17)$$

These coefficients can be computed directly from Eqn. (2.17) or by computing the power spectral coefficients of  $\{x_j\}$  and then using an FFT algorithm to take the inverse Fourier transform of the power spectrum. Both methods are available in RAP. The direct method (from (2.17)) will be more efficient if only a few coefficients are to be computed, otherwise the second method is preferred.

The computational steps for obtaining all  $N$  of the  $\{r_k\}$  autocorrelation coefficients using an FFT algorithm is as follows:

1. Imbed the original time series of length  $N$  in a new series of length  $2N$  where the last  $N$  entries are zero and the first  $N$  entries are the original time series.
2. Compute  $2N$  power spectral coefficients for the new time series.
3. Take the inverse Fourier transform of the power spectrum to obtain  $2N$  unscaled autocorrelation coefficients  $\{R_k, k=1, 1 \dots 2N-1\}$ .
4. From the first  $N$  unscaled coefficients compute  $N$  scaled coefficients as

$$r_k = \frac{2N}{N-k} R_k \quad k=0, 1, 2 \dots N-1 \quad (2.18)$$

The padding with zeros in step 1. is required because of the circular indexing employed within the FFT algorithm. If this padding were not utilized the resultant autocorrelation coefficients would be given by

$$\tilde{r}_k = r_k + r_{N-k} \quad (2.19)$$

where  $\tilde{r}_k$  are the coefficients obtained by taking the inverse Fourier transform of the power spectrum of the original unpadded time series and  $r_k$  are the autocorrelation coefficients defined in Eqn. (2.17).

## 2.8 Cross Spectral Coefficients

Given two real data sequences  $\{x_i, i=0, 1, 2, \dots, N-1\}$  and  $\{y_j, j=0, 1, 2, \dots, N-1\}$ , the Fourier transforms of these data sequences are defined from Equation 2.7 as

$$\begin{aligned} X_k &= \frac{1}{N} \sum_{i=0}^{N-1} x_i \exp \left( \sqrt{-1} \frac{2\pi i k}{N} \right) \quad k=0, 1, 2, \dots, N-1 \\ Y_k &= \frac{1}{N} \sum_{j=0}^{N-1} y_j \exp \left( \sqrt{-1} \frac{2\pi j k}{N} \right) \quad k=0, 1, 2, \dots, N-1 \end{aligned} \quad (2.20)$$

From Reference 3 the cross spectral coefficients are defined as

$$G_k = \overline{X_k} Y_k \quad k=0, 1, 2, \dots, N-1 \quad (2.21)$$

Where  $*$  signifies complex conjugate and  $X_k, Y_k$  are in general complex. Note that for real data sets

$$\overline{G_{N/2+k}} = G_{N/2-k} \quad k=0, 1, 2, \dots, N/2-1 \quad (2.22)$$

In RAP the Singleton fast Fourier transform algorithm, described in Reference 4, is used to compute the complex Fourier coefficients defined in Eqn. (2.20). An option is available, as described in Section 2.6, to smooth the Fourier coefficients with a Hanning window prior to computing the cross spectral coefficients as in Eqn. (2.21). Because of the "mirror image" effect described in Eqn. (2.22) the cross spectral coefficients,  $G_k$ , are computed only for  $k=0, 1, 2, \dots, N/2$ .

## 2.9 Cross Correlation Coefficients

Given two real data sequences  $\{x_i, i=0, 1, 2, \dots, N-1\}$  and  $\{y_i, i=0, 1, 2, \dots, N-1\}$ , the cross correlation coefficients are defined as

$$R_k = \frac{1}{N-|k|} \sum_i x_i y_{i+k} \quad k = -(N-1), \dots, 0, \dots, N-1 \quad (2.23)$$

where the summation over  $i$  is such that  $i+k$  is always between 0 and  $N-1$ .

The computational steps for obtaining all  $2N-1$  cross correlation coefficients  $\{R_k\}$  using the Singleton FFT algorithm is as follows:

1. Imbed each time series of length  $N$  in a new series of length  $2N$  as follows

$$\{x'_i\} = \{x_0, x_1, \dots, x_{N-1}, 0_N, 0_{N+1}, \dots, 0_{2N-1}\}$$

$$\{y'_i\} = \{0_0, 0_1, \dots, 0_{N-1}, y_0, y_1, \dots, y_{N-1}\}$$

2. Compute the  $2N$  complex Fourier coefficients  $\{X_k\}$  and  $\{Y_k\}$  for each of these padded series as in Eqn. (2.20).

3. Compute the cross spectral coefficients as

$$G_k = X_k Y_k \quad k = 0, 1, 2, \dots, 2N-1$$

4. Take the inverse Fourier transform of the power spectral coefficients  $\{G_k\}$  to obtain  $2N$  unscaled cross correlation coefficients  $\{\hat{R}_k, k = -N, \dots, 0, \dots, N-1\}$

5. Compute the scaled cross correlation coefficients as

$$R_k = \frac{2N}{N-|k|} \hat{R}_k \quad k = -(N-1), \dots, 0, \dots, N-1 \quad (2.24)$$

## 2.10 Autoregressive Model

In Sections 2.5 and 2.6, the serial interrelationships of a discrete stationary time series are described by  $N/2$  power spectral coefficients and  $N-1$  autocorrelation coefficients. Box and Jenkins (Reference 2) describe parametric modeling techniques which represent these serial interrelationships with a much smaller number of parameters. Their approach consists of modeling the discrete series as the output of a linear digital filter with white noise input. The filter output is given as

$$H(z) = \frac{F(z)}{D(z)} \cdot \sigma \quad (2.25)$$

where  $\sigma$  is the standard deviation of the white noise process  $Z$  is the complex exponential  $e^{-j2\pi fT}$ ,  $f$  is the frequency in Hz,  $T$  is the sample time in seconds, and  $F(z)$ ,  $H(z)$  are finite polynomials in  $Z$ . The parameters to be estimated are the polynomial coefficients. In general this requires iterative nonlinear estimation procedures. Parzan (Reference 7) and Graupe (Reference 4) suggest an intermediate procedure which requires the estimation of a larger number of parameters but requires only a single iteration linear estimator to recover these parameters. The transfer function,  $H(z)$  is expressed as

$$H(z) = \frac{1}{\tilde{D}(z)} = \frac{a}{1 - \phi_1 z - \phi_2 z^2 + \dots} \quad (2.26)$$

where  $\tilde{D}(z)$  is the infinite partial fraction expansion of

$$\tilde{D}(z) = \frac{D(z)}{F(z)} \quad (2.27)$$

and the  $\phi_i$  are the autoregressive coefficients. For practical applications this infinite polynomial  $\tilde{D}(z)$  is truncated after a finite number of terms. Graupe has derived error bands for this truncation.

Since, in general, the user will have no a priori feel for where  $\tilde{D}(z)$  should be truncated RAP solves for all coefficients for polynomials of order two through twenty. The solutions are obtained by recursive solution of the Yule-Walker equations which obtain the autoregressive coefficients as a linear function of the autocorrelation coefficients as suggested by Box and Jenkins (Reference 2). The program also computes and plots the power transfer function  $|H(z)|^2$  for the polynomial of order twenty.

## 2.11 References

1. Blackman and Tukey, The Measurement of Power Spectra, Dover, 1959.
2. Box and Jenkins, Time Series Analysis, Forecasting and Control, Holden-Day, 1970.
3. Cleveland, "The Inverse Autocorrelations of a Time Series and Their Applications", Technometrics Vol. 14, No. 2, May 1972.
4. Graupe, "Estimation of Upper Bounds of Errors in Identifying AR Models," Fourth Symposium on Nonlinear Estimation Theory and its Applications, September 10-12, 1973, San Diego, Calif.
5. Maynard, "An Evaluation of Ten Fast Fourier Transform (FFT) Programs," Technical Report ECOM-5476, Atmospheric Sciences Laboratory, White Sands Missile Range, New Mexico.
6. Otnes and Enochson, Digital Time Series Analysis, Wiley, 1972.
7. Parzan, "Some Solutions to the Time Series Modeling and Prediction Problem," Technical report No. 5, State University of New York at Buffalo, Department of Computer Science, February 1974.
8. Singleton, "An Algorithm for Computing the Mixed Radix Fast Fourier Transform," IEEE Trans. Audio Electroacoust, Vol. AU-17, pp. 93-103, June 1969.

### 3.0 TESTS FOR STATIONARITY AND NORMALITY

If an altimeter residual time series is stationary, this implies that the parameters of the underlying probability distribution are constants (i.e. not time varying). RAP includes the capability to assess stationarity and to test the hypothesis: "given that the series is stationary, then the underlying probability distribution is normal."

Non stationarity would be indicated if the data contains significant secular (trend) or periodic components, or if the random component (noise) statistics change with time. To obtain a simple assessment of stationarity RAP subdivides the time series into several segments and computes the mean and standard deviation for each segment. Overall "F" statistics will be computed to 1) assess the significance of differences in variability about the segment means, and 2) assess the significance of variability of the segment means about the overall mean. Because of the anticipated sample sizes, these statistics will be quite robust to departures of the underlying probability distribution from normality. The power spectrum, described in Section 2.6 provides a more comprehensive assessment of stationarity.

The data normality will be assessed by computing chi square statistics which measure the difference between the sample distribution function and normal distribution function having the same mean and standard deviation. Kolmogorov-Smirnov two-sample test is used to assess the consistency of the underlying probability distribution function between segments.

#### 3.1 Chi Square Test for Distribution Normality

To test for normality the sample histogram is tabulated and the following statistic computed (reference 3)

$$x^2 = \sum_{i=1}^r \frac{(n_i - e_i)^2}{e_i} \quad (3.1)$$

where  $r$  is the number of cells in the histogram,  $n_i$  is the number of sample values falling within the  $i$ th cell and  $e_i$  is theoretical expected number of sample values for the  $i$ th cell. The theoretical value,  $e_i$  is

evaluated as

$$e_i = n \int_{l_i}^{u_i} f(x) dx \quad (3.2)$$

where  $f(x)$  is the normal probability density function with mean and standard deviation estimated from the sample,  $l_i$  is the lower cell boundary,  $u_i$  is the upper cell boundary and  $n$  is the total sample size. The series approximation used in RAP for the integral of the normal distribution function was taken directly from reference 1. Since the mean and standard deviations are estimated from the sample the number of degrees of freedom associated with the  $\chi^2$  statistic is  $r-2$ . Under the assumption that the underlying sample distribution is normal RAP computes the probability that  $\chi^2$  is less than or equal to the computed value. This is done by integrating the chi square density function as

$$\text{Prob } (\chi^2_{r-2} \leq x^2) = \int_0^{x^2} \phi(t) dt \quad (3.3)$$

where  $\phi(t)$  is the chi square density function with  $r-2$  degrees of freedom. The method used in evaluating this integral is described in reference 4.

### 3.2 "t" Statistic to Test for Zero Residual Mean

If a sample is drawn from a normal population the "t" statistic defined as

$$"t" = \frac{\bar{x} - a}{s/\sqrt{n}} \quad (3.4)$$

follows a students "t" distribution with  $n-1$  degrees of freedom where  $a$  is the hypothesized population mean. In RAP this statistic is computed for each column of data with  $a=0$  to test the hypothesis that the column means are zero.

### 3.3 F Test for Homogeneity of Variances

In order to test the hypothesis that a time series (i.e. a column of data)

has constant variance the series is partitioned into several segments and the testing procedure recommended in reference 2 is used. This procedure is summarized as follows:

- (1) Partition the time series into  $g$  segments and compute the trimmed mean for each segment. The trimmed mean is obtained after deleting the largest ten percent and the smallest ten percent of the segment data points.
- (2) Replace each data point by the absolute value of its deviation from the trimmed segment mean

$$z_{ij} = |x_{ij} - \bar{x}_i| \quad (3.5)$$

- (3) Compute the test statistic

$$W = \frac{\sum_{i=1}^g n_i (\bar{z}_i - \bar{z})^2 / (g-1)}{\sum_{i=1}^g \sum_{j=1}^{n_i} (z_{ij} - \bar{z}_i)^2 / (n-g)} \quad (3.6)$$

where

$$\bar{z}_i = \sum_j \bar{z}_{ij} / n_i \quad \text{and} \quad \bar{z} = \sum_{i=1}^g \sum_{j=1}^{n_i} z_{ij} / n$$

If the time series data consists of *independent, normally distributed variates* with constant variance then the test statistic,  $W$ , will follow an "F" distribution with  $g-1$ ,  $n-g$  degrees of freedom. Large values of  $W$  indicate that the variances are not constant. Results of monte carlo test, summarized in reference 2 demonstrate that  $W$  is quite robust to departures from normality; however, no analytic or numerical results were published to indicate what happens when the variates are autocorrelated.

### 3.4 F Test for Homogeneity of Means

In order to test the hypothesis that a time series (i.e. a column of data) has constant mean the series is partitioned into several segments and the following computational steps performed:

(a) Compute the mean for each segment

$$\bar{x}_i = \frac{1}{n_i} \sum_{j=1}^{n_i} x_{ij} \quad i=1, 2, \dots, g \quad \text{where } g = \text{number of segments} \quad (3.7)$$

(b) Compute the sum of squares about the mean for each segment

$$ssm_i = \sum_{j=1}^{n_i} (x_{ij} - \bar{x}_i)^2 \quad (3.8)$$

(c) Compute the test statistic

$$G = \frac{\sum_{i=1}^g n_i (\bar{x}_i - \bar{x})^2 / (g-1)}{\sum_{i=1}^g ssm_i / (n-g)} \quad (3.9)$$

If the time series consists of *independent normal* variates with constant mean and variance then  $G$  follows an F distribution with  $g-1$ ,  $n-g$  degrees of freedom. A large value of  $G$  and a "small" value of the  $W$  statistic (Eqn. (3.6)) would indicate the value of the mean is not constant.

### 3.5 Kolmogorov-Smirnov Testing for Homogeneity of Sample Distribution Functions

The homogeneity of the sample distribution function is tested, for each column of data, by partitioning the time series into several segments. Kolmogorov-Smirnov two-sample statistics are computed to compare the empirical distribution for each segment with the empirical distribution function obtained by grouping all of the remaining segments. Thus, if there are  $g$  segments there will be  $g$  test statistics computed.

Following the procedure described in reference 5 the Kolmogorov-Smirnov two-sample statistic is computed as follows:

Define  $\{x_1, x_2 \dots x_n\}$  as one sample of size  $n$  and  $\{y_1, y_2 \dots y_m\}$  as the other sample of size  $m$ .

- (a) The samples  $\{x_1, x_2 \dots x_n\}$  and  $\{y_1, y_2 \dots y_m\}$  are sorted into the ordered sets  $\{x_{(1)}, x_{(2)} \dots x_{(m)}\}$  and  $\{y_{(1)}, y_{(2)} \dots y_{(n)}\}$  which are non decreasing sequences
- (b) The empirical cumulative distribution functions  $F_n(x)$  and  $G_m(y)$  are computed. For example  $F_n(x)$  is defined by

$$F_n(x) = \begin{cases} 0 & \text{for } x < x_{(1)} \\ k/n & \text{for } x_{(k)} \leq x < x_{(k+1)} \quad k=1, 2 \dots n-1 \\ 1 & \text{for } x_{(n)} \leq x \end{cases} \quad (3.10)$$

- (c) The maximum difference in absolute value between the two sample distribution functions is computed as

$$D_{m,n} = \max_{x,y} |F_n(x) - G_m(y)| \quad (3.11)$$

The limiting distribution function  $L(z)$  for the test statistic  $\sqrt{\frac{mn}{m+n}} D_{m,n}$  is given by (reference 5)

$$L(z) = \begin{cases} 0 & z \leq 0.27 \\ (\sqrt{2\pi}/z) \sum_{k=1}^3 \exp[-(2k-1)^2 \pi^2 / 8z^2] + E_1(z); & 0.27 < z < 1.0 \\ 1 - 2 \sum_{k=1}^4 (-1)^k \exp(-2k^2 z^2) + E_2(z) & 1.0 \leq z < 3.1 \\ 1 & 3.1 \leq z \end{cases} \quad (3.12)$$

where:

$$E_1(x) \leq 6 \cdot 10^{-15} \quad \text{when } x < 1$$

$$E_2(x) < 10^{-20} \quad \text{when } x \geq 1$$

### 3.6 References

1. Abramowitz and Stegun, Handbook of Mathematical Functions, Department of Commerce, National Bureau of Standards, Applied Mathematics Series 55.
2. Brown and Forsythe, "Robust Tests for the Equality of Variances," Journal of the American Statistical Association, June 1974, Vol. 69, Number 346, pp. 364-368.
3. Crow, Davis and Maxfield, Statistics Manual, Dover, 1960.
4. Huang and Bolch, "On the Testing of Regressing Disturbance for Normality," Journal of the American Statistical Association, June 1974, Vol. 69, Number 346, pp. 325-329.
5. IBM System 360 Scientific Subroutine Package, Version III, Programmers Manual, Program Number 350A-CM-03X.

**APPENDIX B**

PROGRAM SAMPL MATHEMATICAL DESCRIPTION

TABLE OF CONTENTS

	Page
1.0 INTRODUCTION.....	B-3
2.0 FILTER DESCRIPTIONS.....	B-4
2.1 Fixed Weight Moving Average Filter.....	B-5
2.2 Butterworth Filter.....	B-7
2.3 Adaptive Polynomial Filter.....	B-8
3.0 REFERENCES.....	B-11

## 1.0 INTRODUCTION

The SAMPFL Program is designed to filter and subsample time series data for input to the Residual Analysis Program (RAP). Three filtering options are included.

These are:

- 6th order Butterworth filter
- Adaptive polynomial filter
- Fixed weight moving average filter

The data may be low or high pass filtered. The three basic filters are low pass filters. The high pass output is obtained by taking the difference (or residual) between the input and the low pass filter output.

Typically, a low pass filter would be used to remove high frequency noise prior to an analysis of the systematic components of the data. If a particularly long time series is to be analyzed to determine the low frequency spectral structure of the data it is advisable to subsample the data after low pass filtering to eliminate aliasing effects.

A high pass filter would be used to remove the systematic or low frequency components of the time series prior to evaluation of the measurement noise statistics.

SAMPFL contains logic for the extraction of data from an input tape between given start and stop times. Outlying observations are deleted and replaced with a local average. The program also has the capability to either apply a fixed correction or entirely delete data between specified start and stop times.

## 2.0 FILTER DESCRIPTIONS

Each of the three basic filters described in the following sections is a low pass filter, or smoother. The input is a discrete time sequence  $\{y_i\}$  and the output is a discrete time sequence  $\{x_i\}$ . Here the time sequence  $\{x_i\}$  is smoother than  $\{y_i\}$ .

A discrete filter satisfies the following difference equation

$$x_i = \sum_l g_l y_{i-l} + \sum_k h_k x_{i-k} \quad (2.1)$$

If  $h_k = 0$  for all  $k$  then the filter is called a non recursive filter and the output is simply a weighted average of the adjacent values of the input time series. If, in addition, the  $\{g_l\}$  are constant, then the filter is called a fixed weight moving average filter. This type of filter is described in Section 2.1. If the  $\{h_k\}$  are non zero the filter is called a recursive filter. Section 2.2 describes a Butterworth filter for which the  $\{g_l\}$  and  $\{h_k\}$  are constant and Section 2.3 describes an adaptive polynomial filter which has time varying coefficients.

## 2.1 Fixed Weight Moving Average Filter

As defined in Section 2.0  $\{y_i\}$  is the filter input sequence and  $\{x_i\}$  is the filter output sequence. With a fixed weight moving average filter each  $x_i$  is a linear combination of the  $2n+1$  surrounding values of the input sequence. Thus the filter output can be expressed as:

$$x_i = \sum_{j=-n}^n a_j y_{i+j} \quad (2.2)$$

where  $\{a_j\}$  is a fixed weight sequence.

SAMPFL has two moving average options. These are:

- An arbitrary, externally determined set of weights  $\{a_j\}$  stored in BLOCK DATA are used;
- The weights  $\{a_j\}$  are computed so as to give a  $2n+1$  point polynomial midpoint fit.

For an  $(m-1)^{\text{th}}$  order polynomial midpoint fit the regression equation is given by

$$y_i = \beta_0 + \beta_1 (t_i - t_0) + \dots + \beta_{m-1} (t_i - t_0)^{m-1} + \epsilon_i \quad (2.3)$$

where  $i = -n, \dots, 0 \dots n$  and  $\epsilon_i$  is assumed to be a zero mean random error. Since the data is assumed to be equispaced in time, the time difference terms can be expressed as

$$t_i - t_0 = i\Delta t \quad (2.4)$$

For equispaced data the value of  $\Delta t$  is irrelevant in determining the weight sequence; therefore, in the following discussion it is assumed that  $\Delta t = 1.0$ .

In matrix notation the least squares estimate of the regression coefficients  $\{\beta_0 \dots \beta_{m-1}\}$  is given by

$$\hat{\beta} = (\mathbf{A}^T \mathbf{A})^{-1} \mathbf{A}^T \mathbf{y} \quad (2.5)$$

where  $\mathbf{y}^T = (y_{t-n} \dots y_t \dots y_{t+n})$  contains  $2n+1$  consecutive values of the time series. The normal matrix  $\mathbf{A}$  has  $2n+1$  rows with the  $i$ th row containing the partial derivatives of  $x_i$ , as defined from equation 2-3, with respect to the

regression coefficients. Thus the  $i$ th row of  $A$  is given by (for  $\Delta t = 1$ .)

$$a^{(i)} = [1 \ i \ i^2 \ \dots \ i^{m-1}] \quad (2.6)$$

For the filter midpoint  $i = 0$  and

$$a^{(0)} = [1 \ 0 \ 0 \ \dots \ 0] \quad (2.7)$$

The smoothed midpoint value is given by

$$x_i = a^{(0)} \hat{\beta} = \beta_0 \quad (2.8)$$

Substituting into (2.8) from (2.5), the expression for  $x_i$  in matrix notation is given by

$$x_i = a^{(0)} (A^T A)^{-1} A^T y \quad (2.9)$$

Comparing (2.9) with (2.2) which defines a moving average filter it is obvious that the weight sequence is given by

$$\underline{a} = a^{(0)} (A^T A)^{-1} A^T \quad (2.10)$$

Equation 2.10 is implemented in SAMPFL to compute the weight sequence for an  $(m-1)$ th order polynomial midpoint fit spanning  $2n+1$  elements of the input time sequence.

If a high pass filter is specified, the filter output is given by

$$x_i = y_i - \sum_{j=-n}^n a_j y_{i+j} \quad (2.10a)$$

## 2.2 Butterworth Filter

Repeating equation 2.1, a digital filter satisfies the difference equation

$$x_i = \sum_k g_k y_{i-k} + \sum_k h_k x_{i-k}$$

For a second order Butterworth filter this specializes to

$$x_i = g_1 (y_i + 2y_{i-1} + y_{i-2}) + h_1 x_{i-1} + h_2 x_{i-2} \quad (2.11)$$

In SAMPL a sixth order Butterworth filter is implemented as three cascaded second order filters. The coefficients  $g_1$ ,  $h_1$  and  $h_2$  are computed for each stage as described in references 1 and 2 to give a maximally flat frequency response in the passband.

The coefficients  $g_1$ ,  $h_1$  and  $h_2$  for the  $j$ th stage ( $j = 1, 2, 3$ ) are given by

$$g_1 = \frac{\omega_a^2}{\omega_a^2 + a_j \omega_a + 1}$$

$$h_1 = -2g_1 \left( \frac{\omega_a^2 - 1}{\omega_a^2} \right) \quad (2.12)$$

$$h_2 = -g_1 \left( \frac{\omega_a^2 - a_1 \omega_a + 1}{\omega_a^2} \right)$$

If  $\omega_d$  is the desired cutoff frequency for the digital filter and  $\Delta t$  the sampling interval then  $\omega_a$  is given by

$$\omega_a = \tan \left( \frac{\omega_d \Delta t}{2} \right) \quad (2.13)$$

The coefficients  $\{a_j, j = 1, 2, 3\}$  for a sixth order filter are given in reference 2 as

$$\begin{aligned} a_1 &= .5176 \\ a_2 &= 1.4142 \\ a_3 &= 1.9318 \end{aligned} \quad (2.14)$$

### 2.3 Adaptive Polynomial Filter

For a fixed length polynomial filter as described in Section 2.1, the length of the filter ( $2n+1$ ) and the polynomial order ( $m-1$ ) are arbitrarily specified. The adaptive polynomial filter attempts to adjust the effective filter length to the data structure for an arbitrary polynomial order. The filter is implemented as a Kalman filter which adaptively adjusts a single state noise parameter.

The following paragraphs describe the adaptive polynomial filter equations as implemented in SAMPFL. In these discussions the subscripts of each of the vectors or matrices refer to first the data point at which the matrix or vector is being evaluated, and second, the data point at which observation data was last incorporated into the estimate. Thus  $\underline{\beta}_{i|i-1}$  means the estimate prediction of  $\underline{\beta}$  at data point  $i$ , based on observation data through data point  $i-1$ .  $\underline{\beta}_{i-1|i-1}$  means the estimate of  $\underline{\beta}$  at data point  $i-1$ , based on observation data through data point  $i-1$ .  $\underline{\beta}_{i,i-1}$  is evaluated at  $\underline{\beta}_{i-1} = \underline{\beta}_{i-1|i-1}$ .

A particular component of a vector or matrix is denoted by superscript. For example,  $\underline{\beta}_{i|i-1}^{(1)}$  is the first component of the vector  $\underline{\beta}_{i|i-1}$ .

The state vector,  $\underline{\beta} = (\beta^{(0)}, \beta^{(1)} \dots \beta^{(m-1)})$ , contains regression coefficients similar to those defined in Section 2.1.

The incremental state model relating the filter state at time  $t_i$  to the state at  $t_{i+1}$  ( $t_{i+1} = t_i + \Delta t$ ) is defined by the equations

$$\begin{aligned}
 \beta_i^{(0)} &= \beta_{i-1}^{(0)} + \beta_{i-1}^{(1)} \Delta t + \dots + \beta_{i-1}^{(m-1)} (\Delta t)^{m-1} + q \\
 \beta_i^{(1)} &= \beta_{i-1}^{(1)} + q \sqrt{\Delta t} \\
 \beta_i^{(2)} &= \beta_{i-1}^{(2)} + q \Delta t \\
 &\vdots \\
 \beta_i^{(m-1)} &= \beta_{i-1}^{(m-1)} + q (\Delta t)^{m-1}/2
 \end{aligned} \tag{2.15}$$

Here  $q$  is assumed to be a zero mean white noise process with unknown variances  $Q$ . The measurement or input,  $y_i$ , is related to the filter state as

$$y_i = \beta_i^{(0)} + r_i \tag{2.16}$$

where  $r_i$  is a zero mean white noise process with known variance  $R_i$ .

The recursive filter update steps are as follows:

(a) Update the filter state

$$\hat{x}_{i|i-1} = \Phi_{i,i-1} \hat{x}_{i-1|i-1} \quad (2.17)$$

where the state transition matrix,  $\Phi_{i,i-1}$ , is given by

$$\Phi_{i,i-1} = \begin{bmatrix} 1 & \Delta t & \Delta t^2 & \dots & \Delta t^{m-1} \\ 0 & 1 & 0 & \dots & 0 \\ 0 & 0 & 1 & \dots & 0 \\ \vdots & \vdots & \vdots & & \vdots \\ 0 & 0 & 0 & \dots & 1 \end{bmatrix} \quad (2.18)$$

(b) Update the filter state covariance matrix

$$P_{i|i-1} = \Phi_{i,i-1} P_{i-1|i-1} \Phi_{i,i-1}^T + Q \Gamma \quad (2.19)$$

where  $Q$  is a scalar and  $\Gamma$  is a diagonal matrix having

$$\Gamma_{ii} = (\Delta t)^{i-1} \quad i = 1, 2, \dots, m \quad (2.20)$$

(c) Compute the residual variance

$$C_i = P_{i|i-1}^{(1,1)} + R_i \quad (2.21)$$

(d) Compute the filter gain matrix

$$K_i = \frac{1}{C_i} \begin{bmatrix} P_{i|i-1}^{(1,1)} \\ P_{i|i-1}^{(1,2)} \\ \vdots \\ P_{i|i-1}^{(1,m)} \end{bmatrix} \quad (2.22)$$

(f) Compute the filter residual

$$\Delta y_i = y_i - \hat{y}_{i|i-1}^{(0)} \quad (2.23)$$

(g) Using the measurement residual update the filter state estimate

$$\hat{y}_{i|i} = \hat{y}_{i|i-1} + K_i \Delta y \quad (2.24)$$

(h) Update the filter state covariance matrix to include the measurement information

$$P_{i|i} = [I - K_i M_i] P_{i|i-1} [I - K_i M_i]^T + K_i R_i K_i^T \quad (2.25)$$

where  $M_i$  is the  $m$  element row vector  $(1, 0, 0, \dots, 0)$

(i) Obtain an updated estimate of the scalar state noise parameter

$$Q_{i|i} = Q_{i|i-1} + \alpha(\Delta y^2 - c) \quad (2.26)$$

In SAMPFL, to insure filter stability,  $Q_{i|i}$  is restricted to the range of values given by

$$Q_{\min} \leq Q_{i|i} \leq Q_{\max} \quad (2.27)$$

where  $Q_{\min}$  and  $Q_{\max}$  are input parameters.

### 3.0 REFERENCES

1. Beauchamp and Williamson, "The Design of Cascaded Digital Recursive Filters Using the Bi-Linear Transform," Cranfield Institute of Technology, July 1971, Cranfield Memo No. 41.
2. Guilleman, Syntheses of Passive Networks, Wiley 1957.
3. Rader and Gold, "Digital Filter Design Techniques In the Frequency Domain," Proc. IEEE, Vol. 55, pp. 149-171, February 1967.
4. Weinberg, Network Analysis and Synthesis, McGraw-Hill, 1962.
5. Otnes and Enochsom, Digital Time Series Analyses, Wiley 1972.